MONASH University

Characterisation of novel paramyxoviruses isolated from pteropid bat urine

Rebecca Isobel Johnson

BBiomed(Hons)

A thesis submitted for the degree of *Doctor of Philosophy* at

Monash University in 2018

Department of Microbiology, Faculty of Medicine, Nursing and Health Sciences

CSIRO Health and Biosecurity, Australian Animal Health Laboratory

COPYRIGHT NOTICE

ABSTRACT

Bats are the reservoir hosts of multiple zoonotic viruses, making them important targets for virus discovery studies. In 2011, there was a large increase in the incidence of Hendra virus (HeV) disease events in horses in Queensland and New South Wales, concurrent with an increase in HeV prevalence in Australian pteropid bat urine. It has previously been observed that an increase in HeV prevalence is representative of an increase in the prevalence of other viruses in bat urine. Pteropid bat urine samples collected in 2011 from Alstonville, New South Wales were therefore assessed for the presence of novel viruses.

Virus isolations and PCR analysis of the bat urine revealed the presence of paramyxoviruses, paramyxovirus RNA, adenoviruses and a polyomavirus. One sample containing a potential henipa-like virus, Lumley virus (LumPV), was further analysed by next generation sequencing and the majority of the paramyxovirus coding sequence was obtained. Characterisation of the sequence revealed that it encoded an attachment glycoprotein that was divergent from those of known paramyxoviruses. In addition, two paramyxoviruses were isolated from the bat urine, Teviot virus (TevPV) and Alston virus (AlsPV), and were characterised *in vitro* and *in vivo* to determine their pathogenic potential. Phylogenetic and antigenic analysis of TevPV indicated that it was most closely related to Tioman virus. Although currently classified as a rubulavirus, TevPV has a divergent cell attachment glycoprotein and does not require sialic acid for infection. Animal infection trials demonstrated that mice could not be infected with TevPV and that oronasal exposure of ferrets to TevPV resulted in seroconversion but no further evidence of infection, suggesting that TevPV has a low pathogenic potential in mammals.

In contrast, AlsPV is a novel bat-borne rubulavirus that was demonstrated by phylogenetic and antigenic assessment to be most similar to parainfluenza virus 5 (PIV5). Nasal exposure of mice to AlsPV resulted in no clinical signs of infection, however, viral RNA could be detected in the olfactory bulb of the brains of two mice at 21 days post infection. Ferrets exposed to AlsPV through the oronasal route shed the virus in respiratory secretions during acute stages of infection, followed by seroconversion at 10 days post infection. AlsPV caused an upper respiratory tract infection in ferrets, with virus detected predominately in the nasal turbinates and tonsils throughout acute infection, although ferrets remained clinically normal for the duration of the trial. AlsPV also progressed from the nasal turbinates to the olfactory bulb where viral RNA and low levels of viral antigen were detected. These results indicated that AlsPV may be able to infect multiple host species, similar to what has been observed for PIV5. The discovery of these viruses and viral sequences highlights the

diversity found in Australian pteropid bats and emphasises the significance of continued surveillance of bats for the discovery of emerging viruses.

PUBLICATIONS DURING ENROLMENT

Johnson RI, Smith IL. 2017. Virus discovery in bats. Microbiology Australia **38:**25-27.

THESIS INCLUDING PUBLISHED WORKS DECLARATION

I hereby declare that this thesis contains no material which has been accepted for the award of any other degree or diploma at any university or equivalent institution and that, to the best of my knowledge and belief, this thesis contains no material previously published or written by another person, except where due reference is made in the text of the thesis.

This thesis includes two original papers submitted and under review at peer-reviewed journals, the *Journal of General Virology* (Chapter 4) and *Viruses* (Chapter 5). The core theme of the thesis is the discovery and characterisation of paramyxoviruses isolated from Australian pteropid bat urine. The ideas, development and writing up of all the papers in the thesis were the principal responsibility of myself, the student, working within CSIRO Health and Biosecurity and the Monash University Department of Microbiology under the supervision of Dr Glenn Marsh.

The inclusion of co-authors reflects the fact that the work came from active collaboration between researchers and acknowledges input into team-based research. In the case of Chapters 4 and 5 my contribution to the work involved the following: development and design of methodology, conducting *in vitro* and *in vivo* experiments (except for animal handling), data analysis and interpretation, data visualisation, writing and editing of manuscripts.

Since submitting this thesis for examination, Chapter 5: “Alston virus, a novel paramyxovirus isolated from bats causes upper respiratory tract infection in experimentally challenged ferrets” was accepted for publication in *Viruses*.

Thesis Chapter	Publication Title	Status *(published, in press, accepted or returned for revision, submitted)*	Nature and % of student contribution	Co-author name(s) Nature and % of Co-author's contribution*	Monash student Y/N*
4	**Characterisation of Teviot virus, an Australian bat-borne paramyxovirus**	Submitted (*Journal of General Virology*)	Development and design of methodology, conducting experiments, data analysis and interpretation, data visualisation, writing and editing of manuscripts, 80%	1) Mary Tachedjian, methodology and data analysis (sequencing), 5% 2) Bronwyn Clayton, concept and methodology (*in vivo* experiment), critical revision of manuscript, 4% 3) Rachel Layton, investigation (animal handling), 5% 4) Jemma Bergfeld, data analysis (histopathological) 2% 5) Lin-Fa Wang, conceptualisation, critical revision of manuscript, 2% 6) Glenn Marsh, conceptualisation, critical revision of manuscript, 2%	No No No No No No
5	**Alston virus, a novel paramyxovirus isolated from bats that causes upper respiratory tract infection in ferrets**	At submission of thesis: Returned for revision (*Viruses*)	Development and design of methodology, conducting experiments, data analysis and interpretation, data visualisation, writing and editing of manuscripts, 80%	1) Mary Tachedjian, methodology and data analysis (sequencing), 5% 2) Brenton Rowe, investigation (animal handling), 4% 3) Bronwyn Clayton, concept and methodology (*in vivo* experiments), critical revision of manuscript, 2% 4) Rachel Layton, investigation (animal handling), 3%	No No No No

				5) Jemma Bergfeld, data analysis (histopathological), 2% 6) Lin-Fa Wang, conceptualisation, critical revision of manuscript, 2% 7) Glenn Marsh, conceptualisation, critical revision of manuscript, 2%	No No No

I have renumbered sections of submitted papers in order to generate a consistent presentation within the thesis.

Student signature: [redacted] **Date:** 1/11/2018

The undersigned hereby certify that the above declaration correctly reflects the nature and extent of the student's and co-authors' contributions to this work. In instances where I am not the responsible author I have consulted with the responsible author to agree on the respective contributions of the authors.

Main Supervisor signature: [redacted] **Date:** 1/11/2018

ACKNOWLEDGEMENTS

I am greatly appreciative of the many people who have contributed to the completion of this work. I would firstly like to thank my supervisors, Dr Glenn Marsh and A/Prof Hans Netter. I discovered my interest in bats and viruses following a lecture by Glenn in the third year of my undergraduate degree. Eighteen months later I was still fascinated by the topic, so I contacted Glenn to start discussing a possible project that has now become this thesis. Glenn's generosity throughout my PhD has given me so many opportunities to travel and present my work around Australia and internationally. I was trusted to take control of my project and now feel ready to embark on the next stage of my career working as a postdoc overseas. For this, I am highly appreciative. I am thankful of Hans for always being happy to go out of his way to give advice or to address last minute requests. This research was supported by an Australian Government Research Training Program (RTP) Scholarship. Without this financial support, I would not have been able to complete my PhD journey.

Centre suite and the Dangerous Pathogens Team at AAHL were a constant source of advice, support and technical help, in particular from Shawn Todd and Jenn Barr. Thank you also to Reuben Klein, Ina Smith, Vicky Boyd, Paul Selleck, Sue Lowther, Lee Trinidad and Bronwyn Clayton. An extra thank you to Mary Tachedjian for your work generating the sequencing data. My PhD would have taken a lot longer without your assistance. I am very grateful to the animal services group for all of their work conducting the animal infection trials, and to Jemma Bergfeld, Jenni Harper and Jean Payne for carrying out the histopathological processing and analysis for these studies.

My family and friends have encouraged me throughout every stage of my PhD. Mum and Dad, Sharon and Brian Johnson, have been my biggest supporters and are always excited to hear about what I am doing next. Thank you for being my best friends and for encouraging my passion for science my whole life. I know I can always count on you for your love and support.

To Jenn, Lee, Sarah and Sue – thank you especially for all the crosswords - and to everyone else at the lunch table for quiz o'clock. I'm sure it helped with the PhD! To Sarah Edwards, I will be lucky to ever find a lab buddy as good as you! Thank you for making sure I took up every opportunity during my PhD and for being a great friend over the last few years. To my housemates, Caroline Cousins and Nicole Milenkovski, thank you for a fun four years! It was great to come home at the end of the day to such a welcoming and understanding household (and delicious food).

To Christian, it would have been a very stressful few years if it weren't for you. I am lucky to have you! Spending weekends with you let me take a break from the pressure of finishing a PhD. Thank you for supporting me and for keeping me motivated the whole way.

TABLE OF CONTENTS

LIST OF UNITS

°C	Degrees Celsius
Da	Daltons
g	Gram
h	Hour(s)
L	Litre
M	Molar
min	Minute(s)
mol	Mole
ms	Millisecond
mU	Milliunit
n/µ/mg	Nano/micro/milligram
n/µ/ml	Nano/micro/millilitre
p/n/µ/mM	Pico/nano/micro/millimolar
rpm	Revolutions per minute
s	Second(s)
$TCID_{50}$/ml	50% Tissue culture infectious dose per millilitre
U	Enzyme unit

LIST OF ABBREVIATIONS

aa	Amino acid
AAHL	Australian Animal Health Laboratory
BDT	Big Dye Terminator
BLAST	Basic Local Alignment Search Tool
bp	Base pair
BSA	Bovine serum albumin
BSCII	Biosafety cabinet II
cDNA	Complementary DNA
C_t	Cycle threshold
CPE	Cytopathic effect
DAPI	4',6-diamidino-2-phenylindole
DMEM	Dulbecco's minimal essential medium
DNA	Deoxyribonucleic acid
dNTP	Deoxyribonucleic triphosphate
Dpi	Days post infection
E. coli	*Escherichia coli*
EDTA	Ethylenediaminetetraacetic acid
F	Fusion protein/gene
FBS	Foetal bovine serum
H/HN/G	Attachment protein/gene
H&E	Haematoxylin and eosin
HEPES	4-(2-hydroxyethyl)-1-piperazineethanesulfonic acid
IDT	Integrated DNA Technologies

IFA	Immunofluorescence assay
IFNα/β	Interferon alpha/beta
IGR	Intergenic region
IRF-3	Interferon regulatory factor 3
L	Large protein/gene
LB	Luria-Bertani
LN	Lymph node
M	Matrix protein/gene
MDA5	Melanoma differentiation-associated protein 5
MDBK	Madin-Darby Bovine Kidney
MDCK	Madin-Darby Canine Kidney
MOI	Multiplicity of infection
mRNA	Messenger RNA
N	Nucleoprotein protein/gene
NCBI	National Centre for Biotechnology Information
NEB	New England Biolabs
NSW	New South Wales
nt	Nucleotide
ORF	Open reading frame
P	Phosphoprotein/gene
PaKi	*Pteropus alecto* kidney
PAPR	Powered air purifying respirator
PBS	Phosphate buffered saline
PBS-T	Phosphate buffered saline plus Tween 20
PCR	Polymerase chain reaction
PK15a	Porcine kidney-15
Qld	Queensland
qRT-PCR	Quantitative reverse transcription-polymerase chain reaction
RACE	Rapid amplification of cDNA ends
RNA	Ribonucleic acid
RT	Reverse transcription
RT-PCR	Reverse transcription-polymerase chain reaction
SH	Short hydrophobic protein/gene
SPAdes	St. Petersburg genome assembler
STAT	Signal transducer and activator of transcription
$TCID_{50}$	50% Tissue culture infectious dose
TPCK-trypsin	Trypsin L-1-tosylamide-2-phenylethyl chloromethyl ketone
UTR	Untranslated region
w/v	Weight per volume
w/w	Weight per weight

LIST OF VIRUS ABBREVIATIONS

AchPV1/2	Achimota virus 1 or 2
AlsPV	Alston virus
CedPV	Cedar virus
HeV	Hendra virus
hPIV2	Human parainfluenza virus 2
LumPV	Lumley virus
MapV	Mapuera virus
MenPV	Menangle virus
MojPV	Mojiang virus
MuV	Mumps virus
NiV	Nipah virus
PIV5	Parainfluenza virus 5
PorV	Porcine rubulavirus
SosPV	Sosuga virus
TevPV	Teviot virus
TioPV	Tioman virus
ThkPV1/2/3	Tuhoko virus 1, 2 or 3

LIST OF FIGURES

LIST OF TABLES

CHAPTER 1: LITERATURE REVIEW

1.1 INTRODUCTION

Over recent decades, we have seen the continual emergence of new pathogens into the human population, sometimes with devastating outcomes (1). Of these newly emerging pathogens, wildlife have been the source of more than 70%, with bats harbouring a significant number (2). Surveillance of Australian bats is essential to identify future emerging viruses and to prepare for the potential transmission of viruses into other mammalian populations, also known as a spillover event (2-4). Factors such as the urban habituation of bats means that the spillover of potentially zoonotic viruses will increase in frequency (5), thus having significant effects on public health and the economy. The improvement of wildlife surveillance would allow early detection of emerging viruses and a more efficient response in the future (6). In particular, the isolation of novel viruses allows characterisation, which leads to an increased understanding of the potential for these viruses to cause disease.

One of these highly pathogenic emerging viruses is Hendra virus (HeV, described further in section 1.4.1 and 1.6.1), a henipavirus of the family *Paramyxoviridae*, which circulates in the Australian pteropid bat population and has repeatedly spilled over to cause fatal disease into horses and humans (7). Henipa-like virus RNA has been detected in bats globally, indicating that there is a risk of similar viruses spilling over to cause disease in non-pteropid mammals and having a significant impact on public health (8, 9). In 2011, during a year of unprecedented numbers of HeV disease events, pteropid bat urine samples were collected in Alstonville, New South Wales. This increase in HeV spillover was of note as it has previously been proposed that HeV and novel paramyxoviruses have similar patterns of shedding (10). It was hypothesised that these urine samples likely contained novel viruses, in particular paramyxoviruses, which may have the potential to spillover into human or animal populations. In Chapter 3 of this thesis, the isolation of two paramyxoviruses, Teviot virus (TevPV) and Alston virus (AlsPV), along with the detection of multiple paramyxovirus sequences, adenoviruses and a polyomavirus, provided a greater understanding of the viral diversity present in Australian pteropid bats. TevPV and AlsPV were then characterised in Chapters 4 and 5 respectively to determine the antigenic relatedness, growth kinetics, seroprevalence and pathogenic potential of these bat-borne viruses. These data would help facilitate a rapid response to any detected spillover events. The information presented in this thesis provides an insight into the diversity of viruses infecting bats and the pathogenic potential of selected bat-borne viruses of the family *Paramyxoviridae*.

1.2 ZOONOTIC VIRUS EMERGENCE

Emerging diseases and zoonotic viruses are priority infectious disease concerns (11). The majority of emerging and re-emerging infectious diseases are caused by zoonotic pathogens with a broad host range (12). Over 70% of recently emerged infectious diseases originated in wildlife before being passed to humans either directly or indirectly *via* domestic animals, a proportion that has risen significantly since 2000 (2). Human population density and wildlife host richness are both important drivers of emerging infectious diseases (2, 13, 14). Increased human population density can contribute to the loss of wildlife habitats, therefore leading to an increase in wildlife density in the remaining restricted habitat (15). This creates an ideal environment for the maintenance of disease in wildlife and increases the potential for localised transmission of viruses from one species to another. Other factors predicted to influence the risk of infectious disease emergence are changes in land use, increased urbanisation, animal trade and the reduced ability to respond to infectious diseases in developing countries (11).

Initially, the virus is maintained in the reservoir host population (16). Changes to the environment can contribute to changes in host dynamics, such environmental changes leading to urban habituation of the host species, resulting in increased risk of human exposure (17). Human exposure can result in localised emergence of the virus with limited or no human-to-human transmission. The final stage of emergence is when sustained human-to-human transmission is achieved (16). The likelihood of a virus progressing from reservoir host infection to pandemic emergence is low, particularly as adaptation may be required for a virus to be successful in a new host (18). Despite the barriers to infection of a new species, the probability of transmission over time increases as the number of exposures between host and recipient species increase (19).

There are still many unknowns surrounding zoonotic disease emergence (18). Continued surveillance of animals and humans is required to rapidly detect zoonotic transmission events for the early management of outbreaks. In turn, this minimises infection rates and the clinical impact in the human population (16, 20). Targeted wildlife surveillance is an effective way of identifying potentially zoonotic viruses (3), but as pathogen discovery programs are expanding (16), it is essential that we also characterise novel viruses. The International Committee on Taxonomy of Viruses (ICTV) currently requires a complete viral genome before a virus can be listed as a new species (21). While novel viral sequences provide important data on viral diversity and evolution (20), *in vitro* and *in vivo* characterisation of these viruses can provide valuable information regarding their pathogenic potential.

1.3 BATS AS RESERVOIR HOSTS

The role of bats as reservoir hosts for zoonotic pathogens means that surveillance of bats and discovery of novel bat-borne pathogens is a fundamental task in the preparation for virus emergence (3, 15, 16). The significance of bats as reservoir hosts has become more evident in recent years as an increasing number of emerging viruses have been isolated from multiple bat species (22-24). A study of zoonotic viruses and mammalian hosts indicated that bats host a higher proportion of zoonotic viruses than any other mammalian order (3). The surveillance of bats has revealed an extensive list of over one hundred viruses from many different families (5) including coronaviruses (25), adenoviruses (26), filoviruses (27), reoviruses (28), herpesviruses (29) and paramyxoviruses (30). In fact, it has been estimated that each species of bat would have to be sampled approximately 1500 times in order to identify 85% of the viral diversity in that species (31).

With some exceptions, including Australian bat lyssavirus from the family *Rhabdoviridae* (32), these viruses have been isolated from bats in the absence of clinical symptoms. The lack of symptoms indicates that they are a possible reservoir host as it allows these viruses to be permanently maintained in the bat population and therefore able to be continually transmitted to susceptible target populations (33).

It has been suggested that the large number of viruses identified in bats can be attributed to some unique chiropteran features. Bats are migratory, long-lived animals with a wide global distribution (34). Their long life span, 3.5 times greater than non-flying mammals (35), increases the time for potential shedding of the virus and transmission to other susceptible hosts. Furthermore, bats roost in close quarters in large numbers, enhancing inter-host transmission of viruses through urine and faeces (34, 36). As well as being a highly prevalent taxonomic order, bat lineages can be traced back millions of years, making them one of the oldest surviving mammals (37). Viruses have potentially co-evolved with bats for fifty million years; facilitating the development of the host-virus dynamics that allow bats to be reservoir hosts for a range of viruses (34). This hypothesis of bat-virus co-evolution is supported by evidence that viruses such as henipaviruses also have ancient origins (22).

Bats are also the only mammals with the capability of powered flight. It has been hypothesised that the ability to fly, and the increased metabolic rate associated with it, requires increased resistance to DNA damage (33). Whole-genome sequence analysis of *Pteropus alecto* and *Myotis davidii* genomes revealed genetic changes in shared components of the DNA damage repair pathway and the innate immune system, possibly contributing to the increased resistance of bats to symptomatic infection by viruses (38). Furthermore, interferon α (IFN α) is constitutively expressed in bats, providing immediate protection from viruses that can be further induced during infection (39). In comparison,

another study has detected dampening of the STING-dependent interferon response, potentially to ensure a balanced response to viral infection (40).

1.4 BATS IN AUSTRALIA

Bats, belonging to the order Chiroptera, are the world's second most abundant mammalian order with over 1200 species. The order Chiroptera is divided into suborders of Yinpterochiroptera and Yangochiroptera, which were established based on extensive phylogenomic studies and replaced the previous phenotypic classification of Megachiroptera and Microchiroptera (41, 42). Yinpterochiroptera comprises the families *Pteropodidae, Rhinopomatidae, Megadermatidae* and *Rhinolophidae* (43). The genus *Pteropus,* which is the genus targeted for virus discovery in this thesis, is classified into the family *Pteropodidae*. There are four pteropid bat species found on mainland Australia; the grey-headed flying fox, *Pteropus poliocephalus*; the black flying fox, *P. alecto*; the little red flying fox, *P. scapulatus;* and the spectacled flying fox, *P. conspicillatus* (44).

1.4.1 VIRUS DYNAMICS IN AUSTRALIAN BATS

Virus spillover requires a host to be present, infected with and often actively shedding the virus, as well the presence of a susceptible recipient and the exposure of the recipient to a sufficient quantity of the virus (36). In Australia, anthropogenic environmental changes, seasonal conditions and behavioural changes have resulted in bats seeking alternative food sources, often in urban gardens. This urban habituation, combined with a decrease in migration, leads to increased contact between bats, domestic animals and humans, and therefore an increased likelihood of virus transmission (17, 45).

HeV, a pathogen transmitted from Australian pteropid bats to horses, is mainly detected in the spleen and kidney of naturally infected flying foxes, and to a lesser extent in the lungs, liver and blood, indicating systemic infection (46). Higher amounts of viral RNA have been detected in urine from wild *P. alecto* flying foxes compared to other samples such as serum, nasal swabs and faeces, making urine a useful specimen for HeV surveillance (47). HeV antibodies have been detected in all Australian mainland pteropid bat species, however, evidence suggests that *P. alecto and P. conspicillatus* are the primary reservoir hosts (46, 47). *P. alecto* flying foxes are found in coastal northern and eastern Australia, down as far as south-eastern New South Wales, whereas *P. conspicillatus* is found in northern Queensland down to the Queensland central coast (48, 49).

Although HeV can be detected in bat urine at any time of the year (50), it is not continually detected from individual bat colonies, implying that viral shedding may occur in pulses with only very low levels of virus circulating in between pulses (36). It has been proposed that these pulses of HeV

shedding could be occurring either due to episodic shedding of a latent infection or transient epidemics that are characterised by reinfection after a decrease in population immunity (36). HeV has been detected more often in female bats with increased viral shedding occurring around mid-gestation between April and June (47). However, vertical transmission is not thought to occur very often and reproductive material is not a major source of transmission (46). The role of stress in flying foxes has also been investigated as a potential cause of increased virus transmission, but results vary on whether it is a driver of viral spillover (51, 52).

The most significant route of transmission for HeV is through excretion of the virus in urine (47). Despite HeV shedding occurring throughout the year, there is a seasonal clustering of spillover events. In the subtropics, the majority of HeV spillover events into horses occur between May and October with the peak number of events occurring in July. This pattern of spillover is not consistent in the tropical north of Australia where spillover events have also been detected in summer (36). During 2011 when an unprecedented number of HeV spillover events occurred, virus shedding was more prevalent than previously detected and occurred for a longer period of time in southeast Queensland and northern New South Wales (53). It has been proposed that the shedding of other viruses may also be more prevalent in urine collected from Australian pteropid bats during the winter months of 2011. It is therefore an ideal sample for detecting and isolating novel viruses.

1.5 PARAMYXOVIRUSES

Bats are reservoir hosts to two highly pathogenic members of the family *Paramyxoviridae*, HeV and Nipah virus (NiV), along with many other paramyxoviruses that have been detected in bats globally (30, 54, 55). There are currently seven genera in the family *Paramyxoviridae*: *Morbillivirus*, *Henipavirus*, *Rubulavirus*, *Respirovirus*, *Avulavirus, Ferlavirus and Aquaparamyxovirus.* Recent proposals to the International Committee on Taxonomy of Viruses have suggested the formation of additional genera to incorporate currently unclassified viruses such as J virus and Beilong virus (56).

Paramyxoviruses are enveloped viruses with a linear non-segmented, negative sense RNA genome (57). The genomes of paramyxoviruses are between 15kb to 19kb in length and must comply with the rule of six, which requires the length of the genome to be a multiple of six in order to correctly associate with the nucleocapsid protein (58). Six nucleotides helically assemble with a single nucleocapsid protein allowing efficient replication and transcription (59, 60). The paramyxovirus genome is flanked by 3' leader and 5' trailer sequences that play an important role as promoters of transcription and replication. Paramyxovirus genes are made up of coding sequences adjacent to 5' and 3' untranslated regions (UTRs). The transcription of paramyxovirus genes is controlled by conserved transcriptional start and stop sequences at the beginning and end of these UTRs. For most

paramyxoviruses, the transcriptional initiation sequence begins with a uridine residue (57), although exceptions to this are the gene start sequences of Menangle and Tioman virus that begin with a cytosine residue (61, 62). Between these paramyxovirus genes are intergenic regions that are either highly conserved, such as the trinucleotide sequence between henipavirus genes, or variable in length or sequence, such as the intergenic regions of rubulaviruses (57).

1.5.1 PARAMYXOVIRUS PROTEINS

The paramyxovirus genome is made up of six major genes encoding at least seven proteins (Figure 1.1). These genes encode the nucleocapsid protein (N), phosphoprotein (P), matrix protein (M), fusion protein (F), attachment glycoprotein (H, HN or G), and the large polymerase subunit (L). Mumps virus (MuV) and parainfluenza virus 5 (PIV5) also encode a transmembrane small hydrophobic protein (SH) (57). Furthermore, RNA editing of the P gene results in the expression of additional accessory proteins including the multi-functional V and W proteins due to the addition of non-templated G residues (Figure 1.2) (57, 63). For viruses in the genus *Rubulavirus,* it is the unedited transcript that encodes the V protein and the addition of two non-templated G residues due to polymerase stuttering that results in expression of the phosphoprotein. Members of the genera *Morbillivirus*, *Henipavirus* and *Respirovirus* express a C protein from an alternative start site in the P gene (57).

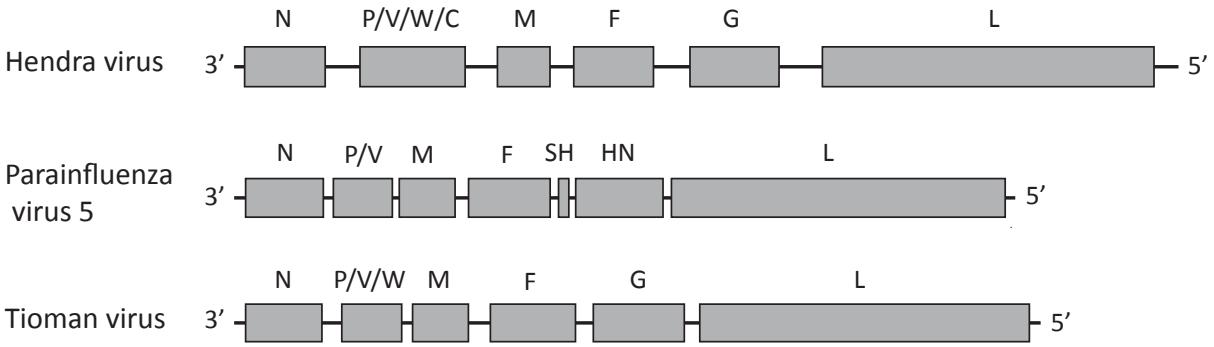

Figure 1.1: Genome layout of representative paramyxoviruses. Hendra virus represents viruses of the genus *Henipavirus* with a genome length of 18234 nt. Parainfluenza virus 5 and Tioman virus are members of the genus *Rubulavirus* with genome lengths of 15246 nt and 15522 nt respectively. The SH gene is only encoded by parainfluenza virus 5 and mumps virus. Grey boxes represent coding sequences and black lines represent untranslated and intergenic regions drawn to approximate scale.

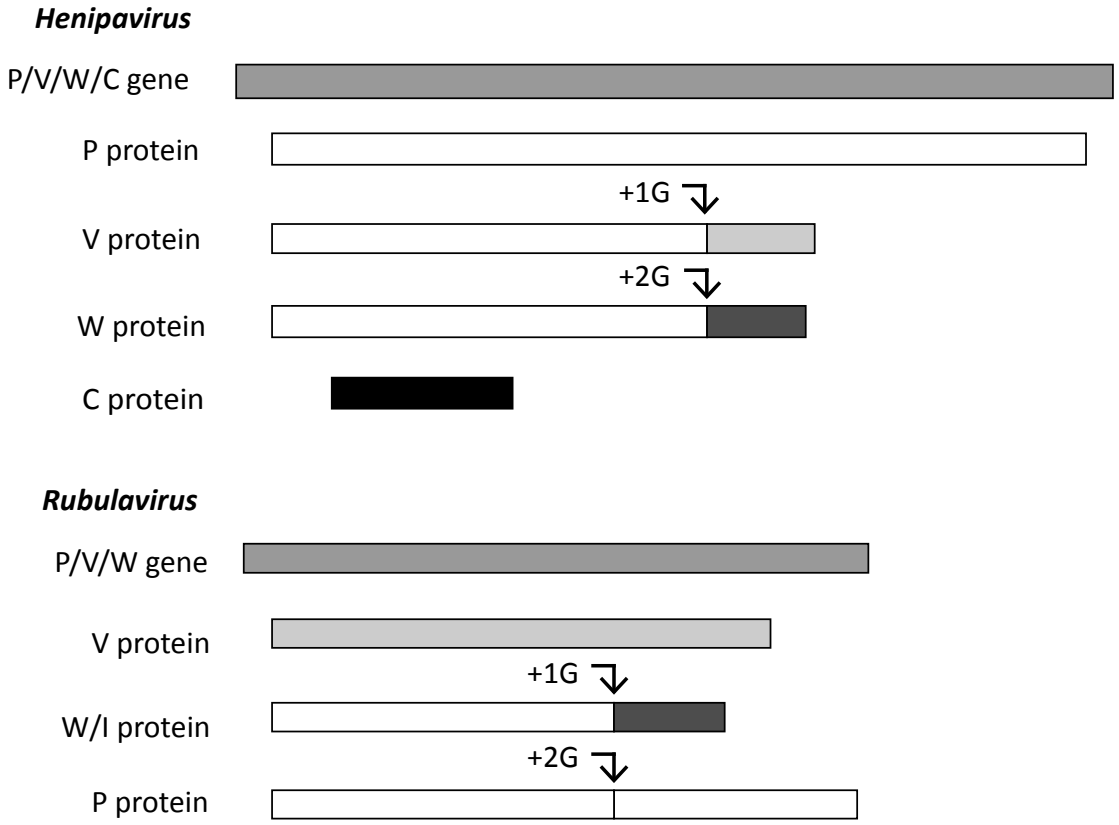

Figure 1.2: Proteins expressed from the P/V gene of viruses in the genera *Henipavirus* and *Rubulavirus.* The addition of non-templated G residues to the P gene mRNA of henipaviruses results in the expression of a V or W protein. The C protein is expressed from an alternative start site. For rubulaviruses, the unedited transcript encodes the V protein and the addition of non-templated G residues results in the expression of the P or W protein. The W protein is sometimes referred to as the I protein for rubulaviruses.

1.5.2 PARAMYXOVIRUS CYCLE OF INFECTION

Invasion of the host cell by paramyxoviruses occurs when the viral attachment glycoprotein adsorbs to specific cell surface receptors, such as host cell sialoglycoconjugates that are bound by the attachment glycoproteins of rubulaviruses and respiroviruses. This protein can have hemagglutinating and neuraminidase activity (HN), hemagglutinating activity alone (H) or neither of these enzymatic abilities (G) (64, 65). After binding of the attachment glycoprotein to a cellular receptor, the F protein undergoes conformational changes in order to facilitate fusion with the host cell membrane at a neutral pH (66, 67). Following fusion of the viral envelope with the host cell membrane and release of the viral nucleocapsid into the cytoplasm of the host cell, primary transcription by the viral RNA-dependent RNA polymerase (RdRp) and translation by host machinery can occur in the cell cytoplasm. The viral RdRp, consisting of a P protein tetramer and a monomer of the L protein, sequentially transcribes the negative sense paramyxovirus genes into positive sense

monocistronic or dicistronic mRNA. These genes are expressed at different ratios due to the instability of the viral polymerase on the genome, with expression decreasing at the junction between the M and F genes, then again between the G and L genes (68).

Once enough N protein has accumulated, the viral polymerase produces full length, positive sense antigenomes, which are encapsidated by the N protein. The antigenome can then be used as the template for production of the full-length genome, also encapsidated by the N protein, forming the ribonucleoprotein complex (69, 70). The N protein coats both the negative sense genome and the positive sense antigenome to allow replication and further transcription. From these progeny full-length genomes, a secondary round of transcription or replication can occur, or the encapsidated negative sense genome can be directly incorporated into a budding virion. Viral envelope proteins are transported to the host cell membrane through the secretory pathway, but the inactive precursor of the F protein (F_0) must be cleaved in order to form the active heterodimer and to expose the hydrophobic fusion peptide (71). For most paramyxoviruses, this occurs during transport through the *trans*-Golgi network, whereas the F proteins of some paramyxoviruses, such as Sendai virus, are cleaved at the cell surface by extracellular proteases. Henipavirus F proteins are cleaved by cathepsin L following endocytosis of F_0 back from the cell surface (72). A feature of paramyxovirus infection is their ability to form multi-nucleated cells, syncytia. After translation, the fusion protein is expressed on the host cell membrane, allowing fusion with the surrounding cells. This cytopathic effect (CPE) allows identification of paramyxoviruses in cell culture and *in vivo* can result in tissue necrosis (57). The SH protein is an additional short transmembrane protein only expressed by two rubulaviruses, MuV and PIV5, which is thought to block apoptosis through a tumour necrosis factor-alpha (TNFα) mediated pathway (73).

The ribonucleoprotein complexes are trafficked to the cell membrane by the host cytoskeleton (74), potentially dependent on the M protein (75). The M protein is located under the virus membrane in the mature virion (Figure 1.3) where it interacts with the cytoplasmic tails of envelope glycoproteins, forming a bridge to the ribonucleoprotein complex (76). During infection, the M protein coordinates the assembly of the components of the virion at the cell membrane and is essential for virus budding (77). To promote budding of viral particles, the M protein interacts with the host membrane and induces the required deformation and curvature (75). For some paramyxoviruses, this process of virus release is driven by host proteins in the vacuolar protein sorting pathway (57, 77).

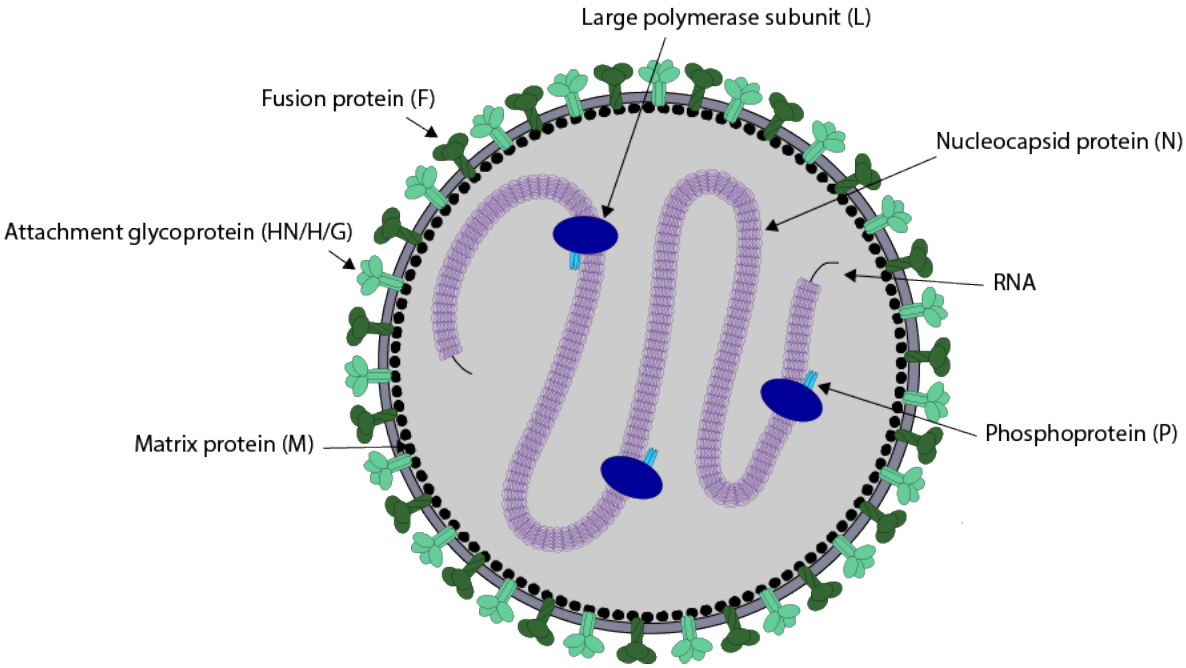

Figure 1.3: Paramyxovirus virion. Two envelope proteins, the trimeric fusion protein (dark green) and tetrameric attachment glycoprotein (light green), are expressed on the viral envelope (dark grey) with cytoplasmic tails that interact with the matrix layer (black circles). The viral RNA genome is encapsidated with the nucleocapsid protein (purple). A tetramer of the phosphoprotein (light blue) interacts with a monomer of L protein (dark blue) and the encapsidated genome. Viral components are not drawn to scale.

1.5.3 PARAMYXOVIRUS ACCESSORY PROTEINS

Paramyxoviruses encode multiple accessory proteins, most of which are involved in the antagonism of the host innate immune response, in particular by targeting multiple stages of the interferon (IFN) pathway. The V proteins of many paramyxoviruses are involved in blocking IFN signalling by mechanisms such as the degradation of signal transducer and activator of transcription 1 (STAT1) or by forming multiprotein complexes to block the signalling of STAT1 (78, 79). Other paramyxovirus V proteins inhibit the induction of IFN by interfering with pattern recognition receptors such as melanoma differentiation-associated protein 5 (MDA5), or by preventing the activation and signalling of interferon regulatory factor 3 (IRF-3) (80). The henipavirus W protein contributes to the interference of IFN signalling by sequestering inactive STAT1 in the nucleus (81), whereas the C protein of henipaviruses has been shown to interfere with host interferon induction and signalling, as well as negatively regulating viral RNA production (82) and moderating genome polarity (83).

1.6 HENIPAVIRUSES

The genus *Henipavirus* was established following the discoveries of HeV and NiV, two zoonotic bat-borne pathogens (84). Since then, many henipavirus sequences have been detected (54), along with

the discovery of three additional henipaviruses, Cedar virus (85), Kumasi virus (54) and Mojiang virus (86). Henipaviruses have genomes that are more than 10% larger than the average genome size of other genera in the family *Paramyxoviridae* (84, 87). These large genomes include long 3' and 5' UTRs and express an attachment glycoprotein that lacks hemagglutinating and neuraminidase activities (88). Both HeV and NiV have a broad host range that is largely attributed to their use of the highly conserved ephrin-B2 and B3 host cell surface molecules as entry receptors (89, 90).

1.6.1 Hendra virus

HeV was first isolated after an outbreak in September 1994 that resulted in the deaths of fourteen horses and one human on a property in Brisbane, Queensland (91). Infection with HeV causes severe respiratory or neurological illness in horses that is often fatal (92). Humans in close contact with infected horses can also become ill with severe respiratory symptoms or encephalitis (93). Infection of humans resulted in death in four out of the seven recorded cases (7), one of which was caused by relapsing encephalitis thirteen months after contact with an infected horse (94). From its discovery in 1994 until 2010, fourteen recorded HeV spillover events from bats to horses occurred in coastal Queensland and northern New South Wales, followed by an unprecedented eighteen spillover events occurring in 2011 alone (7, 95). In 2012, a vaccine was released to protect horses by eliciting an antibody response against a soluble HeV G glycoprotein (96). More recently, there was one confirmed case of HeV in 2016, four confirmed cases in 2017 and one confirmed case in 2018 in horses in Queensland and northern New South Wales (97).

During HeV surveillance of bat urine collected in southeast Queensland, a closely related virus was isolated. Despite genetic and antigenic similarities to HeV, infection with this novel virus, Cedar virus (CedPV), was asymptomatic in both ferrets and guinea pigs. *In vitro* infection of a human cell line with CedPV resulted in greater interferon β production than HeV, potentially due to the lack of an RNA editing site and V ORF in the CedPV phosphoprotein gene (85). Furthermore, the CedPV P protein did not target STAT1 or STAT2 and had a significantly reduced ability to inhibit the nuclear translocation of STAT1 (98). The lack of a V protein and the functional differences of the P protein make CedPV a vital tool to research virus pathogenicity and highlights the importance of isolating novel viruses.

1.6.3 Nipah virus

Initially detected in Malaysia in 1998, NiV causes respiratory disease and often fatal febrile encephalitis in humans (99). It was transmitted from fruit bats to pigs, causing respiratory and neurological disease, then transmitted from pigs to humans (100, 101). The outbreak resulted in the culling of over one million pigs and the deaths of 105 out of 265 reported human cases (99, 100). A

genetically distinct NiV strain emerged in Bangladesh and India in 2001 with important epidemiological and clinical differences. The Bangladesh NiV strain can be directly transmitted from bats to humans through contaminated palm sap, as well as between humans without an intermediate host (102, 103). Annual outbreaks of NiV in humans have occurred in Bangladesh since 2001 (103, 104). In May 2018, an outbreak of NiV occurred in Kerala, India, resulting in the deaths of sixteen out of eighteen laboratory confirmed cases. The outbreak was reported to be contained by mid-June 2018 (105).

1.6.4 MOJIANG VIRUS

More recently, a henipa-like virus, Mojiang virus (MojPV), was detected in rats (*Rattus flavipectus*) in China. In 2012, three people working in an abandoned mine in the Yunnan province of China died following diagnosis of severe pneumonia. No viruses could be isolated from patient specimens, however, a henipa-like virus was detected in anal swabs collected from rats located in the abandoned mine (86). Although this novel virus could not be isolated, the whole genome was obtained and the virus attachment protein was functionally and structurally assessed by cloning the sequence into mammalian expression vectors. These experiments revealed that the MojPV attachment protein was divergent from the G proteins of previously characterised henipaviruses and that it utilised a different entry receptor (106). Despite this divergence, MojPV is currently classified in the genus *Henipavirus*.

1.6.5 KUMASI VIRUS

The whole genome sequence of a henipavirus, Kumasi virus (KV), was identified in an *Eidolon helvum* bat spleen in Ghana (54). Similar to MojPV, this virus could not be isolated despite multiple attempts, however, KV proteins have been studied *in vitro*. Initially, the KV F protein demonstrated no fusogenic activity. *In silico* editing of the F gene sequence was required to correct what appeared to be an error obtained due to polymerase stuttering over an AT-rich region. The addition of a single nucleotide (either A, C or G), restored efficient expression and cleavage of the F protein, as well as restoring fusogenic activity (107). Expression of KV glycoproteins on pseudotyped particles has been used to determine that the KV G protein binds to ephrin-B2 but not ephrin-B3 (108).

1.7 RUBULAVIRUSES

Rubulavirus is a broad genus in the family *Paramyxoviridae.* It encompasses a number of human pathogens, animal pathogens and zoonotic viruses. Seventeen viruses have been classified as rubulaviruses, with the majority isolated from or detected in bats. Rubulaviruses are classified based on the attachment glycoprotein having hemagglutininating and neuraminidase capability, along with

a genetic similarity to the type species, MuV (88). The earliest paramyxoviruses to be isolated from bats were of the genus *Rubulavirus.* A bat parainfluenza virus was isolated from frugivorous bats in India that was serologically related to simian virus 41 (109). This was followed by the isolation of Mapuera virus from bats in the absence of clinical disease in Brazil, 1979. It was later classified as a rubulavirus closely related to porcine rubulavirus, which in turn was isolated as the causative agent of disease in pigs in Mexico (110). Major human pathogens in this genus include MuV and human parainfluenza virus 2 and 4 (54).

1.7.1 PARAINFLUENZA VIRUS 5

PIV5, previously called simian virus 5 or canine parainfluenza virus 2, has been isolated from multiple host species, including from bone marrow aspirate from humans with and without Multiple Sclerosis (MS) (111). It was controversially suggested to cause some cases of MS (112), but this association was not supported by additional studies (113). Nevertheless, this evidence suggested that PIV5 may persist in human cells (111). PIV5 has, however, been associated with disease in other hosts. PIV5 is one of the causative agents of the canine infectious respiratory disease complex, normally causing a self-limiting tracheobronchitis. Secondary infection with another respiratory virus or *Bordetella bronchiseptica* can result in more severe symptoms (114). Due to the highly contagious nature of PIV5, dogs can be vaccinated with a modified live vaccine beginning at 6-8 weeks of age (115). PIV5 has also been isolated from a dog with temporary posterior paralysis (116), the lung of a foetus from a breeding sow with porcine respiratory and reproductive syndrome (117), and has been identified as the possible cause of respiratory disease in weaning calves in China (118).

The ability of PIV5 to infect humans in the absence of clinical disease has meant that it is a candidate to be used as a live recombinant vaccine for viruses such as influenza, respiratory syncytial virus and rabies virus (119-122). Mice and dogs infected with a recombinant PIV5 expressing the HA of influenza virus generated neutralising antibody responses against influenza virus, despite having previously developed neutralising antibodies against PIV5 (123).

1.7.2 RUBULA-LIKE VIRUSES

Within the genus *Rubulavirus*, there is another phylogenetic branch of rubula-like viruses that cluster away from the classical rubulaviruses. Recently, it has been proposed by the ICTV that these two phylogenetic clusters should actually form two genera, *Pararubulavirus* and *Orthorubulavirus*, within the subfamily *Rubulavirinae* (56). These rubula-like viruses, which would be classified as pararubulaviruses, have been detected in or isolated from bats in Australia (30, 124), Ghana (125), Uganda (126), China (127) and Malaysia (128).

Tioman virus (TioPV) was discovered off the coast of Malaysia on Tioman Island during the search for the reservoir host of NiV (128). Although neutralising antibodies against TioPV or a Tioman-like virus were detected in human sera from a village nearby, exposure to the virus has not been linked to clinical disease (129). It is most closely related to Teviot virus (TevPV), a virus that has been isolated multiple times from pteropid bat urine collected throughout southeast Queensland, northern New South Wales and in Geelong, Victoria. Although two isolates of TevPV have previously been sequenced, only limited additional characterisation was conducted; therefore, its pathogenic potential in non-pteropid mammals remains undetermined (30, 130).

Menangle virus (MenPV) was first detected during an outbreak of reproductive disease in a piggery in New South Wales in 1997 (131). Post-natal pigs did not show clinical signs, however, there was an increase in the rate of abortion and birth defects, such as the degeneration of the brain and spinal cord. Over 90% of pigs at the affected piggery had neutralising antibodies against MenPV. Serological screening identified that two piggery workers had also likely been infected with MenPV, resulting in an influenza-like illness (132). MenPV has since been isolated from Australian pteropid bats and serological evidence indicated that the outbreak may have originated from a nearby colony of grey-headed flying foxes (124, 131).

Sosuga virus (SosPV) was discovered when an American wildlife biologist developed fever, malaise, generalised myalgia and arthralgia, sore throat and neck stiffness after conducting fieldwork involving bats in South Sudan and Uganda (133). After admission to hospital, the patient developed a maculopapular rash, oropharynx ulcerations, mild diarrhoea and bloody emesis. The patient was discharged after two weeks in hospital. SosPV was identified by deep sequencing of RNA from blood and serum samples from the patient and the complete genome was determined by reverse transcription PCR and Sanger sequencing (133). The virus was later detected in tissues collected from Egyptian fruit bats (*Rousettus aegyptiacus*) collected prior to the detection of human illness, as well as in archived Egyptian fruit bat tissues collected in Uganda across a three-year period (126).

Achimota viruses 1 and 2 (AchPV1, AchPV2) are distinct virus species that were isolated from straw-coloured fruit bats, *Eidolon helvum,* in Ghana. Neutralising activity to AchPV2 was detected in serum samples from humans from Ghana and Tanzania, indicating that it has the potential to spillover into human populations, however, these viruses have not been associated with clinical symptoms in humans (125). Three rubulaviruses were detected in alimentary and respiratory specimens from *Rousettus leschenaulti* in China. The whole genome sequences of the three viruses were determined, although the viruses could not be isolated in cell culture, and the three novel viruses were assigned the names Tuhoko virus 1, 2 and 3 (127). In addition to these viruses, other rubulaviruses have been

detected in and isolated from bats globally (30, 54), but have not yet been officially classified as part of the genus *Rubulavirus* by the ICTV. Rubulaviruses and rubula-like viruses have the ability to significantly impact animal and human populations when spillover from bats occurs.

1.8 ADENOVIRUSES

Adenoviruses consist of a linear, double-stranded DNA genome between 26 to 45kb in size enclosed within an icosahedral capsid (134). Viruses within the family *Adenoviridae* are classified into five genera; *Aviadenovirus*, *Atadenovirus, Siadenovirus, Ichtadenovirus* and *Mastadenovirus* (88, 135). *Mastadenovirus* comprises mammalian viruses that are usually species specific (135). Although infection is often subclinical, human mastadenoviruses have been associated with conjunctivitis, gastroenteritis and respiratory symptoms including severe pneumonia (136, 137). Canine adenovirus 1 and 2 are also associated with disease, infectious canine hepatitis and infectious tracheobronchitis respectively, in several species and subspecies including dogs, foxes and wolves (138).

Aviadenovirus contains the majority of avian adenoviruses (135), including avian pathogens associated with inclusion body hepatitis (139), gizzard erosion (140) and hepatitis hydropericardium syndrome (141). The genus *Atadenovirus* encompasses bovine, avian and ovine adenoviruses that have genomes with high AT content, along with distinctive genome organisation (142). *Siadenovirus* contains avian adenoviruses and an amphibian adenovirus. These viruses are characterised by a putative sialidase gene and serological distinction from other genera (135, 143). *Ichtadenovirus* currently contains one virus isolated from white sturgeon and is so far the only adenovirus isolated from fish (144).

The potential to use adenoviruses as vectors for gene therapy, cancer treatments and vaccines has been well studied. Although there are promising results for the therapeutic use of adenoviruses as oncolytic viruses, their use as gene therapy vectors has not progressed beyond early clinical trials (145). It has been proposed that mastadenoviruses isolated from other animals may be more efficient vectors for gene therapy due to the absence of pre-existing immunity in humans (146), and that bat adenoviruses may be good candidate vectors (26).

1.8.1 ADENOVIRUS CYCLE OF INFECTION

The adenovirus protein capsid is made up of a hexon protein and includes vertices of a trimeric fibre protein extending from a penton base. The fibre proteins interact with host cells with high affinity, followed by association between the penton base and host cell integrins to trigger endocytosis (134). The virion begins to disassemble upon endocytosis and is released into the cytoplasm before viral DNA and a core viral protein are transported into the nucleus. Transcription occurs from both

strands of DNA. Around 20 early genes and 15 late genes are transcribed into early, intermediate and late transcriptional units, many of which are alternatively spliced into multiple mRNAs (Figure 1.4) (147).

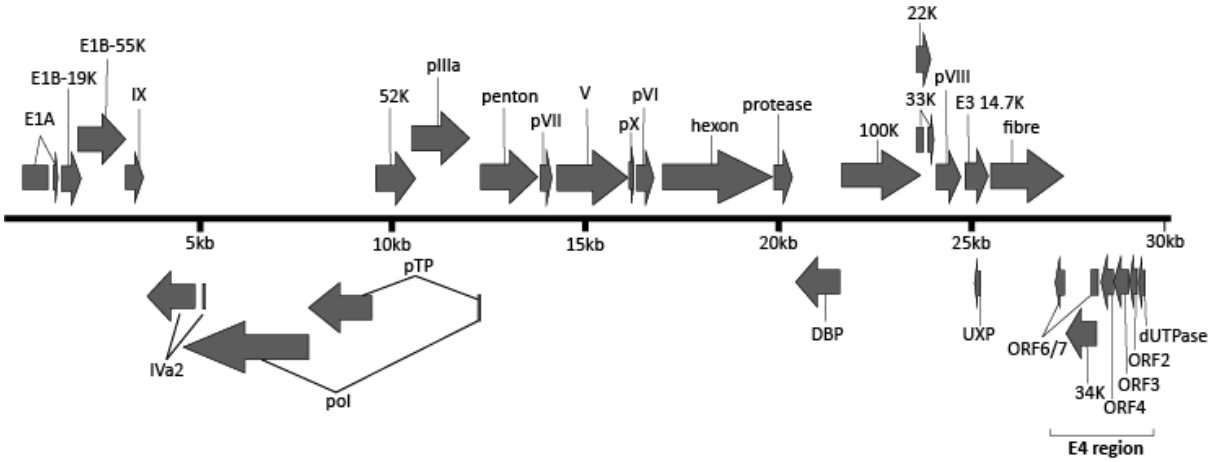

Figure 1.4: Representative genome arrangement of a member of the genus *Mastadenovirus*. Grey arrows represent coding sequences and indicate the direction of transcription. Coding sequences are approximately to scale.

Transcription, translation and virus replication occurs, before viral proteins are imported into the nucleus for virion assembly (134). During this infectious cycle, adenoviruses inhibit cellular transcription, translation and replication. Cells round up, swell and detach from the monolayer, and nuclei enlarge as virions assemble, causing characteristic CPE in cell culture. The virus triggers lysis of the host cell by various mechanisms and progeny virus is released (147).

1.8.2 Adenoviruses in bats

A diverse range of adenoviruses from the genus *Mastadenovirus* have been isolated from bats globally (26, 148, 149). Thus far, these viruses have been classified into seven species, *Bat mastadenovirus A-G* (150). Divergent adenovirus genomes have been sequenced from different bats of the same species living at the same location (26). Although adenoviruses are generally species specific due to virus-host codivergence (135), phylogenetic and structural similarities between some bat adenoviruses and canine adenoviruses imply that cross-species transmission may have occurred from bats to carnivores (151). This is supported by the broader host range and more severe clinical disease exhibited by the canine adenoviruses. Isolation of bat-borne adenoviruses with shorter genomes and low GC content contributes to the hypothesis that these bat viruses may be ancestral

species to other mammalian adenoviruses, and are therefore key to understanding adenovirus evolution (148).

1.9 POLYOMAVIRUSES

The family *Polyomaviridae* is currently divided into four genera*; Alphapolyomavirus, Betapolyomavirus*, *Gammapolyomavirus* and *Deltapolyomavirus* (152). Polyomaviruses are non-enveloped viruses with a circular double-stranded DNA genome approximately 5000 base pairs in length, which wraps around cellular histones (153). The genome encodes an early and late region, as well as a non-coding control region (NCCR, Figure 1.5) (152). The majority of the human population have been infected with a polyomavirus during childhood. These polyomaviruses normally establish an asymptomatic persistent infection, although the virus can reactivate in immunosuppressed individuals. For example, BK virus is thought to persist in the kidney and can reactivate following kidney transplant causing interstitial nephritis and allograft failure (154). Over 80% of adults are seropositive to BK virus (155) and asymptomatic shedding of BK virus in urine occurs in 14-44% of adults, increasing with age (156).

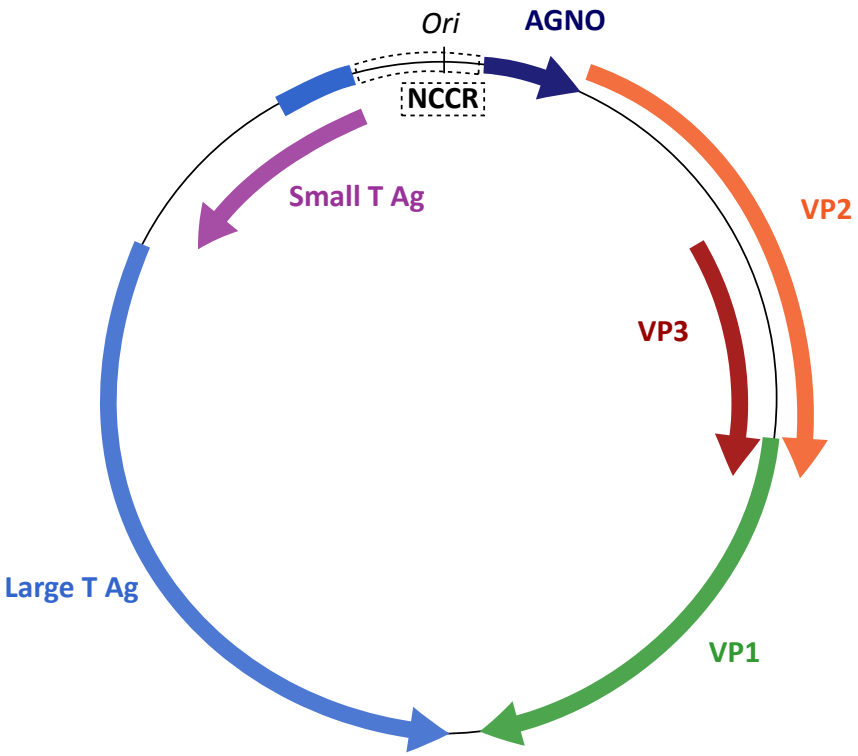

Figure 1.5: Genome arrangement of a polyomavirus. NCCR represents the non-coding control region of the genome. Bidirectional replication occurs from the origin of replication, *Ori.* The early region of the genome encodes the large tumour (T) antigen and the small T antigen. The late region of the genome encodes VP1, VP2, VP3 and sometimes an agnoprotein.

1.9.1 POLYOMAVIRUS CYCLE OF INFECTION

Attachment occurs through the binding of the major capsid protein, VP1, to different gangliosides or sialylated oligosaccharides depending on the species of polyomavirus. Virions are endocytosed, transferred to the endoplasmic reticulum and then to the nucleus. During this trafficking, the capsid disassembles. Once the genome is inside the nucleus, transcription by cellular RNA polymerase II occurs, first transcribing the early region of the genome (153). This transcript is alternatively spliced and translated, resulting in the expression of the large tumour antigen (LTAg) and small tumour antigen (STAg) (152). Bidirectional replication of the viral genome occurs after recruitment of the LTAg to the origin of replication (153). Once the LTAg is expressed at a high enough concentration, it binds to motifs in the control region of the genome, facilitating transcription of the late region by blocking early region transcription. The late region encodes the three proteins that make up the icosahedral capsid; VP1, VP2 and VP3 (153). Alternative splicing and alternate start sites leads to the translation of these capsid proteins (152). Some polyomaviruses also express an agnoprotein. The role of the agnoprotein is not fully understood, but it is proposed to have multiple functions in viral transcription, replication and assembly (157). The capsid proteins are translocated into the nucleus where they assemble into capsomeres. The DNA genome is incorporated to form viral particles (153). The virus is released from the cell by poorly understood mechanisms, although both lytic and non-lytic release have been observed (158, 159).

1.9.2 POLYOMAVIRUSES IN BATS

Bat-borne polyomaviruses have been detected in North America (160), Asia (161), Africa (162, 163) and South America (164) from at least thirteen different bat species (152). The prevalence of these polyomaviruses ranges between 8-30% (161-163), although isolation of these viruses is rare (152). Bat polyomavirus lineages are paraphyletic and these viruses have been phylogenetically classified into the genera *Alphapolyomavirus* and *Betapolyomavirus* (152). The diversity of bat polyomaviruses that group with polyomaviruses from rodents, cows and other mammals indicates that transfer between these hosts is likely to have occurred over evolutionary time. In particular, bat polyomaviruses form monophyletic groups with polyomaviruses from non-human primates (162), although this could be affected by sampling bias (163). It has also been proposed that recombination has occurred to facilitate these changes in host tropism (163).

1.10 RESEARCH OBJECTIVES AND SIGNIFICANCE

The discovery of henipa-like virus RNA in multiple bat species (8, 9, 165) indicates that there are many undiscovered viruses carried by bats globally, some of which are hypothesised to have pathogenic potential in non-pteropid mammals, resulting in significant economic and public health impacts. Australian pteropid bat urine has previously been demonstrated to be a good source of novel viruses (30). The characterisation of two rubulaviruses isolated from Australian pteropid bat urine, TevPV and AlsPV, is described in this thesis. Preliminary analysis of the genomes of these two viruses indicated that further investigation was warranted. Based on the similarity between TevPV and MenPV and the similarity between AlsPV and PIV5, it was hypothesised that these two viruses have the potential to cause disease in non-pteropid mammals.

To investigate these hypotheses, specific research aims were developed:

1) To identify the viral RNA and viruses present in Australian pteropid bat urine, collected from a colony of *P. alecto* and *P. poliocephalus* flying foxes in 2011;
2) To isolate paramyxoviruses from the urine for *in vitro* characterisation, in order to determine their taxonomic classification, their relationship with previously isolated paramyxoviruses and their prevalence in Australian pteropid bats;
3) To investigate the pathogenic potential of these isolated paramyxoviruses by conducting animal infection trials.

The continued emergence of zoonotic viruses, such as the infection of a wildlife biologist with SosPV (133), demonstrates the value of understanding more about viruses before a spillover event occurs. The isolation and characterisation of novel viruses allows for pre-emptive development of diagnostic tools and the establishment of active surveillance programs, resulting in greater preparedness and reduction of the impact of any spillover event that may occur.

Although previous outbreaks and spillover events suggest that there is a risk of novel paramyxoviruses spilling over and causing disease (7, 105, 131, 133), bats host many other viral families (26, 162, 166, 167). The discovery of novel virus sequences, such as adenovirus and polyomavirus sequences, is important for understanding the viral diversity present in bats (168, 169), virus evolution (54, 148), and the global distribution of particular viral families (170). Even in the absence of any pathogenic disease potential, the study of novel viruses can help elucidate pathogenic determinants of related viruses (85), investigate new viral entry mechanisms (106) and be used as sentinels for the surveillance of more pathogenic virus (10), making them an important contribution to the field of emerging zoonotic viruses.

CHAPTER 2: MATERIALS AND METHODS

2.1 BUFFERS, MEDIA AND SOLUTIONS

2.1.1 CELL CULTURE MEDIA

Cells were maintained in Dulbecco's Modified Eagle Medium (DMEM, Gibco) supplemented with 10% foetal bovine serum (FBS, Gibco), 100 U/ml penicillin, 100 µg/ml streptomycin and 0.25 µg/ml amphotericin B (Antibiotic-Antimycotic, Gibco) and 7.5 mM HEPES (Gibco). Cells for growing virus stocks were passaged in this media supplemented with ciprofloxacin (20 µg/ml). All cells were maintained at 37°C with 5% CO_2.

2.1.2 PAKI CELL MEDIA

The primary bat kidney cells used for this study were previously generated from *Pteropus alecto* as described in (171). PaKi cells were maintained in Ham's Nutrient Mixture F12 (Sigma-Aldrich) supplemented with 10% foetal bovine serum (FBS, Gibco), 100 U/ml penicillin, 100 µg/ml streptomycin and 0.25 µg/ml amphotericin B (Antibiotic-Antimycotic, Gibco).

2.1.3 VIRUS ISOLATION MEDIA

Virus isolations were conducted in Ham's F12 Nutrient Mixture (Gibco), supplemented as described in section 2.1.2 except for the Antibiotic-Antimycotic that was added at a final concentration of 200 U/ml penicillin, 200 µg/ml streptomycin and 0.5 µg/ml amphotericin B.

2.1.4 PHOSPHATE BUFFERED SALINE (PBS)

Deionised water containing 0.02% (w/v) KCl, 0.8% (w/v) NaCl, 0.02% (w/v) KH_2PO_4, 0.115% (w/v) Na_2HPO_4, pH 7.4, made using 10 phosphate buffered saline tablets (Dulbecco A solution, Oxoid) per litre of deionised water.

2.1.5 PBS-T

PBS with 0.05% w/v Tween 20 (VWR International).

2.1.6 TAE BUFFER

40x solution (Promega) containing 1.6M Tris-acetate and 40mM EDTA diluted to 1x solution in deionised H_2O.

2.1.7 LURIA BERTONI (LB) BROTH

Deionised water with 5 g/L NaCl (Merck), 5 g/L yeast extract (BD Bacto) and 10 g/L tryptone (MP Biomedical).

2.1.8 Luria Bertoni (LB) agar

Deionised water supplemented as above for LB broth, with the addition of 15 g/L agar (BD Bacto).

2.1.9 LB agar plates

LB agar was heated until melted, then allowed to cool slightly before the addition of 100 µg/ml ampicillin (Gold Biotechnology). LB agar-ampicillin solution was poured into petri dishes and allowed to set in a BSCII.

2.1.10 Virus transport media

Sterile PBS with 1% bovine serum albumin (BSA), 200 U/ml penicillin, 200 µg/ml streptomycin and 0.5 µg/ml amphotericin B (Antibiotic-Antimycotic, Gibco).

2.1.11 Nasal wash and urine collection media

10% BSA with 200 U/ml penicillin, 200 µg/ml streptomycin and 0.5 µg/ml amphotericin B (Antibiotic-Antimycotic, Gibco).

2.2 PRIMERS

Table 2.1: List of primers used throughout this thesis. Sequence encoding a FLAG protein tag is underlined. Restriction enzyme sites are in bold. Letters used are standard International Union of Pure and Applied Chemistry (IUPAC) notation, plus 'I' representing inosine. T_a represents the annealing temperature.

#	Name	Primer sequence 5'-3'	T_a (°C)	Reference	Use
1	PAR-F1	GAAGGITATTGTCAIAARNTNTGGAC	~54.9	(172)	Identifying members of the family *Paramyxoviridae* F1 is external to F2, reverse primer contains M13R sequence
	PAR-F2	GTTGCTTCAATGGTTCARGGNGAYAA	~58.6	(172)	
	PAR-R	CAGGAAACAGCTATGACGCTGAAGTTACIGGITCICCDATRTTNC	~67.9	(172)	
2	RES-MOR-HEN-F1	TCITTCTTTAGAACITTYGGNCAYCC	~59.6	(172)	Identifying members of the genera *Respirovirus, Morbillivirus* and *Henipavirus* F1 is external to F2, reverse primer contains M13R sequence
	RES-MOR-HEN-F2	GCCATATTTTGTGGAATAATHATHAAYGG	~53.3	(172)	
	RES-MOR-HEN-R	CAGGAAACAGCTATGACCTCATTTTGTAIGTCATYTTNGCRAA	~63.7	(172)	
3	AdV-F	TGTTTATGAYATHTGTGGMATGTATGC	~53.4	I. Smith (unpublished, CSIRO)	Identifying members of the family *Adenoviridae* (Reverse contains M13R sequence)
	AdV-R	CAGGAAACAGCTATGACAAKGTTTGRTTTTTDTYYTTRTCTGC	~62.7	I Smith (unpublished, CSIRO)	
4	Herpes-DFA	GAYTTYGCNAGYYTITAYCC	~53.2	(173)	Identifying members of the family *Herpesviridae*
	Herpes-ILK	TCCTGGACAAGCAGCARIYSGCIMTIAA	~67.6	(173)	
	Herpes-TGV	TGTAACTCGGTGTAYGGITTYACIGGIGT	~65.3	(173)	
	Herpes-KG1	GTCTTGCTCACCAGITCIACICCYTT	~64.8	(173)	
	Herpes-IYG	CACAGAGTCCGTRTCICCRTAIAT	~59.7	(173)	

5	Orthoreo1 607F	CARMGNCGNSCHMGHTCHAT HATGCC	~63.2	(174)	Identifying members of the genus *Orthoreovirus*
	Orthoreo2 608R	TAVAYRAAVGWCCASMHNGG RTAYTG	~57.6	(174)	
	Orthoreo2 090F	GGBTCMACNGCYACYTCBACY GAGCA	~65.6	(174)	
	Orthoreo2 334R	CDATGTCRTAHWYCCANCCRA A	~54.1	(174)	
6	Coronavir us-F	ACWCARHTVAAYYTNAARTAY GC	~51.4	(175)	Identifying members of the family *Coronaviridae*
	Coronavir us-R	TCRCAYTTDGGRTARTCCCA	~54.2	(175)	
7	pcDNA3-F	CTAACTAGAGAACCCACTGC	52.1	This study	Sequencing and colony screens of pcDNA3.1(+) constructs
	pcDNA3-R	TAGAAGGCACAGTCGAGG	53.6	This study	
8	M13F	GTAAAACGACGGCCAG	50.7	(176)	Sequencing of paramyxovirus, henipavirus and adenovirus PCR products and pGEM-T Easy constructs, colony screens of pGEM-T Easy constructs
	M13R	CAGGAAACAGCTATGAC	47	(176)	
9	PyV-F1	CCTTACAGCTATACAAACGAG GT	54.2	This study	Sequencing of the bat polyomavirus genome
	PyV-R1	GCTACAGCAGCACTTAGTACT	54.2	This study	
10	PyV-F2	GTGCACTCAGCTATGCTAAG	53.3	This study	
	PyV-R2	CACACAATCCGGGCATG	54.2	This study	
11	PyV-F3	CAGTAAGTATGCAAGCAAGCA G	54.2	This study	
	PyV-R3	ATGTCTGGGGTCATTGCTTC	55.1	This study	
12	PyV-F4	GCTTATGAAATTGAGATCTCAT AGCAT	53.5	This study	
	PyV-R4	GCAGTACTCCCAGACAACTTG	55.5	This study	
13	PyV-246F	ATCTGATCAGCTACCATCTGG	53.7	This study	

	PyV-1110R	CTCCCAACAGCTCTAAAGAGAT	54	This study	
14	PyV-1660F	GAGGCCTTCCTTAACCCT	53.9	This study	
	PyV-2172R	TCTCAATTGGGTATGCATCATCC	55	This study	
15	PyV-2735F	GGATGAACCTTCTTGTGACAG	53.3	This study	
	PyV-3208R	GTTAAGGGTCAGCAAACAGAG	53.6	This study	
16	PyV-3722F	GCATTTAGTACAATACTCTGTTTCCTC	53.8	This study	
	PyV-33R	CCGAGGCAGATAACCTGTA	53.6	This study	
17	AlsPVMF-F	AGGTATCGAGCAAACATAAGAG	52.1	This study	Confirming regions of high variability in the AlsPV genome
	AlsPVMF-R	CTGTCGTACATTGGTAGGAATAAC	53.1	This study	
18	AlsPVFF-F	CTCCCAATCGACCCTCTAGATATAT	54.9	This study	
	AlsPVFF-R	CCGAGACGGTTCTTTCAATACTAG	54.9	This study	
19	AL30-M-F	CTCAGATGGGATTTCATCGTC	53	This study	Determining gaps in AL30 whole genome sequence
	AL30-F-R	CTAAGCATGATGAGAGATTGCC	53.4	This study	
20	AL30-G-F	GATAACTCAGCAGGTATTGAAGG	53.1	This study	
	AL30-L-R	ATGGGATATCTCAGCATACTCT	52.5	This study	
21	AL30-383R1	CAATAATGGTGACACTGATGTC	50.5	This study	Used in attempts to sequence AL30 genome termini
	AL30-279R2	ATGCTTTCAGATGCAATCTG	51.1	This study	
	AL30-6424F1	CCTTATCCTGTGCTAGAGG	51.5	This study	
	AL30-6514F2	GCAAGATCCTTAGAATTCATCAG	51.4	This study	
	AL30-6582F3	CAGTCACTTTAAAAGAACTGCT	51.1	This study	

	AL30-La-R	GAAADATCTCGTTATTAAGTTTTTCTTAATA	~50.3	This study	
	AL30-Lb-R	GAAATCTTGATCTTAAGTTTTTATTAATAG	48.5	This study	
	AL30-Lc-R	GCATAACTTGGATTTGGTTCTGG	54.4	This study	
22	TevPV5'F1	GATTTCGACATCTTTGGCGAC	54.3	This study	Nested primers for sequencing across ligated TevPV genome ends F2 is external to F1
	TevPV5'F2	GACCTCTTCACTCACCATCTC	54.5	This study	
	TevPV3'R	GAAGACATCCTTGCACAGTGAG	55.7	This study	
23	AlsPV5’F1	GATGGCGAGGAGTTGTAATCAG	55.4	This study	Nested primers for sequencing across ligated AlsPV genome ends F2 is external to F1
	AlsPV5’F2	GACTGCAACATTGAACTAACTAGAC	53.8	This study	
	AlsPV3’R	CTCTGATGACAGGTTTTAGTGTG	53.3	This study	
24	DT88	Phosphate - GAAGAGAAGGTGGAAATGGCGTTTTGG - Phosphate	60.2	(177)	Adapter to ligate to the 5’ genome ends of AlsPV and TevPV
25	DT89	CCAAAACGCCATTTCCACCTTCTCTTC	60.2	(177)	Adapter specific primer to sequence the 5’ genome ends of AlsPV and TevPV
26	AlsPV-RACE 14911F	GGATCTGGAATTTGGAATCTTC	51.4	This study	Sequencing the 5’ genome end of AlsPV
	AlsPV-RACE 14993F	CTAGTCTCCTTACTAACAGCTG	51.8	This study	
	AlsPV-RACE-15049F	CTGTATTGGTCTAGTTAGTTCAATG	51.3	This study	
27	TevPV-RACE 15104F	GATTTGACTGTGAGAAATTGGC	52.4	This study	Sequencing the 5’ genome end of TevPV
	TevPV-RACE 15192F	GATCTGTTATCCCTTGGGATG	52.6	This study	

	TevPV-RACE 15296F	CTCATTGTACAATTGGACCG	51.2	This study	
28	TevPV-edit-F	CGTCGGCAGCGTCAGATGTGTATAAGAGACAGGCCGCCTCAAGATAATGCCCAGAACC	71.8	This study, adaptor sequences from Illumina	Determine the prevalence of RNA editing during TevPV infection
	TevPV-edit-R	GTCTCGTGGGCTCGGAGATGTGTATAAGAGACAGCAC AGA GAG CAG ACA TCT GGG CAG	71	This study, adaptor sequences from Illumina	
29	AlsPV-edit-F	TCGTCGGCAGCGTCAGATGTGTATAAGAGACAGCCCAACCCTCTACTTGGCTTGGATTC	71.1	This study, adaptor sequences from Illumina	Determine the prevalence of RNA editing during AlsPV infection
	AlsPV-edit-R	GTCTCGTGGGCTCGGAGATGTGTATAAGAGACAGGCCGGGTATCCATCCCTCTCACTG	71.4	This study, adaptor sequences from Illumina	
30	AlsPV N-287F	AATCCCGAGCTACGTTCAAAACT	56.7	This study	Detecting AlsPV by qRT-PCT
	AlsPV N-360R	TGGGAGTCACGAGCTCCATT	58.4	This study	
	AlsPV N-311-FAM probe	FAM - CTGCTATTTTGCCTACGCATTGTGCTGA -TAMRA	61.3	This study	
31	TevPV N F	ACCTGCTAACTACCCGCTGT	58.4	G.A. Marsh (unpublished, CSIRO)	Detecting TevPV by qRT-PCR
	TevPV N R	TCGGTTTGCTGTCTCAACTC	55.1	G.A. Marsh (unpublished, CSIRO)	
	TevPV N probe	FAM - TCCTGAACGCTTCCGATACCCA -TAMRA	60.1	G.A. Marsh (unpublished, CSIRO)	
32	18S F	GGCCCTGTAATTGGAATGAGTCCA	59	This study	Detecting 18S by qRT-PCR
	18S R	GCTGGAATTACCGCGGCT	61.1	(178)	Generating controls

	18S probe	VIC - TGCTGGCACCAGACTTGCCCTC - TAMRA	64.3	(179)	for qRT-PCR
33	AlsPV-N-F	CC**GGATCC**ATGGACTACAAAG ACGATGACGACAAGTCCTCCG TACTCAAAG	68.5	This study	Generating control plasmids for AlsPV standard curve assay (*Bam*HI and *Xho*I digestion sites, nucleotide sequence encoding a FLAG tag in forward primer)
	AlsPV-N-R	TGCAT**CTCGAG**TTAGATGTCAA GATCACCGAGAGCAGCGTT C	67.2	This study	
34	TevPV-N-F	CC**GAATTC**ATGTCTTCCGTGTT CAG	58	This study	Generating control plasmids for TevPV standard curve assay (*Eco*RI and *Xho*I digestion sites)
	TevPV-N-R	TGCAT**CTCGAG**CTACATGTCTA GATCCAAGTAGCTCGAG	60.7	This study	

2.3 CELL CULTURE

2.3.1 PRIMARY CELLS AND CELL LINES

African Green Monkey kidney (Vero) cells (ATCC), primary *Pteropus alecto* kidney (PaKi) cells (171), Madin-Darby Canine Kidney (MDCK) cells (CSL Ltd), Madin-Darby Bovine Kidney (MDBK) cells (ATCC), porcine kidney (PK15a) cells (National Animal Disease Centre, Iowa, USA), and human cervical (HeLa) cells (ATCC) were used throughout this thesis.

2.3.2 PASSAGING CELLS

Cells were passaged when the monolayer was approximately 80% confluent. Cell culture medium was discarded and cells were washed twice with sterile PBS. The monolayer was then covered with trypsin-EDTA (0.25%, Gibco) and incubated at 37°C until the monolayer detached from the cell culture flask. Cells were resuspended in cell culture medium and diluted into a new cell culture flask.

When an accurate count of cells was required, 75 µl of resuspended cells were loaded onto a Type S cassette of a MOXI Z Mini Automated Cell Counter (Orflo) to calculate the number of cells per ml in suspension. The suspension was then diluted as required.

2.4 VIRUSES

2.4.1 *IN SILICO* ANALYSIS

Virus sequences used in phylogenetic analysis were Teviot virus (TevPV, Alstonville isolate, MH708896; Cedar Grove isolate, KP271124; Geelong isolate, KP271123), Alston virus (AlsPV, MH972568), Tioman virus (TioPV, NC_004074.1), Menangle virus (MenPV, NC_007620.1), parainfluenza virus 5 (PIV5, NC_006430.1), human parainfluenza virus 2 (hPIV2, NC_003443.1), Achimota virus 1 (AchPV1, NC_025403), Achimota virus 2 (AchPV2, NC_025404), Beilong virus (BeiV, NC_007803), Cedar virus (CedPV, NC_025351), Hendra virus (HeV, NC_001906), human parainfluenza virus 4 (hPIV4, NC_021928), human parainfluenza virus 3 (hPIV3, NC_001796), bat mumps virus (MuV-Bat, HQ660095), J virus (JV, NC_007454), Mapuera virus (MapV, NC_009489), measles virus (MeV, NC_001498), mumps virus (MuV, NC_002200), simian virus 41 (SV41, NC_006428), porcine rubulavirus (PorV, NC_009640), Tuhoko virus 1 (ThkPV1, NC_025410), Tuhoko virus 2 (ThkPV2, NC_025348), Tuhoko virus 3 (ThkPV3, NC_025350), Newcastle disease virus (NDV, NC_002617), Nipah virus (NiV, NC_002728), Sendai virus (SeV, NC_001552), Sosuga virus (SosPV, NC_025343), Atlantic salmon paramyxovirus (AsaPV, EF646380), fer-de-lance virus (FDLV, NC_005084), canine distemper virus (CDV, NC_001921), Mojiang virus (MojPV, NC_025352), Kumasi virus (HQ660129.1) and avian paramyxovirus 6 (APMV-6, NC_003043).

2.4.2 Parainfluenza virus 5 sequences

PIV5 strains used in the phylogenetic analysis of AlsPV include 1168 (KC237064), ZJQ-221 (KX100034), SER (JQ743328), BC14 (KM067467), CC-14 (KP893891), W3A (JQ743318), KNU-11 (KC852177), AGS (KX060176), CPI- (JQ743320), CPI+ (JQ743321), 78524 (JQ743319), H221 (JQ743323), 08-1990 (KC237063), D277 (KC237065), DEN (JQ743322), LN (JQ743324), RQ (JQ743327), MEL (JQ743325) and MIL (JQ743326).

2.4.3 Viruses for *in vitro* characterisation

Australian Animal Health Laboratory (AAHL) stocks of TioPV, MenPV, PorV, MapV and HeV were utilised for tissue culture infections to compare to TevPV and AlsPV. PIV5, 21005-2WR (Tissue Culture Adapted), NR-42515 and hPIV2, Greer, NR-3229 were obtained through BEI Resources, NIAID, NIH.

2.4.4 Preparation of virus stocks

TevPV and AlsPV were both initially isolated using PaKi cells. Three rounds of limiting dilutions in Vero cells were conducted to purify the viruses. Virus was transferred to T150 flasks of Vero cell monolayers (75% confluency) to grow virus stocks. Stock virus had been passaged a total of 6 times, including limiting dilution passages, upon storage at -80°C.

2.5 VIRUS ISOLATION

2.5.1 Urine collection

Pooled urine was collected from plastic drop sheets situated under bat colonies in Lumley Park, Alstonville on 12th July 2011 and 3rd August 2011 as previously described (30). Only samples that were negative for Hendra virus by reverse transcription PCR were included in this study to avoid having to isolate mixed viral species from the one urine sample.

2.5.2 Isolation

Urine samples were rapidly thawed then centrifuged at maximum speed (18000 g) for 2 min. Urine was diluted 1:10 in virus isolation media and centrifuged again for 5 min at 4500 rpm to clarify. Media in T75 flasks of PaKi or Vero cell monolayers (75% confluency) was replaced with 2.5 ml of inoculum. Cells were incubated for 45 min at 37°C, topped up to 15 ml with virus isolation media and incubated for at least 7 days while monitoring daily for cytopathic effect (CPE). Volumes of 0.5-1 ml of supernatant were passed onto fresh PaKi or Vero cell monolayers weekly for another two weeks. Flasks were continually monitored for signs of CPE. Aliquots of supernatant were collected weekly for three weeks and stored at -80°C.

2.5.3 OTHER ISOLATION METHODS

Other methods were trialled when viral sequences were detected intermittently in the supernatant or when multiple viruses were present. These methods were selected to account for the unknown virus potentially requiring an external protease to complete the replicative cycle, replicating more efficiently in different pteropid tissues, or only being present at low titres.

- PCR positive supernatant or urine were inoculated onto Vero cell monolayers and incubated in DMEM supplemented with HEPES, Antibiotic-Antimycotic and 2 µg/ml TPCK-trypsin (Sigma-Aldrich). Cells were monitored for cytopathic effect, aliquots of supernatant were harvested for analysis by PCR and supernatant was passaged weekly onto fresh Vero cells in the presence of TPCK-trypsin.
- PCR positive supernatant was inoculated onto a mixed culture of PaKi and Vero cells.
- PCR positive supernatant was inoculated onto confluent *Pteropus alecto* fibroblast cells (171).
- The allantoic cavity of embryonated chicken eggs was inoculated with 100 µl PCR positive supernatant using a 22-gauge needle through a hole in the eggshell made with an egg hole punch. Eggs were sealed, incubated for one week at 37°C and monitored for signs of CPE. Allantoic fluid was harvested after one week. RNA was extracted from allantoic fluid and assessed by PCR for evidence of viral growth.
- Supernatant of infected cells was concentrated by ultracentrifugation over a 20% sucrose cushion at 35000 rpm for 2 h at 4°C. Virus pellet was then resuspended in PaKi cell culture media (Section 2.1.2), added to confluent PaKi cells and monitored for CPE.

2.6 RNA EXTRACTION

Viral nucleic acid was extracted using the QIAamp Viral RNA extraction kit (Qiagen) as per manufacturer's instructions.

Urine samples and samples collected during animal infection studies were extracted by the MagMAX-96 Viral RNA Isolation Kit (Applied Biosystems) according to the manufacturer's instructions because it allowed a higher throughput due to the use of a Kingfisher Flex purification system (Thermofisher Scientific).

Samples for sequencing were extracted using Direct-zol RNA Miniprep kit (Zymo Research) after resuspension in 350 µl of Trizol.

2.7 PCR

PCR reactions were cycled in either a Veriti Thermal Cycler (Applied Biosystems) or a SimpliAmp Thermal Cycler (Applied Biosystems). Amplified PCR products were assessed by agarose gel electrophoresis.

2.7.1 *Paramyxoviridae*-specific and *Respirovirus-Morbillivirus-Henipavirus*-specific PCR

Paramyxoviruses were detected using hemi-nested PCRs with primer sets 1 or 2 (Table 2.1, *Paramyxoviridae*-specific or *Respirovirus-Morbillivirus-Henipavirus*-specific respectively), adapted from (172). Reactions were set up using the Superscript III One-Step RT-PCR System (Invitrogen). A volume of 2 µl extracted RNA was combined with 12.5 µl of 2x reaction mix, 2.5 µl each of 10 µM forward and reverse primers to a final primer concentration of 1 µM, 0.4 uM additional $MgSO_4$ to a final concentration of 2 mM, 2 µl Superscript III/Platinum Taq mix, and H_2O to a final volume of 25 µl. Reactions were run under the following conditions: 1 cycle of 60°C for 1 min, 1 cycle of 48°C for 30 min, 1 cycle of 94°C for 2 min, 40 cycles of 94°C for 15 s, 49°C for 30 s and 68°C for 1 min, and 1 cycle of 68°C for 5 min.

First round PCR product was then amplified with the Expand High Fidelity PCR System (Roche). One µl of template was combined with 2.5 µl Expand High Fidelity buffer without Mg, 2 mM $MgCl_2$, 0.5 µl of 10 mM dNTP, 2.5 µl each of 10 µM forward and reverse primers to a final primer concentration of 1 µM, 0.5 µl (1.75 U) Expand High Fidelity Taq polymerase and H_2O to a final volume of 25 µl. Reactions were run under the following conditions: 1 cycle of 94°C for 2 min, 40 cycles of 94°C for 15 s, 49°C for 30 s and 72°C for 1 min, and 1 cycle of 72°C for 5 min. Positive samples were sequenced by Sanger sequencing then identified using the Basic Local Alignment Search Tool (BLAST, NCBI).

2.7.2 Bat adenovirus-specific PCR

Bat adenoviruses were detected using the Expand High Fidelity PCR System (Roche) with primer set 3 (Table 2.1). A volume of 2 µl of extracted nucleic acid was combined with 2.5 µl Expand High Fidelity Buffer with $MgCl_2$, 2.5 µl each of 10 µM forward and reverse primers to a final primer concentration of 1 µM, 0.5 µl of 10 mM dNTPs, 0.5 µl (1.75 U) Expand High Fidelity Taq polymerase and H_2O to a final volume of 25 µl. The PCR was conducted under the following conditions: 1 cycle of 94°C for 2 min, forty cycles of 94°C for 30 s, 50°C for 1 min and 68°C for 30 s, and 1 cycle of 68°C for 7 min. Positive samples were sequenced by Sanger sequencing then identified using BLAST.

2.7.3 OTHER VIRAL FAMILY OR GENUS SPECIFIC PCRS

Unknown samples exhibiting CPE were screened for the presence of coronaviruses, orthoreoviruses and herpesviruses.

2.7.3.1 HERPESVIRIDAE-SPECIFIC PCR

Samples were screened for the presence of herpesviruses using primer set 4 (Table 2.1) and a protocol adapted from previously described methods (173). Reactions were set up using the Expand High Fidelity PCR System. Two µl of extracted DNA were combined with 2.5 µl Expand High Fidelity buffer without Mg, 2 mM $MgCl_2$, 0.5 µl of 10 mM dNTP, 2.5 µl each of 10 µM DFA primer, ILK primer and KG1 primer to a final primer concentration of 1 µM, 0.5 µl (1.75 U) Expand High Fidelity Taq polymerase and H_2O to a final volume of 25 µl. Reactions were run under the following conditions: 1 cycle of 94°C for 2 min, 40 cycles of 94°C for 15 s, 49°C for 30 s and 72°C for 1 min, and 1 cycle of 72°C for 5 min.

First round PCR product was then amplified using the same protocol, except with the primers TGV and IYG.

2.7.3.2 ORTHOREOVIRUS-SPECIFIC PCR

Samples were screened for the presence of orthoreoviruses using primer set 5 (Table 2.1) and a protocol adapted from previously described methods (174). Reactions were set up using the Superscript III One-Step RT-PCR System (Invitrogen). A volume of 2 µl extracted RNA was denatured for 5 min at 95°C, quenched on ice and then combined with 12.5 µl of 2x reaction mix, 1.5 µl each of 10 µM forward and reverse primers to a final primer concentration of 0.6 µM, 1 µl Superscript III/Platinum Taq mix, and H_2O to a final volume of 25 µl. Reactions were run under the following conditions: 1 cycle of 50°C for 30 min, 1 cycle of 94°C for 2 min, 40 cycles of 94°C for 1 min, 47°C for 1 min and 68°C for 1 min, and 1 cycle of 68°C for 5 min.

First round PCR product was then amplified using GoTaq Hot Start Green Master Mix (Promega). Two µl of template were combined with 12.5 µl 2x master mix, 2.5 µl each of 10 µM forward and reverse primers to a final primer concentration of 1 µM, and H_2O to a final volume of 25 µl. Reactions were run under the following conditions: 1 cycle of 94°C for 3 min, 40 cycles of 94°C for 20 s, 46°C for 30 s and 72°C for 30 s, and 1 cycle of 72°C for 10 min.

2.7.3.3 CORONAVIRIDAE-SPECIFIC PCR

Samples were screened for the presence of coronaviruses using primer set 6 (Table 2.1) and a protocol adapted from previously described methods (175). Reactions were set up using the Superscript III One-Step RT-PCR System (Invitrogen). A volume of 2 µl extracted RNA was combined

with 12.5 µl of 2x reaction mix, 1 µl each of 10 µM forward and reverse primers to a final primer concentration of 0.4 µM, 1 µl of 10mM dNTP mix, 1 µl Superscript III/Platinum Taq mix, and H_2O to a final volume of 25 µl. Reactions were run under the following conditions: 1 cycle of 50°C for 30 min, 1 cycle of 95°C for 2 min, 40 cycles of 95°C for 15 s, 48°C for 30 s and 68°C for 1 min, and 1 cycle of 68°C for 5 min.

2.7.4 Colony screen

To screen for positive transformed colonies, individual colonies were mixed with 4 µl H_2O, 5 µl of 2x GoTaq Mastermix, and 2.5 µl each of 10 µM forward and reverse primers (primer pair 7 or 8, Table 2.1) to a final primer concentration of 0.5 µM. Reactions were cycled under the following conditions: 1 cycle of 95°C for 2 min, 25 cycles of 94°C for 30 s, 45°C for 30 s and 72°C for 1 min, and 1 cycle of 72°C for 5 min.

Cultures for minipreps of the colonies were set up simultaneously.

2.7.5 Polyomavirus-specific PCR

The polyomavirus was initially identified using the *Paramyxoviridae*-specific PCR as described above. Sequencing of the virus was done by inverse PCR then primer walking along the ~5 kb genome. PCR amplification was conducted using the Platinum Taq DNA Polymerase High Fidelity Kit. Extracted nucleic acid was combined with 2.5 µl 10x High Fidelity PCR Buffer, 1 µl of 50 mM $MgSO_4$, 0.5 µl 10 mM dNTP mix, 1 µl each of 10 µM forward and reverse primers to a final primer concentration of 0.4 µM, 0.1 µl (0.5 U) Platinum Taq DNA Polymerase High Fidelity and H_2O to 25 µl. Reactions were run under the following conditions: 1 cycle of 94°C for 30 s, 30 cycles of 94°C for 15 s, 50°C for 30 s and 68°C for 1 min/kb, and 1 cycle of 68°C for 5 min. Primer pairs 9-16 (Table 2.1) were used.

2.8 GEL ELECTROPHORESIS

1% agarose gels were prepared using Analytical Grade Agarose (Promega) in TAE buffer (Promega) and SYBR Safe DNA Gel Stain (Invitrogen) diluted 1:20000.

PCR products were electrophoresed at 100V for 1 h through a 1% agarose gel in TAE Buffer for visualisation of separated products on a Safe Imager Transilluminator (Invitrogen). Samples were mixed with 6x Gel Loading Buffer (0.25% bromophenol blue, 0.25% xylene cyanol FF, 30% glycerol in H_2O) or 6x Loading Buffer (NEB) and loaded alongside a 1 kb Plus DNA Ladder (Invitrogen). Gels were imaged using a GelDoc-It Imaging System (UVP) and analysed using VisionWorks LS Software (UVP).

2.9 PURIFICATION OF DNA FROM AGAROSE GELS

Amplified PCR products were excised from the agarose gel and extracted from the gel matrix using a Wizard SV Gel and PCR Clean-Up System (Promega) according to manufacturer's instructions.

2.10 RESTRICTION ENDONUCLEASE DIGESTION

Digestion with restriction enzymes was required before ligating gel purified templates into pcDNA3.1(+) or pCAGGS vectors. One hundred ng DNA was combined with 10 U of one or two restriction enzymes, 2.5 µl of the preferred buffer for those enzymes, and H_2O to 25 µl. Reactions were incubated at 37°C for approximately 2 h. Digested products were isolated by gel electrophoresis.

2.11 LIGATION

DNA fragments were ligated into vectors for subsequent transformation into electrocompetent *E. coli*. For ligation into pGEM-T Easy vectors, gel extracted PCR products could be used as template. For all other vectors, both the vector and insert were first digested with the relevant restriction endonucleases. Vector and insert were combined at a 1:3 ratio with 1 µl 10x T4 DNA Ligase Buffer (Promega), 1 µl T4 DNA Ligase (Promega) and H_2O to 10 µl and incubated at room temperature for 3 h. If the 2x Rapid Ligation Buffer (Promega) was used, samples were only incubated at room temperature for 15 min. If this method was unsuccessful, reactions were incubated overnight at 16°C.

2.12 TRANSFORMATION

Fifty µl of electrocompetent Top10f *E. coli* (Invitrogen) were thawed on ice and combined with 2 µl of ligated plasmid. The *E. coli* mix was transferred into a 1 mm electroporation cuvette (Sigma-Aldrich) and electroporated using a Gene Pulser electroporator (Bio-Rad) with the following conditions: 1.8 kV, 200 Ω, 25 µF and a time constant of approximately 4 ms. Cells were immediately resuspended in 500 µl of LB broth and shaken at 200 rpm for 1 h at 37°C. Fifty µl of cell suspension were plated onto LB agar plates with 100 µg ampicillin per ml LB agar. Plates were incubated overnight at 37°C.

2.13 MINIPREP

Colonies of transformed bacteria were inoculated into 3 ml LB broth with 300 µg ampicillin and cultured overnight at 37°C while shaking at 200 rpm. Plasmids were isolated from bacterial cultures using a PureYield Plasmid Miniprep System (Promega).

2.14 DNA CONCENTRATION

The DNA concentrations of gel extracted products or plasmids were determined using a Nanodrop Spectrophotometer (Thermo Fisher Scientific).

2.15 SEQUENCING

2.15.1 SANGER SEQUENCING

One hundred ng DNA (PCR products) or 500 ng DNA (plasmids) were combined with 1.6 µM primer, 3.5 µl 5x Big Dye Terminator (BDT) reaction buffer and 1 µl of BDT3.1 Ready Reaction Premix (Applied Biosystems). Product was reacted before sequencing by running under the following conditions: 1 cycle of 96°C for 1 min and 25 cycles of 96°C for 10 s, 50°C for 5 s and 60°C for 4 min. Sanger sequencing was conducted at the AAHL Sequencing Facility (Geelong, Australia) using a 3500xl Genetic Analyser (Thermofisher).

2.15.2 PREPARATION OF VIRUSES FOR WHOLE GENOME SEQUENCING

In preparation for whole genome sequencing, TevPV and AlsPV virus stocks were concentrated by centrifugation over sucrose cushion before RNA extraction. A Vero or Paki cell monolayer was infected with AlsPV or TevPV, respectively, and incubated at 37°C for 5 days in a T75 tissue culture flask. Supernatant was clarified by centrifuging at 4000 rpm for 10 min using a Heraeus Multifuge X3R centrifuge (Thermo Scientific). Clarified supernatant was ultracentrifuged over a 20% sucrose cushion at 35000 rpm for 2 h at 4°C. Centrifugation was conducted in 13.2 mL Ultra-Clear centrifuge tubes (Beckman-Coulter) inserted into an SW41 Ti swinging bucket rotor and run on an L-80 XP Ultracentrifuge (Beckman Coulter). After centrifugation, liquid was removed and the pellet was resuspended in 350 µl Trizol for RNA extraction using the Direct-zol Miniprep kit (Zymo Research) with an in column DNase I digestion according to the manufacturer's instructions. This was followed by processing with an RNA Clean and Concentrator kit (Zymo).

2.15.3 WHOLE GENOME SEQUENCING OF TEVPV

Isothermal amplification was conducted using the REPLI-g WTA Single Cell kit (Qiagen) and purified using the Genomic DNA and Concentrator 10 kit (Zymo). Five hundred ng DNA was fragmented for 30 min using DS DNA Fragmentase (NEB) without the addition of magnesium, followed by reaction clean-up with a Minelute kit (Qiagen). Verification of DNA fragmentation was determined by running 4 ng DNA on a 2100 Bioanalyzer (Agilent) with a High Sensitivity (HS) DNA chip. Dual-index libraries were prepared using an Accel-NGS 2S DNA Library Kit for Illumina Platforms (Swift Biosciences). Clean-up and double-sided size selection of the PCR amplified libraries with SPRIselect beads (Beckman Coulter) resulted in a library with an average size of 367 bp (size range 200-550 bp) as

determined using the 2100 Bioanalyzer HS DNA chip. Denatured libraries, diluted to a final concentration 10 pM and spiked with 1% PhiX control library, were sequenced on the 300 cycle MiSeq Reagent kit v2 (Illumina) generating 150 bp paired-end reads. RNA or DNA samples and Illumina library concentrations were accurately determined with the Qubit RNA or DNA High sensitivity assays (Thermofisher Scientific) respectively. The Generate FASTQ and Illumina adapter trimming workflows were selected for the run using the MiSeq reporter software.

Illumina FASTQ paired-end reads were imported into CLC Genomics Workbench v 8.5.1 using default Illumina import parameters, then trimmed for size, quality and ambiguous bases using default parameters except for the following: Quality Limit = 0.01, Ambiguous limit = 2 and Minimum number of nucleotides in reads = 30. Trimmed reads were mapped to the Cedar Grove isolate of TevPV (KP271124) using CLC Genomics Workbench Map Reads to Reference tool and confirmed by *de novo* assembly. Genome ends were confirmed as described below (section 2.15.6).

2.15.4 Whole genome sequencing of AlsPV

Whole genome sequencing of AlsPV was executed as above (section 2.15.3), except fragmentation and dual-index library preparation were conducted with 1 ng DNA using Nextera XT DNA Library Preparation kit (Illumina). Library size distribution was determined by loading 3 ng of sample on a 2100 Bioanalyzer using a HS DNA chip.

As the genome of AlsPV was too divergent to assemble by mapping to a PIV5 reference genome, a total of 100000 paired-end reads were imported into the VirAMP Galaxy pipeline, trimmed and assembled using the SPAdes *de novo* assembly algorithm (180, 181). This produced an assembled contig of 15047 nt that was missing the leader sequence, trailer sequence and the 5' end of the N gene. Therefore, the genome sequence was iteratively extended by mapping trimmed reads back to the PIV5 genome (NC_006430). Regions of high variability and iteratively extended regions were confirmed by Sanger sequencing. Genome ends were confirmed as described below (section 2.15.6).

2.15.5 Sequencing of Lumley virus Coding Sequence

Following RNA extraction from bat urine using the MagMAX-96 Viral RNA Isolation Kit (Applied Biosystems), fragmentation and dual-index library preparation were conducted as above (section 2.15.4). Whole genome sequencing was performed as described for AlsPV except the denatured Illumina libraries were diluted to a final concentration of 1.3 pM spiked with 2% PhiX control library. Libraries were sequenced on a MiniSeq system (Illumina) using a Miniseq mid output kit (300-cycles, Illumina) generating 150 bp paired-end reads.

Illumina FASTQ paired-end reads (4,246,158 and 12,900,314 reads) from two separate MiniSeq runs were imported into CLC Genomics Workbench 11.0.1 using default Illumina import parameters, then trimmed for size, quality and ambiguous bases using default parameters except for the following: Quality Limit = 0.01, Ambiguous limit = 2 and Minimum number of nucleotides in reads = 30. Trimmed FASTQ paired end reads (3,827,218 and 10,980,060 reads) were imported into Geneious 11.1.4, error corrected and normalised with BBNorm 37.64 using default settings (182). Combined BBNorm processed reads (1,157,834 and 2,669,384 reads) were assembled with the SPAdes *de novo* assembly algorithm 3.10.0, using default settings and selecting the multi-cell data source option. Henipavirus-like contigs were identified by BLASTX and subsequently were input as "trusted contig sequences" for additional rounds of SPAdes *de novo* assemblies. This was continued until the henipavirus-like contig number was reduced to 16. Using CLC Genomics Workbench, the 16 contigs were further verified and extended by read mapping using 3,827,218 and 10,980,060 paired end trimmed reads. Read-map extended open reading frames (ORFs) were verified by BLASTX and overlapping contigs were manually joined, resulting in 3 large non-overlapping contigs: 5217 bp (coding for N, P and M), 4468 bp (F partial and G) and 6731 bp (L partial).

Gaps between the assembled contigs were determined by PCR amplification and Sanger sequencing of viral RNA following the protocol in section 2.7.1 and using the primer sets 19 and 20 (Table 2.1). Rapid amplification of cDNA ends (RACE, section 2.15.6) and amplification of genome ends using primers recognising conserved regions (PCR protocol from section 2.7.1) were attempted to try to determine the genome ends using primers in set 21 (Table 2.1).

2.15.6 CONFIRMATION OF GENOME TERMINI

The genome termini were confirmed using a combination of ligation and RACE followed by Sanger sequencing. The 3' terminus was confirmed sequencing across ligated genome ends, adapted from a method described previously (183). A volume of 15 µl viral RNA was combined with T4 RNA ligase reaction buffer (NEB) and 20 units of RNasin (Promega), denatured at 65°C for 5 min and cooled on ice. Twenty units of T4 RNA ligase, 20 units of RNasin, 50 µM ATP and 10% PEG8000 were added to the reaction and incubated at 16°C overnight. The ligated genome ends were amplified by hemi-nested PCR using Superscript III One-Step RT-PCR System with Platinum Taq DNA Polymerase (Invitrogen) and Expand High Fidelity PCR System (Roche) following the protocol described in section 2.7.1. Primer set 22 was used for TevPV amplification and primer set 23 for AlsPV (Table 2.1). PCR fragments were separated by gel electrophoresis, extracted and transformed into pGEM-T Easy for Sanger sequencing.

Due to difficulties determining the 5' terminus by ligation of genome ends, the 5' terminus was instead determined by RACE, adapted from (177). Viral RNA was reverse transcribed using Superscript III First-Strand Synthesis Supermix (ThermoFisher Scientific) according to manufacturer's instructions with a virus specific primer; AlsPV-RACE-14911F for AlsPV and TevPV-RACE-15104F for TevPV (Table 2.1). Viral cDNA was treated by RNase H for 20 min at 37°C, then purified using a NucleoSpin PCR Clean-up and Gel Extraction kit (Macherey Nagel). Viral cDNA was ligated to a 5'-phosphorylated and 3'-blocked oligonucleotide (DT88) using T4 RNA Ligase (NEB) at 25°C for 16 hours. Two hemi-nested PCRs using an adaptor specific reverse primer (DT89) and nested virus specific forward primers (AlsPV-RACE 14993F and AlsPV-RACE-15049F for AlsPV, TevPV-RACE 15192F and TevPV-RACE 15296F for TevPV, Table 2.1) were conducted using a Platinum Taq DNA Polymerase High Fidelity system (Invitrogen). The PCR reactions were set up according to manufacturer's instructions, except with an annealing temperature of 50°C for the first PCR and 49°C for the second round of PCR. Fragments of the predicted length were gel purified using a NucleoSpin PCR Clean-up and Gel Extraction kit before Sanger sequencing.

2.15.7 Amplicon sequencing

Amplicon sequencing was adapted from previously described methods (184) to determine the prevalence of P gene editing for AlsPV and TevPV. Vero cells were infected in triplicate at an MOI of 0.01, followed by total RNA extraction at 72 h post infection. Total cDNA was produced from mRNA using Superscript III Reverse Transcriptase (Invitrogen) with oligo(dT) primers following the manufacturer's protocol. Short P gene editing site fragments were amplified with primers attached to Nextera adaptors (primer set 28 for TevPV, and set 29 for AlsPV, Table 2.1) using the Expand Hi-fidelity PCR kit.

PCR products were amplified with a HiFi HotStart ReadyMix PCR system (Kapa Biosystems) and a Nextera XT Index Kit (Illumina) for Nextera XT barcode incorporation. A volume of 25 µl of KAPA HiFi HotStart ReadyMix was combined with 5 µl Nextera XT Index 1 primers, 5 µl Nextera XT Index 2 primers, 10 µl H_2O and 0.5-5ng PCR product. This PCR was conducted under the following conditions: 1 cycle of 95°C for 3 min, then 8 cycles of 95°C for 30 s, 55°C for 30 s and 72°C for 30 s, followed by 1 cycle of 72°C for 5 min. Amplified PCR products were cleaned up using AMPure XP beads (Beckman Coulter Genomics) as per Illumina sample preparation protocol (185). The denatured DNA libraries (diluted to 12 pM) were spiked with 10% PhiX control library due to the low diversity of the amplicons, then denatured at 96°C for 2 min immediately before sequencing on a MiSeq using a 600-cycle MiSeq Reagent Kit v3 (Illumina).

Data was analysed using CLC Genomics Workbench. Paired end reads were merged, trimmed on size and quality and reads with large deletions and insertions were removed. Basic variant detection, with a minimum frequency output of 0.05%, was conducted and standardised to 100000 reads. Manual scanning detected longer insertions at rates below 0.05%. Data was confirmed using unmerged, untrimmed or non-standardised read inputs.

2.15.7.1 AMPLICON SEQUENCING CONTROLS

RNA extracted from infected cell supernatant was used as the template to generate the editing site controls. Controls were amplified using the primer set 28 for TevPV and 29 for AlsPV (Table 2.1) using the PCR protocol described in section 2.7.1. Amplified fragments were extracted from agarose gel and cloned into pGEM-T Easy (section 2.9, 2.11-13). The absence of G residue insertions was confirmed by Sanger sequencing. The AlsPV editing site-pGEM construct, TevPV editing site-pGEM construct and pCAGGS were digested with SacII and NsiI in buffer H (Promega) for 2h at 37°C (section 2.10), then agarose gel purified. Digested constructs were cloned into pCAGGS (section 2.11-13). These pCAGGs constructs were either amplified in triplicate with the Expand Hi-Fi PCR kit and gel purified to act as a control for the DNA polymerase, or transfected into Vero cells to act as a control for the reverse transcriptase.

As a control for any G residues potentially introduced by the reverse transcriptase, confluent Vero cells in 24 well plates were transfected with pCAGGS constructs in triplicate. Per well, approximately 500 ng of AlsPV editing site-pCAGGS or TevPV editing site-pCAGGS were combined with 0.5 µl PLUS reagent (Invitrogen) and Opti-MEM medium (Gibco), then incubated for 5 min. A volume of 1.5 µl Lipofectamine LTX diluted into Opti-MEM was added to the diluted DNA and incubated at room temperature for 30 min. The DNA-lipid complex was then added to confluent Vero cells and incubated at 37°C for 24 h. After 24 h, RNA was extracted from transfected cells, reverse transcribed and amplified as for the test amplicons in section 2.15.7.

2.15.8 ANALYSIS OF SEQUENCES

Sequences were analysed using Geneious 10.2.2. Nucleotide and amino acid alignments were completed using the ClustalW alignment tool in Geneious or the Clustal Omega multiple sequence alignment program (186) and visualised using Jalview 2 (187). Trees were reconstructed following a maximum likelihood model using MEGA 6.06 with a bootstrap test of phylogeny (1000 bootstrap replications). Other analysis preferences were set to default. Where used, outgroups were selected by examining paramyxovirus phylogenetic trees. Putative protein sequences were analysed using various prediction tools; TMHMM 2.0 (188), Phobius (189), SignalP 4.1 (190).

2.16 VIRUS QUANTIFICATION ($TCID_{50}$ ASSAY)

Serial 10-fold dilutions of virus were added to a 96-well plate. A suspension of $2x10^4$ Vero cells was added per well and plates were incubated at 37°C for 5-7 days then checked for cytopathic effect. The $TCID_{50}$/ml of the virus was determined using the Reed-Muench method (191).

2.17 ANTIBODIES

Table 2.2: Primary polyclonal antibodies used in immunofluorescence assays (IFA), neutralisation assays and immunohistochemical analysis.

Antibody target	Source animal	Source	Additional information
AlsPV	Ferret	AAHL	Antisera obtained from three different ferrets during animal infection study 1, section 2.22.8
AlsPV N protein	Rabbit	GenScript, USA	Raised against the peptide CRQQGRINPRYLLQP (from position 200 in the AlsPV N protein)
TevPV	Ferret	AAHL	Antisera obtained from three different ferrets during animal infection study 1, section 2.22.8
TioPV	Pig	AAHL	
TioPV N protein	Rabbit	AAHL (Bioassay R&D Group)	
MenPV	Pig	AAHL	
MenPV N protein	Rabbit	AAHL (Bioassay R&D Group)	
MapV N protein	Rabbit	AAHL	
PorV N protein	Rabbit	AAHL	
PIV5	Guinea pig	BEI Resources, NAIID, NIH	
hPIV2	Guinea pig	BEI Resources, NAIID, NIH	
MuV	Guinea pig	BEI Resources, NAIID, NIH	
HeV	Horse	AAHL	
HeV N protein	Rabbit	AAHL (Bioassay R&D Group)	

2.18 IMMUNOFLUORESCENCE ASSAY

Immunofluorescence assays were used to detect the presence of AlsPV and TevPV in cell culture and to assess cross-reactivity with other paramyxoviruses. Vero cells at 70-90% confluency were infected with virus and incubated for 24-72 h. Infected cells were fixed in ice cold methanol for 15 min, before being blocked with 1% BSA in PBS for 30 min at 37°C. HeV infections were done at BSL4 and fixed in ice cold methanol for 30 min before being transferred to BSL3 for blocking with 1% BSA in PBS. Cells were incubated with primary antibodies for 1 h at 37°C and washed 4 times with PBS-T. Antibodies were diluted in 1% BSA/PBS and ranged from 1:100 for ferret antisera to 1:1000 for rabbit antisera against viral N proteins. Cells were then incubated with either Alexa Fluor 488 goat anti-rabbit IgG (1:1000, Life Technologies) or Alexa Fluor 488-protein A conjugate (1:1000, Life Technologies, used to detected ferret, pig, guinea pig and horse derived antisera) and DAPI (1:5000, Fluka) diluted in 1% BSA/PBS for 1 h at 37°C. Cells were washed 4 times with PBS-T, covered with PBS and imaged on an EVOS FL Cell Imaging System (Invitrogen).

2.19 NEUTRALISATION ASSAY

Neutralising antibodies were detected by virus neutralisation test. Sera were first inactivated by incubating at 56°C for 35 min. Antisera against a number of different paramyxoviruses were two-fold serially diluted in quadruplicate, starting at a 1:10 dilution. Antibodies were incubated with 100 $TCID_{50}$ of virus stock for 30 min at 37°C. A suspension of $2x10^4$ Vero cells was added per well and plates were incubated at 37°C for 5 days while monitoring cells for viral CPE. Back titrations were completed to confirm the addition of 100 $TCID_{50}$ of virus stock. Neutralising titres were calculated using the Reed-Muench method as the reciprocal of the highest dilution of serum at which the infectivity of 100 $TCID_{50}$ of virus is neutralised in 50% of the wells (192).

2.20 SEROPREVALENCE ASSAY

Sera from 120 Australian pteropid bats were initially screened for reactivity to TevPV and AlsPV using the immunofluorescence assay described above (section 2.18). Samples were then analysed by neutralisation assay at a 1:10 dilution in quadruplicate (section 2.19) to determine the prevalence of TevPV or AlsPV in the Australian bat population. Sera were obtained for previous studies and were collected between 1999 and 2007 from pteropid bats in Queensland or in 2012 from pteropid bats in Victoria. Sera were inactivated by incubating at 56°C for 35 min.

2.21 SIALIDASE ASSAY

Analysis of the TevPV genome revealed that the sequence of its attachment glycoprotein was divergent from those of other classical rubulaviruses, such as PIV5 and MuV. To investigate this

further, a sialidase assay was designed to assess whether TevPV required sialic acid for the infection of Vero cells. This assay was also completed during the characterisation of AlsPV to confirm its similarity to the classical rubulaviruses. Vero cells at 75% confluency in 48-well plates were treated with 15 mU neuraminidase from *Arthrobacter ureafaciens* (Sigma-Aldrich) in cell culture media for 2 h at 37°C. Some wells were simultaneously treated with 0.01% (w/w) sodium deoxycholate to increase the solubility of glycolipids. Cells were washed twice with PBS and infected with different rubulaviruses, MOI = 2. After cells were incubated with virus at 37°C for 1 h, cells were washed 4x with PBS and incubated at 37°C for 24 h in cell culture media.

After 24 h, plates were processed for IFA as described above (section 2.18). Plates were viewed on an ImageXpress Micro XLS Widefield High-Content Analysis System (Molecular Devices). Fluorescent cells were counted in nine fields of view per well (n=2 wells per treatment per biological repeat) and the mean was expressed as a percentage of the mean number of untreated cells that were infected. The relative number of infected cells was compared by one-way ANOVA followed by Dunnett's multiple comparison test (compared to untreated cells) using GraphPad Prism 5.

2.22 ANIMAL INFECTION STUDIES

2.22.1 ETHICS

These experiments were approved by the Commonwealth Scientific and Industrial Research Organisation (CSIRO) AAHL Animal Ethics Committee (AEC), approval numbers 1814 and 1865.

2.22.2 BIOSECURITY

These animal infection studies were conducted under BSL3-Z conditions. All operators wore powered air purifying respirators (PAPR, 3M). Operators underwent a three-minute personal shower upon exiting the animal research rooms.

2.22.3 PREPARATION OF INOCULUM

Virus stocks were clarified by centrifugation at 4000 rpm for 5 min. Clarified stock was diluted 1/10 in sterile PBS. The high dose was selected to ensure the maximum likelihood of infection, while dilution in PBS was required to reduce the risk of adverse reactions during virus challenge. Inoculum titre was confirmed by back titration of aliquots of the inoculum (collected before and after animal exposure) onto Vero cells (described in section 2.16).

2.22.4 Animals

All mice used in the following experiments were female BALB/c mice. Juvenile mice were 8 weeks of age and adult mice were between 6-9 months of age. Ferrets were outbred animals approximately 1 year old. All ferrets were female except for the three ferrets exposed to TevPV.

2.22.5 Handling and euthanasia

Ferrets were anaesthetised for microchip implantation, virus challenge, sampling and euthanasia using a combination of medetomidine (0.05 mg/kg) and ketamine (5 mg/kg) injected intramuscularly. Except at euthanasia, the anaesthetic reversal agent atipamezole (0.25 mg/kg) was administered intramuscularly to provide rapid recovery from anaesthesia. Ferrets were euthanased by intracardiac exsanguination and intracardiac barbiturate (Pentabarbitone at 150 mg/kg).

Mice were anaesthetised for microchip injection, virus challenge and euthanasia using a combination of medetomidine (1 mg/kg) and ketamine (75 mg/kg) intraperitoneally. Except at euthanasia, sedation was reversed with an intramuscular injection of atipamezole (1 mg/kg). Mice were euthanased by intracardiac exsanguination followed by cervical dislocation or cervical snip.

2.22.6 Sample collection

Oral swabs and rectal swabs were collected from ferrets into 1 ml viral transport media (section 2.1.10). Sterile PBS was used to collect nasal washes from ferrets, then aliquoted into a tube containing 100 µl nasal wash collection media (section 2.1.11). When possible, ferret urine was collected into tubes containing 100 µl nasal wash collection media. Blood was collected from ferrets and mice into tubes containing EDTA (1.8 mg EDTA per mL blood, Vacutainer or Microtainer Purple, BD Biosciences) to be assessed for viraemia, and into serum separation tubes (Vacutainer or Microtainer Gold, BD Biosciences) for serology.

Tissue samples were collected into tubes containing 750 µl viral transport media and 250 µl silicon carbide beads (Biospec Products Inc.). Tissues for histology were collected into 10% neutral phosphate buffered formalin and fixed for at least 48 h at room temperature.

2.22.7 Study 1: Pathogenicity study

Pathogenicity studies were conducted in mice and ferrets to determine if either TevPV or AlsPV could infect or cause disease in a non-pteropid mammal.

2.22.7.1 FERRETS

Ferrets were anaesthetised and implanted with subcutaneous temperature microchips (LifeChip, Destron Fearing) at least one week before virus challenge. Pre-challenge samples, temperature and weight readings were collected for baseline data.

Ferrets were oronasally exposed to 1 ml of diluted TevPV virus stock (n = 3 ferrets) or diluted AlsPV virus stock (n = 3 ferrets), confirmed by back titration to be $7x10^4$ $TCID_{50}$ of TevPV and $3x10^5$ $TCID_{50}$ of AlsPV. The route of infection was selected based on previous HeV infection trials in ferrets (193). Furthermore, the most likely route of exposure for non-pteropid mammals to viruses in bat urine is through the mucosal membrane. Subcutaneous microchip temperature data was recorded daily. Clinical samples were collected on days 3, 5, 7, 10 and 14 post infection, as well as at euthanasia. Body weight measurements, rectal temperatures, blood, nasal washes, oral swabs and rectal swabs were measured and collected. Attempts were made to collect urine, however, this was only successful at euthanasia when the urine could be collected directly from the bladder. Sera were collected on days 7, 10, 14 and 21 (euthanasia) to assess for seroconversion.

Tissues were collected at euthanasia and assessed for viral replication. Sections of kidney, liver, spleen, lung, retropharyngeal lymph nodes and brain (olfactory bulb plus 2 mm of the rostral cerebral cortex) were collected for analysis by quantitative RT-PCR. Remaining tissues (thoracic pluck including the pharynx/tonsils, retropharyngeal lymph nodes, mesenteric lymph nodes, representative sections of the liver lobes, kidney, spleen, gonads (testes if male; ovary and uterus if female), skull, brain and any abnormal areas of tissue seen on post mortem examination) were collected into 10% neutral buffered formalin for histopathological and histochemical analysis. Animals were assessed daily for clinical signs of disease. Changes in play scores (Table 2.3) were utilised to determine the progression of disease.

Table 2.3: Ferret play scores

0	Alert and fully playful
1	Alert but playful only when induced to play
2	Alert but not playful when stimulated
3	Neither alert nor playful

Predetermined humane end-points were defined by mild, moderate and severe non-specific signs of disease that could have developed during infection (Table 2.4). If ferrets displayed moderate disease signs that persisted for 24 hours; a play score of 2 or more was noted; or total weight loss of 20%

(from pre-challenge bodyweight) or more was recorded, the animal was euthanised due to reaching the humane endpoint.

Table 2.4: Possible symptoms during AlsPV or TevPV infection of ferrets for determining if the humane endpoint had been reached.

Mild	Onset of fever (>40°C); reluctance to rise from bed but bright and active once up; "puffy" faced appearance, squinting, clear ocular or nasal discharge, sneezing. Play score <2.
Moderate	Any of the following: Fever (≥42°C). One of more of the following: coughing, vomiting, diarrhoea; purulent or crusty nasal discharge; intermittent bouts of reduced activity; increased respiratory effort; hunched posture; straining to defecate; swelling of the throat; hollow flanks; weight loss of 10-20%. Play score 2.
Severe	Any of the following: Tremor, limb weakness, severe respiratory distress (significant abdominal sucking during breathing), play score >2; immediate euthanasia is warranted. Weight loss >20%.

2.22.7.2 MICE

Mice were injected with subcutaneous temperature microchips (LifeChip, Destron Fearing) at least one week prior to virus challenge. Pre-challenge blood, temperature and weight readings were collected for baseline data.

Mice were intranasally exposed to 30 µl of the diluted virus stock (n = 5 juvenile mice per virus, n = 5 adult mice per virus). The virus titre in this volume was confirmed by back titration to be $2x10^3$ $TCID_{50}$ for TevPV and $9x10^3$ $TCID_{50}$ for AlsPV. The route of infection was selected based on previous HeV infection trials in mice (194). Animals were monitored daily for 21 days for clinical signs of disease. Mice were monitored for pain using the mouse grimace scale (MGS) (195). Orbital tightening, nose bulge, cheek bulge, ear position and whisker change were scored on a scale of 0-2, where 0 indicated not present, 1 indicated an expression was moderately visible and 2 indicated the expression was severe or clearly apparent. An overall score was calculated as an average of each expression score. An overall score of greater than 1 would have warranted euthanasia due to the presence of moderate to severe pain.

Predetermined humane end-points were defined by mild, moderate and severe non-specific signs of disease that could have developed (Table 2.5). If mice exhibited moderate disease signs that

persisted for 24 hours, an overall MGS of 1 or more, three days of continuous weight loss, or a total of 20% weight loss was reached, the animal was euthanised.

Table 2.5: Possible symptoms during AlsPV or TevPV infection of mice for determining if the humane endpoint had been reached.

Mild	Mild lethargy with decreased curiosity in surroundings and/or mild weight loss (less than 10%) but still performing normal mouse behaviours
Moderate	Any of the following: Lethargic, disinclined to examine surroundings but some normal mouse behaviours; intermittently isolated from cage mates; overall score on the MGS of 1 or more; weight loss of 10-20%.
Severe	Any of the following: Fluffed up fur; inactivity; wasp-waisted or hunched appearance; isolated; agitated on stimulation; ataxia; tremors; weight loss >20%.

Body weight and temperature data were recorded daily. Blood and sera were collected following euthanasia. Samples of brain (olfactory bulb plus 2 mm of the rostral cerebral cortex), lung, kidney, liver and spleen were collected for analysis by quantitative RT-PCR. Remaining tissues (entire thoracic/abdominal pluck, skull and remainder of brain) were collected into 10% neutral buffered formalin for histopathological and histochemical analysis.

2.22.8 Study 2: Pathogenesis study

As virus shedding and seroconversion were observed in ferrets exposed to AlsPV in study 1, a follow up animal infection trial was conducted. This study involved the serial euthanasia of ferrets exposed to AlsPV in order to investigate the pathogenesis of the virus during acute infection.

Ferrets (n = 12) were randomly assigned to a date of euthanasia prior to exposure to AlsPV. Ferrets were anaesthetised and implanted with subcutaneous temperature microchips at least one week before virus challenge. Pre-challenge samples, temperature and weight readings were collected for baseline data.

Ferrets were oronasally exposed to 1 ml of diluted virus stock, confirmed by back titration to be $3x10^5$ $TCID_{50}$ of AlsPV. Temperature data was recorded daily from subcutaneous temperature microchips and animals were monitored daily for clinical signs of disease as outlined above for experiment 1. On each day of euthanasia, days 3, 5, 7 and 10 post infection, three ferrets were euthanised and samples were collected for assessment for viral replication.

Animals were first anaesthetised, then body weight data and rectal temperatures were recorded. Following euthanasia, oral swabs, nasal washes, rectal swabs, urine, and blood were collected. Sera samples were collected from ferrets that were euthanised on day 10 post infection. Sections of ferret brain (olfactory bulb plus 2 mm of the rostral cerebral cortex), nasal turbinates, trachea, tonsil, lung (hilar), lung (peripheral), kidney, heart, spleen, liver, small intestine, large intestine, bronchial lymph node and retropharyngeal lymph node were collected to determine the tissue tropism of AlsPV during acute infection. Remaining tissues (thoracic pluck including the pharynx/tonsils, retropharyngeal lymph node, mesenteric lymph nodes, representative sections of the liver lobes, kidney, spleen, gonads (ovary and uterus), skull, brain and any abnormal areas of tissue seen on post mortem examination) were collected into 10% neutral buffered formalin.

2.22.9 SAMPLE PROCESSING

2.22.9.1 PROCESSING OF ANIMAL SERA

Whole blood was allowed to clot in serum separation tubes for at least 30 min. Tubes were centrifuged at 1200 g for 10 min in swinging bucket rotors. Serum was then pipetted from above the polymer barrier and stored at -20°C.

2.22.9.2 PROCESSING OF ANIMAL TISSUES

Tissues samples were homogenised by bead beating (4.0 m/s for 30 s) and then centrifuged for 2 min at maximum speed. Samples were then used for virus isolation or for RNA extraction.

2.22.9.3 PROCESSING OF SAMPLES FOR RT-PCR

A volume of 100 µl of sample (clinical samples, blood or homogenised tissue) was added into tubes containing 260 µl of a guanidinium thiocyanate-based solution (MagMAX Lysis/Binding Solution, Applied Biosystems). The solution was made of a 50/50 mix of isopropanol and Lysis/Binding Solution Concentrate, with 1 µl carrier RNA. Samples were extracted using a MagMAX-96 Viral RNA Isolation Kit.

2.22.10 HISTOPATHOLOGY AND IMMUNOHISTOPATHOLOGY

Tissues were fixed in 10% neutral phosphate buffered formalin for 48 h at room temperature. Fixed tissues were dehydrated in graded alcohols, paraffin embedded and sectioned into 3-4 µm slices. Sections were stained with haematoxylin and eosin (Lillie-Mayer Haematoxylin; Australian Biostain Pty Ltd and Alcoholic Eosin/Phloxine 0.1%; Australian Biostain Pty Ltd) for assessment by light microscopy.

For immunohistochemistry, sections were mounted onto positively charged adhesion microscope slides (Hurst Scientific Pty Ltd). Paraffin sections were treated for 10 min with 10% hydrogen

peroxide. Slides were incubated at 97°C for 30 min with high pH target retrieval solution (EnVision FLEX Target Retrieval Solution, Dako Omnis) using a PT Link module (Dako), then treated with a 3% hydrogen peroxide solution. Sections were incubated for 1 h with either Menangle virus N protein rabbit antisera (1:100, produced by the Bioassay R&D Team, AAHL) for TevPV infected samples or AlsPV N protein rabbit antisera (1:1600, produced by Genscript, USA). Following this, sections were incubated for 45 min with a horseradish peroxidase-conjugated secondary antibody (Envision Flex HRP; Dako) and reacted with aminoethyl carbazole substrate chromogen (DAKO Envision) for 10 min. Sections were counterstained with Lillie-Mayer's haematoxylin (Lillie-Mayer Haematoxylin; Australian Biostain Pty Ltd). Cover slips were mounted using aqueous mounting media (Faramount Aqueous Mounting Medium Ready-to-use; Dako). Slides were examined by light microscopy.

2.23 REAL-TIME PCR (TAQMAN)

2.23.1 PRIMERS AND PROBES

The presence of viral RNA in clinical samples or tissues was determined by quantitative RT-PCR. Primers and probe for detecting the N gene of AlsPV were designed using Primer Express 3.0.1 (primer set 30, Table 2.1). Three different concentrations of forward and reverse primers were compared. 300 nM of forward primer and 500 nM of reverse primer were selected for the assay when using 133 nM for the probe concentration.

Existing primers, probes and concentrations were used for detecting TevPV N gene (final concentration of 200 nM for forward and reverse primers, 100 nM for probe, primer set 31, Table 2.1) and 18S RNA (50 nM forward and reverse primers, 200 nM for probe), except a new forward primer was designed for the detection of 18S (primer set 32, Table 2.1).

2.23.2 REAL-TIME PCR RUNNING CONDITIONS

Viral N gene RNA was detected by multiplex quantitative RT-PCR using AgPath-ID One-Step RT-PCR reagents (Applied Biosystems). RT-PCR buffer was combined with virus specific forward and reverse primers, virus specific probe, 50 nM 18S forward and reverse primers, 200 nM 18S probe, 0.6 µl RT-PCR Enzyme Mix, 2 µl sample and H_2O to 15 µl. Reactions were then run in duplicate on a QuantStudio 6 Flex Real-Time PCR System (Applied Biosystems) under the following conditions: one cycle of 45°C for 10 min and 95°C for 10 min, then 40 cycles of 95°C for 15 s and 60°C for 45 s.

2.23.3 CONTROL PLASMIDS

Control plasmids were developed so that standard curves could be produced for the qRT-PCR reactions. Inserts for control plasmids were amplified using the PCR protocol described above (section 2.7.1) with primer sets 32-34 (Table 2.1). PCR products were separated by gel

electrophoresis and fragments of the predicted size were excised from the gel and extracted from the gel matrix. The 18S control fragments were ligated into the pGEM-T Easy vector (section 2.11). AlsPV and TevPV N gene control fragments were first digested with the corresponding restriction enzymes (section 2.10) before ligation into the digested pcDNA3.1(+) vector (section 2.11). Ligated plasmids were transformed into electrocompetent *E. coli* and incubated on L.B. agar plates supplemented with ampicillin overnight (section 2.12). Colonies were selected for overnight culture by colony screen PCR (section 2.7.4). Plasmids were isolated from overnight cultures (section 2.13) and the correct sequence was confirmed by Sanger sequencing.

2.23.4 RNA TRANSCRIPTION

Plasmids were transcribed into RNA to make them more accurate controls for viral RNA. 18S-pGEM was digested with SpeI-HF in Cutsmart buffer (NEB), while TevPV N-pcDNA3.1 and AlsPV N-pcDNA3.1 were digested with KasI in Cutsmart buffer. This allowed transcription of the insert from a nearby T7 promoter for 2 h at 37°C using the Hiscribe T7 *In Vitro* Transcription kit (NEB) according to the manufacturer's instructions. The transcribed sample was then digested with DNase I (NEB) for 15 min at 37°C, followed by reaction clean-up using an RNeasy Mini kit (Qiagen).

2.23.5 RNA CONCENTRATION

RNA concentration was determined using a Qubit RNA HS Assay Kit (Invitrogen). Qubit Working Solution was prepared by diluting the Qubit RNA Reagent 1:200 into the Qubit RNA Buffer. RNA standards (0 ng/ml and 10 ng/ml) were diluted into the Working Solution, vortexed and incubated at room temperature for 2 min before being used to calibrate a Qubit 2.0 Fluorometer (Invitrogen). Test samples were diluted 1:100 in Working Solution, vortexed and incubated at room temperature for 2 min, then assessed on a fluorometer.

2.23.6 COPY NUMBER CALCULATION

The RNA concentrations (converted to g/µl) were used to calculate the copy number of control RNA per µl using an online calculator (196). The formula assumes that the mass of each RNA nucleotide is 340 Da, therefore the mass of the fragment of RNA is the length in RNA bases multiplied by 340, where 1 Da = 1 g/mol. The size of the insert was from the T7 transcription start site to the selected restriction endonuclease digestion site (SpeI or KasI).

$$g/mol = \left(size\ of\ insert_{bp}\right) * 340\ Da$$

$$g/molecule = (\frac{g}{mol})/(Avogadro's\ number: 6.02214199 * 10^{23})$$

$$molecules/\mu l = \left(\frac{g}{\mu l}\right)/(\frac{g}{molecule})$$

2.23.7 STANDARD CURVES

Standard curves were generated to quantify the amount of viral RNA present in samples and to confirm the efficiency of the reaction. Ten-fold serial dilutions of control plasmids were added in triplicate to the reaction and the reactions were cycled on a QuantStudio 6 Flex Real-Time PCR System as described above (Section 2.23.2). For analysis of the standard curves, data was imported into QuantStudio Real-Time PCR Software (v1.1). First, the fixed threshold ΔRn value was selected to best represent the phase of exponential target amplification. This was determined to be 0.2 (study 1) or 0.13 (study 2) for 18S-specific products, 0.05 (study 1) or 0.135 (study 2) for AlsPV-specific products and 0.018 for TevPV-specific products. The baseline start and end points were automatically calculated by the QuantStudio software.

Eight control RNA dilutions representing the range of potential results were selected to generate the standard curves. Copy numbers calculated from the RNA concentrations were applied to the standard curves so that they could be used for quantification. Efficiencies of all the reactions were between 95-101% with an R^2 value of >0.99.

The following formulas were used:

Study 1

$$Copy\ number_{AlsPV\ N\ gene} = 10^{\left(\frac{C_T - 42.55}{-3.34}\right)}$$

$$Copy\ number_{TevPV\ N\ gene} = 10^{\left(\frac{C_T - 46.21}{-3.44}\right)}$$

$$Copy\ number_{18S\ rRNA} = 10^{\left(\frac{C_T - 40.4}{-3.44}\right)}$$

Study 2

$$Copy\ number_{AlsPV\ N\ gene} = 10^{\left(\frac{C_T - 38.74}{-3.3}\right)}$$

$$Copy\ number_{18S\ rRNA} = 10^{\left(\frac{C_T - 40.62}{-3.4}\right)}$$

2.23.8 ANALYSIS

Data was imported into QuantStudio Real-Time PCR Software for analysis. The same thresholds that were determined for the standard curve control reactions were applied to the test results. Standard curves were imported so that positive results could be quantified. These steps required the assumption that reverse transcription and amplification efficiencies were comparable across different plates due to running with the same protocol, cycle conditions and using the same platform. Standard curves were redone for the analysis of animal infection study 2. To facilitate data

interpretation for AlsPV experiments, a copy number of 5 in both replicates, correlating with a C_T value of 40 (experiment 1) or 37.4 (experiment 2) was used as the minimum of detection. For 18S, this correlated to a C_T value of 38 (study 1) or 38.2 (study 2). No samples were positive for the TevPV N gene within 40 cycles therefore this additional threshold was not required.

Viral N gene copies detected in animal tissues were normalised to 18S values and expressed as a log transformation of the number of copies of viral N gene RNA per 10^{10} copies of 18S RNA, relative to the respective standard curves. C_T values and conversion to copy numbers were calculated using QuantStudio software. Log transformations and graphs were produced using GraphPad Prism 5.02. For shedding samples, positive results were expressed as the number of N gene copies per ml of sample.

CHAPTER 3: DETECTION AND ISOLATION OF MULTIPLE VIRUSES FROM PTEROPID BAT URINE

3.1 INTRODUCTION

High diversity and prevalence of viruses in bats has been observed during the surveillance of pteropid bats globally. Genetically diverse viruses have been isolated from, or detected in, a range of bat genera, including adenoviruses (26), paramyxoviruses (54), polyomaviruses (162), coronaviruses (166), and herpesviruses (197). These studies suggest that there are still many undiscovered viruses in bats, some of which may have the potential to transmit to a non-reservoir host in what is known as a spillover event.

In particular, a number of these studies have been aimed at detecting novel paramyxoviruses (54, 165, 168, 198). A survey of Australian pteropid bats screened bat urine by PCR for henipa or henipa-like viruses, resulting in 100 detections of unknown paramyxovirus sequences. These sequences were potentially derived from 31 new species and eight new genera (198). They proposed that these viral sequences represented paramyxoviruses that had co-evolved with their specific host for millions of years, since the dispersal of bats from Asia (198). Another survey of paramyxoviruses in 86 species of bats globally discovered many new paramyxovirus sequences, but conversely, these sequences supported the conclusion that henipaviruses originated in African bats based on analysis of key L protein motifs (54). Detection of additional paramyxovirus sequences may help to resolve the evolution of paramyxovirus and bats.

A targeted approach can be more successful at identifying particular viral families than a hypothesis-free method such as deep sequencing. Drexler *et al*. identified multiple novel paramyxovirus species in bat samples by hemi-nested PCR, but when they attempted random cDNA amplification followed by deep sequencing of serum samples, they concluded that the method wasn't sensitive enough to detect any paramyxovirus sequences (54). Similarly, a study of *Eidolon helvum* urine, throat swabs and lung tissue by metagenomic analysis did not detect any paramyxoviruses despite previously demonstrating a high prevalence of paramyxoviruses by PCR in the same population of bats (199).

During 2011, there was an unprecedented increase in the number of Hendra virus (HeV) disease events in southeast Queensland and northern New South Wales, predicating the collection of bat urine samples for HeV surveillance. The HeV prevalence was higher in these samples than previously detected and HeV was shed in bat urine across a longer period of time (53). It has also previously been observed that when the incidence of HeV detection increases, the incidence of other viruses in the urine also increases. Therefore, it was hypothesised that the urine samples collected in 2011 would also contain a range of unidentified viruses, including adenoviruses and paramyxoviruses, that would contribute to our understanding of viral diversity and evolution, as well as potentially having public health implications if the identified viruses had zoonotic potential. Targeting these samples

has previously proven successful, resulting in the isolation of novel paramyxoviruses (30). These previous isolations justify the assessment of additional urine samples collected in 2011 for the presence of novel viruses.

Urine collected from a pteropid bat colony in Alstonville, New South Wales in 2011 was selected for analysis due to the colony having a HeV prevalence of >30%. This chapter demonstrates the presence of multiple viruses and viral nucleic acid circulating in a colony of Australian pteropid bats. Furthermore, almost the whole coding sequence of a novel paramyxovirus was obtained through next generation sequencing, as well as the whole genome sequence of a polyomavirus species previously only detected in Indonesian pteropid bats. Two paramyxoviruses identified in this chapter were then characterised in Chapters 4 and 5 of this thesis.

3.2 RESULTS

Virus isolations were attempted on all Alstonville bat urine samples by inoculating 59 urine samples onto PaKi and Vero cell monolayers. Samples causing cytopathic effect (CPE) and aliquots of supernatant collected weekly were assessed by a range of viral family-specific PCRs; *Paramyxoviridae, Adenoviridae*, *Coronaviridae* and *Herpesviridae*, as well as a genus-specific PCR; *Orthoreovirus*. PCR positive samples were then identified by Sanger sequencing and BLAST analysis. Nucleic acid extracted from the 59 urine samples was also assessed for the presence of viral sequences. Although all samples were negative when assessed using PCRs specific for the virus families *Coronaviridae* or *Herpesviridae* or the genus *Orthoreovirus*, the *Paramyxoviridae* and *Adenoviridae* family specific PCRs were successful in identifying a range of viruses and viral sequences in the bat urine.

3.2.1 DETECTION AND ISOLATION OF PARAMYXOVIRUSES AND PARAMYXOVIRUS RNA

3.2.1.1 PCR DETECTION OF PARAMYXOVIRUS RNA

Paramyxovirus RNA sequences were detected in multiple bat urine samples by PCR amplification utilising consensus primers for the family *Paramyxoviridae* and the genera *Respirovirus*, *Morbillivirus* and *Henipavirus* (Appendix, Table A1)(172). Viruses could not be isolated from most of these samples. A total of 22.7% (5/22) of samples collected on the 12/7/11 and 32.4% (12/37) of samples collected on the 3/8/11 had evidence of either paramyxovirus RNA or a paramyxovirus.

Analysis of the highly conserved 600 nt fragment amplified by this PCR provided evidence that some of these viral sequences were likely to be derived from the same species of virus (Figure 3.1, 3.2). Four of the viral sequences (AL30, AL34, AL38 and AL50) were between 93-99% identical at the nucleotide level. AL23 and AL42 (urine extract) were also almost identical at the nucleotide level

(99%), as were AL15 and AL21 (96%). Some of the detected sequences were almost identical to rubula-like viruses isolated from bat urine collected during previous surveillance of Australian bats such as Grove virus, Menangle virus and Teviot virus. The remaining sequences were 61-74% identical to each other and were not similar to known, isolated paramyxoviruses, suggesting that they were derived from unique viruses. Although the short fragments of sequence meant that some of the phylogenetic distinctions were not strongly supported, there was a trend toward these viral RNA sequences clustering away from previously isolated henipaviruses. BLAST analysis indicated similarity between the Alstonville paramyxovirus RNA and RNA detected in *Eidolon helvum* bats from Ghana (Table A1). Although this could imply similarity between African and Australian henipa-like viruses, whole genome sequences are required before drawing any conclusions.

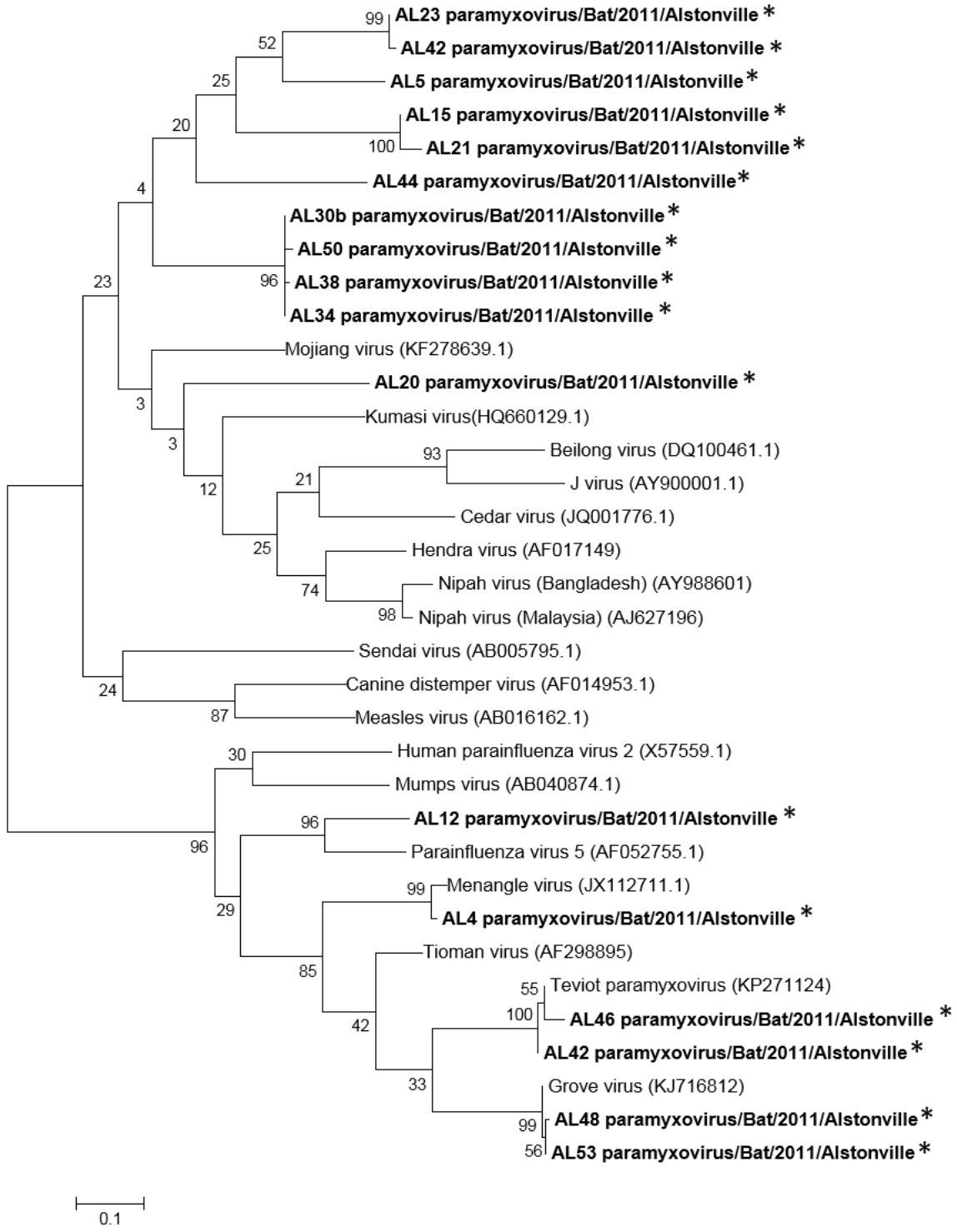

Figure 3.1: Phylogenetic analysis of selected paramyxoviruses and bat-borne viral sequences identified using *Paramyxoviridae*-specific primers (using the protocol described in section 2.7.1). Maximum-likelihood tree based on partial and complete L gene nucleotide sequences and reconstructed with MEGA 6.06, bootstrapping to 1000 replicates. Sequences identified in this study are marked by an asterisk. Genbank accession numbers are provided in parentheses.

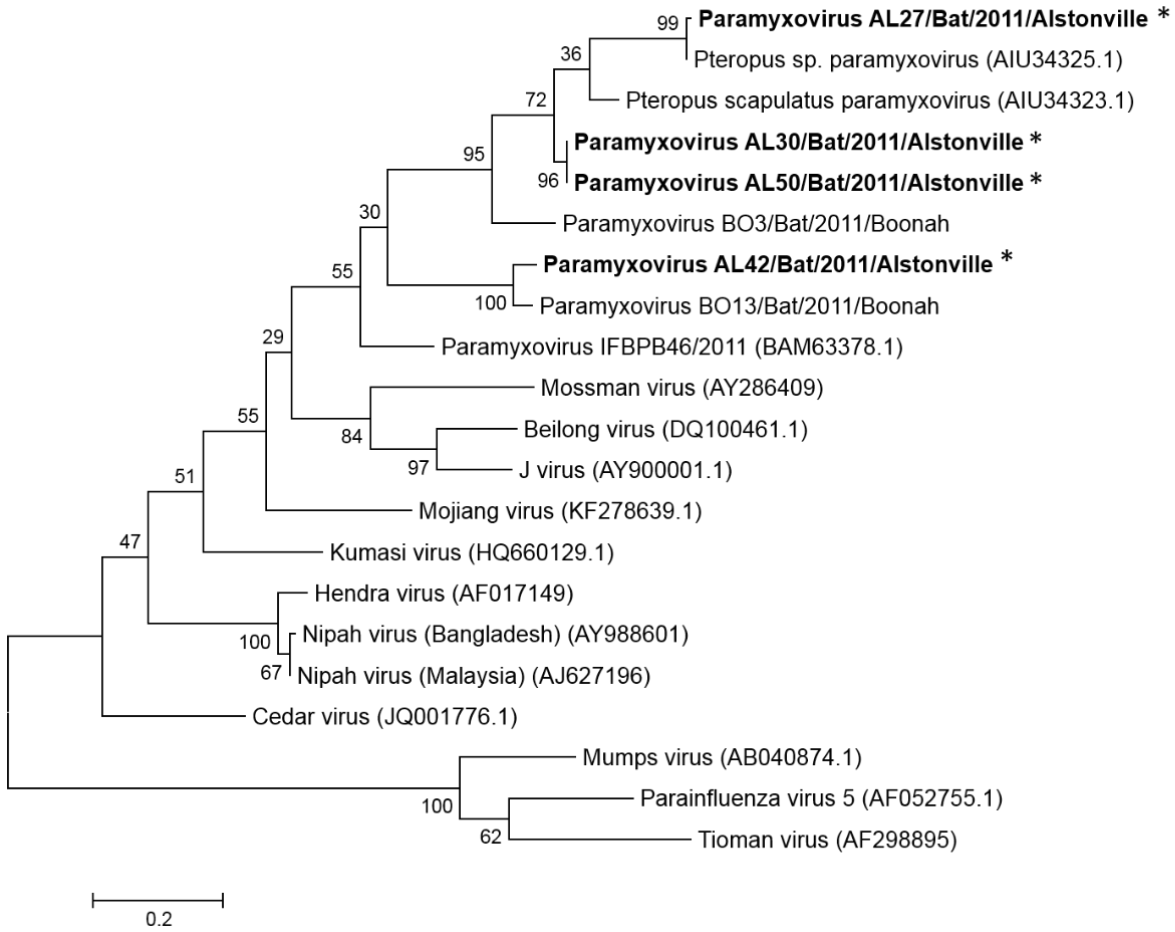

Figure 3.2: Phylogenetic analysis of selected paramyxoviruses and bat-borne viral sequences identified using *Respirovirus-Morbillivirus-Henipavirus* specific primers (using the protocol described in section 2.7.1). Maximum-likelihood tree based on partial and complete L protein sequences reconstructed with MEGA 6.06, bootstrapping to 1000 replicates. Sequences identified in this study are marked by an asterisk. Genbank accession numbers are provided in parentheses.

3.2.1.2 ISOLATION OF PARAMYXOVIRUSES

Inoculation of 59 urine samples urine onto cell monolayers resulted in the isolation of two previously uncharacterised paramyxoviruses from urine samples 12 and 42 (Appendix, Table A1). The first of these isolated viruses, Teviot virus (TevPV) from sample 42, had previously been isolated from pteropid bat urine collected in Queensland, northern New South Wales and Victoria (30, 200). The full genome sequence of this Alstonville isolate of TevPV was obtained and submitted to GenBank (MH708896). The characterisation of this virus is described in Chapter 4. The second paramyxovirus, isolated from urine sample 12, is a completely novel virus classified in the genus *Rubulavirus*. We have named this virus Alston virus (AlsPV, MH972568) based on the location of urine collection. Full

genome sequencing, along with *in vitro* and *in vivo* characterisation of this virus, forms the basis of Chapter 5. Cytopathic effect was also detected in cells inoculated with two other urine samples, designated AL23 and AL30. Further characterisation was prevented due to these putative viruses failing to grow in serial passages of the samples.

3.2.1.3 DETECTION OF PUTATIVE PARAMYXOVIRUS IN SAMPLE AL23

Although subsequent growth of the virus present in sample AL23 was not detected, a small fragment of paramyxovirus RNA was obtained. This RNA was detected in the supernatant of PaKi cells at 21 days post inoculation. The sequence was demonstrated by BLAST analysis to be most similar to Paramyxovirus IFBPV01/2010, which was detected in the spleen of a *Pteropus vampyrus* flying fox in Indonesia (Appendix, Table A1) (165). Although multiple methods for the concentration and re-isolation of this novel virus were attempted (section 2.5.3), the putative virus in sample AL23 did not appear to be able to consistently replicate in the tested cell lines and therefore was not able to be characterised. No additional sequence was obtained for this paramyxovirus.

3.2.1.4 DETECTION OF LUMLEY VIRUS

Four days post-inoculation with sample AL30, CPE consistent with adenovirus growth was observed in PaKi cells. PCR followed by Sanger sequencing revealed that both an adenovirus and a paramyxovirus were present in the supernatant. Several methods were utilised in order to isolate the paramyxovirus, named Lumley virus (LumPV) based on the location of urine collection, in the absence of the adenovirus. These methods included inoculating alternative *P. alecto* cell lines, inoculating mixed PaKi/Vero cell cultures and conducting limiting dilutions of the positive virus supernatant.

After three rounds of limiting dilution, PCR analysis demonstrated the absence of any adenovirus contamination, with CPE suggestive of paramyxovirus growth in Vero cells. Attempts to consistently culture this virus after the limiting dilution were unsuccessful, with no virus detected by PCR in subsequent passages of supernatant. Several unsuccessful attempts were made to culture this virus, including adding trypsin to the supernatant in case the virus required an external protease to cleave the fusion protein, concentrating the supernatant by ultracentrifugation over a sucrose cushion (as described in section 2.5.3), and attempting to detect the virus by IFA using Hendra virus-specific antibodies.

Despite the inability to isolate the virus, a near-complete coding sequence was obtained directly from the urine sample. Two rounds of Illumina sequencing were conducted on RNA extracted from bat urine. Reads were then assembled through multiple rounds of SPAdes *de novo* assembly (180) and read mapping (as described in section 2.15.5). The two rounds of sequencing produced

relatively low numbers of virus specific reads, however, three contigs that covered the majority of the genome were successfully assembled. These contigs included a 5217 nt fragment that comprised the entire N, P and M coding sequence, a 4468 nt fragment that covered the majority of the F and all of the G coding sequence, and a 6731 contig that covered the majority of the L coding sequence. These contigs were used to design primers and determine the missing sequences between the three contigs by Sanger sequencing. Reads were successfully mapped back to these Sanger sequenced fragments as confirmation, albeit at a very low coverage (range 1-60 reads, mean 14 reads in the M-F region, range 0-21 reads, mean 6 reads in the G-L region). No reads mapped back to a 3 nt region within the L gene 3'UTR. Across the entire genome, the coverage range was 0-2441 reads with a mean of 257 reads. Rapid amplification of cDNA ends (RACE) was attempted to determine the sequence of the genome termini and the 5' end of the L gene, and primers against the 5' UTR of the Mojiang virus (MojPV) L gene were used to try and complete the coding sequence (as described in section 2.15.5-6). Neither of these methods was successful, leaving the genome termini unsequenced.

3.2.1.4.1 ANALYSIS OF PUTATIVE GENES AND PROTEINS OF LUMLEY VIRUS

GENOMIC FEATURES

Despite having low sequence homology with other paramyxoviruses, conserved motifs were identified throughout the sequence. The trinculeotide intergenic region, CTT, is located between all the predicted open reading frames (ORFs) and surrounded by putative gene boundaries that are relatively conserved with other paramyxovirus gene boundaries (Appendix, Table A2). The lengths of untranslated regions are variable when compared with other paramyxoviruses, although this variability has also been observed in the genome of MojPV. The genome organisation of LumPV corresponds to the organisation of known paramyxoviruses, with six open reading frames correlating with six major genes, the N, P, M, F, G and L genes (Table 3.1). LumPV also appears to have the potential to express additional proteins from the P gene. Phylogenetic analysis indicated that LumPV is most closely related to MojPV when comparing the whole nucleotide sequence (Figure 3.3), but is more divergent when comparing G protein sequences (Figure 3.4, Table 3.2).

Table 3.1: Comparison of LumPV predicted coding regions and other genomic features. LumPV coding sequences are compared to those of MojPV and HeV.

		Virus	Length (nt)	Length (aa)
3' leader		LumPV	-	
		MojPV	51	
		HeV	55	
N	CDS	LumPV	1638	545
		MojPV	1620	539
		HeV	1599	532
P	V CDS	LumPV	924	307
		MojPV	1197	398
		HeV	1374	457
	P CDS	LumPV	1605	534
		MojPV	2085	694
		HeV	2124	707
	W CDS	LumPV	885	294
		MojPV	1209	402
		HeV	1347	448
	C CDS	LumPV	519	172
		MojPV	534	177
		HeV	501	166
M	CDS	LumPV	1026	341
		MojPV	1023	340
		HeV	1059	352
F	CDS	LumPV	1653	550
		MojPV	1638	545
		HeV	1641	546
G	CDS	LumPV	2115	704
		MojPV	1878	625
		HeV	1815	604
L	CDS	LumPV	-	-
		MojPV	6834	2277
		HeV	6735	2244
5' trailer		LumPV	-	
		MojPV	40	
		HeV	33	

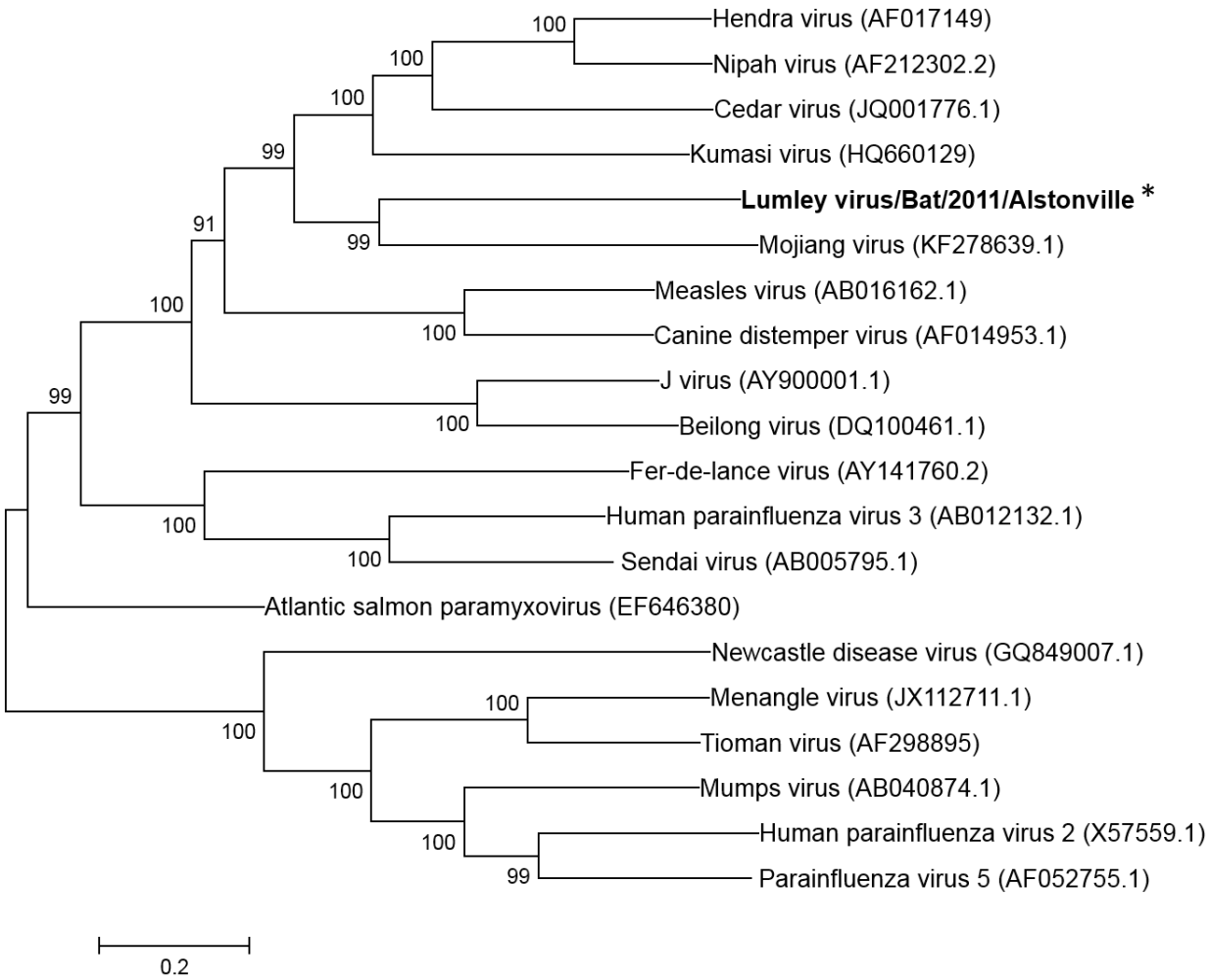

Figure 3.3: Phylogenetic analysis of whole genome nucleotide sequences of representative paramyxoviruses. Analysis includes the majority of the LumPV coding sequence. Maximum-likelihood tree reconstructed with MEGA 6.06, bootstrapping to 1000 replicates. The paramyxovirus sequence identified in this study is marked by an asterisk. Genbank accession numbers are provided in parentheses.

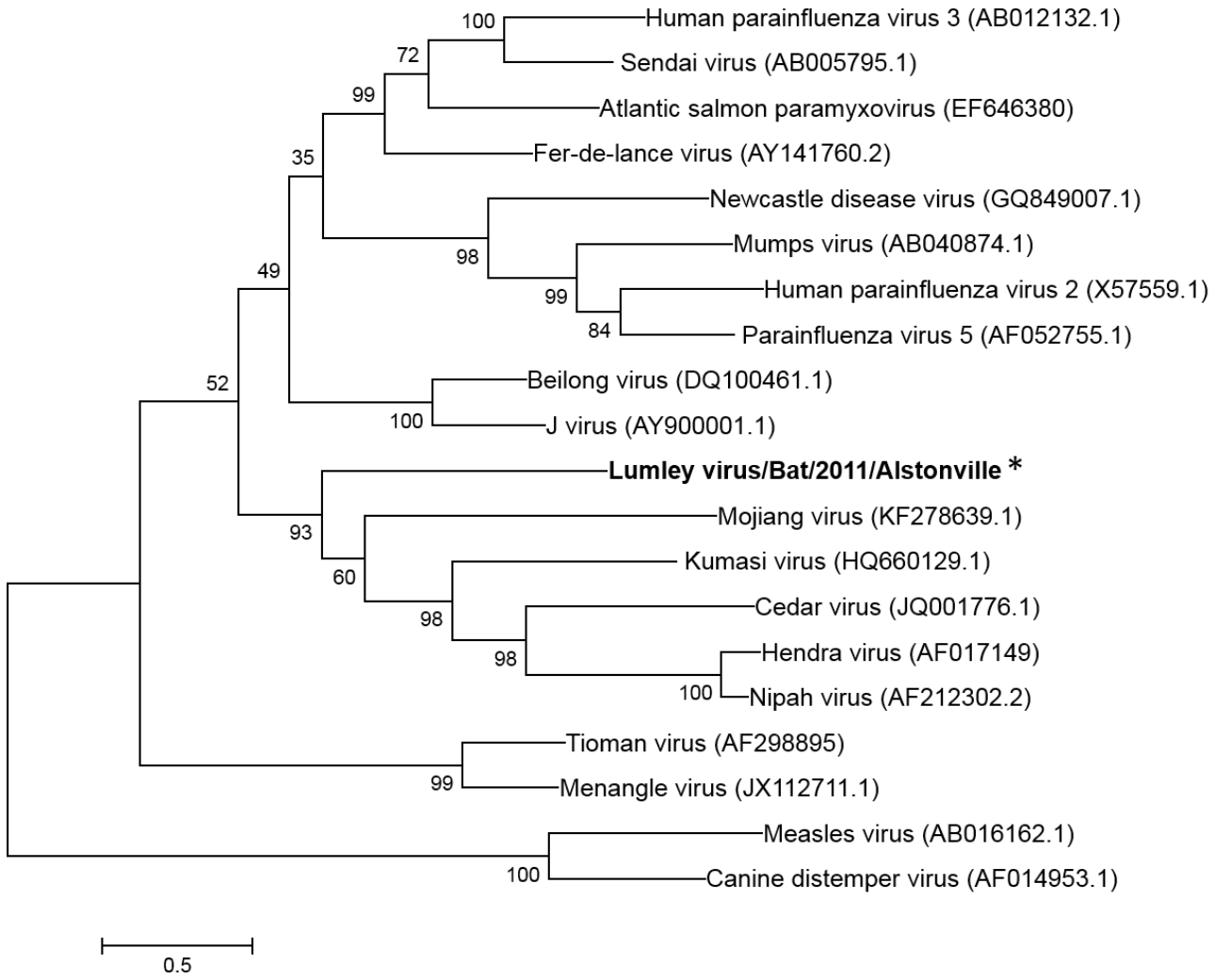

Figure 3.4: Phylogenetic analysis of representative paramyxovirus attachment glycoprotein sequences. Maximum-likelihood tree reconstructed with MEGA 6.06, bootstrapping to 1000 replicates. The paramyxovirus sequence identified in this study is marked by an asterisk. Genbank accession numbers are provided in parentheses.

Table 3.2: Comparison of LumPV putative protein sequences. Values represent the percentage amino acid sequence identity compared to MojPV, HeV and Beilong virus (BeiPV). Sequences aligned and identities calculated by ClustalW alignment in Geneious 10.2.2.

	LumPV								
	N	P	V	W	C	M	F	G	L
MojPV	41.9	16.9	19.2	14.0	25.0	54.4	36.7	18.8	50.6
HeV	45.7	21.9	19.0	19.2	30.3	53.9	35.4	21.3	52.0
BeiPV	31.9	17.6	21.9	13.9	14.9	48.8	32.7	18.6	46.9

N

The putative N protein of LumPV contains a central region that is conserved with other paramyxovirus N proteins. For viruses in the family *Paramyxoviridae*, this central region contains the motif F-X4-Y-X3-Φ-S-Φ-A-M (where Φ is a hydrophobic amino acid) (57). The LumPV N protein is missing the final methionine residue of this motif (Appendix, Figure A1.1), despite relatively good sequencing coverage in this region. Overall, the LumPV N protein is more similar to the N proteins of henipaviruses than those of other paramyxoviruses.

P

The LumPV P gene encodes a conserved RNA editing site (Table 3.3). Consistent with other paramyxoviruses, the unedited transcript encodes the P protein and the addition of one or two non-templated G residues produces open reading frames encoding a putative V protein or W protein respectively (Figure 1.2). LumPV also appears to have the coding capacity for a C protein from an alternative start site located 35 nt downstream of the standard start site. Expression from this alternative start site would result in the expression of a 172 aa protein. Although this is similar in length to C proteins expressed from henipaviruses, there are only low levels of amino acid and nucleotide identity in this sequence.

The predicted P and V proteins of LumPV have low overall sequence similarity to other paramyxoviruses and are at least 150 aa shorter than the long P and V proteins expressed by the henipaviruses. The C-terminal of the LumPV V protein is highly conserved with other paramyxoviruses, containing one conserved histidine and seven cysteine aa residues that are associated with zinc molecule binding (Appendix, Figure A1.3) (57).

Table 3.3: Comparison of RNA editing sites of paramyxoviruses. Difference in conserved site is highlighted in bold and lowercase.

	Editing site
LumPV	ATTAAAA**g**GGGCACAGA
HeV	ATTAAAAAGGGCACAGA
NiV	ATTAAAAAGGGCACAGA

M

The M protein of LumPV is the most highly conserved with ~55% amino acid conservation with the M proteins of the henipaviruses (Table 3.2). It encodes the 'YMYL' motif and five out of six residues of the 'YPLGVG' motif that are associated with viral budding in the NiV M protein (Appendix, Figure A1.6) (201, 202).

F

There are multiple potential start sites for the LumPV F protein that are all in the same reading frame. The second potential start site, encoding a 550 amino acid fusion protein, is predicted to be the expressed protein due to similarities in length and sequence with henipaviruses. The lack of a virus isolate means that this cannot be confirmed. None of the potential ORFs have a strongly predicted N-terminal signal sequence. Other out-of-frame start sites were investigated to see if, similar to Kumasi virus, polymerase error resulted in the deletion of a nucleotide in an AT-rich region near the N-terminus, however, no alternative ORFs could be generated *in silico*. *In silico* analysis (section 2.15.8) also indicated that there are four hydrophobic regions that have the potential to be transmembrane. One of these putative transmembrane regions would result in a 25-30 aa cytoplasmic tail at the C-terminus of the LumPV protein, similar to what is observed for the F proteins of other paramyxoviruses.

Similar to henipaviruses, the LumPV F protein has a monobasic cleavage site followed by a region of higher conservation that corresponds to the hydrophobic fusion peptide (Appendix, Figure A1.7) (71). The LumPV F protein encodes all 10 conserved cysteine aa residues that are found in paramyxovirus fusion proteins and are critical for correct protein folding (203). It also encodes a conserved endocytosis motif, YXXΦ (where Φ is a hydrophobic amino acid) in the putative cytoplasmic tail that has been shown to facilitate efficient internalisation of Hendra and Nipah virus F proteins (204, 205).

G

LumPV encodes a divergent G protein that is longer than most paramyxovirus attachment glycoproteins. Alignment of henipavirus attachment glycoproteins indicated that this increase in length is due to an extension of the C-terminus of the protein (Appendix, Figure A1.8). Despite the lack of sequence similarity to other paramyxovirus attachment proteins, the LumPV G protein is predicted *in silico* (section 2.15.8) to be a type 2 membrane protein with a 53 aa N-terminal cytoplasmic tail, consistent with other paramyxovirus attachment proteins. It lacks the motif, NRKSCS, which is part of the neuraminidase active site, as well as only having two out of seven aa residues that are associated with neuraminidase function. Furthermore, the LumPV G protein lacks 12 out of 14 sites that were identified in either HeV or NiV as important for ephrin binding (206, 207), although further studies are required to investigate the potential of this G glycoprotein to use ephrins as cellular receptors for attachment.

L

The paramyxovirus L protein, responsible for transcription and replication of the viral RNA, can be divided into six domains of high sequence conservation with the highest level of conservation in

domains II to V (57, 208). These domains appear to be present in the LumPV L protein (Appendix, Figure A1.9). In particular, the motif GDNQ, thought to be the active site of paramyxovirus polymerases (57, 61, 208), is found in domain III of the LumPV L protein.

3.2.2 ISOLATION OF MULTIPLE ADENOVIRUSES

3.2.2.1 ISOLATION

Adenovirus induced cytopathic effect was characterised by cells becoming refractory to light in localised sections of the cell monolayer (Appendix, Figure A2). Cells then started to shrink and become rounded, before the monolayer of cells became completely detached from the tissue culture flask surface. For the majority of isolates, this occurred between 4-7 days post inoculation, although some needed additional passages or longer incubation times for the infection to become visually evident (Table 3.4).

Table 3.4: Adenovirus isolation information. Dpi indicates days post infection

Date collected	**Urine no.**	**Passage CPE first seen**	**Dpi**
12/7/11	9	PaKi 1st passage	7
	11	PaKi 1st passage	4
	32	PaKi 1st/2nd/3rd passage	18/11/7
3/8/11	6	PaKi 1st passage	6
	30	PaKi 1st passage Vero 1st passage	4
	31	PaKi 2nd passage	4
	32	PaKi 1st passage	7
	34	PaKi 1st passage	6

3.2.2.2 PHYLOGENETIC ANALYSIS

Eight urine samples contained adenoviruses that could be isolated in cell culture, resulting in a detection rate of ~13.5% in urine collected at either time point. Out of those eight adenovirus isolates, sequencing of the PCR amplified fragments of DNA polymerase indicated that potentially three species had been isolated. These three viral DNA polymerase protein sequences are between 81-86% identical to each other and appear to be highly similar to unpublished adenovirus sequences that were obtained from bat urine collected throughout southeast Queensland and northern New South Wales. A whole genome sequence is not available for any of these Australian bat isolates (Figure 3.5).

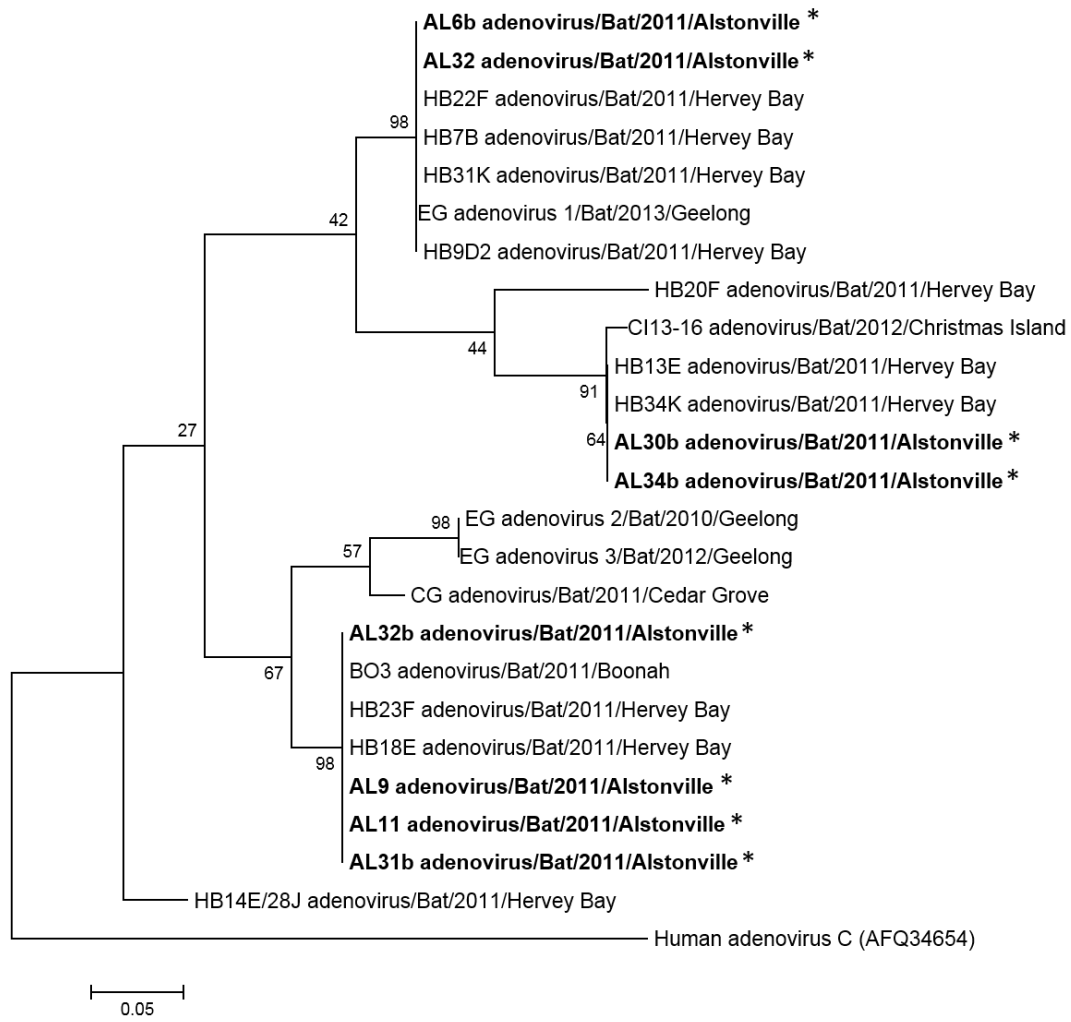

Figure 3.5: Phylogenetic comparison of adenoviruses isolated from Australian and Christmas Island pteropid bats. Maximum-likelihood tree is based on partial polymerase amino acid sequences and reconstructed with MEGA 6.06, bootstrapping to 1000 replicates. Isolates identified in this study are marked by an asterisk.

The Alstonville bat isolates are also closely related to some of the short polymerase sequences obtained from *Pteropus giganteus* flying foxes in Bangladesh, but more divergent from another pteropid isolate, bat adenovirus FBV1 from *Pteropus dasymallus yayeyamae* in Japan (Figure 3.6). When only comparing to adenoviruses with a published whole genome sequence, the Alstonville bat isolates are the most similar to an adenovirus recently isolated from *Rousettus aegyptiacus* in South Africa (isolate 3085) (209) and isolates belonging to the newly classified species *Bat mastadenovirus D* and *E*, both isolated from *Miniopterus schreibersii* in China (148, 150). No additional adenoviruses could be detected by conducting PCRs directly on nucleic acid extracted from the bat urine.

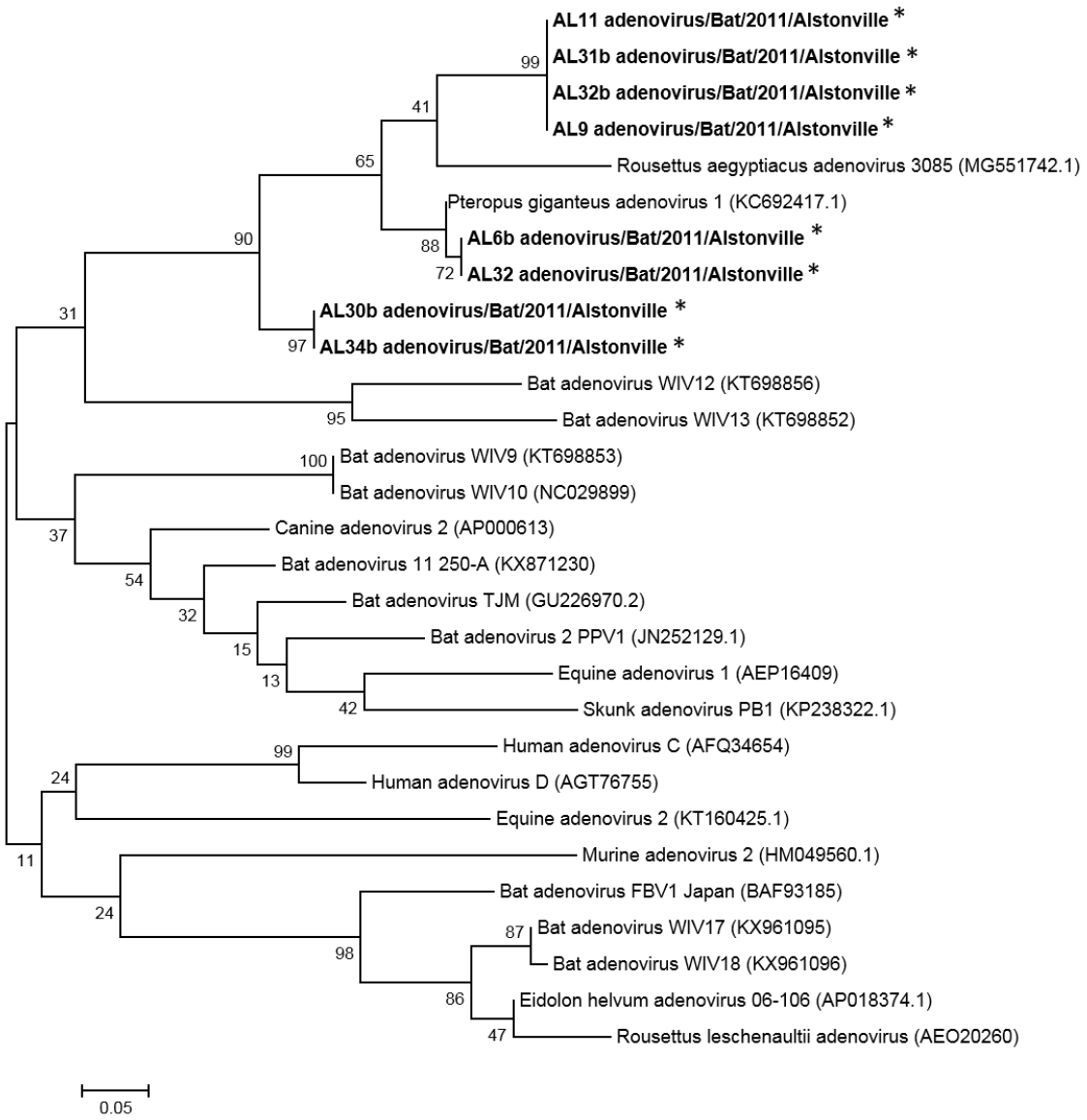

Figure 3.6: Phylogenetic tree of selected adenovirus isolates. Maximum-likelihood tree is based on partial and complete polymerase amino acid sequences and reconstructed with MEGA 6.06, bootstrapping to 1000 replicates. Isolates identified in this study are marked by an asterisk. Genbank accession numbers are provided in parentheses.

3.2.3 ISOLATION OF A POLYOMAVIRUS

A polyomavirus was isolated following the inoculation of PaKi cells with bat urine collected on the 3rd August 2011. No obvious cytopathic effect was observed, however, aliquots of supernatant were collected weekly. Nucleic acid was extracted from the supernatant and PCR identification was attempted using *Paramyxoviridae*-specific degenerate primers due to the detection of a paramyxovirus sequence in the source urine sample. A 600 bp fragment was obtained from nucleic acid extracted 14 and 21 days post inoculation. Sequencing and BLAST analysis revealed this sequence corresponded to a polyomavirus and was amplified due to a partial match with the degenerate primers. Further PCR and Sanger sequencing was conducted to obtain the complete virus genome sequence.

Polyomavirus genomes are comprised of circular double-stranded DNA. Analysis of this virus revealed a 4958 bp long genome with open reading frames that corresponded to the polyomavirus large T antigen, small T antigen and viral capsid proteins, VP1, VP2 and VP3. Phylogenetic analysis indicated that this isolate, Pteropus sp. PyV/Bat/2011/Alstonville, was the same species as an Indonesian bat polyomavirus that was isolated from a *Pteropus sp*. flying fox in Paguyaman, Indonesia (Pteropus sp. PyV 6d/Bat/2013/Paguyaman) (161), with 96.59% nucleotide identity across the whole genome (Table 3.5, Figure 3.7, 3.8). There were two nucleotide insertions in the non-coding control region (NCCR) of the Australian isolate when compared to Pteropus sp. PyV 6d/Bat/2013/Paguyaman, but protein coding sequences were almost identical (Table 3.5). Pteropus sp. PyV/Bat/2011/Alstonville also encodes four ORFs adjacent to the NCCR that potentially correspond to an agnogene, however, the putative proteins from these sequences have no sequence similarity to known agnoproteins.

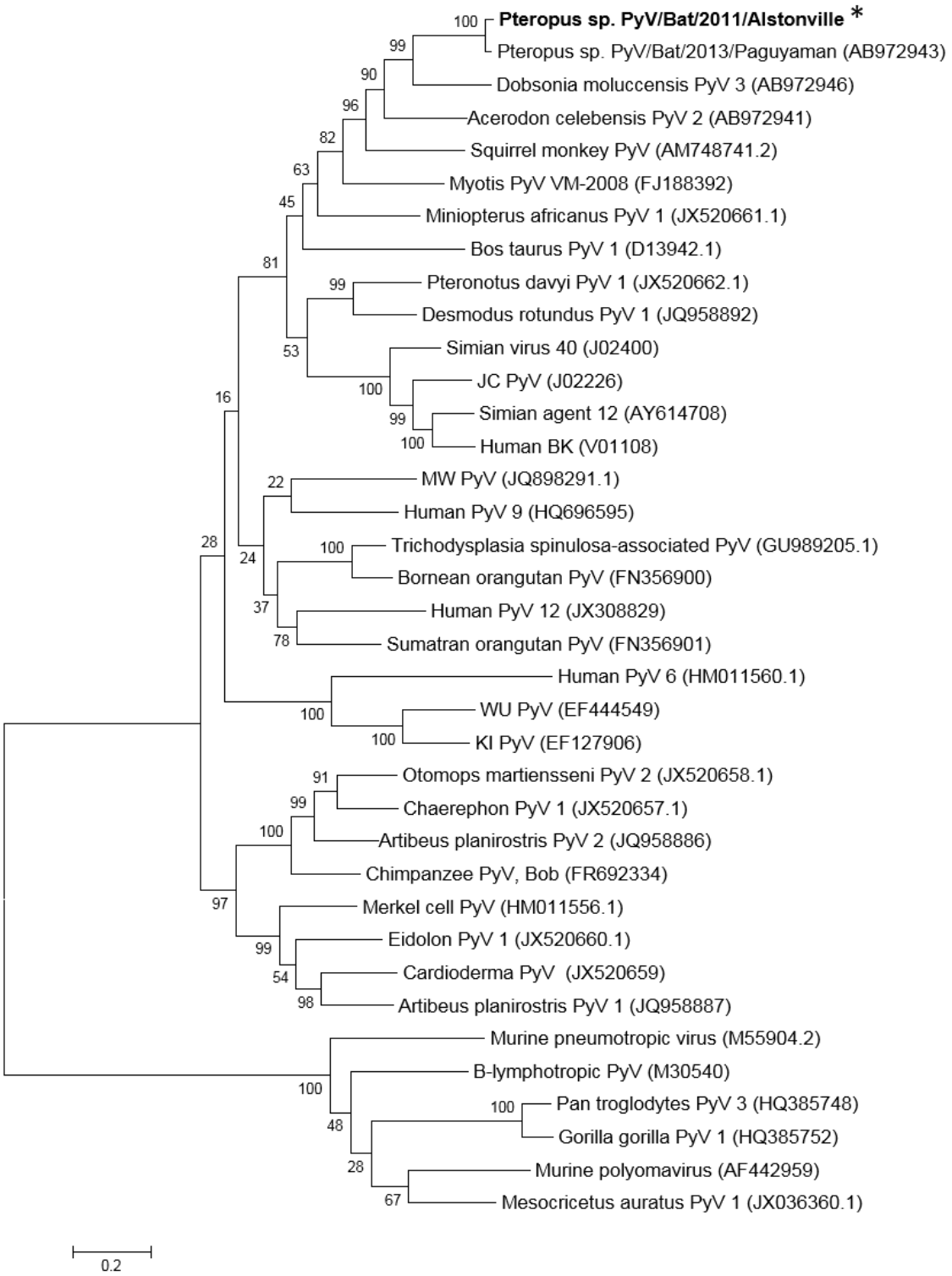

Figure 3.7: Phylogenetic analysis of whole genome nucleotide sequences of representative polyomaviruses. Maximum-likelihood tree reconstructed with MEGA 6.06, bootstrapping to 1000 replicates. The isolate identified in this study is marked by an asterisk. Genbank accession numbers are provided in parentheses.

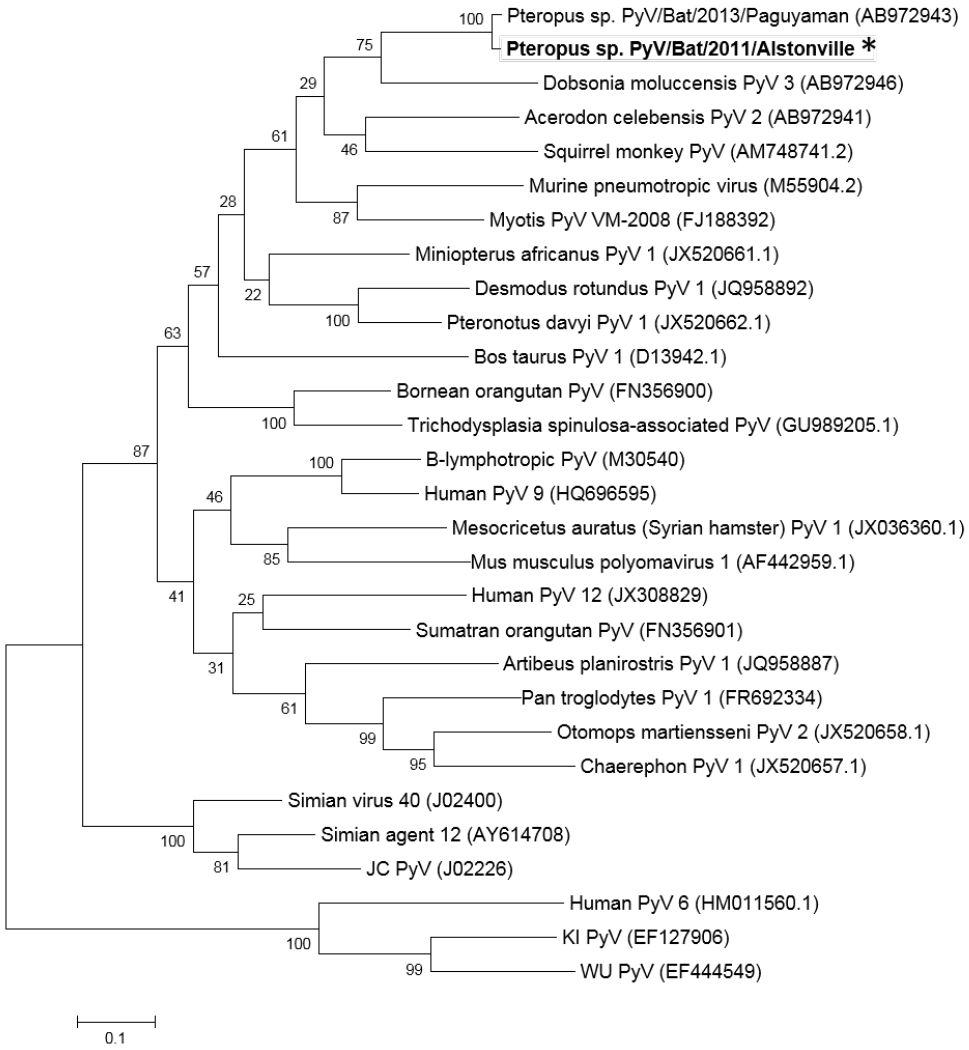

Figure 3.8: Phylogenetic analysis of VP1 protein sequences of representative polyomaviruses. Maximum-likelihood tree reconstructed with MEGA 6.06, bootstrapping to 1000 replicates. The isolate identified in this study is marked by an asterisk. Genbank accession numbers are provided in parentheses.

Table 3.5: Gene and protein lengths of Pteropus sp. PyV/Bat/2011/Alstonville and comparison to Pteropus sp. PyV 6d/Bat/2013/Paguyaman.

	Length (bp)	Nucleotide differences	Identity (%)	Length (aa)	Amino acid differences	Identity (%)
VP1	1104	32	97.1	367	6	98.37
VP2	975	33	96.62	324	2	99.38
VP3	615	23	96.26	204	1	99.51
*Agnoprotein**	213	0	100	70	0	100
LTAg	1986	87	95.62	661	11	98.34
STAg	501	16	96.81	166	0	100
Whole genome	4958	169	96.59			
NCCR	629	11	98.25			

*Based on open reading frame that encodes a protein most similar in size to other bat polyomavirus agnoproteins

3.3 DISCUSSION

Fifty-nine urine samples collected in Alstonville in 2011 were assessed for the presence of unknown viruses. It was predicted that these samples would contain multiple paramyxoviruses and adenoviruses based on the high percentage of these urine samples that contained HeV RNA, as well as previous studies that isolated paramyxoviruses or detected paramyxovirus RNA in Australian pteropid bat urine (9, 30). In this chapter, urine samples collected in Alstonville were demonstrated to contain paramyxovirus RNA potentially derived from a range of novel viruses, in addition to adenoviruses and a polyomavirus.

The urine samples were collected from a mixed colony of flying foxes, made up of an approximate 50/50 split of *P. poliocephalus* and *P. alecto.* Therefore, information regarding the host specificity of these viral sequences, and thus conclusions about host-virus co-evolution and infection dynamics, cannot be determined. Previously, co-evolution of paramyxoviruses and their host species has been supported by host specificity and the particular geographical distribution of these viruses or viral sequences (198). For example, *P. alecto* and *P. conspicillatus* are considered the main reservoir hosts of HeV, whereas infection rates are low in *P. poliocephalus* colonies despite the geographical overlap with *P. alecto* colonies (47). Further work is required to determine the source species for each sequence based on cytochrome B gene PCR (210), however, the results may not be accurate due to potential pooling of the urine samples on the plastic collection sheets.

PARAMYXOVIRUSES

In addition to the isolation of Teviot virus and Alston virus that are described in Chapters 4 and 5, analysis of the urine samples revealed a number of distinct sequences that could contribute to the generation of a novel genus within the family *Paramyxoviridae* (Figure 3.1-2). Almost the whole coding sequence of a novel paramyxovirus, Lumley virus (LumPV), was detected in a bat urine sample as described in section 3.2.1.4. Initially, the virus was detected in the supernatant of cells inoculated with the urine sample, but did not appear to replicate efficiently. It is possible that LumPV requires a specific protease for efficient infection following cleavage of the fusion protein, although no increase in growth was observed when LumPV was grown in the presence of trypsin. As paramyxovirus-derived RNA could also be detected in the bat urine, it is possible that no replication occurred at all and the sensitive hemi-nested PCR only detected residual viral RNA from the urine. In comparison, the putative virus in sample AL23 could only be detected in the cell culture supernatant and not in the urine, suggesting that some replication had occurred.

A cleavable signal sequence in the N-terminus of the F protein, present in all paramyxoviruses but apparently lacking in LumPV, is required for targeting to the endoplasmic reticulum membrane (57).

The fusion protein of Kumasi virus also appeared to lack an N-terminal signal sequence. This was later determined to be due to an polymerase error and was adjusted by the *in silico* addition of another nucleotide near the N-terminus (107). For the LumPV F protein, conserved features such as the fusion peptide and a C-terminal endocytosis motif indicate that the protein is in the correct reading frame when using the current start site. Other potential start sites in alternative reading frames were investigated to see if there was a similar polymerase error to Kumasi virus, but this was unsuccessful. Furthermore, *in vitro* investigation is required to confirm the membrane orientation of the LumPV F protein as the *in silico* prediction of four potentially transmembrane regions is not consistent with other paramyxovirus fusion proteins.

The lack of sequence similarity to other paramyxovirus attachment proteins (Figure 3.4) is similar to what has been observed with MojPV. It has been demonstrated that MojPV does not use an ephrinB2/B3-, sialic acid- or human CD150-dependent pathway for cell attachment (106). The functional assessment of MojPV was conducted by co-expression of the fusion protein and attachment glycoprotein from mammalian expression vectors. This method could be utilised for the characterisation of LumPV as it only requires the sequences of the F and G genes instead of an isolate of the virus. The sequence divergence of LumPV from other virus attachment proteins and the lack of conserved neuraminidase or ephrin binding motifs indicate that it likely also uses an alternative entry receptor to sialic acid or ephrinB2, or that it binds these host cell receptors in a novel way. Obtaining the entire coding sequence of LumPV would allow this to be investigated even further by developing a reverse genetics system.

A number of other short sequences of paramyxovirus-derived RNA were detected in bat urine by PCR (section 3.2.1.1). Although metagenomic analysis of these samples would have potentially yielded additional viral sequences, the aim of this thesis was to isolate and characterise paramyxoviruses, therefore a targeted approach was used instead. For the majority of the samples described in section 3.2.1, only fragments of RNA were detected, but no replicating virus could be isolated or whole genome sequences obtained. This is because the nested RT-PCR assay used for detecting paramyxoviruses was more sensitive than virus isolation and could detect viral RNA even after the inactivation of the virus or degradation of the genome. The urine samples used for analysis were collected off plastic sheets below bat colonies, potentially allowing time for the viral RNA to degrade before collection into viral transport media. Following transport to the Australian Animal Health Laboratory, the urine samples were thawed for HeV detection, before being frozen again and stored for 4 years at -80°C.

The urine samples used for this thesis had already been tested for the presence of Hendra virus (HeV) RNA, which revealed that 39% of urine samples collected on the 12th July 2011 and 31% of samples collected on the 3rd August 2011 were HeV positive. These HeV positive samples were removed from analysis, meaning that the prevalence of paramyxoviruses in the Alstonville bat colony in 2011 was actually 52.8% and 53.7% for the two collection dates. The observed prevalence of adenoviruses may have also been misrepresented depending on the adenovirus prevalence in the removed samples and how infection with HeV affects viral coinfections.

The sequences described in section 3.2.1.1 cannot currently be identified as 'novel viruses' due to the lack of whole genome sequences. Some of these viral sequences may have been derived from the same virus species as sequences identified during previous surveillance of Australian bats (198). However, this cannot be confirmed due to the use of different primers and the lack of whole genome sequences. Many previously identified sequences were detected by screening bat urine using only the *Respirovirus-Morbillivirus-Henipavirus* degenerate primers (198), whereas this study also utilised *Paramyxoviridae* degenerate primers, resulting in the detection of viral RNA in an additional twelve urine samples. These two sets of primers amplify different, non-overlapping regions of the L gene, therefore it is possible that the virus sequences detected using *Paramyxoviridae*-specific primers in section 3.2.1.1 have been identified during previous Australian surveillance using *Respirovirus-Morbillivirus-Henipavirus*-specific primers. Similarly, a major international study of bat paramyxoviruses did not use the *Paramyxoviridae* degenerate primers (54); therefore, comparisons to international sequences were limited to specific studies (31, 165, 168).

Phylogenetic analysis of the detected paramyxovirus sequences indicated that their closest relatives were from the genus *Henipavirus*. We have used a similar method to Vidgen *et al*. to distinguish between the virus-derived sequences based on the variation of the L gene within the genus *Henipavirus* (198). A group of viral sequences, potentially representing a genus, contained sequences with variation between 6.2-35.4% at the nucleotide level. Variation <6.2% potentially represented a single species, based on the variation between the Malaysia and Bangladesh isolates of NiV. By this definition, we have identified or isolated eleven sequences representative of virus species (Figure 3.1-2), four of which were potentially representative of novel virus species (Appendix, Table A1). The high similarity, less than 6.2% variation, between particular identified sequences suggested that some of the detected viral RNA originated from the same viral species. Despite RNA viruses having a high mutation rate due to their highly error-prone RNA-dependent RNA polymerases (211), it has been observed in multiple paramyxoviruses that mutations are often not tolerated in the field and that the genome sequences of paramyxoviruses remain fairly stable (212, 213). Therefore, based on the observed variation between the sequences described in section 3.2.1.1, it is likely that these

representative sequences equate to unique viral species that were circulating throughout Australian bat populations in 2011 and shed in their urine. Further inferences cannot be made because the phylogenetic tree was not well supported by bootstrapping.

Many henipa-like virus RNA fragments have been detected globally, but there has been limited success in isolating the viruses that correspond to these sequences (54, 198). As more whole-genome sequences of these viruses are elucidated, it is likely that the paramyxoviruses from which the sequences discussed in this chapter are derived will form at least one novel genus, consistent with what has been hypothesised during other surveillance studies (168, 198). Although inferences can be made about the range of viruses present in this population of bats, definite conclusions must wait until whole-genome sequences or isolates of these viruses can be obtained. The whole-genome sequence of LumPV is therefore an important tool for learning more about this potential new genus of paramyxoviruses.

ADENOVIRUSES

Multiple adenoviruses were isolated from bat urine collected in Alstonville (section 3.2.2). The sequence similarity of the adenovirus isolates with previously isolated Australian bat adenoviruses suggests that these adenoviruses may be consistently maintained in the Australian flying fox population, but a larger study size and regular sampling would be required to investigate this hypothesis. Other bat adenoviruses have shown tissue tropism for the intestines, liver and kidney of bats (214), and multiple bat adenoviruses have been isolated from bat faeces samples (148) or from bat urine (199). Care was taken to avoid contamination with bat faeces, therefore it seems that these adenoviruses were shed in the bat urine. Further investigation using a more sensitive PCR would be useful for detecting any additional adenovirus DNA in the urine. This mechanism of virus shedding would facilitate continuous exposure of the bat colony to the adenoviruses, contributing to a higher probability of bat infection and maintenance of the virus circulation in the population (36).

Previous bat isolates have been classified as belonging to one of the seven recently formed species, *Bat mastadenovirus* A-G (150). Species demarcation within the *Mastadenovirus* genus is dependent on a number of criteria that cannot be determined from a short PCR fragment alone, including cross-neutralisation and genome organisation (135). Although the adenoviruses described in this chapter were isolated, no characterisation or further sequencing was completed. One criterion for the formation of a new species is a phylogenetic distance of >5-15% based on the DNA polymerase amino acid sequence (135). Although these isolates have a phylogenetic distance of ~15% or greater from previously described adenovirus species, it is only based on a 126 aa fragment of the DNA

polymerase, therefore whole genome sequencing is required to confirm their description as unique species.

Mastadenoviruses are considered to be very host species-specific (215), however, the similarity of the Alstonville bat isolates to *Rousettus aegyptiacus* adenovirus-3085 (209) suggests that host switching events may have occurred instead of exclusively co-diverging with their host species. *R. aegyptiacus* are also members of the *Pteropodidae* family, but cluster under the *Rousettinae* subfamily that are estimated to have diverged from the *Pteropodinae* subfamily 20 million years ago (216). As sampling and surveillance of bats continues, the phylogeny of bat adenoviruses may become more distinct and this apparent relationship between adenoviruses from divergent host species may disappear (209).

Furthermore, the isolates to which the Australian bat adenoviruses are most closely related have a lower GC content than most mastadenoviruses. A similarly low GC content of between 34-39% is observed in the DNA polymerase fragment obtained from the Australian isolates, although definite conclusions cannot be made from only short fragments of genome. It has been suggested that mastadenoviruses evolved to have longer genomes with higher GC content over millions of years and that isolates with a low GC content may represent ancestral mammalian viruses (148). The controlling factors behind the diversity and evolution of adenoviruses need further investigation by obtaining the whole genome sequence of these Australian isolates. Characterisation of the Australian isolates is also required to understand more about their potential for host switching.

POLYOMAVIRUS

The presence of a polyomavirus in bat urine is not surprising given the tissue tropism of BK virus, a human polyomavirus. While usually caught as a respiratory infection in childhood, it later establishes a latent infection in the urothelium and tubular epithelial cells (154). BK virus is highly prevalent in humans with over 80% of adults seropositive for the virus (155) and up to half of these adults exhibiting viruria of BK virus (156). Although normally asymptomatic, reactivation of BK virus can occur after kidney transplant due to immunosuppression, resulting in interstitial nephritis and allograft failure (154). Due to the differences in the bat immune system, bat polyomaviruses might not establish a completely latent infection of the kidney and the urothelium. Further screening of bat urine at regular intervals would be required to determine if there is periodic reactivation of the virus or constant viruria.

Despite this, urine has not previously been used to detect bat polyomaviruses (152, 161-164). This study indicates that urine is a viable sample for the isolation of polyomaviruses from bats. So far, there is no documented evidence of bat polyomavirus isolation in cell culture from any bat sample

and only genomic characterisations of bat polyomaviruses have been completed and published (152, 161-164). Therefore, this isolation provides a new opportunity for future characterisation of a bat polyomavirus.

The polyomavirus species identified in this chapter has previously been detected in an Indonesian pteropid bat (Table 3.5). Although similar viruses have been detected in Australian and Indonesian pteropid bats, this is the first instance of the same viral species being identified in both countries. The genome of the Indonesian isolate was detected in the spleen of an unidentified species of pteropid bat in the Paguyaman District (161). Due to the lack of a confirmed host species, this virus is yet to be officially classified as a new species by the ICTV. Bat samples collected from the Paguyaman District in previous years indicate that *Pteropus hypomelanus* and close relatives are present in this district (165).

As dsDNA viruses, polyomaviruses have a low level of mutation and substitution, with some strains shown to have identical nucleotide sequences over a range of times and locations (217). However, it has been hypothesised that the virus-host co-evolution of polyomaviruses follows an intrahost divergence model, which allows for transmission between closely related species. This model suggests that viruses diverge faster than host species evolution, resulting in multiple clades of polyomavirus in one host species. (217). Therefore, given the minimal number of nucleotide changes between these two isolates, it is likely that the virus transmission event occurred more recently than the divergence of Australian and Indonesian pteropid bats. This once again raises the question of the likelihood of Nipah virus (NiV) transmitting to Australian bats. NiV has been detected in fruit bat populations within 500 km of Australia (218). It has previously been determined that the risk of NiV introduction into the Australian bat population by a migratory route is medium, although the presence of Hendra virus neutralising antibodies means that the risk of establishment of NiV in the population is less due to cross protection (219).

Pteropid bats, including *Pteropus alecto*, have been shown by satellite telemetry to be able to fly between Australia, Papua New Guinea and Indonesia, with one *P. alecto* travelling >3000 km over the course of 11 months (220). Using the same methods, *P. poliocephalus* have been observed to fly ~1000 km from the initial trapping location over 39 weeks of tracking (221), although its more southern geographical location means this distance is over Australian instead of international borders. It is therefore possible that this polyomavirus has recently transmitted from pteropid bats in Indonesia to Australian flying foxes. Previously, inter-species transmission of polyomaviruses has only been observed for avian polyomaviruses involving captive host animals (217). However, as only

the genus of Pteropus sp. PyV/Bat/2011/Alstonville and Pteropus sp. PyV/Bat/2013/Paguyaman was identified, it remains unconfirmed if interspecies transmission has occurred.

3.4 CONCLUSION

These results build on our knowledge about the vast diversity of viruses in Australian bats. The discovery of diverse paramyxovirus sequences, in addition to the isolation of two paramyxoviruses, multiple adenoviruses and a polyomavirus, could have important public health implications if these viruses spillover into non-pteropid mammalian populations. This knowledge of the primary host of these viruses could enhance recognition and speed up the epidemiological response to viral spillover. As we cannot determine the significance of these viruses based on sequence alone, two isolated paramyxoviruses were selected for *in vitro* and *in vivo* investigation for this thesis.

CHAPTER 4: CHARACTERISATION OF TEVIOT VIRUS, AN AUSTRALIAN BAT-BORNE PARAMYXOVIRUS

This manuscript has been submitted to the Journal of General Virology and is currently under review. It describes the characterisation of a virus, Teviot virus, isolated during the investigation described in Chapter 3 of this thesis.

Page numbers, as well as numbering of figures, tables and sections, have been changed in order to generate a consistent presentation within the thesis.

CHARACTERISATION OF TEVIOT VIRUS, AN AUSTRALIAN BAT-BORNE PARAMYXOVIRUS

Authors: Rebecca I. Johnson[1], Mary Tachedjian[1], Bronwyn A. Clayton[1], Rachel Layton[1], Jemma Bergfeld[1], Lin-Fa Wang[2], Glenn A. Marsh[1]

Affiliations: [1]CSIRO Health and Biosecurity, Australian Animal Health Laboratory, Geelong, Australia

[2]Programme in Emerging Infectious Diseases, Duke-NUS Medical School, Singapore, Singapore

Corresponding author: Glenn Marsh

Keywords: Teviot virus, paramyxovirus, zoonoses, bat-borne

Repositories: The GenBank accession number for the Teviot virus (Alstonville isolate) sequence is MH708896.

4.1 ABSTRACT

Bats are the reservoir hosts for multiple viruses with zoonotic potential including coronaviruses, paramyxoviruses and filoviruses. Urine collected from Australian pteropid bats was assessed for the presence of paramyxoviruses. One of the viruses isolated was Teviot virus (TevPV), a novel rubulavirus previously isolated from pteropid bat urine throughout the east coast of Australia. Here, we further characterise TevPV through analysis of whole-genome sequencing, growth kinetics, antigenic relatedness and the experimental infection of ferrets and mice. TevPV is phylogenetically and antigenically most closely related to Tioman virus (TioPV). Unlike many other rubulaviruses, cell receptor attachment by TevPV does not appear to be sialic-acid dependent, with the receptor for host cell entry unknown. Infection of ferrets and mice suggested TevPV has a low pathogenic potential in mammals. Infected ferrets seroconverted by 10 days post infection without clinical signs of disease. Furthermore, infected ferrets did not shed virus in any respiratory secretions, suggesting a low risk of onward transmission of TevPV. No productive infection was observed in the mouse infection study.

4.2 INTRODUCTION

With the emergence of pathogens occurring at a greater frequency than ever before (2), the discovery and characterisation of novel viruses is important in the prevention of emerging infectious disease outbreaks. In particular, the number of pathogens emerging from wildlife has risen significantly (2). The increased risk of pathogen emergence and infection of non-reservoir hosts (spillover) is attributed to increased urbanisation and higher human population density leading to more contact between humans, livestock and wildlife (2, 3, 16). Bats host a greater proportion of zoonotic viruses than any other mammalian order (3), making them an important target group for a systematic approach to the discovery of viral pathogens. Identifying potentially zoonotic viruses before they emerge can reduce the impact of these viruses, both economically and from a public health perspective, as well as increase our understanding of existing pathogens (16).

Multiple viruses from the family *Paramyxoviridae* have been detected in bats, including Hendra virus and Nipah virus that cause significant disease and fatality in humans (30, 53, 54, 100). This viral family currently contains the genera *Morbillivirus, Henipavirus, Rubulavirus, Respirovirus, Avulavirus, Ferlavirus, and Aquaparamyxovirus,* with a number of viruses yet to be classified (222). Paramyxoviruses are enveloped viruses with a linear negative sense RNA genome. With some variation between genera, the genome encodes at least 6 genes. These are the nucleoprotein (N) gene, phosphoprotein (P) gene, matrix (M) gene, fusion (F) gene, attachment glycoprotein (G, H or HN depending on the enzymatic function of the protein) gene and the large polymerase subunit (L) gene. RNA editing and alternative start sites in the P gene can result in the expression of multiple proteins such as a P, V, W and/or C protein (57).

The genus *Rubulavirus* contains the human pathogens mumps virus and human parainfluenza virus 2, as well as a number of bat-borne viruses, several of which have been associated with zoonotic transmission to humans (57). For example, Menangle virus (MenPV) was identified as the causative agent of an outbreak of reproductive disease in pigs and an influenza-like illness in two humans (131, 132). Sosuga virus was identified after a biologist conducting field work collecting bats and rodents in South Sudan and Uganda developed symptoms including fever, maculopapular rash and oropharynx ulcerations. The virus was then identified in *Rousettus aegyptiacus* fruit bats, suggesting bats were the source of infection (126, 133).

Since the discovery of Hendra virus (HeV), the surveillance of Australian pteropid bats has led to the discovery of multiple novel paramyxoviruses (30). In 2011, there was an unprecedented increase in the number of Hendra virus disease events; 18 spillover events occurred in a single year, compared to 14 events documented between 1994 and 2010 (53). Increased surveillance of pteropid bats

triggered by increased spillover events demonstrated that shedding of Hendra virus from pteropid bats in northern New South Wales and southeast Queensland was more prevalent in 2011 than in previous years (53), making them useful targets for the discovery of novel paramyxoviruses.

In the current study, analysis was carried out on urine collected in 2011 from fruit bats in Alstonville, New South Wales, leading to the isolation of Teviot virus/Bat/2011/Alstonville (TevPV). TevPV has now been isolated 19 times including in Cedar Grove, Queensland, and in Geelong, Victoria (30, 200), making it widespread down the east coast of Australia. Previous study of other isolates of TevPV has revealed its whole genome sequence, its capacity for RNA editing of the P gene to result in the translation of V and P proteins, and its growth in some mammalian cell lines (30, 200). The most recent isolation of TevPV in Alstonville has prompted the current investigation into the ability of this virus to cause pathogenic disease in experimentally infected animals, along with further *in vitro* characterisation.

4.3 RESULTS

4.3.1 ISOLATION OF TEVIOT VIRUS FROM PTEROPID BAT URINE

Fifty-nine pooled urine samples, collected from a combination of *Pteropus alecto* and *P. poliocephalus* bats, were inoculated onto Vero and *P. alecto* kidney (PaKi) cells (171) and monitored for signs of viral cytopathic effect (CPE). One urine sample, collected on the 3rd August 2011 in Alstonville, caused syncytial CPE on day 13 of the first passage, day 6 of the second passage and day 4 of the third passage when inoculated onto PaKi cells. CPE appeared late in the second passage on Vero cells. RT-PCR and Sanger sequencing indicated that the virus was the rubulavirus Teviot virus (TevPV). RNA extracted from the supernatant of the first passage of PaKi cells exposed to the bat urine containing TevPV was used for whole genome sequencing.

4.3.2 WHOLE GENOME SEQUENCING

Whole genome sequencing was conducted to confirm the presence of TevPV and to compare with geographically different isolates of the virus (Fig. 4.1). This was carried out using RNA extracted after pelleting by ultracentrifugation through a 20% sucrose cushion. Consistent with previous TevPV isolates, the genome of the Alstonville isolate was found to be 15522 nucleotides long with a whole genome GC content of 43.4%. This genome satisfies the rule of six, allowing efficient replication (60). The protein coding percentage of the genome is 90%, which is similar to other rubulaviruses (223). Phylogenetic analysis determined that the most closely related paramyxovirus is Tioman virus (TioPV), isolated from pteropid bats in Malaysia during the search for Nipah virus (Table 4.1) (128).

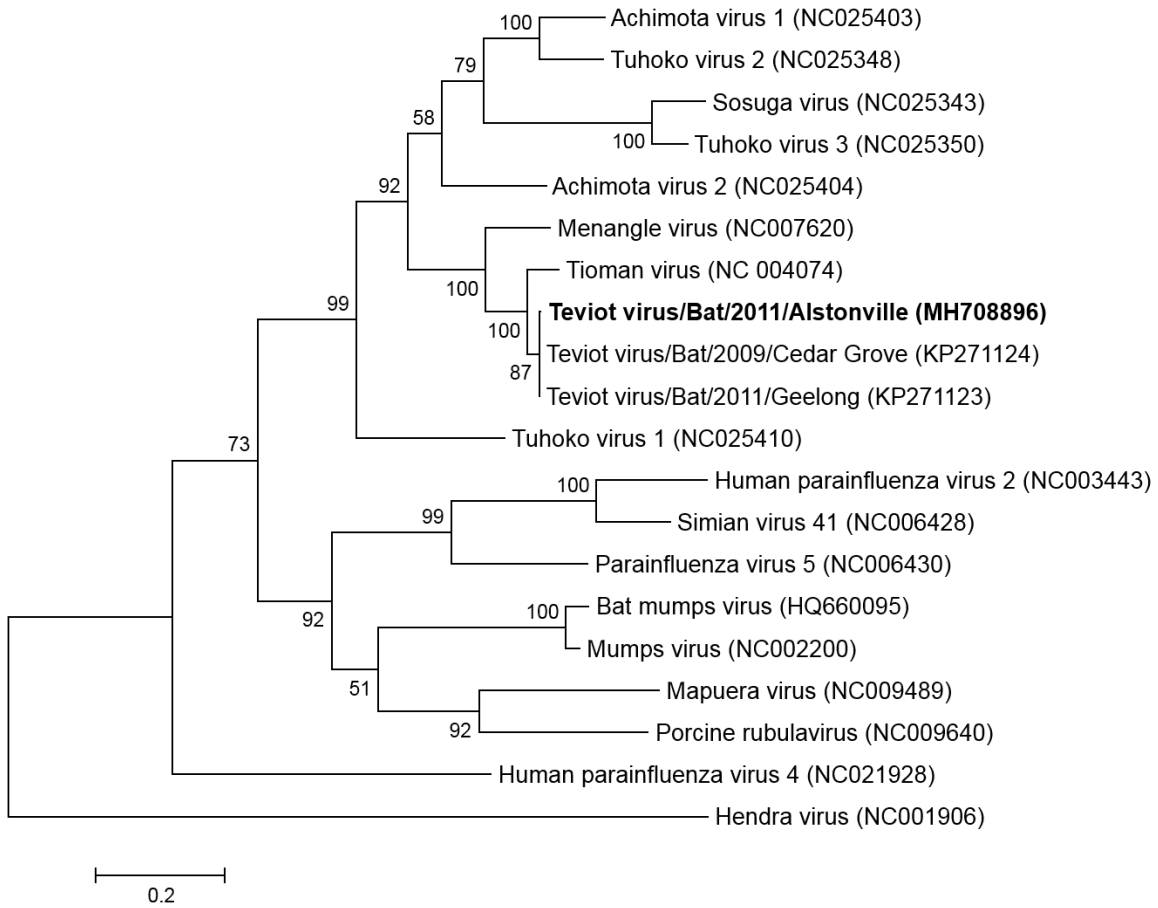

Figure 4.1: Phylogenetic analysis of rubulavirus N proteins. Maximum-likelihood tree constructed with MEGA 6.06, bootstrapping to 1000 replicates. Isolate characterised in this chapter is highlighted in bold. Genbank accession numbers are provided in parentheses.

Table 4.1: TevPV amino acid sequence identity compared to TioPV and MenPV. Sequences aligned and identities calculated by ClustalW alignment in Geneious 10.2.2.

Virus	Percentage amino acid sequence identity						
	N	P	V	M	F	G	L
TioPV	90	72	71	92	83	73	79
MenPV	78	56	59	87	61	51	65

Genome ends were determined by a combination of 5' rapid amplification of cDNA ends (RACE) and sequencing across ligated genome ends. The resulting sequence matched predicted sequences previously inferred from the genome termini of TioPV (200). The leader sequence of TevPV is 55 nucleotides and is highly conserved with other rubulaviruses, while the trailer sequence is 23

nucleotides long and is similar to that of TioPV. The first 15 nucleotides of the leader sequence of the genome are complementary to the 3' terminus of the antigenome.

Similar to TioPV and MenPV, the transcriptional start sites of all TevPV genes begin with a guanine (in the antigenome) and the gene boundaries are conserved (Table S4.1) (61, 62). In comparison, other members of the family *Paramyxoviridae*, including other members of the genus *Rubulavirus*, have adenine at the first position of gene transcription (57). The lengths of the intergenic regions are variable, as are the starting nucleotides of these intergenic sequences, unlike TioPV where all intergenic sequences begin with a cytosine (62).

4.3.3 Analysis of deduced amino acid sequences for key proteins

Teviot virus/Bat/2011/Alstonville was found to be over 99% identical to the two other recorded sequences of TevPV - Teviot virus/Bat/2011/Geelong and Teviot virus/Bat/2009/Cedar Grove. Only 11 amino acid differences were observed in total between the Alstonville isolate and the Geelong isolate, and 14 amino acid (aa) differences between the Alstonville isolate and the Cedar Grove isolate. Consistent with previous isolates, TevPV expresses 8 proteins from 6 genes, with the lengths of coding sequences highly conserved with TioPV (Table 4.2).

Table 4.2: TevPV gene and protein lengths compared to TioPV genes and proteins. Differences between the two viruses are highlighted in bold font.

Gene	Region	Virus	Length (nt)	Length (aa)
3' leader		TevPV	55	
		TioPV	55	
N	CDS	TevPV	1560	519
		TioPV	1560	519
P	V CDS	TevPV	681	226
		TioPV	**687**	**228**
	P CDS	TevPV	1158	385
		TioPV	1158	385
	W CDS	TevPV	636	211
		TioPV	636	211
M	CDS	TevPV	1128	375
		TioPV	**1122**	**373**
F	CDS	TevPV	1617	538
		TioPV	1617	538
G	CDS	TevPV	1788	595
		TioPV	**1782**	**593**
L	CDS	TevPV	6816	2271
		TioPV	6816	2271
5' trailer		TevPV	23	
		TioPV	23	

4.3.3.1 P/V

The gene editing strategy of TevPV was demonstrated to be the same as other rubulaviruses, with the unedited form of the gene encoding the 226 aa long V protein. The addition of 2 non-templated G nucleotides during transcription results in the translation of a P protein of 385 aa in length. Like other paramyxoviruses, the V protein of TevPV has a highly conserved C-terminal domain and has all seven of the conserved cysteines in this domain that have been previously demonstrated to be associated with a zinc binding function (57).

The prevalence of RNA editing per 100000 reads was analysed by amplicon sequencing of the editing site. Three biological replicates were compared to controls, also in triplicate, to eliminate the effect of errors introduced during reverse transcription and PCR amplification of the amplicons. Amplicon sequencing revealed that the transcript remained unedited or had the addition of 3 G residues to maintain the reading frame 66.6% of the time, resulting in the expression of the V protein. The P protein was expressed, on average, from 27.6% of transcripts and the W protein was expressed from 5.9% of transcripts. The majority of these W transcripts were from single G insertions, however approximately 1.7% of transcripts had the insertion of four G residues. Five G insertions could also be detected at a very low prevalence resulting in the expression of the P gene. This is consistent with the editing frequency of the MenPV P gene when analysed by the same method (184).

4.3.3.2 ATTACHMENT GLYCOPROTEIN

The attachment glycoprotein of TevPV is predicted to be a Type 2 transmembrane protein with an N-terminal cytoplasmic domain of 41 aa, however the sequence differs from classical rubulaviruses such as mumps virus and parainfluenza virus 5 (Fig. 4.2a). Specifically, it is less than 20% identical to these rubulaviruses, which is similar to the identity observed when comparing TevPV with other genera of *Paramyxoviridae* (Fig. S4.2). Sequence analysis indicated that, similar to TioPV and MenPV, TevPV is missing the first four residues of a key hexapeptide, NRKSCS. This motif is thought to be part of the neuraminidase active site and is found in many rubulavirus and respirovirus attachment glycoproteins (224, 225). TevPV also only has 2-3 out of seven residues that that are important for neuraminidase function (61, 62, 226).

The attachment glycoprotein of TevPV and other rubula-like viruses also appear to be functionally different to that of classical rubulaviruses. Treatment of Vero cells with sialidase from *Arthrobacter ureafaciens*, which targets α2,3-, α2,6-, and α2,8-linked terminal *N*- or *O*-acylneuraminic acids, resulted in the reduction of viral infection with human parainfluenza virus 2 and parainfluenza virus 5, but not with the rubula-like viruses TevPV and TioPV (Fig. 4.2b). Viral infection with MenPV

increased slightly. The addition of detergent to hydrolyse glycolipids made no difference to viral infection.

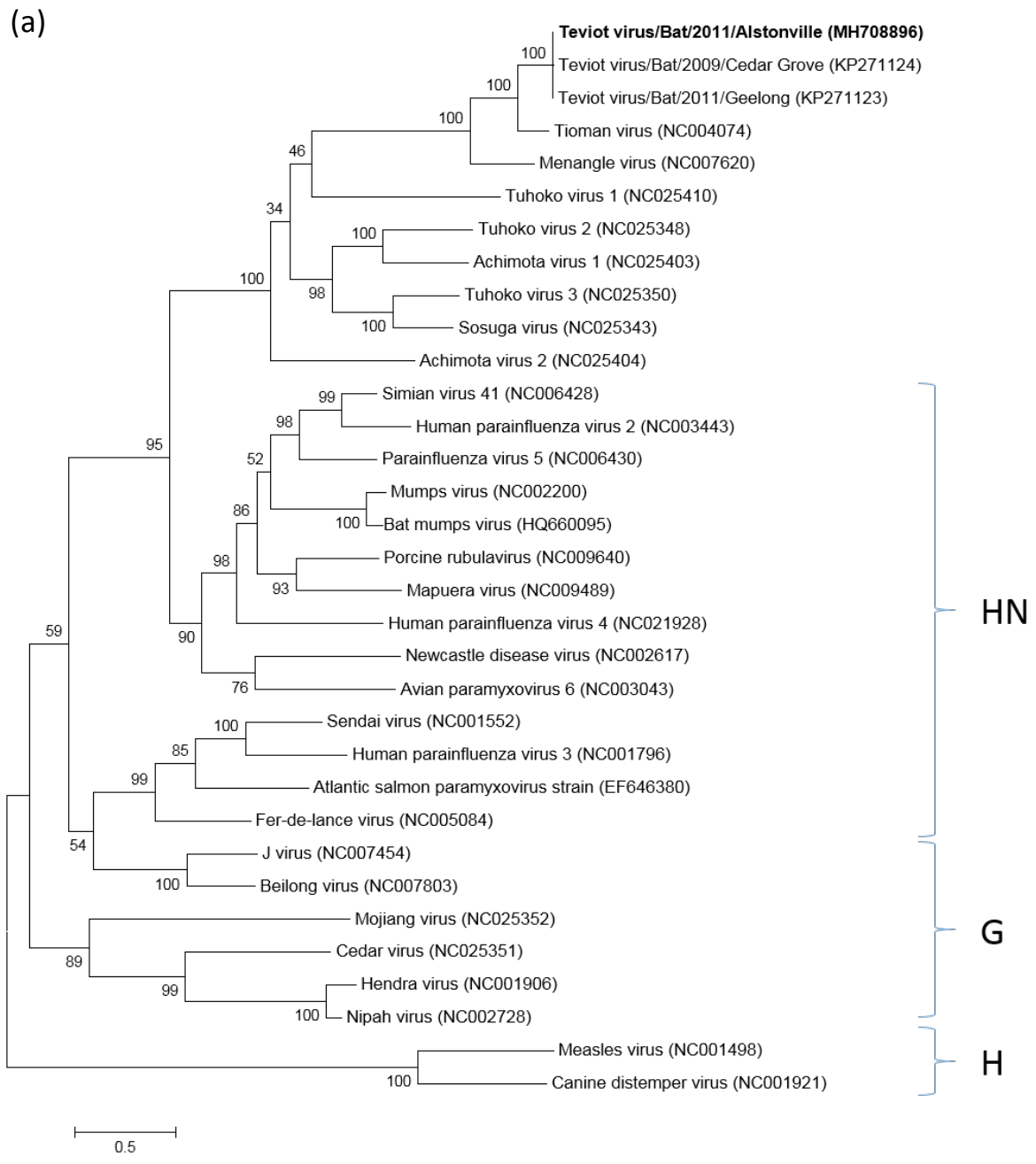

(b)

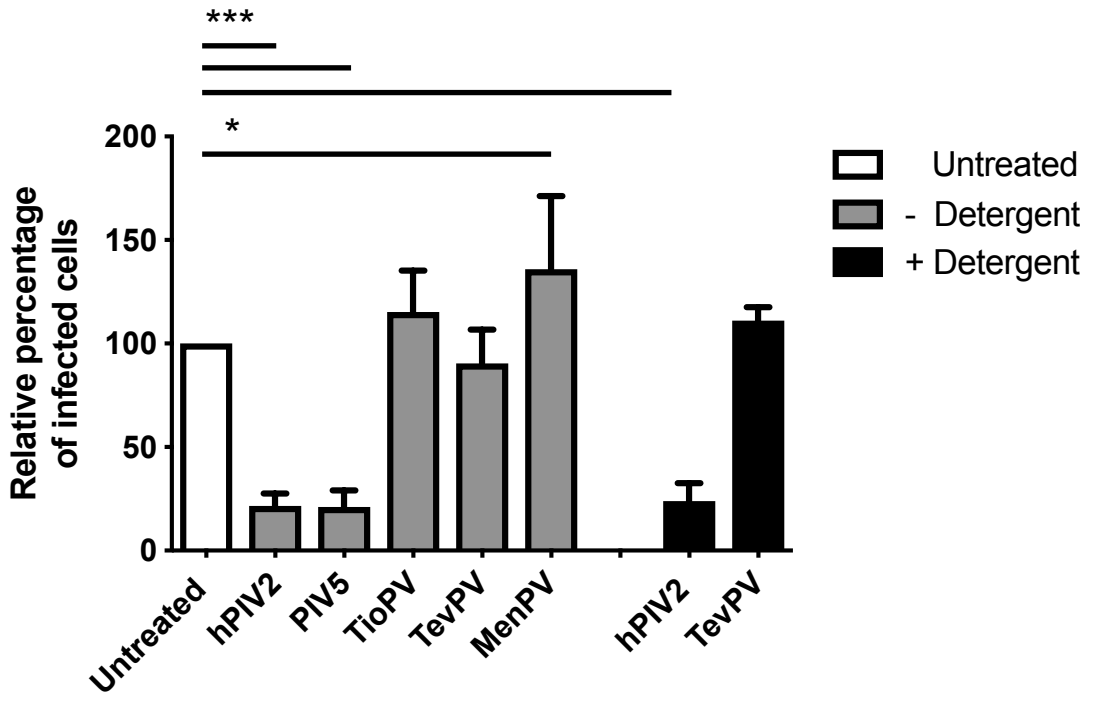

Figure 4.2: Characterisation of the attachment glycoprotein of TevPV. a) Maximum likelihood phylogenetic tree of paramyxovirus attachment glycoproteins, constructed using MEGA 6.06, bootstrapping at 1000 replicates. Genbank accession numbers are provided in parentheses. b) Effect of *Arthrobacter ureafaciens* neuraminidase treatment on rubulavirus infection of Vero cells, with or without treatment with an ionic detergent, sodium deoxycholate. Infected cells were counted in nine fields of view and compared to infected cells not treated with sialidase. Values represent a percentage of the number of infected cells counted in untreated samples. Error bars represent standard deviation. Significance calculated by one-way ANOVA followed by Dunnett's multiple comparison test (compared to untreated cells). *** represents a *p* value of <0.001, * represents a *p* value of <0.05. *n* = 2 independent experiments.

4.3.4 TevPV is antigenically related to Tioman virus

Antibodies from multiple rubulaviruses and antibodies raised against the nucleocapsid protein of Hendra virus were observed to cross-react with TevPV. In comparison, antibodies raised against TevPV in ferrets only bound to MenPV and TioPV (Fig. S4.1), the two rubulaviruses most closely related to TevPV. TioPV and TevPV sera were also cross-neutralising (Table 4.3).

Table 4.3: Cross-neutralising titres of sera generated against TevPV, TioPV and MenPV. Titres represent the reciprocal of the highest dilution of serum at which the infectivity of 100 $TCID_{50}$ of virus is neutralised in 50% of the wells, as calculated using the Reed-Muench method.

Sera from / Infected with	TioPV	TevPV	MenPV
TioPV	**453**	28	<10
TevPV	13	**226**	<10
MenPV	<10	<10	**320**

Sera: ferret TevPV antisera, pig TioPV antisera and pig MenPV antisera; bold numbers indicate homologous sera virus pairs

4.3.5 Seroprevalence study in Australian flying foxes

The prevalence of TevPV in Australian flying foxes was assessed by neutralisation assay and immunofluorescence assay (IFA) using sera collected from Australian flying foxes between 1999 and 2012 (Table 4.4). TevPV was neutralised by 12.5% of the tested sera, however almost two thirds of the sera samples bound TevPV when assessed by immunofluorescence assay, indicating cross-reactivity with a related virus. The prevalence of neutralising antibodies in *P. poliocephalus* sera was 30%.

Table 4.4: Prevalence of neutralising antibodies to TevPV in Australian flying foxes. Sera from pteropid bats collected in Queensland between 1999 and 2007, or Victoria in 2012.

Pteropid bat species	No. positive	Percentage positive
*Pteropus sp.**	7/59	11.9
P. scapulatus	0/15	0
P. alecto	2/26	7.7
P. poliocephalus	6/20	30
Total	**15/120**	**12.5**

*Pteropid bat sera collected in Queensland between 1999 and 2007, species not recorded

4.3.6 TevPV is non-pathogenic in ferrets and mice

To determine the pathogenic potential of TevPV in mammalian species, animal infection studies were carried out in ferrets and mice. Three ferrets, five aged mice and five juvenile mice were exposed to TevPV via the oronasal (ferrets) or intranasal (mice) route and monitored for up to 21 days. Seroconversion was detected by neutralisation assay in all three ferrets on day 10, indicating that infection had occurred (Table 4.5), however, ferrets remained clinically normal with no fever, changes in weight or behaviour until the scheduled day of euthanasia (21 days post infection). Shedding of virus was not detected in ferrets in nasal, oral or rectal swab samples collected over the course of the study. Virus was not detected by qRT-PCR or immunohistochemical analysis in any tissues collected from ferrets following euthanasia.

Table 4.5: TevPV neutralising antibody titres from infected ferrets. Neutralising titres were calculated using the Reed-Muench method.

Ferret No.	Day 7	Day 10	Day 14	Euthanasia
Ferret 1	<10	57	96	101
Ferret 2	<10	100	186	226
Ferret 3	<10	64	135	113

Mice remained clinically normal following intranasal exposure to TevPV. Five mice were euthanised during the predicted peak of infection (one on day 5 and four on day 6) and had no evidence of infection by qRT-PCR or immunohistochemical analysis of various tissues. Remaining mice were euthanised on day 21, at which point there was no detectable neutralising or non-neutralising antibody response.

4.4 DISCUSSION

Bats have been identified as a significant reservoir of zoonotic viruses (3). It has been predicted that with increased urbanisation and the encroachment of humans on bat habitats, the risk of these viruses spilling over and causing disease will increase (3). Bat-borne paramyxoviruses, such as Hendra virus and Nipah virus, can cause significant morbidity and mortality in livestock and humans (7, 100). TevPV has been isolated multiple times from pteropid bats over a range of locations and years (30, 200), suggesting an ongoing risk of human exposures. We demonstrated, through analysis of sequence data and antigenic relatedness that TevPV is most closely related to TioPV. Serological surveillance of humans living in proximity to TioPV-infected flying fox populations showed seroconversion to a Tioman-like virus in a small number of cases, although TioPV infection has not

been attributed to illness in people (129). It was therefore of interest to attempt to characterise the disease-causing potential of TevPV in relevant animal models of paramyxovirus infection.

Although particular viral factors such as cytoplasmic replication, broad host range and low host mortality can indicate a greater likelihood of causing zoonotic infections (3, 227), *in vivo* experiments allow for characterisation of the pathogenic potential of flying fox isolates in non-pteropid mammalian species. To this end, we exposed ferrets to TevPV isolated from flying foxes in Alstonville in 2011. Ferrets developed a neutralising antibody response and had no detectable viral RNA or viral antigen in tissues at 21 days post infection, suggesting oronasal exposure resulted in transient, self-limiting subclinical infection that was cleared following a neutralising host antibody response. While time-course studies would be needed to determine sites of viral replication during early infection of ferrets, virus was not detected in oral or rectal swabs or nasal washes from ferrets sampled over the course of the study, indicating viral replication at sites relevant to transmission did not occur. Mice did not appear to be susceptible to infection with TevPV, indicated by the lack of detectable viral genome or antigen, including in mice euthanised on days 5 and 6 post infection, and absence of a serological response to infection in mice euthanised on day 21 post infection.

Taken together, our findings in ferrets and mice suggest that TevPV may have low pathogenic and transmission potential in non-pteropid mammalian hosts. However, care must be taken in extrapolating these observations to other animals and people. While ferrets are useful models for infection with other paramyxoviruses of significance to human health, the similarity between TevPV, MenPV and TioPV suggests that the infection of pigs with TevPV could provide a better indication of its potential to cause disease in livestock. Experimental infection of pigs with TioPV was characterised by pyrexia between 4-9 days post infection, the production of neutralising antibodies and the presence of TioPV antigen in lymphoid tissues, particularly during acute infection (228). It was proposed that circulating leukocytes were responsible for the dissemination of TioPV. Another closely related bat-borne virus, MenPV, caused a higher rate of birth defects and abortion in pigs, but did not cause disease in post-natal pigs during an outbreak at an Australian piggery. These pigs were thought to act as an intermediate host, leading to the infection of two piggery workers who displayed influenza-like symptoms (132). Further investigation of TevPV infection of pigs or other livestock could also provide a greater understanding of their potential to be an intermediate or amplifying host for the transmission of TevPV to humans.

Instead, ferrets were selected to assess the pathogenic potential of TevPV because they have been shown to be useful models of infection for other paramyxoviruses of significance to human health (193, 229, 230). Mice were selected as they are a useful early experimental model due factors such

as ease of handling (194). Although previous experiments have demonstrated that the closely related TioPV does not cause infection in suckling mice exposed intraperitoneally, age can be a factor in susceptibility to paramyxovirus infection and disease. For example, aged mice more reliably develop encephalitis than juvenile mice when infected with Hendra virus (194), therefore adult and juvenile mice were included in this investigation.

Three isolates of TevPV have now been sequenced with only 11-14 aa differences and 64-101 nt changes observed across the entire genome between the three isolates. This is despite two years and 1400km between the collections of the sources of these isolates. The low number of nucleotide differences between the TevPV isolates indicates that there may be constraining factors preventing high levels of variation. This is seen in studies of other paramyxoviruses where, despite the high error rate of RNA dependent RNA polymerases, the observed sequence diversity of different isolates is very low (213). Multiple factors could influence these low levels of mutation, such as codon usage constraints, nucleocapsid phasing constraints and the suppression of CpG ribonucleotide pairs to reduce recognition by the immune system (213).

Despite the high sequence similarity between TevPV and TioPV, amplicon sequencing of the TevPV RNA editing site indicated a much lower prevalence of P protein expression of 27.6% compared to 50% for TioPV, though the TioPV prevalence was calculated by sequencing only sixty clones of the editing site (128). Analysis of MenPV P gene editing by the same method of amplicon sequencing produces similar results to TevPV (184), indicating the differences may just be due to the low depth of sequencing for the TioPV editing site.

In vitro and *in silico* analysis of the attachment glycoprotein of the rubula-like viruses, TevPV, MenPV and TioPV, indicated that they do not require sialic acid for cell entry and likely lack the ability to bind sialic acid altogether (61, 62). The receptor for these rubula-like viruses remains unknown, although the infection of pigs, bats and, in the case of MenPV, humans, demonstrates that it is likely a conserved receptor. The reduction but not complete ablation of infection by the sialic acid-binding rubulaviruses was similar to that observed after influenza virus infection of desialylated cells. Stray *et al.* hypothesised that this was due to either a sialic acid-independent entry pathway or a multistep pathway involving low affinity binding of sialic acid, which then facilitated higher affinity binding with a secondary receptor (231). This evidence suggests that a new genus needs to be established to reflect the sequence and functional differences. Recently, it has been proposed that these rubula-like viruses be reclassified into a new genus, *Pararubulavirus*, within a new subfamily, *Rubulavirinae* (56).

Cross-reactive antibodies were detected in 65% of tested Australian flying fox sera, indicating that other paramyxoviruses, in particular rubula and rubula-like viruses, are prevalent in these populations. The higher prevalence of TevPV neutralising antibodies in *P. poliocephalus* sera suggests that it is likely to be the primary host species for TevPV. *P. poliocephalus* flying foxes are endemic to southeast Queensland, eastern New South Wales and Victoria (232) and were observed in all the colonies from which TevPV has been isolated.

Enormous sampling efforts are taking place to describe the virome of bats and other animals globally (233). Although detecting novel viruses in bats will increase our understanding of viral diversity, it is necessary that we also continue to isolate and characterise viruses to better understand their potential to cause disease. While our observations in ferrets and mice suggest TevPV poses a low risk of infection causing significant disease or transmission, we cannot rule out this possibility for other animals or people. Furthermore, the repeated isolations from bat colonies around Australia demonstrate a large area for potential spillover, and anthropogenic changes could increase exposure of the virus to other hosts, such as livestock animals, that have greater contact with humans. It is therefore important that we continue to strive for increased understanding of potentially zoonotic viruses, such as TevPV, through ongoing surveillance and discovery efforts in reservoir hosts.

4.5 MATERIALS AND METHODS

4.5.1 PRIMARY CELLS AND CELL LINES

Cell lines used were African green monkey kidney (Vero) cells and primary *Pteropus alecto* kidney (PaKi) cells (171).

4.5.2 CELL CULTURE

Vero cells, MDCK cells, MDBK cells, HeLa cells and PK15a cells were grown in Dulbecco's Modified Eagle Medium (Gibco) supplemented with 10% foetal bovine serum (FBS, Gibco), 100 units/ml penicillin, 100 µg/ml streptomycin and 0.25 µg/ml amphotericin B (Antibiotic-Antimycotic, Gibco), and 7.5mM HEPES (Gibco). PaKi cells were grown in Ham's F12 Nutrient Mixture (Gibco) supplemented as above.

4.5.3 SEQUENCES FOR PHYLOGENETIC ANALYSIS

Virus sequences used in phylogenetic analysis were the Alstonville isolate of Teviot virus (MH708896), Teviot virus (Geelong isolate, KP271123), Teviot virus (Cedar Grove isolate, KP271124), Tioman virus (NC_004074.1), Menangle virus (NC_007620.1), parainfluenza virus 5 (NC_006430.1), human parainfluenza virus 2 (NC_003443.1), Achimota virus 1 (NC_025403), Achimota virus 2 (NC_025404), Beilong virus (NC_007803), Cedar virus (NC_025351), Hendra virus (NC_001906),

human parainfluenza virus 4 (NC_021928), human parainfluenza virus 3 (NC_001796), bat mumps virus (HQ660095), J virus (NC_007454), Mapuera virus (NC_009489), measles virus (NC_001498), mumps virus (NC_002200), simian virus 41 (NC_006428), porcine rubulavirus (NC_009640), Tuhoko virus 1 (NC_025410), Tuhoko virus 2 (NC_025348), Tuhoko virus 3 (NC_025350), Newcastle disease virus B1 (NC_002617), Nipah virus (NC_002728), Sendai virus (NC_001552), Sosuga virus (NC_025343), Atlantic salmon paramyxovirus (EF646380), fer-de-lance virus (NC_005084), canine distemper virus (NC_001921), Mojiang virus (NC_025352) and avian paramyxovirus 6 (NC_003043).

4.5.4 URINE COLLECTION

Pooled urine was collected from plastic drop sheets situated under bat colonies in Lumley Park, Alstonville on 12th July 2011 and 3rd August 2011 as previously described (50). Samples that were negative for Hendra virus by reverse transcription PCR were included in this study. At the time of collection, the Alstonville bat colony comprised approximately 50% *Pteropus alecto* and 50% *Pteropus poliocephalus* flying foxes.

4.5.5 VIRUS ISOLATION

Virus isolations were completed as previously described (124). Pooled urine samples were thawed, centrifuged to remove debris, and then diluted 1:10 in PaKi cell growth media with a double concentration of antibiotics and antimycotic. Diluted samples were added to Vero or PaKi cell monolayers and rocked for 1 h at 37°C. Additional cell culture media was added and the flasks were incubated at 37°C for one week to monitor for signs of viral cytopathic effect (CPE). One ml of supernatant was passed onto Vero and PaKi cell monolayers at one week and again at 2 weeks.

4.5.6 VIRAL RNA EXTRACTION

RNA was extracted using a Viral RNA Isolation Kit (Qiagen) or Direct-zol RNA Miniprep (Zymo) as per manufacturer instructions. A MagMAX-96 Viral RNA Isolation Kit (Applied Biosystems) was utilised for viral RNA extraction from tissues and shedding samples collected from ferrets and mice.

4.5.7 VIRUS IDENTIFICATION

Extracted viral RNA was amplified by hemi-nested PCR using broadly reactive *Paramyxoviridae*-specific primers (172). Reactions were set up using the Superscript III One-Step RT-PCR System (Invitrogen) with a final $MgSO_4$ concentration of 2 mM, then incubated at 60°C for 1 min then 48°C for 30 min for reverse transcription. Reactions were then cycled according to manufacturer's instructions with an annealing temperature of 49°C. First round PCR product was then amplified with the Expand High Fidelity PCR System according to manufacturer's instructions with an annealing

temperature of 49°C. Positive samples were sequenced by Sanger sequencing then identified by BLAST (NCBI).

4.5.8 Whole genome sequencing

Virus stock was prepared for sequencing by incubating a PaKi cell monolayer for 7 days with supernatant from passage 1 of putative TevPV isolation. Virus was pelleted by ultracentrifugation through a 20% sucrose cushion at 35000rpm for 2 h, 4°C, then resuspended in 500 µl of TRIzol Reagent (Invitrogen). Viral RNA was extracted using a Direct-zol RNA Miniprep kit (Zymo Research) with an in column DNAseI digestion, followed by processing with a RNA Clean and Concentrator kit (Zymo Research). Isothermal amplification was conducted using a REPLI-g WTA Single Cell kit (Qiagen) and purified using a Genomic DNA and Concentrator 10 kit (Zymo Research).

DNA was fragmented for 30 min using DS DNA Fragmentase (NEB) without addition of magnesium. Dual-index libraries were prepared using the Accel-NGS 2S DNA Library Kit for Illumina Platforms (Swift Biosciences). Clean-up and double-sided size selection of the PCR amplified libraries with SPRIselect beads (Beckman Coulter) resulted in a library with average size of 367bp (size range 200 to 550bp), as determined using the Agilent Bionalyzer 2100 HS DNA chip. Denatured libraries were sequenced on the 300 cycle MiSeq Reagent kit v2 (Illumina) generating 150 bp paired-end reads.

Illumina FASTQ paired-end reads were imported into CLC Genomics Workbench 8.5.1 and trimmed for size, quality and ambiguous bases. Trimmed reads were mapped to the Cedar Grove isolate of Teviot virus (KP271124) and confirmed by *de novo* assembly.

4.5.9 Confirmation of genome termini

The genome termini were confirmed using a combination of ligation and rapid amplification of cDNA ends (RACE) followed by Sanger sequencing. The 3' terminus was confirmed by ligating the ends of the genome. T4 RNA ligase reaction buffer (NEB) was combined with 20 units of RNasin (Promega), 15 µl viral RNA, denatured at 65°C for 5 min and then cooled on ice. Then 20 units of T4 RNA ligase, 20 units of RNasin, 50 µM ATP and 10% PEG8000 were added to the reaction and incubated at 16°C overnight. The ligated genome ends were amplified by hemi-nested PCR using Superscript III One-Step RT-PCR System with Platinum Taq DNA Polymerase (Invitrogen) and Expand High Fidelity PCR System (Roche) as described above. PCR fragments were gel purified and transformed into pGEM for Sanger sequencing. The 5' terminus was confirmed by rapid amplification of cDNA ends (RACE) adapted from (177). Viral RNA was reverse transcribed with Superscript III First-Strand Synthesis Supermix (ThermoFisher Scientific) according to manufacturer's instructions using a virus specific primer. Viral cDNA was treated by RNase H for 20 min at 37°C, then purified using a NucleoSpin PCR

Clean-up and Gel Extraction kit (Macherey Nagel). Viral cDNA was ligated to a 5'-phosphorylated and 3'-blocked oligonucleotide (5'-GAAGAGAAGGTGGAAATGGCGTTTTGG-3) using T4 RNA Ligase (NEB) at 25°C for 16 h. Two hemi-nested PCRs using an adaptor specific reverse primer and nested virus specific forward primers were set up using a Platinum Taq DNA Polymerase High Fidelity system (Invitrogen). The PCR reactions were set up according to manufacturer's instructions, with an annealing temperature of 50°C for the first PCR and 49°C for the second PCR. Fragments of the correct size were gel purified using a NucleoSpin PCR Clean-up and Gel Extraction kit before Sanger sequencing.

4.5.10 Amplicon sequencing

Amplicon sequencing was adapted from previously described methods (184). Vero cells were infected in triplicate at an MOI of 0.01, followed by total RNA extraction at 72 h post infection. Total cDNA was produced using Superscript III Reverse Transcriptase (Invitrogen) with oligo(dT) primers following the manufacturer's protocol. Short P gene fragments were amplified with primers attached to Nextera adapters using the Expand Hi-fidelity PCR kit (Roche). PCR controls were produced in triplicate by cloning non-edited fragments into pGEM and amplifying the fragments using the Expand Hi-Fi PCR kit (Roche). Reverse transcription controls were produced in triplicate by cloning non-edited fragments into pCAGGS and transfecting the construct into Vero cells using Lipofectamine LTX Reagent (Invitrogen). After 24 h incubation, total RNA was extracted. Reverse transcription and PCR amplification were completed as above. Control and test PCR products were amplified with Nextera adaptor-specific primers and a HiFi HotStart ReadyMix PCR system (Kapa Biosystems). The DNA library was denatured at 96˚C for 2 min before sequencing on a Miseq (Illumina) using a 600-cycle MiSeq Reagent Kit v3 (Illumina). Data was analysed using CLC Genomics Workbench 8.5.1 (Qiagen). Paired end reads were merged, trimmed on size and quality and reads with large deletions and insertions were removed. Basic variant detection, with a minimum frequency output of 0.05%, was conducted and standardised to 100000 reads. Data was confirmed using unmerged, untrimmed or non-standardised read inputs.

4.5.11 Virus titration

The 50% tissue culture infectious dose ($TCID_{50}$) per millilitre of virus stock was determined by conducting serial 10-fold dilutions of virus in Vero cells in a 96-well plate. After 5 days incubation at 37°C, cells were assessed for the presence of cytopathic effect. Titres were then calculated using the Reed-Muench method (191).

4.5.12 IMMUNOFLUORESCENCE

TevPV was inoculated onto Vero cell monolayers in duplicate with an MOI of 0.01 and incubated for 48 h. Cells were fixed with methanol for 15 min at -20°C then blocked with 1% BSA in PBS for 30 min at 37°C. Cells were incubated with primary antibodies for 1 h at 37°C and washed 4 times with PBS-T. Cells were then incubated with either Protein A or anti-rabbit tagged with Alexa Fluor-488 and DAPI for 1 h at 37°C. Cells were imaged using an EVOS FL Cell Imaging System.

4.5.13 NEUTRALISATION ASSAYS

Antibodies were two-fold serially diluted in quadruplicate starting at a 1:10 dilution. Antibodies were then incubated with 100 $TCID_{50}$ of virus for 30 min at 37°C. A suspension of 2 x 10^4 Vero cells per well were added and plates were incubated at 37°C for 5 days while monitoring cells for viral CPE. Neutralising titres were calculated using the Reed-Muench method as the reciprocal of the highest dilution of serum at which the infectivity of 100 $TCID_{50}$ of virus is neutralised in 50% of the wells (192).

4.5.14 AUSTRALIAN FLYING FOX SEROLOGY ASSAY

Sera from 120 Australian pteropid bats were screened for reactivity to TevPV using the immunofluorescence assay described above. Samples were then analysed by neutralisation assay in quadruplicate using a 1:10 dilution of sera. Bat sera were collected between 1999 and 2012 and were obtained for previous studies. All sera were inactivated by incubating at 56°C for 35 min.

4.5.15 ANIMAL EXPERIMENTS

All procedures were approved by the CSIRO Australian Animal Health Laboratory Animal Ethics Committee. Ferrets (n=3), BALB/c mice aged between 6-9 months (n=5) and juvenile BALB/c mice at 8 weeks of age (n=5) were exposed to a 1/10 dilution of virus stock via the oronasal route (ferrets) or the intranasal route (mice) whilst under anaesthesia (ferrets - 0.05 mg/kg medetomidine and 5 mg/kg ketamine; mice 1 mg/kg medetomidine and 75 mg/kg ketamine). The stock was diluted 1/10 to reduce the risk of adverse reactions during virus challenge, while still maximising the likelihood of infection. The inoculum was confirmed by back titration to be 7x10^4 $TCID_{50}$ of TevPV per ferret and 2x10^3 $TCID_{50}$ of TevPV per mouse. Both species were monitored for 21 days for signs of clinical disease and subcutaneous microchip temperature data were recorded daily. Weight data was recorded and nasal washes, oral swabs, rectal swabs and blood were collected from infected ferrets at days 3, 5, 7, 10, 14 and 21 post infection. Sera were collected on days 7, 10, 14 and 21 post infection. Lung, kidney, spleen, brain (olfactory bulb plus 2mm caudal), liver and retropharyngeal lymph node were collected from ferrets following euthanasia. Mice were weighed daily. Lung,

kidney, spleen, brain (olfactory bulb plus 2mm caudal) and liver were collected from mice following euthanasia.

4.5.16 Quantitative RT-PCR

Quantitative RT-PCR was conducted to detect viral RNA using Agpath-ID One-Step RT-PCR reagents (Applied Biosystems). Briefly, 1x AgPath-ID One-Step RT-PCR Mastermix was combined with 300 nM forward primer, 300 nM reverse primer, 100 nM probe, 0.4x RT-PCR Enzyme Mix and H_2O to 20 µl. 18S rRNA was amplified as an internal control using primer concentrations of 50 nM each and probe concentration of 200 nM. Reactions were incubated at 45°C for 10 min and 95°C for 10 min, and then cycled 40 times at 95°C for 15 s and 60°C for 45 s on a QuantStudio6 (Applied Biosystems). Results were analysed using QuantStudio6 software.

4.5.17 Histology

Tissues collected at post mortem examination were assessed for the presence of histopathological lesions and viral antigen following routine hematoxylin and eosin staining and immunohistochemical staining using rabbit polyclonal antisera against MenPV N protein (AAHL Bioassay R&D).

4.5.18 Sialidase assay

Confluent Vero cell monolayers were treated with 15 mU of *Arthrobacter ureafaciens* neuraminidase (Sigma-Aldrich) for 2 h in cell culture media. Culture media was detergent free or contained 0.01% (w/w) sodium deoxycholate (Sigma-Aldrich). Cells were washed 2x with PBS and incubated with virus (MOI 2) in duplicate for 1 h. Cells were then washed four times with PBS and incubated for 24 h in cell culture media, before fixing and immunofluorescence staining as above. Cells were viewed on an ImageXpress Micro XLS Widefield High-Content Analysis System (Molecular Devices). Fluorescent cells were counted in nine fields of view per well and compared to infected cells not treated with sialidase. The relative number of infected cells was compared by one-way ANOVA followed by Dunnett's multiple comparison test (compared to untreated cells) using GraphPad Prism 5.

FUNDING INFORMATION

This work was supported by an Australian Government Research Training Program Scholarship (R.I.J.) and CSIRO internal funding.

ACKNOWLEDGEMENTS

We thank Brian Shiell, Susanne Wilson and Gary Beddome for the production of the TioPV and MenPV N protein antisera. We are grateful to Jenn Barr, Shawn Todd and Ina Smith for their technical assistance; Jean Payne and Jenni Harper for preparation of tissue samples for

histopathologic and immunohistochemical assessment; and Hume Field and his team for their support with the field work. We are also thankful to Brenton Rowe, Jessica Haining and Sarah Riddell for their work with the animal study.

CONFLICTS OF INTEREST

The authors declare that there are no conflicts of interest.

4.6 SUPPLEMENTARY MATERIAL

Table S4.1: Comparison of genomic features of TevPV and TioPV. Nucleotide sequences of transcriptional start and stop signals, untranslated region (UTR) lengths and intergenic region lengths (IGR) are compared. Differences between the two viruses are highlighted in bold font.

			Length	Boundary Sequence
N	5’ UTR	TevPV	109	GAGCCCAGAAG
		TioPV	109	GAGCCCAGAAG
	3’ UTR	TevPV	119	TAAGAAAAAA
		TioPV	119	TAAGAAAAAA
	IGR	TevPV	41	
		TioPV	41	
P	5’UTR	TevPV	148	GAGCCCGAAC
		TioPV	148	GAGCCCGAA**t**
	3’UTR	TevPV	157	TAATAAAAAA
		TioPV	**151**	TAA**g**AAAAAA
	IGR	TevPV	8	
		TioPV	8	
M	5’UTR	TevPV	35	GGGTCCGAAC
		TioPV	35	GGGTCCGAAC
	3’UTR	TevPV	253	TAAGAAAAAA
		TioPV	**220**	TAA**t**AAAAAA
	IGR	TevPV	2	
		TioPV	**35**	
F	5’ UTR	TevPV	74	GAGCCCGGAA
		TioPV	74	GAGCCCG**a**A**c**
	3’ UTR	TevPV	86	AAAGAAAAAA
		TioPV	**84**	**tt**A**agg**AAAA
	IGR	TevPV	40	
		TioPV	**55**	
G	5’ UTR	TevPV	55	GGGCCCGAAC
		TioPV	55	G**a**GCCCGA**ct**
	3’ UTR	TevPV	120	TAAGAAAAAA
		TioPV	**137**	TAAGAAAAAA
	IGR	TevPV	82	
		TioPV	**70**	
L	5’ UTR	TevPV	8	GGGCCAGA
		TioPV	8	GGGCCAGA
	3’ UTR	TevPV	42	TAATAAAAAAA
		TioPV	42	TAA**g**AAAAAAA

Table S4.2: Amino acid sequence comparison of TevPV with selected paramyxoviruses.

	Virus	Percentage amino acid sequence identity						
		N	P	V	M	F	G	L
	TioPV	90	72	71	92	83	73	79
	MenPV	78	56	59	87	61	51	65
Rubulaviruses	SosPV	58	35	33	57	42	29	55
	AchPV2	68	40	34	57	43	26	58
	ThkPV1	61	35	35	56	45	24	55
	PIV5	46	31	30	37	36	19	49
	MuV	49	26	25	46	36	19	51
	PorV	48	28	21	46	37	17	48
	MapV	45	25	21	46	37	17	49
	hPIV2	41	27	25	37	34	18	48
	hPIV4	43	22	19	47	33	17	47
Non-rubulaviruses	HeV	26	8	8	19	23	14	27
	NiV	26	8	9	18	24	14	27
	CedPV	25	5	-	17	25	15	24
	JV	23	12	15	19	25	15	28
	BeiPV	23	11	12	18	24	16	27
	NDV	31	19	21	27	31	17	25
	MeV	24	10	14	19	23	10	28
	hPIV3	18	6	-	18	24	16	28
	SeV	17	8	11	17	24	16	27

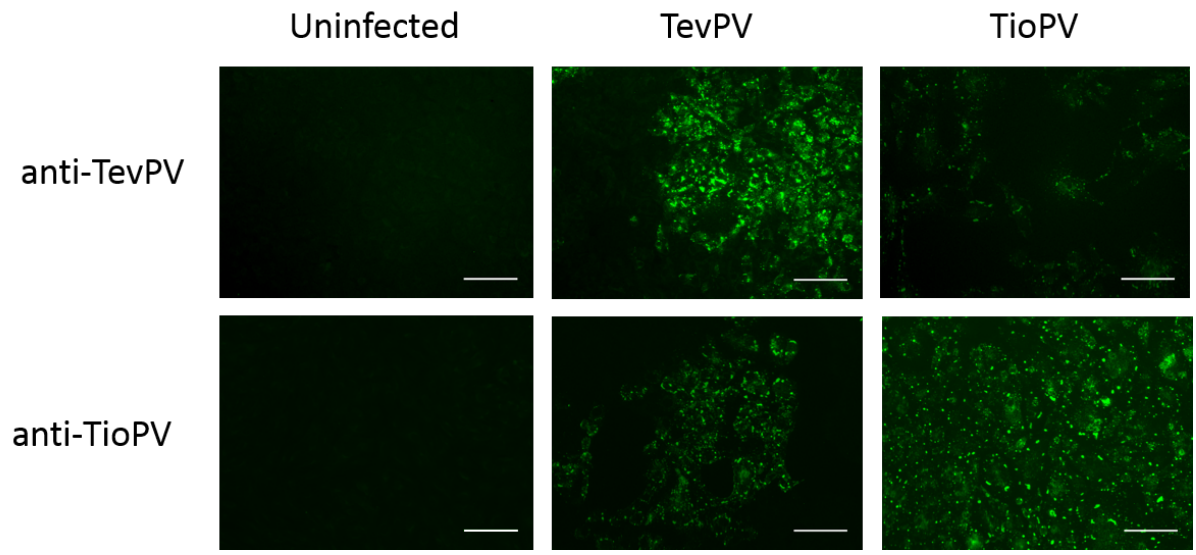

Figure S4.1: Antigenic cross-reactivity between TevPV and TioPV. Vero cells were infected TevPV or TioPV and stained with either rabbit sera raised against recombinant N proteins of TioPV or with ferret sera resulting from infection with TevPV. Magnification X20; scale bar = 100 µm.

CHAPTER 5: ALSTON VIRUS, A NOVEL PARAMYXOVIRUS ISOLATED FROM BATS CAUSES UPPER RESPIRATORY TRACT INFECTION IN EXPERIMENTALLY CHALLENGED FERRETS

This manuscript has been submitted to Viruses and is currently under review. It describes the characterisation of a virus, Alston virus, isolated during the investigation described in Chapter 3 of this thesis.

Page numbers, as well as numbering of figures, tables and sections, have been changed in order to generate a consistent presentation within the thesis.

Article

Alston virus, a novel paramyxovirus isolated from bats causes upper respiratory tract infection in experimentally challenged ferrets

Rebecca I. Johnson[1], Mary Tachedjian[1], Brenton Rowe[1], Bronwyn A. Clayton[1], Rachel Layton[1], Jemma Bergfeld[1], Lin-Fa Wang[2], Glenn A. Marsh[1,*]

[1] CSIRO Health and Biosecurity, Australian Animal Health Laboratory, Geelong, Australia; rebecca.johnson@csiro.au, mary.tachedjian@csiro.au, brenton.rowe@csiro.au, bronwyn.clayton@ecodev.vic.gov.au, rachel.layton@csiro.au, jemma.bergfeld@csiro.au,

[2] Programme in Emerging Infectious Diseases, Duke-NUS Medical School, Singapore, Singapore; linfa.wang@duke-nus.edu.sg

* Correspondence: glenn.marsh@csiro.au; Tel.: +613-5227-5125

Abstract: Multiple viruses with zoonotic potential have been isolated from bats globally. Here we describe the isolation and characterisation of a novel paramyxovirus, Alston virus (AlsPV), isolated from urine collected from an Australian pteropid bat colony in Alstonville, New South Wales. Characterisation of AlsPV by whole-genome sequencing and analysing antigenic relatedness revealed it is a rubulavirus that is closely related to parainfluenza virus 5 (PIV5). Intranasal exposure of mice to AlsPV resulted in no clinical signs of disease, although viral RNA was detected in the olfactory bulbs of two mice at 21 days post exposure. Oronasal challenge of ferrets resulted in subclinical upper respiratory tract infection, viral shedding in respiratory secretions, and detection of viral antigen in the olfactory bulb of the brain. These results imply that AlsPV may be similar to PIV5 in its ability to infect multiple mammalian host species. This isolation of a novel paramyxovirus with the potential to transmit from bats to other mammalian species reinforces the importance of continued surveillance of bats as a source of emerging viruses.

Keywords: Paramyxovirus, bat-borne, zoonoses

5.1 INTRODUCTION

Bats are the source of multiple zoonotic viruses including SARS coronavirus (25), Hendra virus (53), Nipah virus (100) and Marburg virus (27). In fact, evidence suggests that bats host a greater proportion of zoonotic viruses than any other mammalian order (3), highlighting the importance of identifying novel viruses in bats. Australian pteropid bats are becoming more urbanised and fewer bats are migrating, resulting in a greater chance of contact between bats and humans or domestic animals (17, 45). This increased potential for exposure of non-reservoir hosts to bat-borne viruses leads to the increased probability of infection spillovers occurring (18, 19).

Isolation and phenotypic characterisation should be critical components of virus discovery programs because the analysis of novel viral sequences is not currently enough to predict the likelihood of that virus causing a zoonotic disease event (24). The likelihood of viral emergence and sustained human-human transmission is influenced by many factors. In addition to environmental factors and host behaviours, specific viral traits and host-pathogen interactions play important roles. For example, low viral pathogenicity resulting in low host mortality influences opportunities for sustained viral transmission; viral tissue tropism and host immune responses determine shedding at sites relevant to transmission; and the establishment of chronic or latent infection may allow for sustained or recurrent viral shedding (227).

Paramyxoviridae is a family of negative strand RNA viruses currently comprising seven genera - *Rubulavirus, Henipavirus, Respirovirus, Morbillivirus, Ferlavirus, Aquaparamyxovirus* and *Avulavirus* (222). PCR and virus isolation have been used to identify many paramyxoviruses in bats globally, in particular henipaviruses and rubulaviruses (30, 54). The genus *Rubulavirus* contains the human pathogens parainfluenza virus 2 (hPIV2) and mumps virus (MuV), as well as bat-borne viruses such as Mapuera and Menangle viruses (MapV and MenPV). Viruses within this genus have a cell attachment glycoprotein with neuraminidase and haemagglutinin capability (88). In addition to the cell attachment glycoprotein (HN), the rubulavirus genome also encodes a nucleoprotein (N), phosphoprotein (P), V protein, matrix (M) protein, fusion (F) protein and a large polymerase subunit (L) (57). The unedited P gene transcript encodes the V protein, whereas the addition of two non-templated G residues by co-transcriptional stuttering of the RNA-dependent RNA polymerase is required for the expression of the phosphoprotein (57). MuV and parainfluenza virus 5 (PIV5) also express a short hydrophobic (SH) protein that has been associated with blockage of the TNFα-mediated apoptosis pathway (73).

PIV5 is most well known as one of the causative agents of Canine Infectious Respiratory Disease Complex (CIRDC), where infection results in self-limiting tracheobronchitis that resolves in 6-14 days when in the absence of any co-infections (114). Since the discovery of PIV5 in monkey kidney-cell culture in 1954 (234), it has been isolated from a wide range of host species including pigs and cattle (118, 235).

Here we describe the isolation of a novel rubulavirus that we have called Alston virus (AlsPV). AlsPV is closely related to PIV5 and was isolated from pteropid bat urine collected in Alstonville, New South Wales in 2011. A 500 nt sequence that appears to be derived from AlsPV was previously detected by PCR in pteropid bat urine collected in Geelong, Victoria (236), however, this is the first isolation of this novel virus. This paper describes the characterisation of this virus in order to confirm its classification as a rubulavirus, as well as to determine its pathogenic potential.

5.2 MATERIALS AND METHODS

5.2.1 CELL CULTURE

Cell lines used in the characterisation of AlsPV were African Green Monkey (Vero) cells (ATCC), primary *Pteropus alecto* kidney (PaKi) cells (171), Madin-Darby Canine Kidney (MDCK) cells (CSL Ltd), Madin-Darby Bovine Kidney (MDBK) cells (ATCC), porcine kidney (PK15a) cells (National Animal Disease Centre, Iowa, USA) and human cervical (HeLa) cells (ATCC).

With the exception of PaKi cells, all other cell lines were grown in Dulbecco's Modified Eagle's Medium (DMEM, Gibco) supplemented with 10% foetal bovine serum (FBS, Gibco), 100 units/ml penicillin, 100 µg/ml streptomycin and 0.25 µg/ml amphotericin B (Antibiotic-Antimycotic, Gibco), and 7.5mM HEPES (Gibco). PaKi cells were grown in Ham's F12 Nutrient Mixture (Gibco) supplemented as above for normal cell culture media.

5.2.2 VIRUS ISOLATION

For isolations, cells were cultured in Ham's F12 Nutrient Mixture (Gibco), supplemented as above except for the Antibiotic-Antimycotic that was added at double the normal strength. Virus isolations were conducted using pooled bat urine collected from pteropid bat colonies in Alstonville, New South Wales on the 12th July 2011 and 3rd August 2011. Urine collection was conducted as previously described (50). Urine was clarified, diluted and incubated with confluent Vero or PaKi cell monolayers as previously described (124). Cell monolayers were observed for at least one week for evidence of virus-induced cytopathic effect (CPE). Supernatants were further passaged onto fresh Vero and PaKi cell monolayers weekly for another two weeks and observed for signs of CPE.

Isolated paramyxoviruses were initially identified using hemi-nested PCR with degenerate primers following protocols described previously (172), followed by Sanger sequencing of the PCR products.

5.2.3 VIRUSES

In addition to Alston virus, viruses used for *in vitro* analysis included Teviot virus/Bat/2011/Alstonville (TevPV), porcine rubulavirus (PorV), Mapuera virus (MapV), Tioman virus (TioPV), Menangle virus (MenPV) and Hendra virus (HeV). The following reagents were obtained through BEI Resources, NIAID, NIH: human parainfluenza Virus 2 (hPIV2), Greer, NR-3229; parainfluenza virus 5 (PIV5), 21005-2WR (Tissue Culture Adapted), NR-42515; and mumps virus (MuV), Enders, NR-3846.

The GenBank accession number for the Alston virus sequence is MH972568. Virus sequences used in phylogenetic analysis Teviot virus (KP271123), Tioman virus (NP665871), Menangle virus

(AFY09794), parainfluenza virus 5 (YP138518), human parainfluenza virus 2 (X57559), Achimota virus 1 (JX051319), Achimota virus 2 (AFX75118), human parainfluenza virus 4 (AB543336), bat mumps virus (HQ660095), Mapuera virus (EF095490), mumps virus (NP054714), simian virus 41 (X64275), porcine rubulavirus (BK005918), Tuhoko virus 1 (ADI80715), Tuhoko virus 2 (GU128081), Tuhoko virus 3 (GU128082), Sosuga virus (AHH02041), and Hendra virus (NP047113).

5.2.4 PARAINFLUENZA VIRUS 5 SEQUENCES

Parainfluenza virus 5 strains used in the analysis of AlsPV included 1168 (KC237064), ZJQ-221 (KX100034), SER (JQ743328), BC14 (KM067467), CC-14 (KP893891), W3A (JQ743318), KNU-11 (KC852177), AGS (KX060176), CPI- (JQ743320), CPI+ (JQ743321), 78524 (JQ743319), H221 (JQ743323), 08-1990 (KC237063), D277 (KC237065), DEN (JQ743322), LN (JQ743324), RQ (JQ743327), MEL (JQ743325), and MIL (JQ743326).

5.2.5 SEQUENCING

5.2.5.1 WHOLE-GENOME SEQUENCING

Supernatant of AlsPV infected Vero cells was prepared for sequencing by ultracentrifugation through a 20% sucrose cushion at 35000 rpm for 2 h at 4°C. Total RNA was extracted from the resulting pellet using a Direct-zol RNA Miniprep kit (Zymo), including an in column DNaseI digestion, and purified by an RNA Clean and Concentrator kit (Zymo). A REPLI-g WTA Single Cell kit (Qiagen) was utilised for isothermal amplification, followed by processing with a Genomic DNA and Concentrator 10 kit (Zymo). Fragmentation and dual-index library preparation were conducted using Nextera XT DNA Library Preparation kit (Illumina), and denatured libraries were sequenced using a 300-cycle MiSeq Reagent kit v2 (Illumina). 100000 paired-end reads were imported into the VirAMP Galaxy pipeline, trimmed and assembled using the SPAdes de novo assembly algorithm (180, 181). The genome sequence was iteratively extended by mapping trimmed reads back to the parainfluenza virus 5 genome (NC_006430). Genome ends and regions of high variability were confirmed by Sanger sequencing.

5.2.5.2 CONFIRMATION OF GENOME TERMINI

Ligation of genome ends was used to enable sequencing of the 3’ terminus, adapted from a protocol previously developed for influenza virus sequencing (183). Genome ends were ligated overnight at 16°C using 20 U T4 RNA Ligase, 20 U RNasin, 50 µM ATP, 10% PEG8000 and T4 RNA ligase reaction buffer (NEB). Ligation was followed by hemi-nested PCR amplification using a Superscript III One-Step RT-PCR System with Platinum Taq DNA Polymerase (Invitrogen), then an Expand High Fidelity PCR System (Roche).

The rapid amplification of cDNA ends (RACE) (177) was required to determine the 5' terminus, with some adaptations made to the original method. Briefly, viral RNA was reverse transcribed using a virus specific primer and the Superscript III First-Strand Synthesis Supermix (ThermoFisher Scientific). Viral cDNA was RNase H digested, followed by processing with a NucleoSpin PCR Clean-up and Gel Extraction kit (Macherey Nagel). Viral cDNA was ligated to an oligonucleotide adaptor (5'-GAAGAGAAGGTGGAAATGGCGTTTTGG-3') overnight at 16°C using T4 RNA Ligase (NEB) and amplified by hemi-nested PCR using Platinum Taq DNA Polymerase High Fidelity system (Invitrogen) with virus specific primers and an adaptor specific primer. Fragments of the correct size were purified before sequencing by standard Sanger methods.

5.2.5.3 AMPLICON SEQUENCING

Amplicon sequencing of the RNA editing site within the P gene was conducted on RNA extracted from Vero cells infected with AlsPV for 72 h in triplicate. RNA was reverse transcribed using oligo(dT) primers with Superscript III Reverse Transcriptase (Invitrogen). Fragments containing the RNA editing site were amplified using an Expand High Fidelity PCR System with primers containing Nextera adaptors, (5'-TCGTCGGCAGCGTCAGATGTGTATAAGAGACAGCCCAACCCTCTACTTGGCTTGGATTC-3') and (5'-GTCTCGTGGGCTCGGAGATGTGTATAAGAGACAGGCCGGGTATCCATCCCTCTCACTG-3'). Controls were included in triplicate to account for the mutation rate of the reverse transcriptase and the polymerase. PCR controls were produced by amplifying pCAGGS constructs containing non-edited fragments with an Expand High Fidelity PCR System. Reverse transcription controls were produced by transfecting constructs containing non-edited fragments into Vero cells for 24 h using Lipofectamine LTX Reagent (Invitrogen), followed by total RNA extraction, reverse transcription and PCR amplification. All PCR products were amplified with Nextera adaptor-specific primers using a HiFi HotStart ReadyMix PCR system (Kapa Biosystems). The DNA library was sequenced using a 600-cycle MiSeq Reagent Kit v3 (Illumina). Data were analysed using CLC Genomics Workbench 8.5.1 (Qiagen) basic variant detection tool with a minimum frequency output of 0.05%. The prevalence of editing was standardised per 100000 reads.

5.2.6 VIRUS QUANTIFICATION

10-fold serial dilutions of virus stocks were combined with Vero cells in 96-well plates to determine the 50% tissue culture infectious dose per millilitre ($TCID_{50}$/ml). Virus titres were calculated using the Reed-Muench method (191).

5.2.7 GROWTH KINETICS ASSAY

Comparative growth analysis in multiple mammalian cell lines was conducted as described previously (30). Briefly, confluent cells were inoculated with AlsPV at an MOI of 0.01 and incubated

for 1 h at 37°C. Cells were washed four times with PBS and cell culture media was added. Infected cells were incubated at 37°C and aliquots were taken every 24 h for 6 days. Virus titres were determined as above.

5.2.8 IMMUNOFLUORESCENCE ASSAY

Confluent Vero cells were infected with virus at an MOI of 0.01 and incubated for 2-3 days at 37°C. Cells infected with Hendra virus at an MOI of 0.5 were incubated at 37°C for 24 h under BSL4 conditions. Infected cells were fixed with ice-cold methanol for 15 min, or 30 min for cells infected with Hendra virus, before blocking with 1% BSA at 37°C for 30 min. Cells were incubated with primary antibody for 1 h at 37°C and washed four times with PBS-T. Following this, cells were incubated for 1 h at 37°C with a secondary antibody, either Protein A-Alexa Fluor 488 or anti-rabbit-Alexa Fluor 488, and DAPI. Cells were washed four times with PBS-T before imaging using an EVOS FL Cell Imaging System.

5.2.9 NEUTRALISATION ASSAY

Paramyxovirus sera were first inactivated by incubating at 56°C for 35 min. A volume of 100 $TCID_{50}$ of AlsPV or other paramyxoviruses were incubated with two fold dilutions of various paramyxovirus sera or AlsPV ferret sera for 30 min at 37°C. A suspension of $2x10^4$ Vero cells was added to each well, and plates were incubated for 5-7 days and then assessed for the presence of CPE. Neutralising titres were calculated using the Reed-Muench method as described previously as the reciprocal of the highest dilution of serum at which the infectivity of 100 $TCID_{50}$ of virus is neutralised in 50% of the wells (192).

5.2.10 AUSTRALIAN FLYING FOX SEROLOGY

Australian pteropid bat sera, collected between 1999 and 2012, were inactivated by treating at 56°C for 35 min. Sera at a 1:10 dilution were incubated in quadruplicate with 100 $TCID_{50}$ AlsPV for 45 minutes before the addition of a suspension of $2x10^4$ Vero cells per well. Plates were incubated for 7 days before being assessed for the presence of virus-induced CPE.

5.2.11 ANIMAL EXPERIMENTS

All procedures were approved by the CSIRO Australian Animal Health Laboratory Animal Ethics Committee. Study 1, project number 1814, was approved in August 2016. Study 2, project number 1865, was approved in June 2017.

5.2.11.1 STUDY 1:

Female ferrets (n=3) were exposed oronasally to $7x10^5$ $TCID_{50}$ AlsV in 1 ml sterile PBS. Adult female BALB/c mice aged between 6-9 months (n=5) and juvenile (8 week old) female BALB/c mice

(n=5) were exposed intranasally to $2x10^4$ $TCID_{50}$ AlsV in 30 µl sterile PBS whilst under anaesthesia (ferrets - 0.05 mg/kg medetomidine and 5 mg/kg ketamine; mice 1 mg/kg medetomidine and 75 mg/kg ketamine). Ferrets were approximately one year old and had a mean weight of 890g. Virus stock used for animal challenge was diluted 1/10 to reduce the risk of adverse reactions during virus challenge, while still maintaining a high enough dose to maximise the likelihood of infection. The challenge dose of inocula were confirmed by back titration.

Animals were monitored for clinical signs of disease for 21 days following challenge. Oral swabs, nasal washes, rectal swabs and EDTA-treated whole blood samples were collected from ferrets on days 3, 5, 7, 10 and 14 days post-infection and again at euthanasia on day 21. Sera were also collected from ferrets on day 7 onward and urine was collected at euthanasia. Weight, rectal temperature and body temperature measurements were collected from ferrets at each sampling event. Weight and microchip temperature were measured daily for mice.

Tissues collected at euthanasia for assessment by both virus isolation and qRT-PCR were lung, kidney, spleen, brain (olfactory bulb plus 2mm caudal) and liver from mice; and lung, kidney, spleen, brain (olfactory bulb plus 2mm caudal), liver and retropharyngeal lymph node from ferrets. Tissues were fixed in 10% neutral buffered formalin for histology analysis.

5.2.11.2 STUDY 2:

Female ferrets (n=12), approximately one year old with a mean weight of 800g, were exposed to $7x10^5$ $TCID_{50}$ AlsV as for study 1. Three ferrets were euthanised on each of days 3, 5, 7 and 10 post-inoculation, based on random allocation of a time point for euthanasia.

Microchip temperature was recorded daily from all animals following challenge. On the day of euthanasia, oral swabs, nasal washes, rectal swabs, urine and blood were collected from each ferret, and weight and rectal temperature measurements recorded. Tissues collected for the detection of virus by isolation and quantitative RT-PCR were brain (olfactory bulb plus 2mm caudal), nasal turbinates, tonsil, trachea, peripheral lung, hilar lung, spleen, kidney, liver, heart, small intestine, large intestine, bronchial lymph node and retropharyngeal lymph node. Tissues were also stored in 10% neutral buffered formalin for histology analysis.

5.2.11.3 ANALYSIS OF ANIMAL INFECTION STUDY SAMPLES

RNA was extracted from swab, EDTA-blood and homogenised tissue samples using MagMAX-96 Viral RNA Isolation Kit (Applied Biosystems) and analysed by quantitative RT-PCR. RNA was amplified with AgPath-ID One-Step RT-PCR Reagents (Applied Biosystems) using primers and probe targeting a region in the viral nucleocapsid gene – AlsPV-N287F (5'-AATCCCGAGCTACGTTCAAAACT-3'), AlsPV-N360R (5'-TGGGAGTCACGAGCTCCATT-3'), AlsPV N-311-FAM (5'- FAM-CTGCTATTTTGCCTACGCATTGTGCTGA-TAMRA-3') - and 18S as an internal control – 18S-F (5'-

GGCCCTGTAATTGGAATGAGTCCA-3'), 18S-R (5'-GCTGGAATTACCGCGGCT-3'), 18S-VIC (5'-VIC - TGCTGGCACCAGACTTGCCCTC - TAMRA-3'). Reactions were incubated at 45°C for 10 min and 95°C for 10 min, and cycled 40 times at 95°C for 15 s and 60°C for 45 s on a QuantStudio6 (Applied Biosystems). Copy numbers were calculated using standard curves generated by serially diluting RNA transcribed from control DNA plasmids. To facilitate data interpretation, copy numbers of 5 in both qRT-PCR replicates, correlating with a C_T value of 40 (study 1) or 37.4 (study 2) were used as the minimum of detection. Viral N gene copy numbers in tissue samples were standardised to 18S expression (per 10^{10} copies of 18S RNA). Viral N gene copy numbers in shedding samples were calculated per millilitre of sample. Results were analysed using QuantStudio6 software. For virus isolation and titration, 10-fold serial dilutions of clinical samples or homogenised tissue were made in 96-well plates. A suspension of $2x10^4$ Vero cells was added to each well and plates were incubated at 37°C for 7 days before assessing for signs of CPE. Titres were calculated using the Reed-Muench formula (191).

5.2.11.4 HISTOLOGY

Tissues were fixed in 10% neutral buffered formalin, and then trimmed and processed using routine histological methods as previously described (237). Sections were assessed for the presence of histopathological lesions and viral antigen following routine haematoxylin and eosin staining and immunohistochemical staining using rabbit antibodies raised against a recombinant AlsPV N protein peptide (Genscript).

5.2.12 ANTIBODIES

AlsPV polyclonal antibodies were generated in rabbits by Genscript (USA) using the peptide CRQQGRINPRYLLQP from the AlsPV N protein. AlsPV ferret antisera produced in the animal infection trials described in this study were also utilised. Other primary antibodies included rabbit or pig antisera against MenPV (AAHL), rabbit or pig antisera against TioPV (AAHL), TevPV ferret antisera (AAHL), rabbit or horse antisera against HeV (AAHL), PorV rabbit antisera (AAHL) and MapV rabbit antisera (AAHL). Polyclonal anti-PIV5, 21005-2WR (antiserum, guinea pig), NR-3232, polyclonal anti-mumps virus, Enders (antiserum, guinea pig), NR-4019 and polyclonal anti-hPIV2, Greer, (antiserum, guinea pig), NR-3231 were obtained through the NIH Biodefense and Emerging Infections Research Resources Repository, NIAID, NIH.

5.2.13 PROTEIN PREDICTION

Membrane topology of AlsPV proteins was predicted using Phobius (189).

5.2.14 SIALIDASE ASSAY

Confluent Vero cell monolayers were treated with 15 mU of *Arthrobacter ureafaciens* neuraminidase for 2 h at 37°C in cell culture media. Untreated and neuraminidase-treated cells were washed twice with PBS and incubated with AlsPV or PIV5 (MOI 2) in duplicate for 1 h. The cells were then washed four times with PBS and incubated for 24 h in cell culture media, before fixing and immunofluorescence staining as above. Fluorescent cells were counted in nine fields of view per well using an ImageXpress Micro XLS Widefield High-Content Analysis System (Molecular Devices) and compared to untreated infected cells. The relative number of infected cells was compared by one-way ANOVA followed by Dunnett's multiple comparison test (compared to untreated cells) using GraphPad Prism 5.

5.3. RESULTS

5.3.1 ISOLATION OF A NOVEL BAT-BORNE RUBULAVIRUS

Bat urine samples were collected from Alstonville, New South Wales in July and August of 2011. Inoculation of the bat urine onto primary bat kidney (PaKi) cells and Vero cells resulted in the isolation of a novel paramyxovirus. Cytopathic effect was initially observed in PaKi cells 18 days post inoculation. RT-PCR and Sanger sequencing indicated that the virus was the source of a short fragment of L gene previously detected by PCR in urine collected from grey-headed flying foxes, *Pteropus poliocephalus,* in Geelong, Victoria in 2010 (KM359175.1). In that instance, however, the virus was unable to be cultured (236). Whole genome sequencing of first passage supernatant confirmed the presence of a novel paramyxovirus and the name Alston virus (AlsPV) was chosen based on the location of the source bat colony. No other virus or bacteria were detected in the supernatant by next generation sequencing.

5.3.2 ANALYSIS OF THE ALSPV WHOLE-GENOME SEQUENCE

The whole genome sequence of AlsPV was assessed for the presence of paramyxovirus motifs and features, as well as phylogenetically analysed to determine its classification as a novel virus. Whole genome sequencing revealed that AlsPV is a novel virus from the genus *Rubulavirus* (Figure 5.1). The genome of AlsPV is 15270 nucleotides long with a GC content of 41.6%. The coding percentage is 92.2%, which is the average coding percentage of the paramyxoviruses, not including members of the genus *Henipavirus* (223). It has a 55 nt leader sequence and a 31 nt trailer sequence that were confirmed using a combination of 5' rapid amplification of cDNA ends (RACE) and sequencing across ligated genome ends.

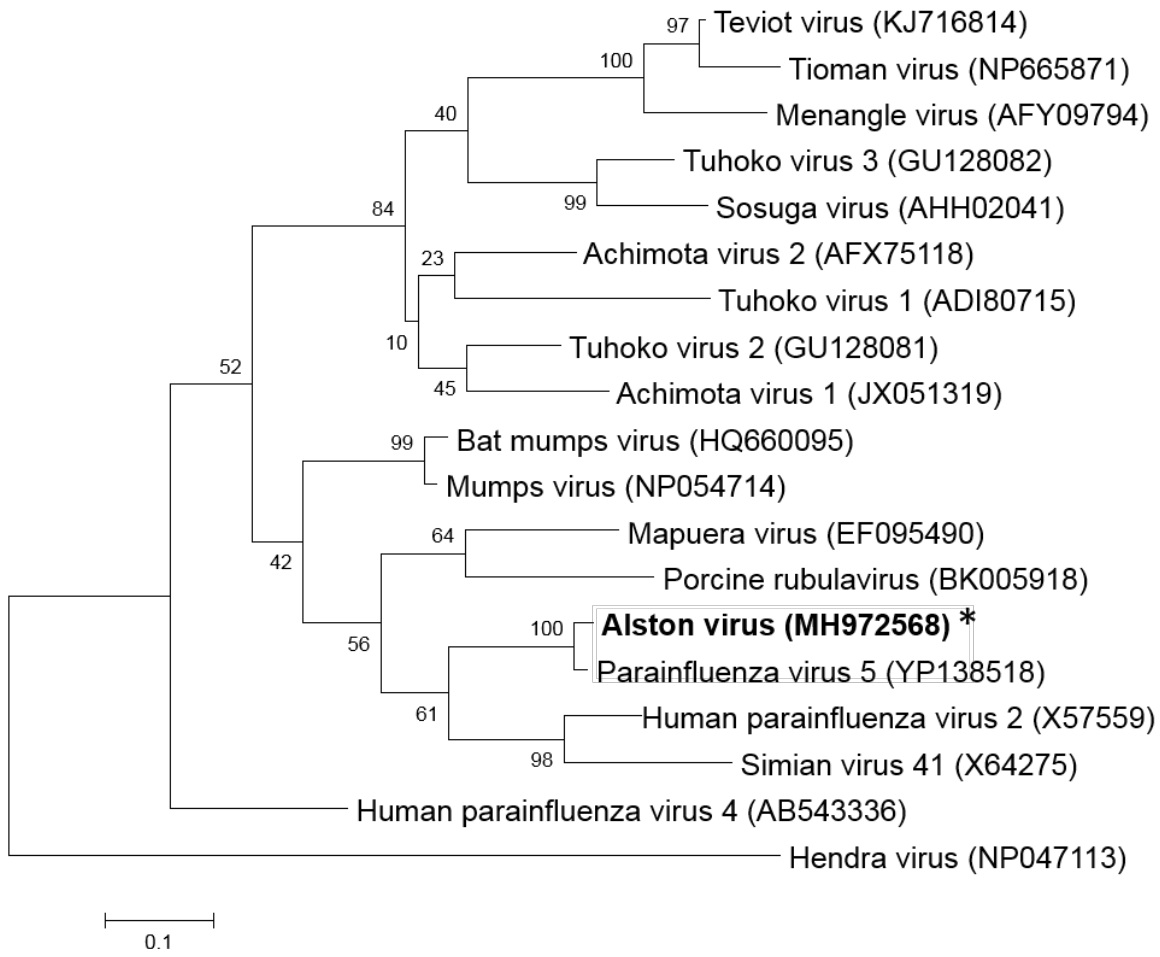

Figure 5.1: Phylogenetic analysis of rubulavirus and Hendra virus L protein. Maximum-likelihood tree reconstructed with MEGA 6.06, bootstrapping to 1000 replicates. Genbank accession numbers are provided in parentheses.

Phylogenetic analysis indicated that AlsPV is most closely related to PIV5 (Figure 5.2). The lengths of the genomes and genes are highly conserved between PIV5 and AlsPV (Table 5.1), as well as the sequences of the gene boundaries and the length of untranslated regions and intergenic regions (Table S5.1). Furthermore, comparison of coding regions of PIV5 and AlsPV revealed nucleotide identities between 63 - 81% and amino acid (aa) identities between 61 - 93% (Table 5.2). Across the whole genome, including non-coding regions, the nucleotide identity between the two viruses was found to be 74%.

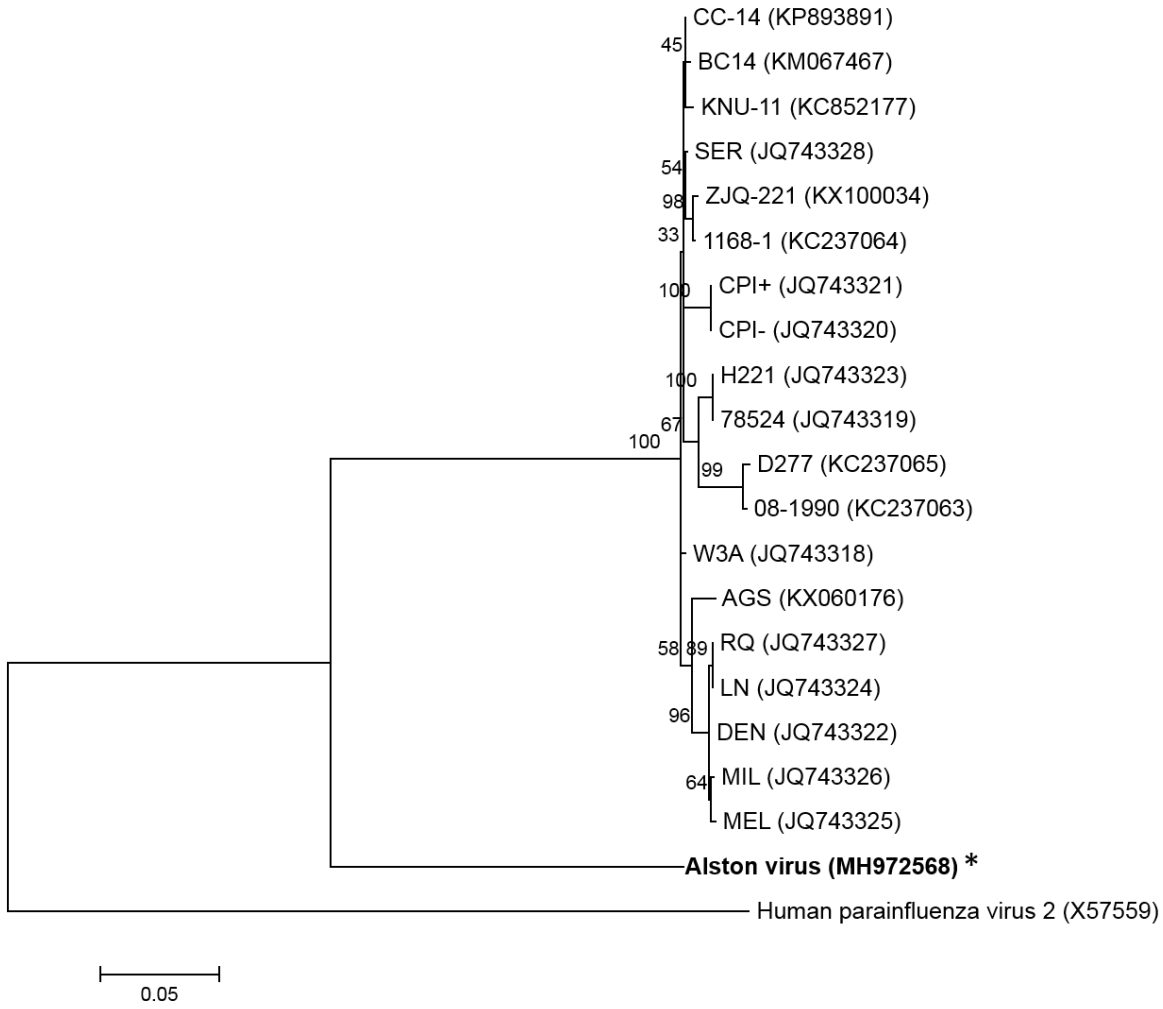

Figure 5.2: Phylogenetic analysis of the N gene of multiple parainfluenza virus 5 strains, AlsPV and human parainfluenza virus 2. Maximum-likelihood tree reconstructed with MEGA 6.06, bootstrapping to 1000 replicates. Genbank accession numbers are provided in parentheses.

Table 5.1: Comparison of AlsPV and PIV5 coding sequences and protein lengths. Differences between AlsPV and PIV5 are in bold.

Gene/feature	Coding region	Virus	Length (nt)	Length (aa)
3′ leader		AlsPV	55	
		PIV5	55	
N	CDS	AlsPV	1530	509
		PIV5	1530	509
P	V CDS	AlsPV	669	222
		PIV5	669	222
	P CDS	AlsPV	1179	392
		PIV5	1179	392
	W CDS	AlsPV	516	171
		PIV5	516	171
M	CDS	AlsPV	1134	377
		PIV5	1134	377
F	CDS	AlsPV	1629	542
		PIV5	**1590**	**529***
SH	CDS	AlsPV	135	44
		PIV5	135	44
HN	CDS	AlsPV	1698	565
		PIV5	1698	565
L	CDS	AlsPV	6768	2255
		PIV5	6768	2255
5′ Trailer		AlsPV	31	
		PIV5	31	

*The F protein length of PIV5 varies from 529 aa to 551 aa

Table 5.2: Nucleotide and amino acid sequence identities between AlsPV and PIV5. Identities calculated by ClustalW alignment in Geneious 10.1.3.

	N	P	V	W	M	F	SH	HN	L
Nucleotide	76	79.4	80.6	76.9	76.6	72.5	63	71	76.7
Amino acid	91	86	89	86.6	93	85	61	81	92

5.3.3 Analysis of deduced amino acid sequences

5.3.3.1 SH

The SH gene is only encoded by the genomes of MuV and PIV5, so the AlsPV genome was assessed for the presence of an additional open reading frame in between the F gene and the HN gene. AlsPV was found to have this additional open reading frame with the capacity to express a short hydrophobic (SH) protein of 44 aa in length. Despite lower similarity with PIV5 in this gene compared to the rest of the coding regions, the SH protein of AlsPV is predicted to have the same cell surface orientation as the SH protein of PIV5 (238). The AlsPV SH protein is predicted to be a

class II integral membrane protein with 16-19 cytoplasmic N-terminal residues and 1-5 C-terminal residues.

5.3.3.2 HN

The AlsPV HN gene contains important motifs and residues associated with neuraminidase function, in particular, the NRKSCS motif (224, 225). Treatment of Vero cells with a broad acting sialidase prior to infection resulted in a significant reduction in the ability of the virus to infect cells (Figure 5.3). It is likely that, similar to PIV5 and multiple other rubulaviruses, sialic acid is the main cellular receptor used for attachment to host cells.

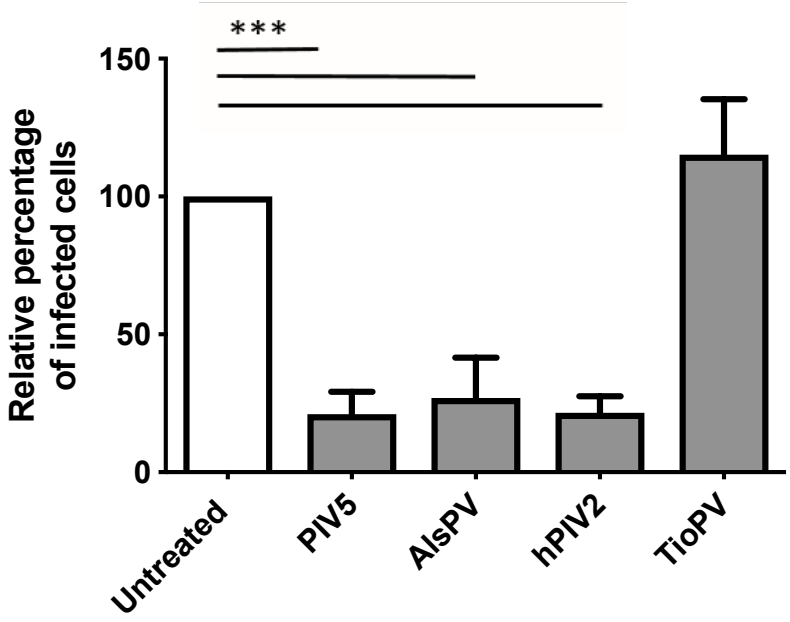

Figure 5.3: Effect of *Arthrobacter ureafaciens* neuraminidase treatment on AlsPV, PIV5, hPIV2 and TioPV infection of Vero cells. Infected cells were counted and averaged across nine fields of view and compared to infected but untreated cells. TioPV was included as a control because it lacks the NRKSCS motif and was therefore not expected to bind sialic acid. Values represent a percentage of the number of infected cells counted in untreated samples. Error bars represent the standard deviation. Significance calculated by one-way ANOVA followed by Dunnett's multiple comparison test (compared to untreated cells). *** represents a *p* value of <0.001. *n* = 2 independent experiments.

5.3.3.3 RNA EDITING OF THE P GENE

Similar to other rubulaviruses, the unedited transcript of the AlsPV P gene encodes the V protein and insertion of two guanine residues at the editing site results in the expression of the P protein. Amplicon sequencing was used to determine the prevalence of edited transcripts per 100000 reads. On average, 79.63% of the transcripts were unedited or had the addition of three G residues resulting in expression of the V protein. Transcripts encoding the P protein through the

addition of two or five G residues occurred 19.09% of the time. In 1.28% of transcripts, the addition of one or four G residues encoded a putative W protein. This totalled an average editing frequency of 21.8%. Insertions of up to eight G residues could be detected at the editing site, although at low frequency.

5.3.4 AlsPV is antigenically related to PIV5

The antigenic relatedness of AlsPV to other paramyxoviruses was determined by immunofluorescence assay (IFA) in order to add evidence to its classification as a novel rubulavirus. Analysis by IFA revealed cross-reactivity between AlsPV and PIV5 (Figure 5.4). There were low levels of cross-reactivity with hPIV2, mumps virus, Menangle virus, Tioman virus and Teviot virus when using antisera against the AlsPV N protein. No cross-reactivity was detected for Hendra virus, porcine rubulavirus or Mapuera virus.

AlsPV was neutralised by low dilutions of PIV5 antisera, however, AlsPV antisera were unable to neutralise PIV5 (Table 5.3). More PIV5 sera need to be tested to confirm the one-way neutralisation. There was no cross-neutralisation between AlsPV and any other tested virus; MenPV, TioPV, TevPV MuV, hPIV2, MapV, PorV and HeV.

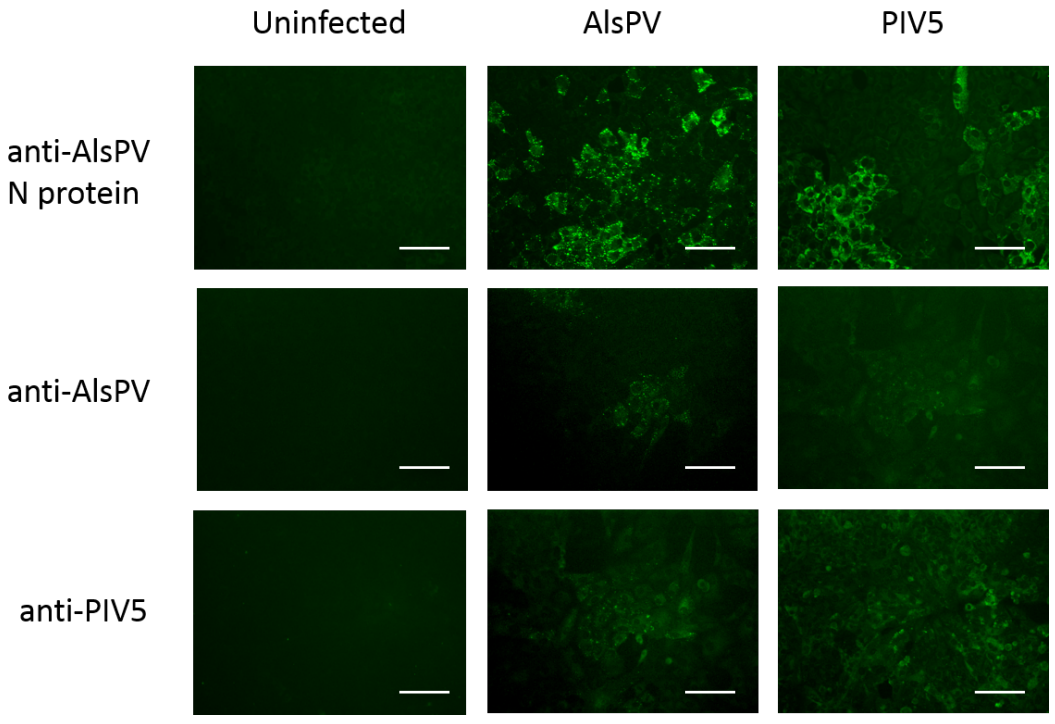

Figure 5.4: Antigenic cross-reactivity between PIV5 and AlsPV by immunofluorescence assay. Vero cells were infected with AlsPV or PIV5 and stained with either rabbit sera raised against an N protein peptide of AlsPV, ferret sera resulting from infection with AlsPV, or anti-PIV5 guinea pig sera. Scale bar = 100 µm.

Table 5.3: Neutralisation titres of ferret AlsPV antisera, guinea pig PIV5 antisera and guinea pig hPIV2 antisera against AlsPV, PIV5 or hPIV2 infection. Viruses were incubated with sera for 30 min before the addition of Vero cells. CPE was assessed after 5-7 days. Neutralisation titres were calculated using the Reed-Muench method, described as the reciprocal of the highest dilution of serum at which the infectivity of 100 $TCID_{50}$ of virus is neutralised in 50% of the wells. Results from matched virus-serum pairs are in bold.

Infected with \ Sera from	AlsPV	PIV5	hPIV2
AlsPV	**202**	14	<10
PIV5	<10	**160**	<10
hPIV2	<10	<10	**226**

5.3.5 Growth analysis of AlsPV in mammalian cell lines

Comparative growth analysis of AlsPV in multiple mammalian cell lines was conducted as a preliminary indication of the potential for AlsPV to infect other mammalian species. AlsPV was found to grow to high titres in all tested mammalian cell lines, with AlsPV growth plateauing at higher titres in MDBK, MDCK and PK15a cells (Figure 5.5). These higher titres may be a consequence of the virus not causing significant damage to the cells as only minimal cytopathic effect (CPE) was observed in MDCK, MDBK and PK15a cells. No signs of CPE were observed in any control cells.

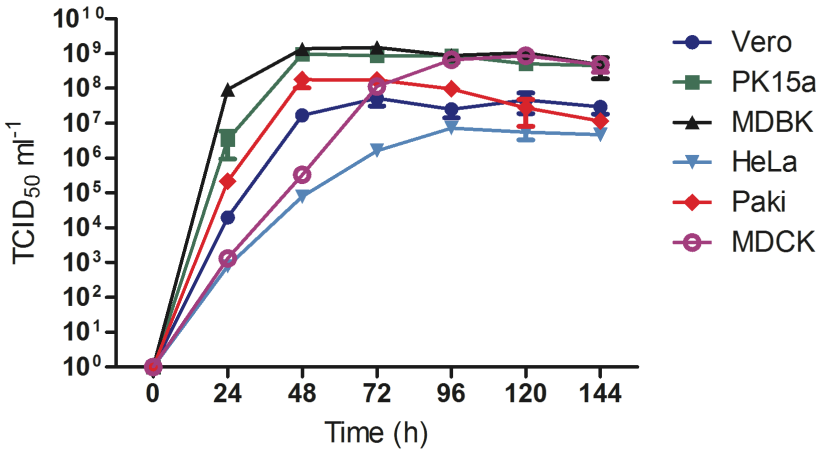

Figure 5.5: Growth kinetics of AlsPV in multiple mammalian cell lines. Mammalian cell lines were infected with AlsPV at MOI 0.01 for 1 h in triplicate. Cells were washed and aliquots were collected every 24 h for 6 days. The $TCID_{50}$/ml was determined by virus titration. Data represents 3 biological repeats and 6 technical repeats. Error bars represent standard error of the mean.

5.3.6 AlsPV NEUTRALISING ANTISERA ARE PREVALENT IN GREY HEADED FLYING FOXES

To determine the potential exposure rate of Australian flying foxes to AlsPV, 120 pteropid bat sera samples were tested by neutralisation assay. Only ~8% (10/120) of total tested pteropid bat sera neutralised the growth of AlsPV, however, 25% (5/20) of *P. poliocephalus* sera neutralised AlsPV, suggesting it may be the primary host species for AlsPV (Table 5.4).

Table 5.4: Prevalence of neutralising antibodies to AlsPV in Australian flying foxes. Sera from pteropid bats collected in Queensland between 1999 and 2007, or Victoria in 2012 were diluted 1/10 and incubated with 100 $TCID_{50}$ AlsPV for 45 min before the addition of Vero cells.

	No. positive	**Percentage positive**
*Pteropus sp.**	4/59	6.8
P. scapulatus	0/15	0
P. alecto	1/26	3.8
P. poliocephalus	5/20	25
Total	**10/120**	**8.3**

*Pteropid bat sera collected in Queensland between 1999 and 2007, species not recorded

5.3.7 ANIMAL INFECTION STUDIES

5.3.7.1 ALSPV IS SHED IN FERRET RESPIRATORY SECRETIONS

Animal infection studies in ferrets (n = 3) and mice (n = 5 juvenile mice, n = 5 adult mice) were completed to attempt to determine the pathogenic potential of AlsPV in mammalian species. Mice remained clinically normal, with no evidence of fever, weight loss or behavioural changes, until scheduled euthanasia at 21 days post infection, and there was no evidence of seroconversion. Low copy numbers of viral RNA could be detected by qRT-PCR in the brains of two mice, one adult (169 copies of AlsPV N per 10^{10} copies of 18S RNA) and one juvenile (5 copies of AlsPV N per 10^{10} copies of 18S RNA), but there was no evidence of viral antigen or inflammation when the brain was assessed by histopathology. Other tissues were negative by qRT-PCR and histopathology.

Ferrets also remained clinically normal with no fever, weight loss or behavioural changes following exposure to AlsPV, however, infectious virus was isolated from oral swab and nasal wash samples collected during acute infection (Figure 5.6). At 10 days post infection, oral and nasal shedding of virus could no longer be detected, correlating with the first detection of seroconversion in one of the three ferrets. Virus neutralisation assays showed that all three ferrets had seroconverted by day 14 (Table 5.5). The shedding samples indicated that virus was replicating, potentially in the upper respiratory tract, but by euthanasia on day 21 no viral RNA could be detected in any tissues by qRT-PCR. Viral RNA could not be detected in ferret urine or blood.

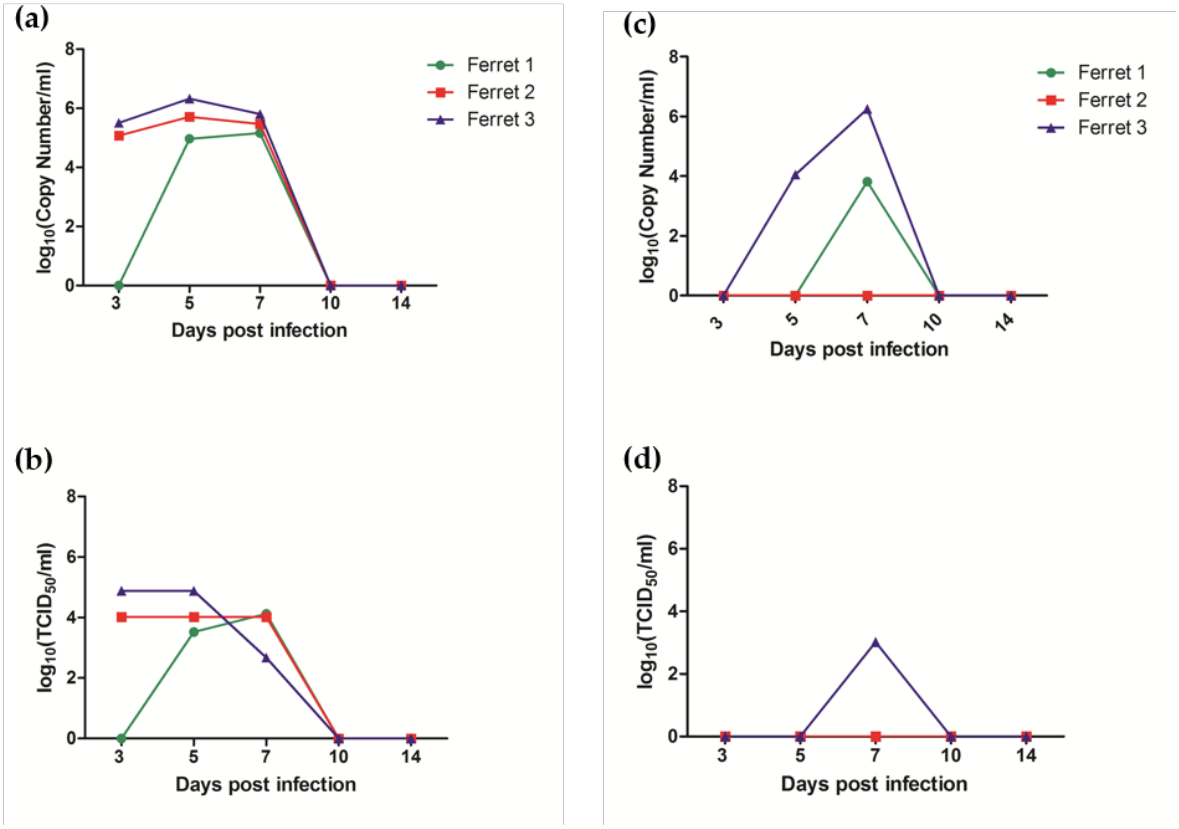

Figure 5.6: Shedding of AlsPV in ferret respiratory secretions following oronasal exposure. Graphs present log transformations of the (a) copy number of AlsPV N gene per ml of nasal wash sample, (b) titre of AlsPV isolated from nasal wash, (c) copy number of AlsPV N gene per ml of oral swab sample, and the (d) titre of AlsPV isolated from oral swabs.

Table 5.5: Neutralising antibody titres from AlsPV-infected ferrets. Ferret sera were incubated with 100 $TCID_{50}$ of virus for 30 min before the addition of Vero cells. CPE was assessed after 7 days. Neutralising titres were calculated using the Reed-Muench method as described previously (192).

	Day 7	Day 10	Day 14	Day 21
Ferret 1	<10	<10	13	101
Ferret 2	<10	13	13	40
Ferret 3	<10	<10	32	202

5.3.7.2 ALSPV INFECTS THE FERRET UPPER RESPIRATORY TRACT AND OLFACTORY LOBE OF THE BRAIN

A second animal infection study was conducted to determine sites of virus replication during the acute stages of infection. Ferrets (n = 12) were exposed to AlsPV and euthanised on either day 3, 5, 7 or 10 post infection. As observed in the previous experiment, ferrets remained clinically normal and no viral RNA could be detected in ferret urine or blood. Seroconversion was detected in one of three ferrets euthanised on day 10. Oral and nasal virus shedding was similar to what was observed in study 1 but virus was shed at higher titres and for a prolonged time (Figure 5.7). Viral RNA was detected in the rectal swab of one ferret euthanized 5 days post infection. This ferret also had low copy numbers of viral RNA detected in the small intestine.

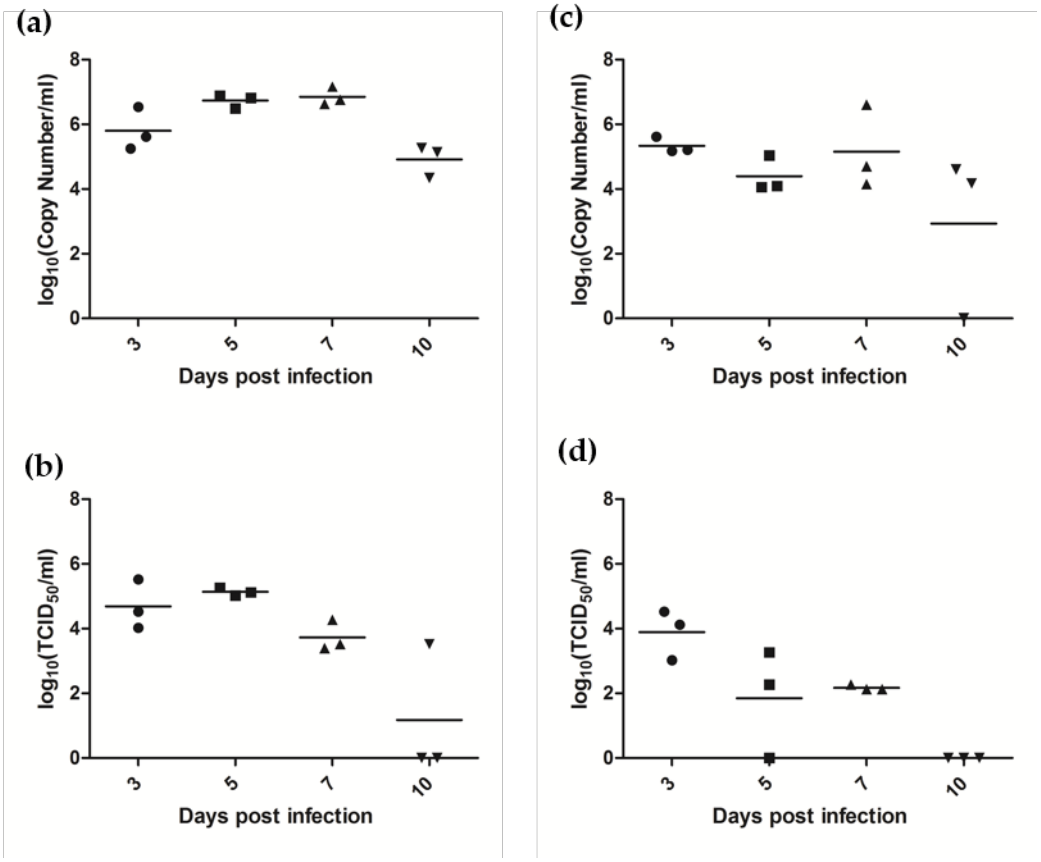

Figure 5.7: Shedding of AlsPV in ferret respiratory secretions following oronasal exposure. Ferrets were sampled prior to euthanasia, at 3, 5, 7 or 10 days post infection. Graphs present log transformations of the (a) copy number of AlsPV N gene per ml of nasal wash sample, (b) titre of AlsPV isolated from nasal wash, (c) copy number of AlsPV N gene per ml of oral swab sample, and the (d) titre of AlsPV isolated from oral swabs.

Viral RNA was detected in a number of tissues at euthanasia (Table 5.6). In particular, viral RNA was detected in the olfactory bulb of the brain, nasal turbinates and palatine tonsils of all twelve ferrets (Figure 5.8). Virus was reisolated from 9/12 nasal turbinate samples, 4/12 tonsil samples and from 2/12 olfactory bulb samples, suggesting that live virus was present in these tissues. Low titres of viral RNA could sometimes be detected in the retropharyngeal lymph node, the main draining lymph node of the upper respiratory tract, as well as the trachea and lung. Occasionally, viral RNA could be detected in other organs at low titres, such as the heart.

Although many of the PCR positive samples, such as the nasal turbinates, tonsils and most olfactory lobes, were unavailable for histology, the olfactory lobe of the brains collected from ferrets euthanised on day 10 were assessed by routine histology. Two out of three olfactory lobes had evidence of inflammation consistent with viral infection, in addition to the presence of low amounts of viral antigen (Figure S5.1). No other organs, including the remainder of the brain, showed signs of inflammation or viral antigen.

Table 5.6: Detection of AlsPV N gene RNA and isolation of AlsPV from tissues collected from AlsPV-infected ferrets. Viral RNA was extracted from homogenised ferret tissues and amplified by qRT-PCR. Virus isolations were conducted by inoculating Vero cells with homogenised tissue and assessing for CPE after 7 days.

	Dpi 3			Dpi 5			Dpi 7			Dpi 10		
Ferret #	1	2	3	4	5	6	7	8	9	10	11	12
Nasal turbinates	+/+	+/+	+/+	+/+	+/+	+/+	+/+	+/+	+/+	+/-	+/-	+/+
Tonsil	+/+	+/-	+/-	+/+	+/+	+/+	+/-	+/-	+/-	+/-	+/-	+/-
Retropharyngeal L.N.	+/-	-	-	+/-	-	+/-	+/-	-	+/-	+/-	-	+/-
Trachea	-	-	-	-	-	+/-	+/-	-	-	-	-	+/-
Lung (hilus)	-	-	-	+/-	-	+/-	-	-	-	-	-	-
Lung (peripheral)	-	-	-	+/-	-	-	-	-	+/-	-	-	-
Bronchial L.N.	-	-	+/-	-	-	-	-	-	-	+/-	+/-	-
Heart	-	-	-	-	-	+/-	-	-	-	-	-	-
Liver	-	-	-	-	-	-	-	-	-	-	-	-
Kidney	-	-	-	-	-	-	-	-	-	-	-	-
Spleen	-	-	-	-	-	-	-	-	-	-	-	-
Brain	+/+	+/-	+/-	+/-	+/-	+/-	+/-	+/-	+/+	+/-	+/-	+/-
Small intestine	-	-	-	-	-	+/-	-	-	-	-	-	-
Large intestine	-	-	-	-	-	-	-	-	-	-	-	-

Virus detection in tissue samples at euthanasia, RNA/virus isolation. +/+ indicates the sample was positive by both qRT-PCR and virus isolation; +/- indicates the sample was only positive by qRT-PCR and not by virus isolation; - indicates virus was not detected by qRT-PCR therefore virus isolation was not attempted. Dpi, days post infection; L.N., lymph node; #, number.

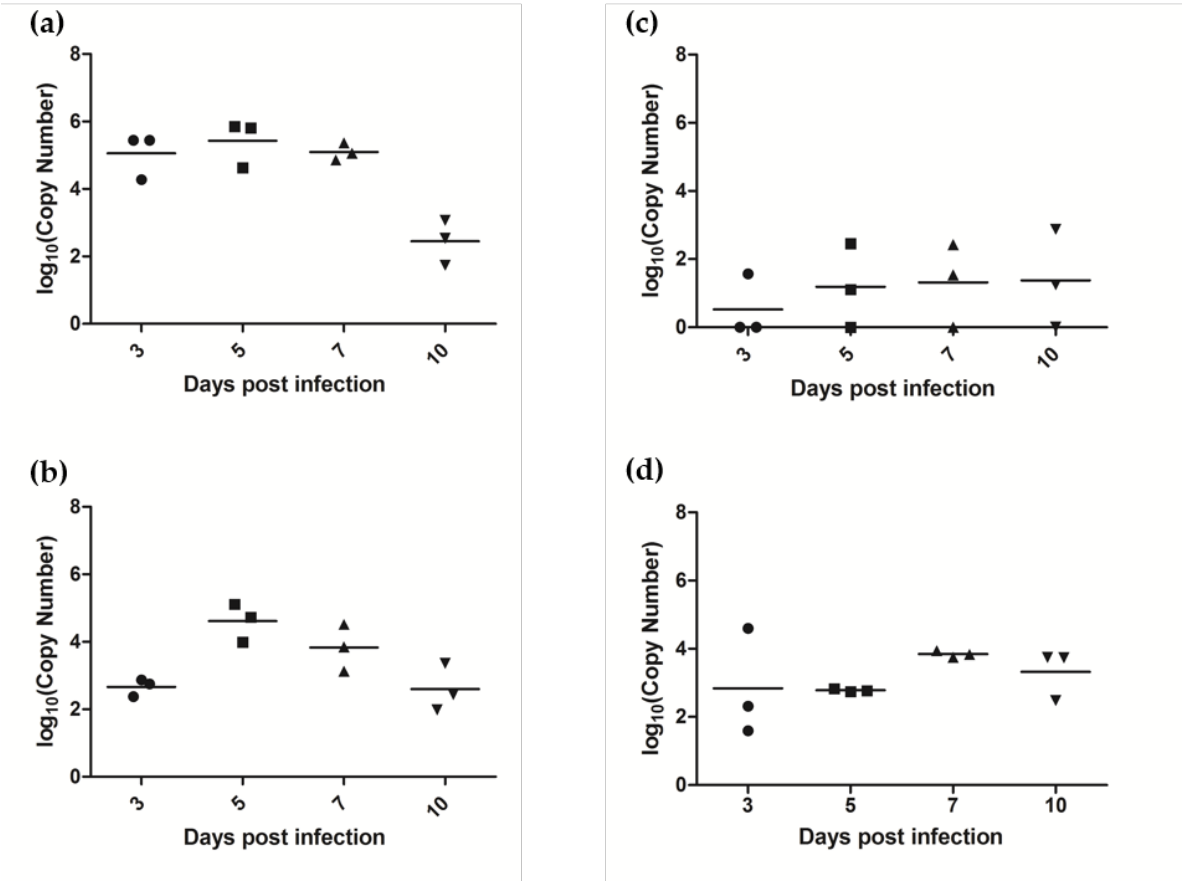

Figure 5.8: Detection of viral RNA in ferret tissues at euthanasia. Graphs represent log transformations of the copy number of AlsPV N gene RNA per 10^{10} copies of 18S rRNA detected in (a) nasal turbinates (b) tonsils (c) retropharyngeal lymph nodes (d) olfactory bulb of the brain by qRT-PCR.

5.4 DISCUSSION

Analysis of pteropid bat urine collected in northern New South Wales in 2011 has led to the isolation of a novel rubulavirus that we have named Alston virus (AlsPV). Phylogenetic and antigenic analyses indicated that this virus is closely related to PIV5. However, in comparison to the average observed variation between AlsPV and PIV5, 26% across the whole genome, isolates of PIV5 are almost identical despite being isolated from a range of host species, geographical locations and over multiple decades (239). In fact, variability of only 7.8% is observed between strains of PIV5, with an average pairwise difference of only 2.1% at the nucleotide level (239). Furthermore, AlsPV antisera did not neutralise PIV5 infection. We therefore propose that AlsPV is a new species of rubulavirus and not a new strain of PIV5.

AlsPV and PIV5 also share phenotypic similarities. Experimental intranasal infection of ferrets with PIV5, similar to the infection studies described here, demonstrated variable results ranging from no clinical symptoms to mild cough with minimal lesions in the nasal cavities and upper trachea

(240, 241). Antigen could only be detected in the trachea with no evidence of virus in the lungs or the brain (240, 241), although it is not known if the olfactory bulb was specifically investigated. Neurological symptoms have been observed in ferrets experimentally infected with PIV5, but only after intracerebral injection as the route of infection. In addition to the *in vivo* similarities, PIV5 and AlsPV are similar in that they utilise sialic acid as a receptor for cell entry (57), grow to high titres in multiple mammalian cell lines with minimal cytopathic effect (242, 243) and encode an SH gene (57). The multiple similarities between the two viruses indicate that, despite the lack of clinical disease in ferrets and mice, AlsPV may also have the potential to infect other mammalian species.

The findings presented here suggest that AlsPV causes an upper respiratory tract infection in ferrets that is followed by infection of the olfactory pole of the brain. It is likely that from the nasal turbinates, the virus has access to the olfactory neurons that extend from the olfactory bulb through the cribriform plate and into the olfactory neuroepithelium in the nasal cavity (244), but further histopathological examination would be required to confirm this hypothesis. This allows direct access for the virus to disseminate through the central nervous system. However, AlsPV was not detected in brain tissue beyond the olfactory bulb. It is likely that the innate immune response had a role in preventing the spread of AlsPV throughout the CNS (244, 245). Further investigation into the persistence of AlsPV is required, particularly as reduced cytopathic effect was observed during infection of some mammalian cell lines with AlsPV and viral RNA was detected in the olfactory pole of mouse brains at 21 days post infection.

The timing of detection of virus shedding in respiratory secretions of ferrets suggests that virus replication peaked around 5-7 days post inoculation. Although there was some variability between shedding in the first and second animal infection studies, it may have been due to variation between cohorts of outbred ferrets. The presence of virus in oronasal shedding samples and in the upper respiratory tract suggests that AlsPV replicates in tissues that are relevant to virus transmission, although transmission studies are required to confirm if transmission occurs in ferrets. Further experiments are also required to determine the effect of the route of virus challenge and if oronasal infection with lower doses of AlsPV still results in subsequent infection of the olfactory nerve.

Although AlsPV neutralising antibodies were found at a low overall prevalence in Australian pteropid bat sera, analysis of individual pteropid species indicated that the *Pteropus poliocephalus* flying foxes may be the primary reservoir host. This species was observed in the colony in Alstonville as well as in Geelong where AlsPV was detected by PCR. The high proportion of positive sera samples from grey headed flying foxes, combined with the increasing urban habituation of pteropid bats (17), suggest that there is risk of exposure and potential transmission of AlsPV to non-pteropid mammalian species.

Supplementary Materials: The following are available online at www.mdpi.com/xxx/s1, Table S1: Comparison of AlsPV and PIV5 untranslated regions and intergenic regions.

Author Contributions: Conceptualization, G.A.M. and L-F.W.; methodology, R.I.J., M.T., and B.A.C.; investigation, R.I.J., B.R. and R.L.; formal analysis, R.I.J., J.B. and M.T.; visualization, R.I.J.; writing – original draft preparation, R.I.J.; writing – review and editing, R.I.J., B.A.C., M.T., L-F.W. and G.A.M.; supervision, G.A.M.

Funding: This work was supported by an Australian Government Research Training Program Scholarship (R.I.J.) and CSIRO internal funding.

Acknowledgments: We are grateful to Jenn Barr, Shawn Todd and Ina Smith for their technical assistance; Jean Payne, Jenni Harper and Teresa Eastwood for the preparation of tissue samples for histopathologic and immunohistochemical assessment; and Hume Field and his team for their support with the field work. We are also thankful to Ben Hubbard and Leah Frazer for their work with the animal study.

Conflicts of Interest: The authors declare no conflict of interest. The funders had no role in the design of the study; in the collection, analyses, or interpretation of data; in the writing of the manuscript, or in the decision to publish the results.

5.5 SUPPLEMENTARY MATERIAL

Table S5.1: Comparison of AlsPV and PIV5 untranslated regions and intergenic regions. Differences between AlsPV and PIV5 are in bold and lowercase.

			Length	Boundary Sequence
N	5’ UTR	AlsPV	102	AGGCCCGGAA
		PIV5	**96**	AGG**u**CCGGAA
	3’ UTR	AlsPV	106	UUUAAGAAAAAAA
		PIV5	106	UUUAA**ag**AAAAAAA
	IGR	AlsPV	1	
		PIV5	1	
P	5’UTR	AlsPV	61	AGGCCCGGAC
		PIV5	61	AGGCCCGGAC
	3’UTR	AlsPV	66	UUUAGAAAAAA
		PIV5	66	UUUAGAAAAAA
	IGR	AlsPV	33	
		PIV5	**16**	
M	5’UTR	AlsPV	33	AGGCCCGAAC
		PIV5	**32**	AG**c**CC**ga**A**ca**
	3’UTR	AlsPV	211	UUCAAAGAAAA**a**
		PIV5	**204**	UUCAAAGAAAA
	IGR	AlsPV	22	
		PIV5	**23**	
F	5’ UTR	AlsPV	28	AGCACGAATC
		PIV5	28	AGCACGAA**c**C
	3’ UTR	AlsPV	60	UUUAAGAAAAAA
		PIV5	**100**	UUUAAGAAAAAA**a**
	IGR	AlsPV	5	
		PIV5	**4**	
SH	5’ UTR	AlsPV	79	AGGACCGAAC
		PIV5	79	AGGACCGAAC
	3’ UTR	AlsPV	72	UUUUAAGAAAAAAA
		PIV5	**78**	UUUUAA**ag**AAAAAA
	IGR	AlsPV	1	
		PIV5	1	
HN	5’ UTR	AlsPV	67	AGGCCCGAAC
		PIV5	67	AGGCCCGAAC
	3’ UTR	AlsPV	111	UUUAAGAAAAA**a**
		PIV5	111	UUUAAGAAAAA
	IGR	AlsPV	13	
		PIV5	13	
L	5’ UTR	AlsPV	8	AGGCCAGA
		PIV5	8	AGGCCAGA
	3’ UTR	AlsPV	34	UUUAAGAAAAAA
		PIV5	34	UUUAAGAAAAAA

(a) (b)

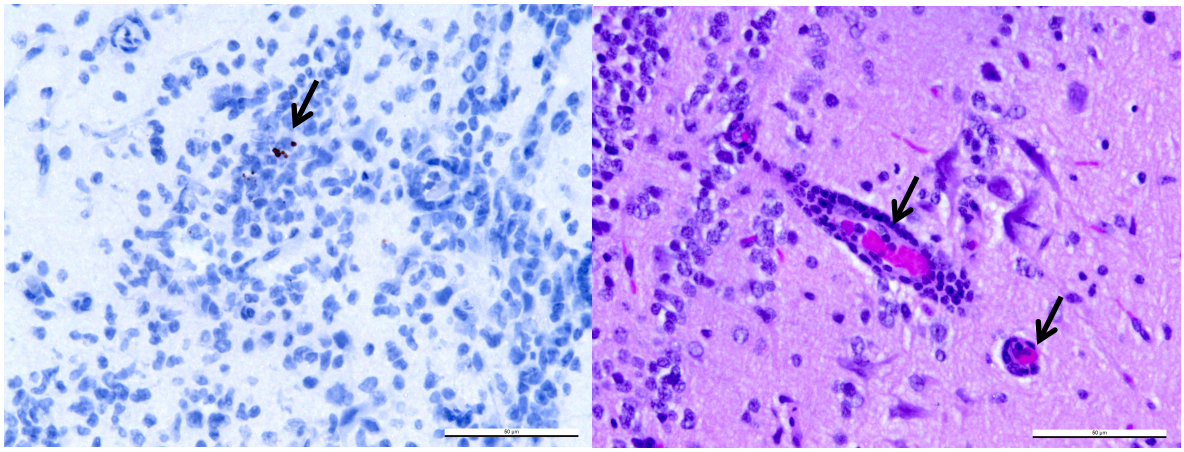

Figure S5.1: Immunohistochemical and histopathological analysis of olfactory bulb of ferret at 10 days post infection with AlsPV. Olfactory bulb of ferret #10, euthanised on day 10 post infection, was (a) stained with rabbit antiserum against the N protein peptide of AlsPV (arrow indicates stained antigen) and (b) assessed by routine H&E staining. Panel (b) shows perivascular cuffing with mononuclear cells, indicating an inflammatory process consistent with viral infection (arrows indicates perivascular cuffing).

CHAPTER 6: GENERAL DISCUSSION

6.1 INTRODUCTION

Bats host a significant number of zoonotic viruses that are continuing to emerge into susceptible populations and have a substantial impact on animals and humans (3, 36). In 2018, Nipah virus (NiV) caused an outbreak in Kerala, India, resulting in sixteen deaths out of eighteen confirmed cases (105). Despite continuing outbreaks, there are no licensed vaccines or treatments for NiV (246, 247), highlighting the difficulties of developing effective vaccines and anti-viral treatments. However, previous characterisation of NiV and epidemiological investigations resulted in the quick implementation of control measures in Kerala, such as patient isolation, surveillance of patient contacts, as well as increased surveillance in surrounding regions (105). The large number of undiscovered bat-borne viruses means that there is also the risk of unknown viruses spilling over and causing disease, this time in the absence of any diagnostic tools or surveillance programs. Virus discovery programs are an important part of preparing for outbreaks of emerging viruses because they allow the development of pre-emptive control measures (16).

In the winter of 2011 there was an increase in HeV disease events detected throughout Queensland and northern New South Wales. Sporadic outbreaks had occurred in the years following the discovery of HeV in 1994. Conversely, there were eighteen disease events reported in 2011 alone (7). It has previously been noted that an increased HeV prevalence reflected an increased prevalence of a range of other paramyxoviruses shed in bat urine. Therefore it was hypothesised that bat urine collected in 2011 would be a useful source for virus discovery projects. Samples collected in Alstonville in July and August of 2011 were selected due to a high prevalence of HeV (31-39%). Based on previous virus isolation studies using samples collected from other Australian bat colonies, it was predicted that multiple adenoviruses and paramyxoviruses would be detected and isolated and that these viruses would provide an important insight into the viral diversity found in Australian bats. Consistent with this hypothesis, this study resulted in the isolation of two paramyxoviruses with unknown pathogenic potential. Furthermore, this thesis describes the identification of multiple paramyxovirus-derived sequences and the isolation of a polyomavirus and multiple adenoviruses.

Virus discovery programs are increasing (31), but there have been questions regarding their contribution to outbreak prevention. The discovery of viral sequences are important for improving our understanding of viral diversity and evolution, however, sequence data alone is not currently sufficient for the prediction of pathogenic potential or likelihood of emergence (20). Therefore, this study included both the discovery of viral sequences, as well as the characterisation of two isolated paramyxoviruses. The isolation of these viruses facilitated whole-genome sequencing, animal

infection studies, seroprevalence surveys, analysis of antigenic relatedness with other paramyxoviruses, and growth kinetics analyses.

6.2 THERE ARE MULTIPLE UNKNOWN VIRUSES PRESENT IN AUSTRALIAN PTEROPID BATS

In Chapter 3, bat urine samples were assessed for the presence of viruses. This resulted in the isolation of two paramyxoviruses, multiple adenoviruses and one polyomavirus, as well as the detection of a range of paramyxovirus RNA sequences. In Chapters 4 and 5, the two isolated paramyxoviruses were characterised *in vitro* and *in vivo* to understand more about their pathogenic potential. The whole genome sequences of the isolated adenoviruses were not determined, however, it is recommended that characterisation and whole genome sequencing of these viruses occurs in the future so that they can provide important data for elucidating the evolution of adenoviruses. The isolation of a polyomavirus was unexpected because it was not targeted for discovery. Sequencing of the whole genome revealed that it was the same species as a polyomavirus isolated from Indonesian pteropid bats (161). This warrants further investigation to determine the direction and frequency of this potential transmission between pteropid bats originating from different countries.

The diversity of paramyxovirus-derived sequences detected by consensus PCR is consistent with observations in previous surveys of bats globally (9, 31, 54, 165). It is of note that our current method for virus isolation seems to be biased toward isolating rubulaviruses (30). It may be because of this bias that all the rubula-like viruses and viral sequences that were detected in the bat urine had been previously detected or isolated. In comparison, there were a multiple unique henipa-like viral sequences, potentially corresponding to novel viruses, which were identified in the bat colony but were unable to be isolated. The difference in the number of detected viral sequences between the two genera may indicate an underlying difference in diversity, potentially due to a difference in the tolerance of mutations and substitutions. Furthermore, other studies have identified similar henipa-like viruses, however, none have been isolated to date (8, 86). This suggests that a different approach to virus isolation may be required to specifically target these viruses.

This study examines urine samples collected in Alstonville in 2011, however, urine has been reported to have low viral prevalence overall (24). Therefore, future virus discovery studies in Australian bats may benefit from assessing a range of samples including faeces and oral swabs (54). However, this must be weighed against the cost efficiency of collecting these extra samples and the stress caused to the bats (248), particularly as *P. poliocephalus* are considered a vulnerable species (232). The benefit of using urine is that it provides a way of regularly screening colonies for viruses without

direct handling of the bats. In addition, other samples are more likely to carry bacterial loads that will replicate in the cell culture media. This is particularly evident when using faecal samples as rapid bacterial overgrowth of the culture often prevents virus isolation.

Almost the whole coding sequence of a novel paramyxovirus, Lumley virus (LumPV), was assembled following next generation sequencing of one urine sample. This paramyxovirus appeared to be prevalent in the Alstonville colony as similar sequences were detected in three other urine samples collected at the same time point. Different detection methods, such as designing a specific qRT-PCR, are required to confirm this hypothesis. It is unknown why the isolation of viruses similar to LumPV has often been unsuccessful (8, 86). The coding sequence of LumPV is therefore an important tool to help elucidate ways of isolating related viruses. In particular, further functional studies of receptor binding, utilising the surface glycoprotein sequences determined in this thesis, may provide an indication as to what is required for the growth of these viruses.

6.3 TEVIOT VIRUS DOES NOT CAUSE CLINICAL DISEASE IN MICE OR FERRETS

In Chapter 4, Teviot virus (TevPV), a rubula-like virus similar to Tioman and Menangle virus (TioPV and MenPV), was characterised following isolation from the Alstonville bat urine samples. This isolation followed eighteen previous isolations from pteropid Australian bats in Victoria, New South Wales and Queensland, however, previous characterisation of the virus was limited (30, 130). Investigation into TevPV was justified based on the apparently high prevalence amongst Australian bats and its similarity to the zoonotic viruses such as MenPV and SosPV. This study therefore describes a full analysis of the genome, *in vitro* investigation and *in vivo* animal infection trials.

Phylogenetic and antigenic assessment indicated that TevPV was more similar to TioPV than to MenPV. Amplicon sequencing revealed that, consistent with other rubulaviruses (57), TevPV expressed the V protein from the unedited P/V gene. Editing of the mRNA resulted in the expression of the P protein and W protein with a prevalence of 27.6% and 5.9% respectively. TevPV also grew to moderate titres in multiple mammalian cell lines. In accordance with the frequent isolations of TevPV, neutralising antibodies were detected in 30% of *Pteropus poliocephalus* sera, suggesting that this species may be the primary host of TevPV. Analysis of the attachment glycoprotein sequence revealed a lack of important neuraminidase motifs. This led to functional studies that implied that TevPV does not utilise sialic acid as a cell entry receptor.

The pathogenic potential of TevPV was investigated through animal infection studies in mice and ferrets. Intranasal exposure of mice resulted in no evidence of infection. Exposure of ferrets *via* the oronasal route resulted in infection, demonstrated by the presence of a neutralising antibody

response, but no clinical disease. These results suggest that TevPV is unlikely to cause a significant, transmissible outbreak in non-pteropid mammalian species.

TevPV is, however, an important tool for understanding more about other paramyxoviruses, particularly rubula-like viruses. Although the risk of pathogenic infection of humans with TevPV is low, it is important to understand its mechanism of host cell entry and how it relates to the entry mechanism of zoonotic viruses such as MenPV and SosPV. The results in Chapter 4 also contribute to the evidence that TevPV, along with MenPV, TioPV and others, should not be classified as rubulaviruses. Recent proposals to the ICTV reflect this variation and suggest that TevPV be classified in the genus *Pararubulavirus*, subfamily *Rubulavirinae* (56). These functional results are essential for confirming the conclusions made from phylogenetic analyses.

6.4 ALSTON VIRUS IS CAPABLE OF INFECTING THE RESPIRATORY TRACT OF FERRETS LEADING TO INFECTION OF THE OLFACTORY BULB OF THE BRAIN

Alston virus (AlsPV) was isolated from a pteropid bat colony in Alstonville and was shown through the investigation described in Chapter 5 to be a novel rubulavirus. Although a sequence likely corresponding to the L gene of this virus had previously been detected in *Pteropus poliocephalus* urine collected in 2010, this was the first isolation of AlsPV. Although electron microscopy was not attempted during the characterisation of this virus, whole genome sequencing indicated that no other bacteria or viruses were present in the virus stock. Inoculation of cells with AlsPV resulted in CPE that could be passed on to fresh cell cultures through the transfer of supernatant. Phylogenetic and antigenic analysis revealed this virus was closely related to parainfluenza virus 5 (PIV5), but was divergent enough to be classified as a novel species. Consistent with observations of PIV5, AlsPV grew to high titres in multiple mammalian cell lines in the absence of strong CPE. The similarities to PIV5 suggested that there was the potential for AlsPV to have a broad host range and to be pathogenic in non-pteropid mammalian species, so this was investigated through animal infection studies.

Two animal infection studies were conducted to understand the pathogenesis and tissue tropism of AlsPV. These two studies revealed that oronasal exposure of ferrets to AlsPV resulted in virus shedding in respiratory secretions, sometimes up to ten days post exposure. AlsPV was detected throughout the upper respiratory tract, particularly the nasal turbinates and tonsils, although no clinical symptoms were observed. AlsPV was also detected in the olfactory bulb of the brain, suggesting trafficking of the virus from the nasal turbinates through the olfactory nerve. Viral RNA was detected in various other organs, including the small intestine and heart, albeit at a low copy number. Mice remained clinically normal and did not seroconvert following intranasal exposure to

AlsPV, however, there was evidence of AlsPV RNA in the brains of two mice at 21 days post-infection. The potential persistence of AlsPV in this immune privileged site was not investigated further.

These *in vivo* results were consistent with what was observed following the experimental exposure of ferrets to PIV5 (240, 241). This implies that AlsPV may have the potential to infect other mammalians species, but might only be pathogenic in select species or in immunocompromised hosts. The shedding of virus in respiratory secretions and the replication of AlsPV in tissues relevant for virus transmission indicate that AlsPV infection also has the potential for ongoing transmission to other susceptible hosts.

The characterisations of TevPV and AlsPV in Chapters 4 and 5 demonstrated the phenotypic diversity of bat-borne paramyxoviruses. This diversity is even observed within a single bat species as both viruses appear to be primarily hosted by *P. poliocephalus*. Although both viruses are currently classified as being part of the same genus, these viruses are phylogenetically distinct based on their attachment glycoproteins and appear to utilise different host cell entry mechanisms. They are also phenotypically distinct, with AlsPV infection causing minimal CPE in cell culture and TevPV causing significant syncytia formation. Furthermore, exposure of ferrets to either virus resulted in very different outcomes and pathogenesis. The differences between these two related viruses highlight the importance of virus characterisation and the benefits of studying isolated viruses.

6.5 LIMITATIONS OF THE STUDY

The virus isolation methods used in this thesis have previously been optimised and have proven successful for the isolation of multiple rubulaviruses and henipaviruses (30). While this is useful for a targeted approach, these methods may not be ideal for the isolation of all genera of paramyxovirus. Furthermore, divergent novel genera of paramyxovirus might not be detected by consensus PCR.

Animal infection studies are currently the most effective way to determine the pathogenic potential of viruses (30). Mice and ferrets were selected for the infection studies because they have been characterised as successful animal models for other paramyxoviruses. For example, HeV infection of ferrets resulted in clinical disease that modelled the course of infection in horses and humans (193). Additionally, intranasal exposure to HeV resulted in transient lung infection and encephalitis in 80% of aged mice (194). In comparison, exposure of ferrets to PIV5 had variable results and was not replicative of clinical disease in dogs (114, 240). Furthermore, despite causing a severe outbreak of reproductive disease at an Australian piggery, MenPV infection was clinically silent during animal infection studies of weaned pigs (237). These studies highlight that there are limitations in what can be interpreted from the results as animal infection trials are considered predictive but not exactly replicative of human infection (249). As such, the absence of clinical disease during experimental

TevPV or AlsPV infection is therefore not conclusive evidence that disease would be absent in all mammalian species. While it is not feasible to test every species that may be exposed to these viruses, the experimental infection of pigs with TevPV may yield useful results based on the pathogenesis of MenPV and TioPV.

Another limitation of the animal infection studies was the small sample size of ferrets in the first study. This was due to it being an observational study aimed at determining whether ferrets could be infected with either virus. AlsPV RNA was observed in the brain tissue of two out of ten mice at 21 days post exposure to AlsPV, but was not detected in any ferret brain tissue at the same time point. It is possible that this evidence of viral persistence could have been found in ferrets if a greater number were exposed to the virus. In addition, the high virus titres used in the animal challenge experiments did not reflect the titres animals would be exposed to under natural conditions. Nevertheless, the ferret is clearly a useful model for determining the pathogenesis of AlsPV and could also be used in the future to understand the potential transmission of the virus given previously established transmission models for influenza virus (250).

6.6 SUMMARY AND FUTURE DIRECTIONS

Multiple viruses and virus-derived sequences were detected in bat urine collected in Alstonville in July and August of 2011, revealing the incredible diversity of unknown viruses in bats. The isolation of two paramyxoviruses, AlsPV and TevPV, facilitated *in vitro* and *in vivo* characterisation. The potential persistence of AlsPV in immune privileged sites warrants further investigation, particularly as the reactivation of other persistently infecting paramyxoviruses has resulted in ongoing transmission or death (94, 251). The growth of high titres of AlsPV causing limited cytopathic effect in multiple mammalian cell lines may also indicate the potential for persistence (252). Additional animal infection studies should be conducted to determine the potential for persistent infection and the presence of any long-term neurological or olfactory effects.

It is also important to determine the whole genome sequences of representative adenoviruses that were isolated from Alstonville bats, as no whole genome sequences of Australian bat adenoviruses have been published thus far. Their low GC content and apparent relationship with geographically and host species distinct adenoviruses suggests that these isolates are an important contribution to our understanding of adenovirus evolution and diversity. The isolations and short sequences described in Chapter 3 reveal that adenoviruses are prevalent in pteropid bats and bat urine, consistent with observations in bats internationally (26).

Although the prevalence of AlsPV and TevPV neutralising antibodies in pteropid bats was assessed in Chapters 4 and 5, it would be useful to conduct similar serosurveillance studies to determine their

prevalence in other animals, particularly in livestock. There may be some difficulties with calculating the prevalence of AlsPV due to the observed neutralisation of AlsPV with low dilutions of PIV5 antisera. PIV5 has been isolated from a wide range of animals and PIV5 neutralising antibodies have even been detected in humans (235, 253), therefore false positives due to cross-reactivity may be recorded. The results in this thesis raise the possibility that some PIV5 neutralising antibodies may be due to another closely related virus, such as AlsPV. These cross-neutralising antibodies mean that humans may be protected against AlsPV infection. Other serological tests would be needed to distinguish antibodies against either of the two viruses.

Bats host a higher proportion of zoonotic viruses than any other mammalian order (3), therefore it is important to identify these viruses with zoonotic potential before they emerge from the reservoir. The viral sequences identified in this thesis are a valuable contribution to our understanding of viral diversity and evolution. Furthermore, knowledge of the source of these viral sequences can assist an epidemiological response if they are detected during disease outbreaks in non-pteropid mammals. Imaging of these viruses by electron microscopy is recommended as a next step in understanding more about the isolated viruses. It would be interesting to compare the viral diversity identified in the Alstonville bat colony in 2011 to the current day to see if the same viral sequences are still present now and if the prevalence of all viruses was affected by the same factors that caused an increased prevalence of HeV in 2011 (53).

The risk of spillover of each virus described in this thesis is low due to the wide range of specific conditions that are required for spillover to occur (23). Effective spillover and infection of a non-reservoir host relies on the distribution, infection dynamics and shedding dynamics of the reservoir host, as well as the susceptibility of the non-reservoir hosts and frequency of exposure (36). However, changes to these factors are leading to an increased likelihood of exposure of non-pteropid mammals to bat-borne viruses. Bats are seeking food and roosting in urban areas due to ecological changes and bat behavioural adaptation (17, 45), and anthropogenic environmental changes such as agricultural intensification are contributing to an increased risk of zoonotic virus emergence (254). Although the individual risk of transmission of one of these viruses is low, regular exposure to bat-borne viruses increases the risk of infecting a new host. It is therefore important that we continue to recommend methods of preventing the transmission of these viruses. These include restricting livestock access to trees that attract flying foxes and providing food and water sources that are protected from bat urine or faecal contamination (255).

Despite multiple virus discovery projects in Australia, novel virus-derived sequences and viruses are continuing to be detected and isolated, indicating that the saturation point of virus discovery has not

yet been reached (9, 30). It is clear from these results that further virus discovery and characterisation studies are warranted. Although the isolation of viruses can be more labour intensive than the detection of nucleic acids, it allows complete phenotypic characterisation of viruses and confirms their description as 'novel' species (24, 256). By conducting phenotypic characterisation, we have been able to fully understand the relationship of AlsPV and TevPV with other isolated viruses and determine the pathogenesis and tissue tropism following infection of representative mammalian species. This information is lacking from the multiple detected paramyxovirus sequences described in Chapter 3 and prevents their classification as novel species. Furthermore, the isolation of a virus can facilitate whole genome sequencing. For the two isolated paramyxoviruses described in Chapters 4 and 5, whole genome sequencing was successful and at high coverage due to the higher virus titres found in infected cell culture supernatant. In comparison, LumPV could not be isolated, with sequencing of the LumPV genome incomplete and at low coverage as a result of the lower levels of viral RNA present in bat urine. Nevertheless, both the detection of viral sequences and the isolation of viruses give an important insight into the remarkable virus diversity in bats and highlight the importance of continued surveillance of Australian bats.

APPENDIX

Table A1: Paramyxovirus RNA detected in urine collected from a pteropid bat colony in Alstonville, or in the supernatant (SNT) of cells inoculated with this urine.

Date collected	**Urine no.**	**Source**	**Primers used**	**Closest relative by BLASTX**	**Closest relative by BLASTn**	**Similarity to HeV**
12/7/11	12	SNT	*Paramyxoviridae*	100% Geelong paramyxovirus (KM359175.1)	99% Geelong paramyxovirus (KM359175.1)	38%
	15	Urine	*Paramyxoviridae*	75% Paramyxovirus PgPMV-10 (KC692412.1)	72% Paramyxovirus PgPMV-10 (KC692412.1)	66%
	20	Urine	*Paramyxoviridae*	95% Bat paramyxovirus (AKG96280.1)	96% Bat paramyxovirus (KM391916.1)	66%
	21	Urine	*Paramyxoviridae*	68% Paramyxovirus PgPMV-10 68% (KC692412.1)	70% Paramyxovirus PgPMV-10 (KC692412.1)	56%
	23	SNT	*Paramyxoviridae*	79% Paramyxovirus IFBPV01/2010 (AB691542.1)	73% Paramyxovirus IFBPV01/2010 (AB691542.1)	67%
3/8/11	4	Urine	*Paramyxoviridae*	97% Menangle virus (YP_009512971.1)	97% Menangle virus isolate Australia/bat/2009/Cedar Grove 97% (JX112711.1)	39%
	5	Urine	*Paramyxoviridae*	98% Paramyxovirus PgPMV-10 (KC692412.1)	100% Yarra Bend paramyxovirus (KM359176.1)	72%
	27	Urine	*Respirovirus-Morbillivirus-Henipavirus*	100% Pteropus sp. paramyxovirus 100% (AIU34325.1)	100% Pteropus sp. paramyxovirus (KF871295.1)	59%
	30	Urine and SNT	*Paramyxoviridae*	76% Eidolon helvum paramyxovirus (AEY68861.1)	75% Eidolon helvum paramyxovirus (JN648079.1)	70%
			Respirovirus-Morbillivirus-Henipavirus	90% Pteropus scapulatus paramyxovirus (AIU34323.1)	76% Pteropus scapulatus paramyxovirus (KF871293.1)	65%
	34	Urine	*Paramyxoviridae*	74% Eidolon	74% Eidolon	65%

				helvum paramyxovirus (AEY68861.1)	helvum paramyxovirus (JN648079.1)	
	38	Urine	*Paramyxoviridae*	74% Eidolon helvum paramyxovirus (AEY68861.1)	78% Eidolon helvum paramyxovirus (JN648079.1)	67%
	42	Urine	*Paramyxoviridae*	82% Paramyxovirus PgPMV-10 (KC692412.1)	74% Paramyxovirus PgPMV-10 (KC692412.1)	68%
			Respirovirus-Morbillivirus-Henipavirus	99% Pteropus alecto paramyxovirus (KF871301.1)	98% Pteropus alecto paramyxovirus (KF871301.1)	60%
	42	SNT	*Paramyxoviridae*	99% Teviot virus isolate Cedar Grove (KP271124.1)	98% Teviot virus isolate Cedar Grove (KP271124.1)	35%
	44	Urine	*Paramyxoviridae*	89% Paramyxovirus PgPMV-9 (KC692411.1)	79% Paramyxovirus PgPMV-9 (KC692411.1)	68%
	46	Urine	*Paramyxoviridae*	100% Teviot virus (AIS82743.1)	100% Teviot virus isolate Cedar Grove (KP271124.1)	40%
	48	Urine	*Paramyxoviridae*	97% Grove virus (AIS82741.1)	98% Grove virus (KJ716812.1)	34%
	50	Urine	*Paramyxoviridae*	75% Eidolon helvum paramyxovirus (AEY68861.1)	75% Eidolon helvum paramyxovirus (JN648079.1)	68%
			Respirovirus-Morbillivirus-Henipavirus	89% Pteropus scapulatus paramyxovirus (AIU34323.1)	76% Pteropus scapulatus paramyxovirus (KF871293.1)	66%
	53	Urine	*Paramyxoviridae*	97% Grove virus (AIS82741.1)	96% Grove virus (KJ716812.1)	31%

Table A2: Comparison of Lumley virus (LumPV) genomic features. Putative gene boundary sequences and intergenic region (IGR) sequences of LumPV are compared to those of Mojiang virus (MojPV) and Hendra virus (HeV).

			Length	Boundary Sequence
N	5’ UTR	LumPV	-	-
		MojPV	85	AGGATTCAGGAC
		HeV	57	AGGAACCAAGAC
	3’ UTR	LumPV	149	ATTATAAAAAA
		MojPV	164	ATTAAACAAAA
		HeV	568	ATTAAGAAAAA
	IGR	LumPV	3	CTT
		MojPV	3	CTT
		HeV	3	CTT
P	5’UTR	LumPV	228	AGGAGCCAAGCC
		MojPV	264	AGGATCCAAGAG
		HeV	105	AGGATCCAAGAC
	3’UTR	LumPV	139	GCTTAAGAAAAA
		MojPV	144	TATCATAAAAAA
		HeV	469	CATTAAGAAAAA
	IGR	LumPV	3	CTT
		MojPV	3	CTT
		HeV	3	CTT
M	5’UTR	LumPV	310	AGGATCCAAGAT
		MojPV	49	AGGAGTCAAGAA
		HeV	100	AGGAGACAGGTA
	3’UTR	LumPV	83	TCTTATGAAAAA
		MojPV	455	CAATATAAAAAA
		HeV	200	TATTAAGAAAAA
	IGR	LumPV	3	CTT
		MojPV	3	CTT
		HeV	3	CTT
F	5’ UTR	LumPV	275	AGGATCCCAGAA
		MojPV	952	AGGTGTCAGGAC
		HeV	272	AGGAGCCAAGTT
	3’ UTR	LumPV	264	CACTATAAAAAA
		MojPV	173	TATTAATAAAAA
		HeV	418	CTTTACAAAAAA
	IGR	LumPV	3	CTT
		MojPV	3	CTT
		HeV	3	CTT
G	5’ UTR	LumPV	283	AGGATTCAAGGC
		MojPV	121	AGGAGTCAGGGT
		HeV	233	AGGACCCAAGTC
	3’ UTR	LumPV	237	AATTATAAAAAA
		MojPV	543	GGTTACAAAAAA
		HeV	516	ATTAAGAAAAA
	IGR	LumPV	3	CTT
		MojPV	3	CTT

		HeV	3	CTT
L	5’ UTR	LumPV	696	AGGGTCCAAGGA
		MojPV	222	AGGATTCACGGA
		HeV	153	AGGACCCAAGTC
	3’ UTR	LumPV	-	-
		MojPV	50	TATTAATAAAAA
		HeV	67	TATTAAGAAAAA

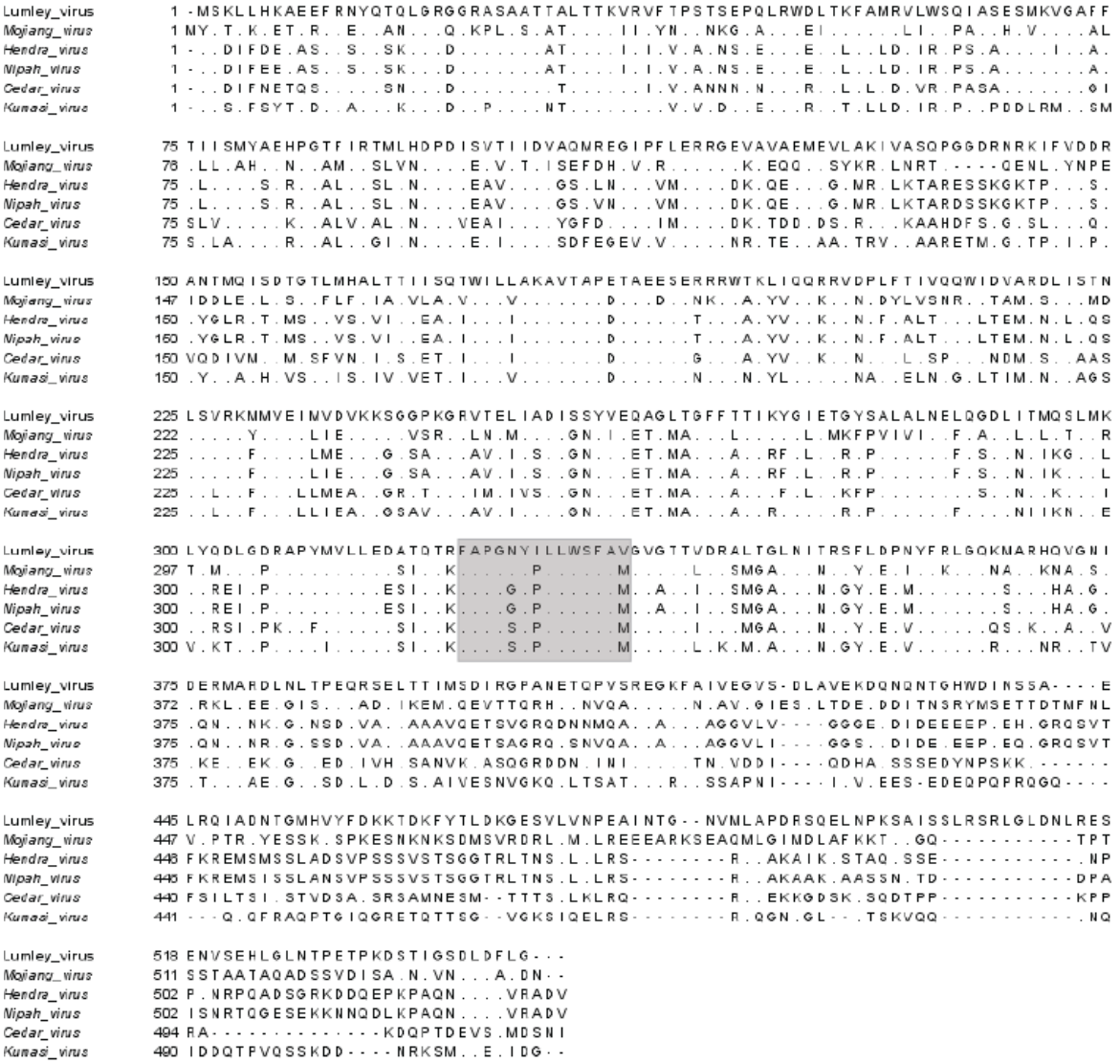

Figure A1.1: Alignment of henipavirus N proteins with putative LumPV N protein. Sequences aligned using Clustal Omega multiple sequence alignment program and visualised using Jalview 2. Conserved motif highlighted in grey.

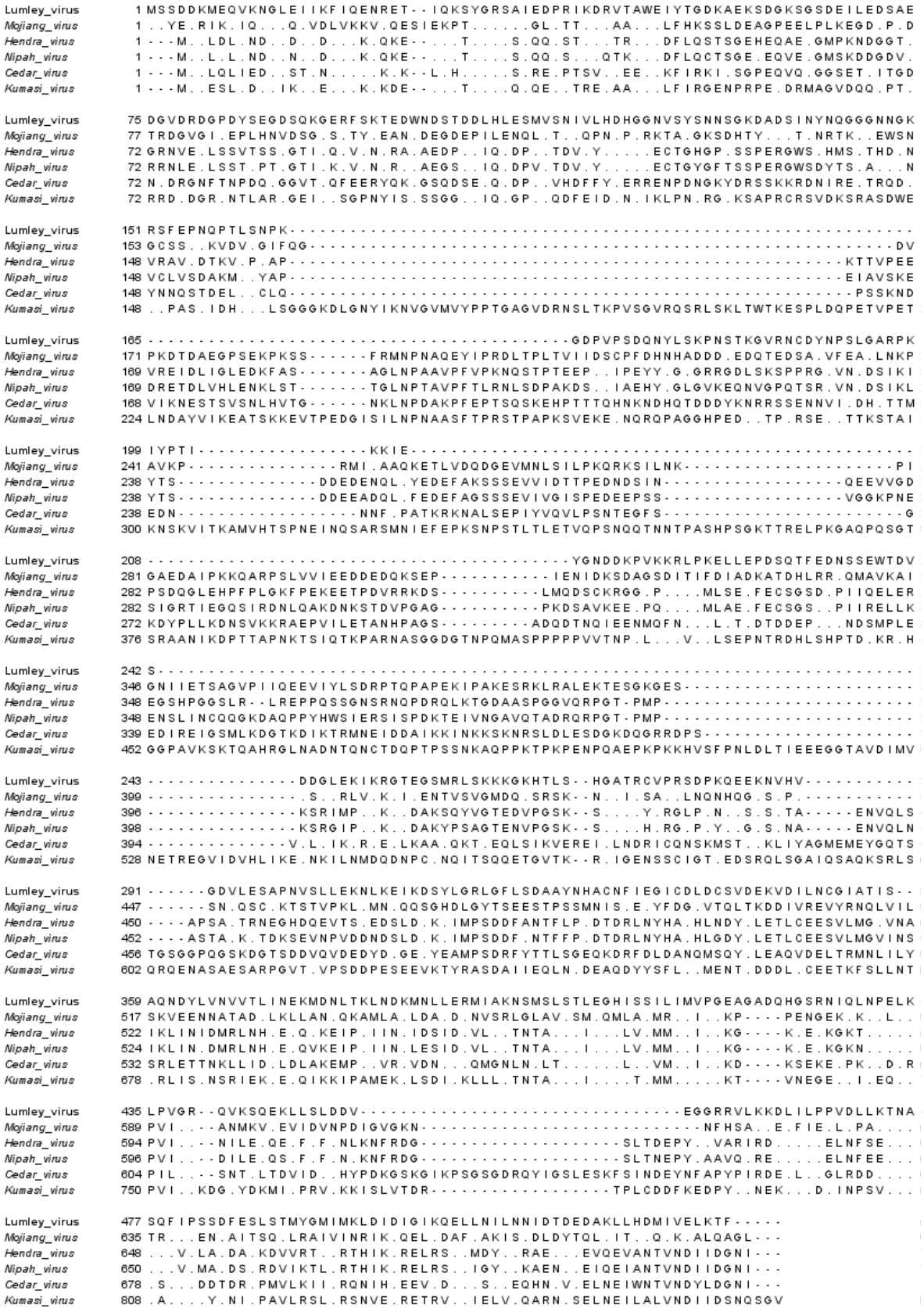

Figure A1.2: Alignment of henipavirus P proteins with putative LumPV P protein. Sequences aligned using Clustal Omega multiple sequence alignment program and visualised using Jalview 2.

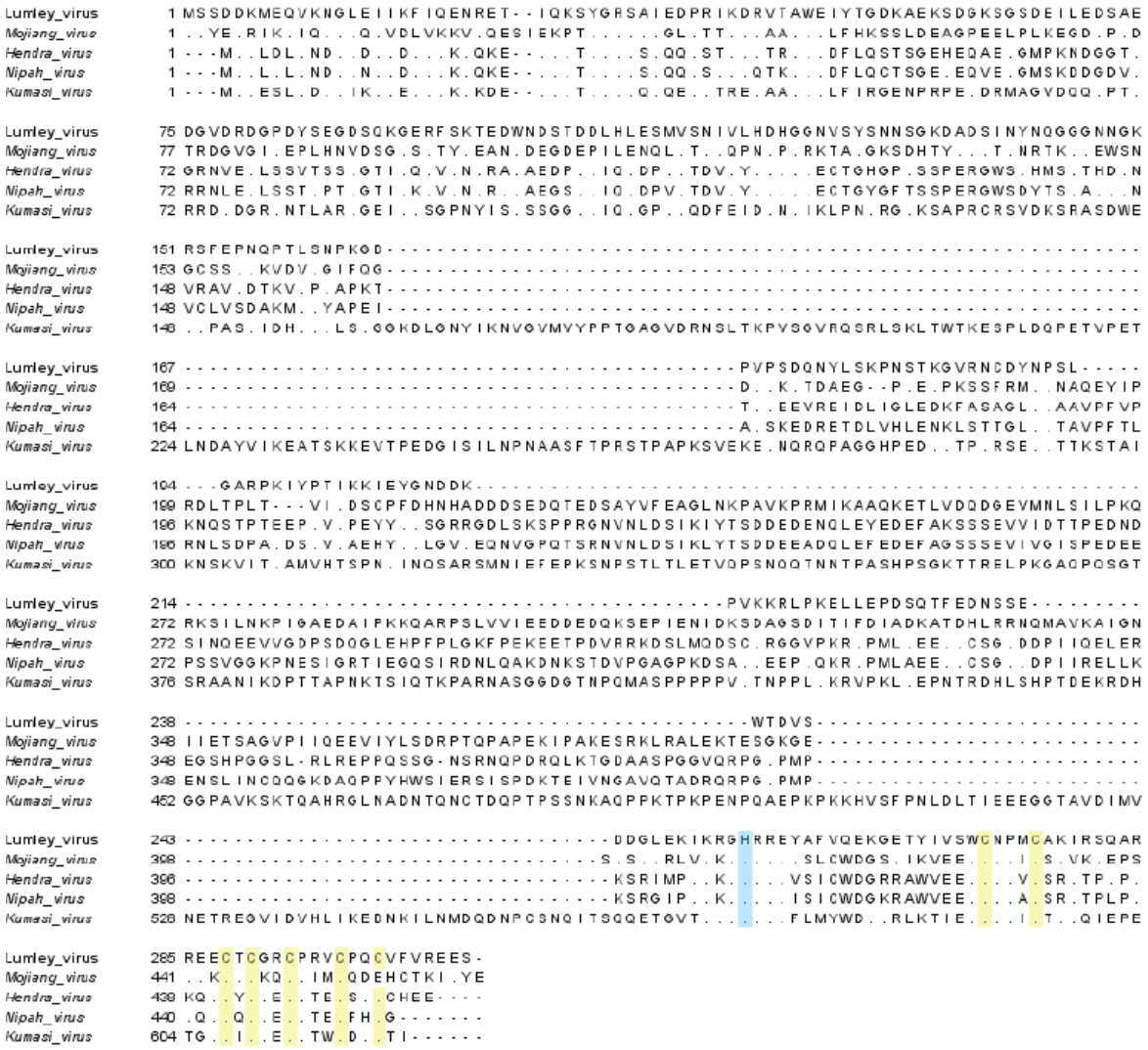

Figure A1.3: Alignment of henipavirus V proteins with putative LumPV V protein. Sequences aligned using Clustal Omega multiple sequence alignment program and visualised using Jalview 2. Conserved histidine (blue) and cysteine (yellow) residues are highlighted.

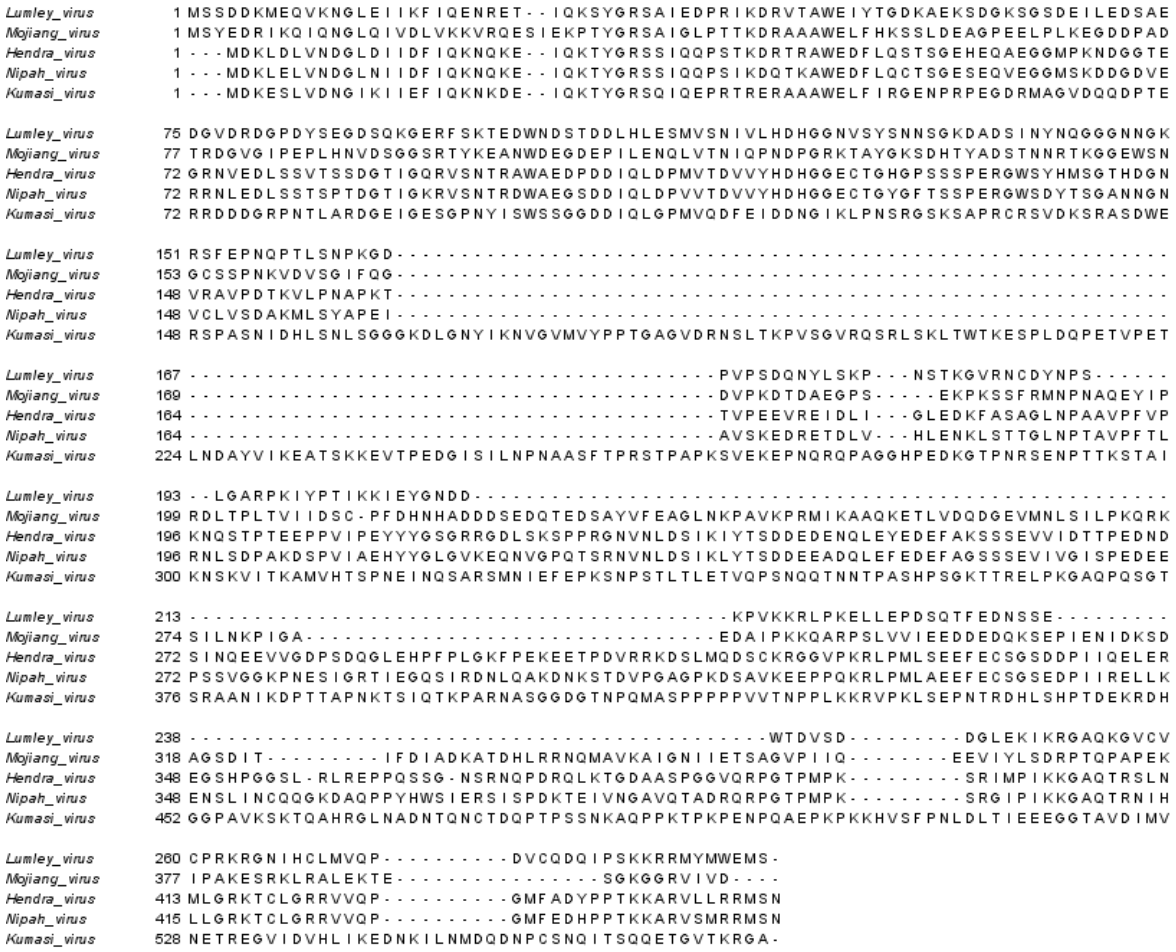

Figure A1.4: Alignment of henipavirus W proteins with putative LumPV W protein. Sequences aligned using Clustal Omega multiple sequence alignment program and visualised using Jalview 2.

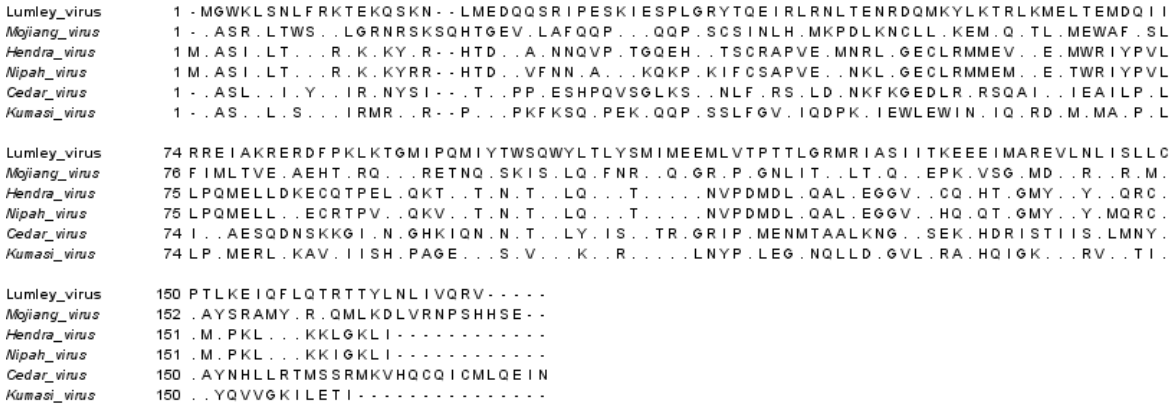

Figure A1.5: Alignment of henipavirus C proteins with putative LumPV C protein. Sequences aligned using Clustal Omega multiple sequence alignment program and visualised using Jalview 2.

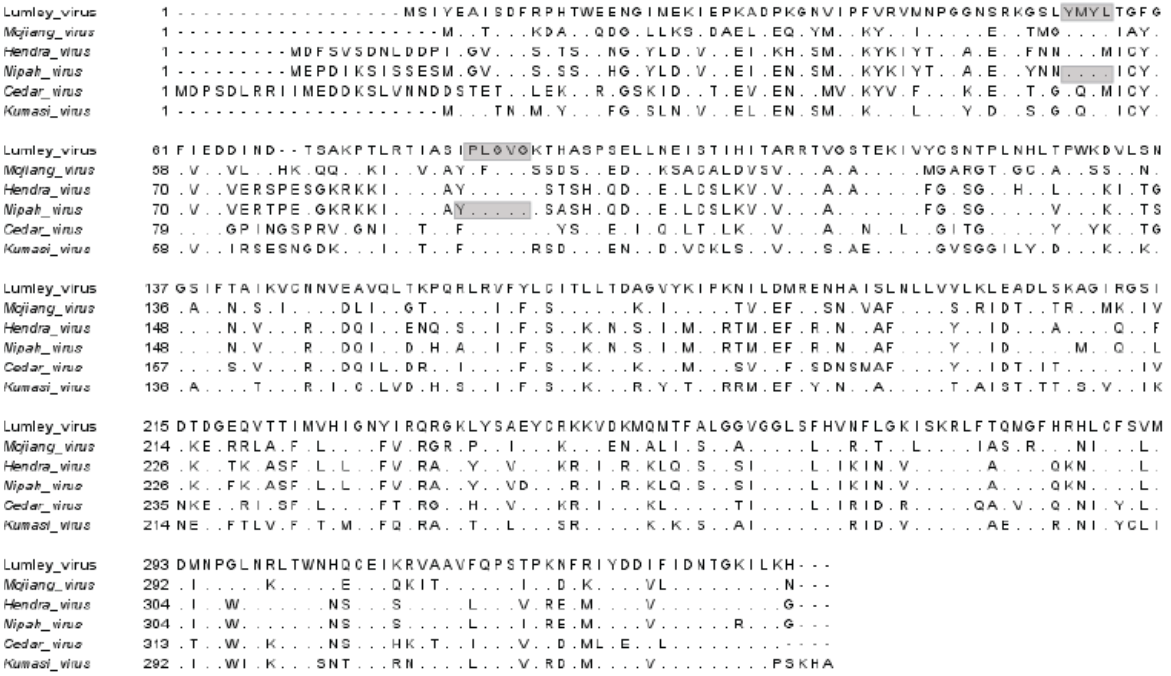

Figure A1.6: Alignment of henipavirus M proteins with putative LumPV M protein. Sequences aligned using Clustal Omega multiple sequence alignment program and visualised using Jalview 2. Conserved motifs are highlighted in grey.

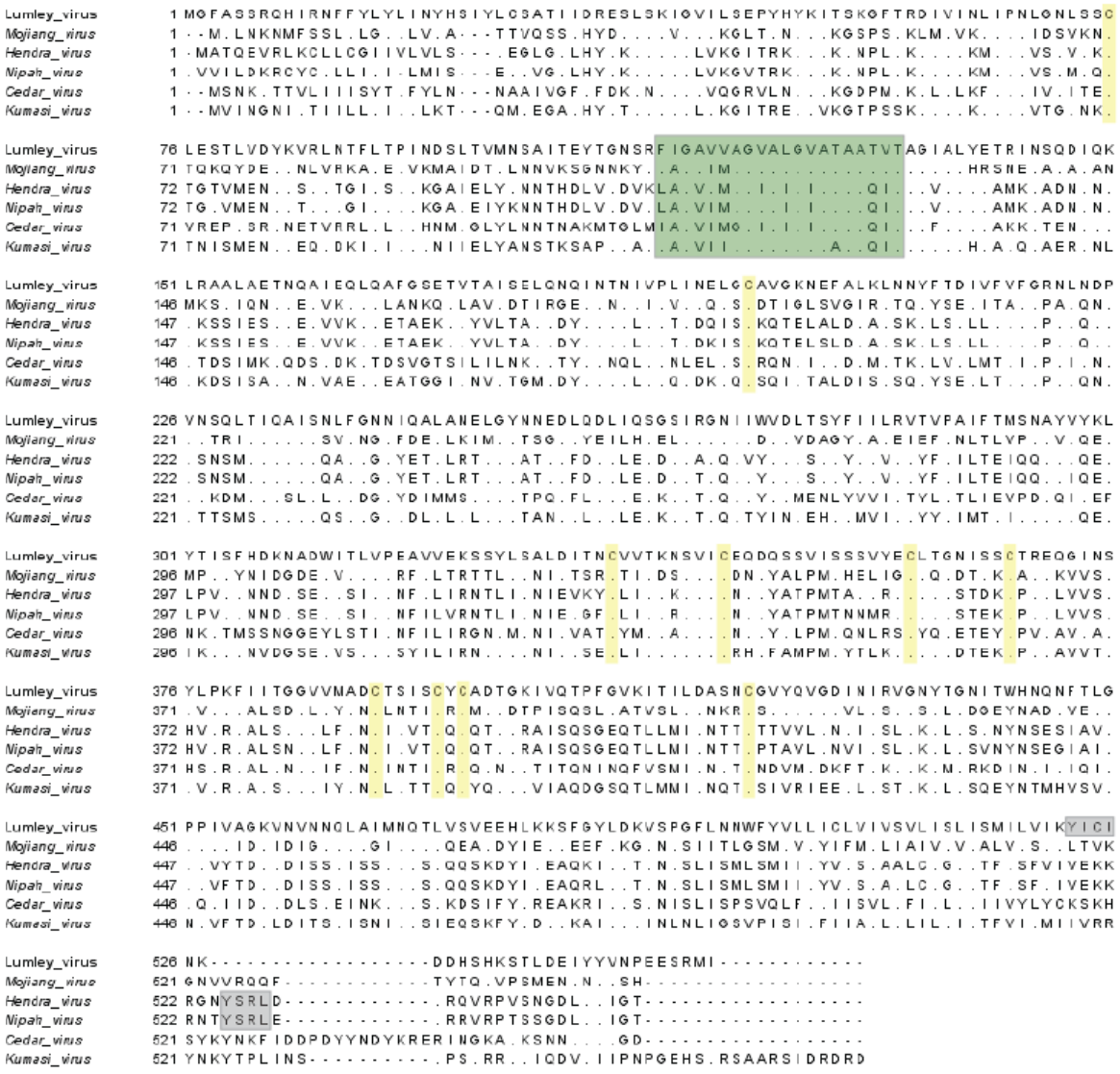

Figure A1.7: Alignment of henipavirus F proteins with putative LumPV F protein. Sequences aligned using Clustal Omega multiple sequence alignment program and visualised using Jalview 2. Fusion peptide is highlighted in green and conserved cysteine residues are highlighted in yellow. The YXXΦ (where Φ is a hydrophobic amino acid) endocytosis motif is highlighted in grey.

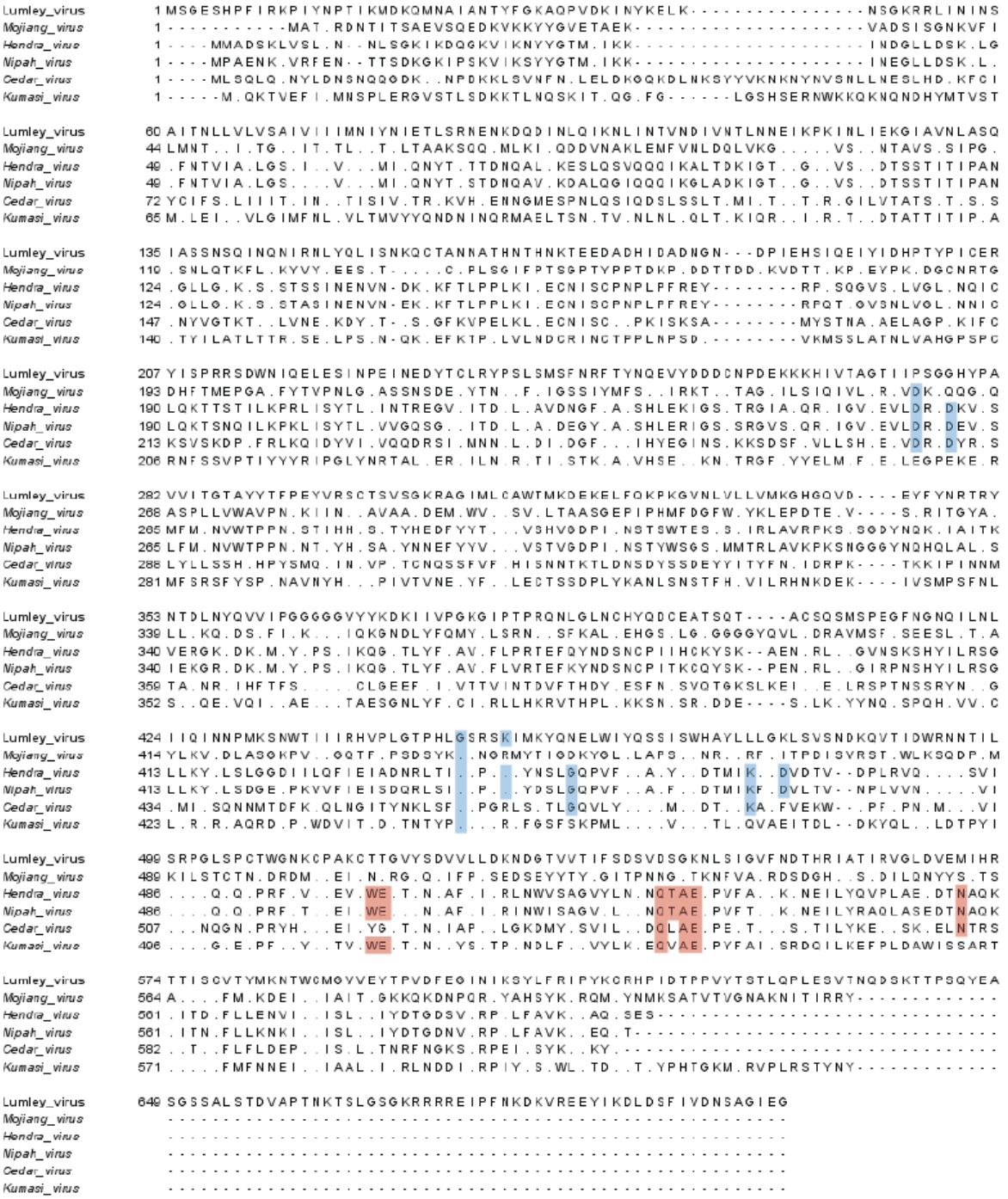

Figure A1.8: Alignment of henipavirus G proteins with putative LumPV G protein. Sequences aligned using Clustal Omega multiple sequence alignment program and visualised using Jalview 2. Residues associated with ephrin binding in Hendra virus (blue) and Nipah virus (red) are highlighted.

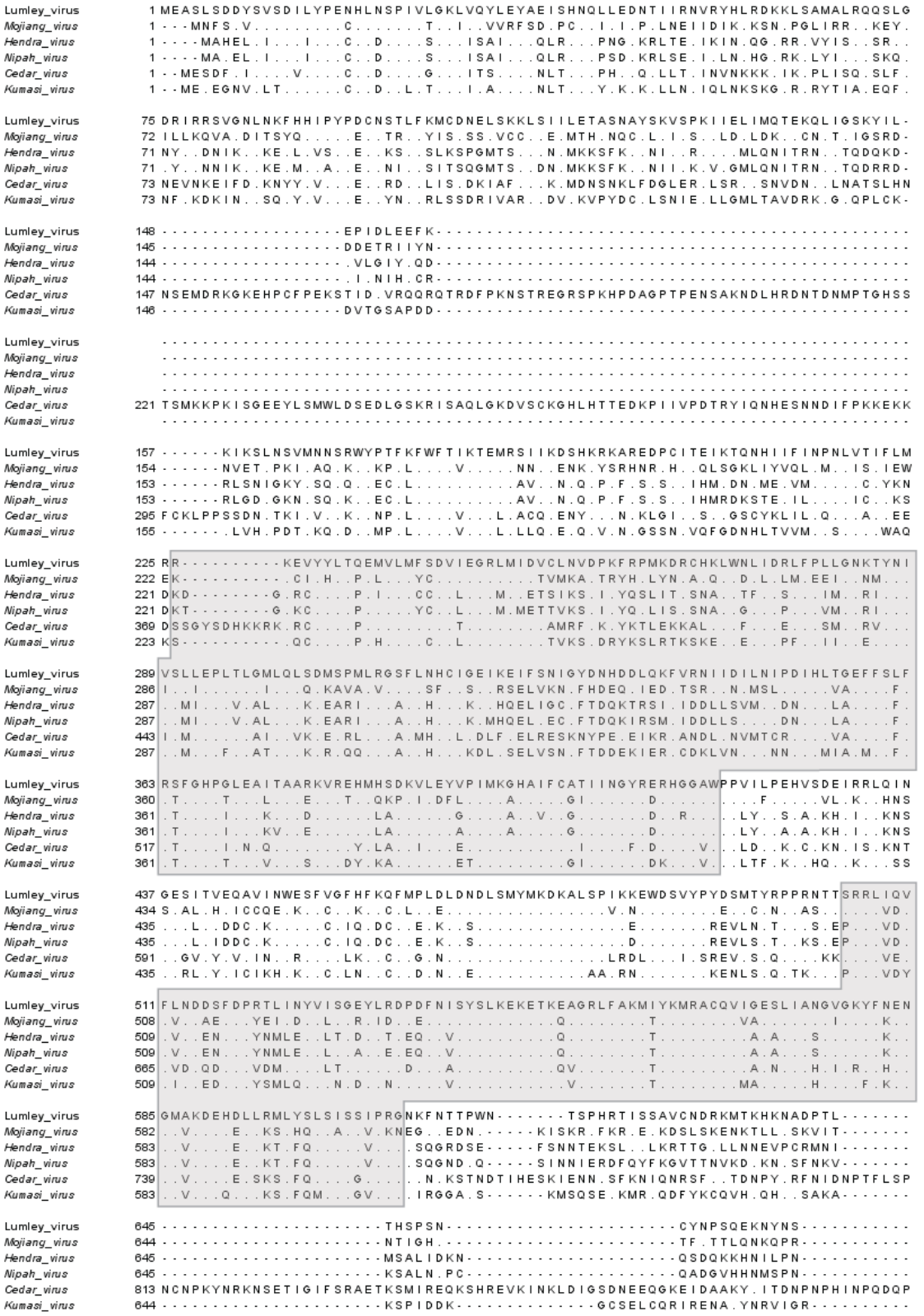
Lumley_virus
Mojiang_virus
Hendra_virus
Nipah_virus
Cedar_virus
Kumasi_virus
I
II

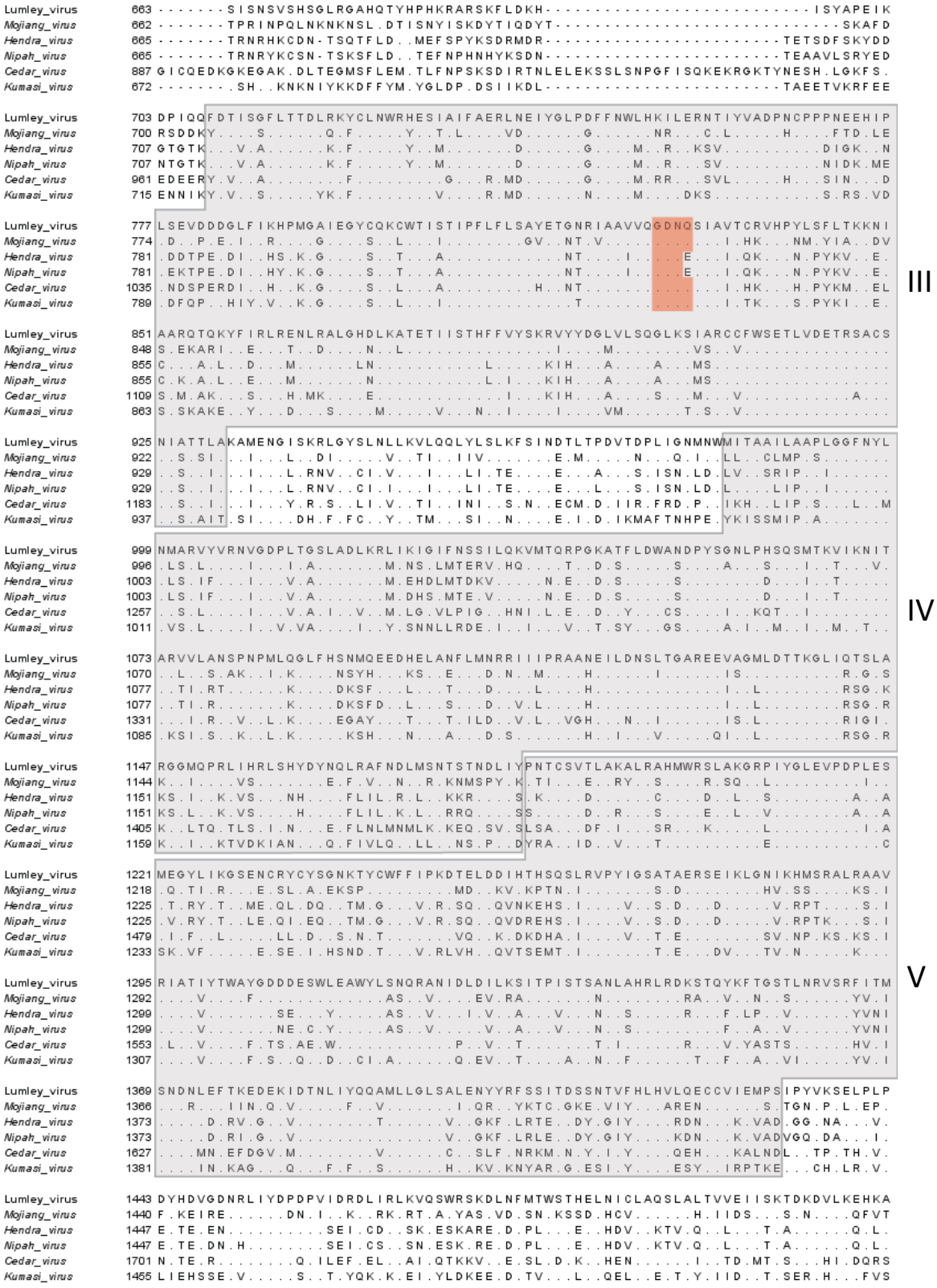
Lumley_virus
Mojiang_virus
Hendra_virus
Nipah_virus
Cedar_virus
Kumasi_virus
III
IV
V

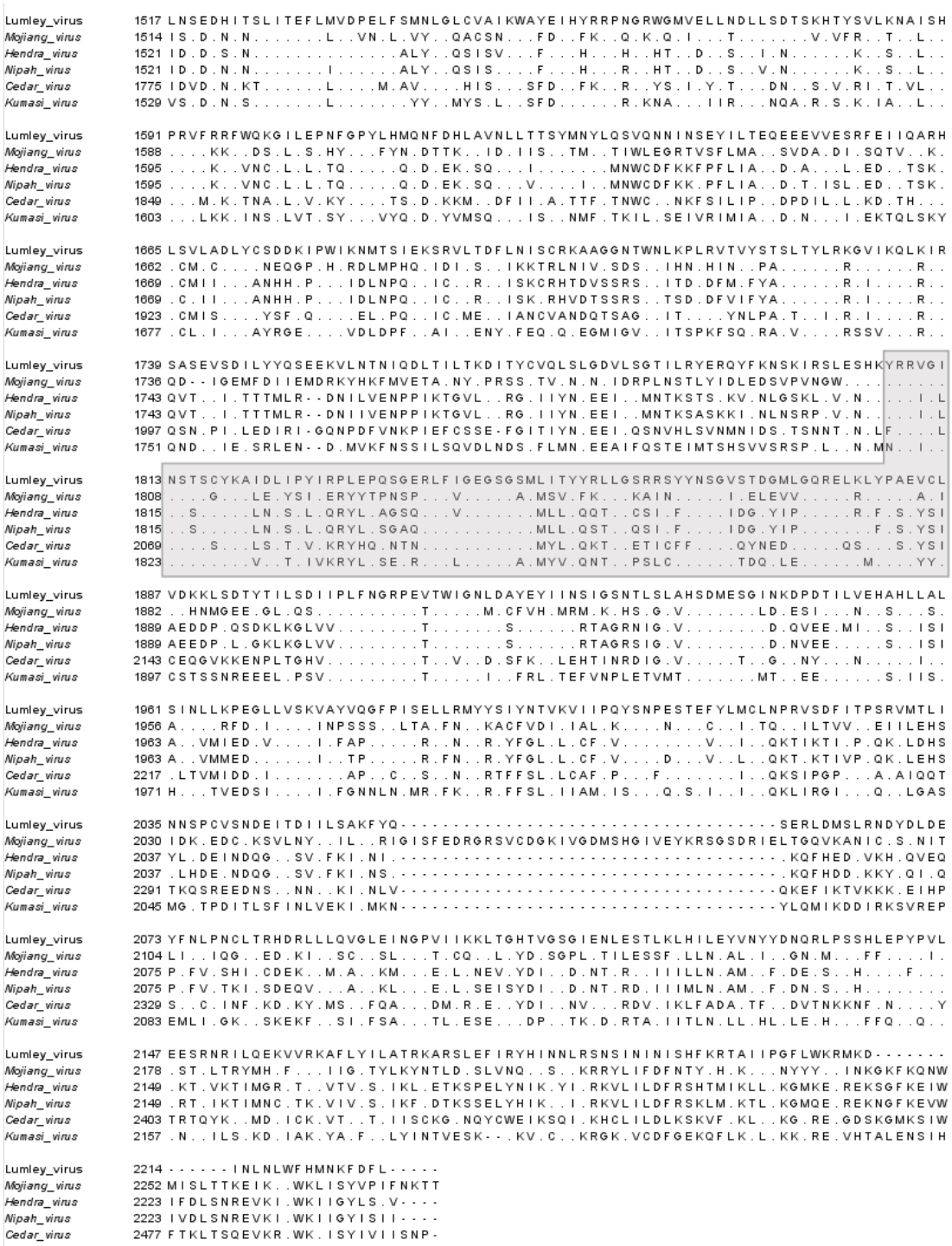

Figure A1.9: Alignment of henipavirus L proteins with putative LumPV L protein. Sequences aligned using Clustal Omega multiple sequence alignment program and visualised using Jalview 2. Conserved domains I-VI are highlighted in grey. The GDNQ motif (red) is in Domain III. The LumPV L protein 3' terminal sequence remains unknown.

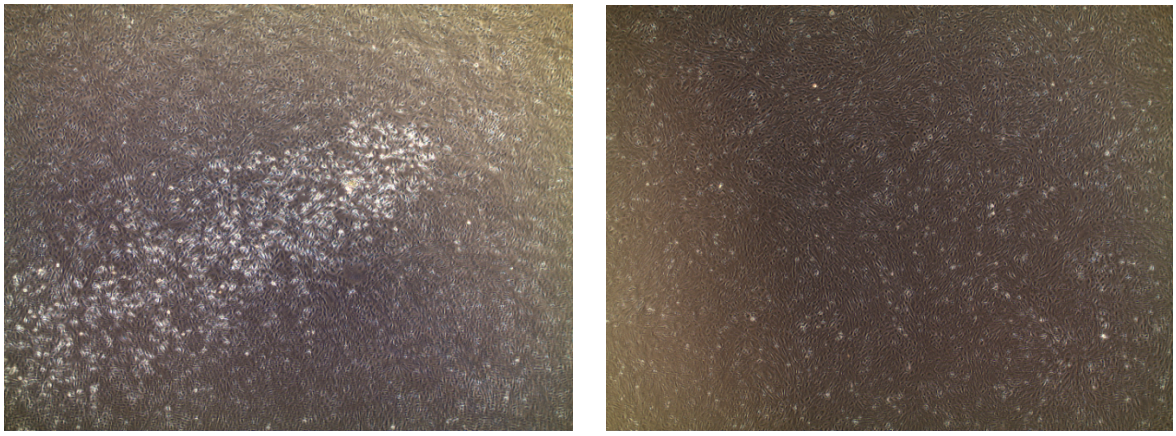

Figure A2: Cytopathic effect caused by an adenovirus in urine sample AL11. Urine was inoculated onto PaKi cells and cytopathic effect was observed at 6 days post inoculation. Left panel shows cytopathic effect at 6 days post inoculation, 4x magnification. Right panel shows uninfected PaKi cells at the same time point and magnification.

REFERENCES

1. **Cunningham AA, Daszak P, Wood JLN.** 2017. One Health, emerging infectious diseases and wildlife: two decades of progress? Philos Trans R Soc Lond B Biol Sci **372**.
2. **Jones KE, Patel NG, Levy MA, Storeygard A, Balk D, Gittleman JL, Daszak P.** 2008. Global trends in emerging infectious diseases. Nature **451:**990-993.
3. **Olival KJ, Hosseini PR, Zambrana-Torrelio C, Ross N, Bogich TL, Daszak P.** 2017. Host and viral traits predict zoonotic spillover from mammals. Nature **546:**646-650.
4. **Levinson J, Bogich TL, Olival KJ, Epstein JH, Johnson CK, Karesh W, Daszak P.** 2013. Targeting surveillance for zoonotic virus discovery. Emerg Infect Dis **19:**743-747.
5. **Schountz T.** 2014. Immunology of bats and their viruses: challenges and opportunities. Viruses **6:**4880-4901.
6. **Kuiken T, Leighton FA, Fouchier RA, LeDuc JW, Peiris JS, Schudel A, Stohr K, Osterhaus AD.** 2005. Public health. Pathogen surveillance in animals. Science **309:**1680-1681.
7. **Middleton D.** 2014. Hendra virus. Vet Clin North Am Equine Pract **30:**579-589.
8. **Drexler JF, Corman VM, Gloza-Rausch F, Seebens A, Annan A, Ipsen A, Kruppa T, Muller MA, Kalko EK, Adu-Sarkodie Y, Oppong S, Drosten C.** 2009. Henipavirus RNA in African bats. PLoS One **4:**e6367.
9. **Vidgen ME, de Jong C, Rose K, Hall J, Field HE, Smith CS.** 2015. Novel paramyxoviruses in Australian flying-fox populations support host-virus coevolution. J Gen Virol doi:10.1099/vir.0.000099.
10. **Kohl C, Tachedjian M, Todd S, Monaghan P, Boyd V, Marsh GA, Crameri G, Field H, Kurth A, Smith I, Wang LF.** 2018. Hervey virus: Study on co-circulation with Henipaviruses in Pteropid bats within their distribution range from Australia to Africa. PLoS One **13:**e0191933.
11. **King DA, Peckham C, Waage JK, Brownlie J, Woolhouse ME.** 2006. Epidemiology. Infectious diseases: preparing for the future. Science **313:**1392-1393.
12. **Woolhouse ME, Gowtage-Sequeria S.** 2005. Host range and emerging and reemerging pathogens. Emerg Infect Dis **11:**1842-1847.
13. **Allen T, Murray KA, Zambrana-Torrelio C, Morse SS, Rondinini C, Di Marco M, Breit N, Olival KJ, Daszak P.** 2017. Global hotspots and correlates of emerging zoonotic diseases. Nature Communications **8:**1124.
14. **Dunn RR, Davies TJ, Harris NC, Gavin MC.** 2010. Global drivers of human pathogen richness and prevalence. Proc Biol Sci **277:**2587-2595.
15. **Daszak P, Cunningham AA, Hyatt AD.** 2000. Emerging infectious diseases of wildlife--threats to biodiversity and human health. Science **287:**443-449.
16. **Morse SS, Mazet JA, Woolhouse M, Parrish CR, Carroll D, Karesh WB, Zambrana-Torrelio C, Lipkin WI, Daszak P.** 2012. Prediction and prevention of the next pandemic zoonosis. Lancet **380:**1956-1965.
17. **Plowright RK, Foley P, Field HE, Dobson AP, Foley JE, Eby P, Daszak P.** 2011. Urban habituation, ecological connectivity and epidemic dampening: the emergence of Hendra virus from flying foxes (Pteropus spp.). Proc Biol Sci **278:**3703-3712.
18. **Parrish CR, Holmes EC, Morens DM, Park EC, Burke DS, Calisher CH, Laughlin CA, Saif LJ, Daszak P.** 2008. Cross-species virus transmission and the emergence of new epidemic diseases. Microbiol Mol Biol Rev **72:**457-470.
19. **Wolfe ND, Dunavan CP, Diamond J.** 2007. Origins of major human infectious diseases. Nature **447:**279-283.
20. **Holmes EC, Rambaut A, Andersen KG.** 2018. Pandemics: spend on surveillance, not prediction. Nature **558:**180-182.
21. **International Committee on Taxonomy of Viruses.** 2018. Help with completing a taxonomic proposal to ICTV. https://talk.ictvonline.org/files/taxonomy-proposal-templates/m/templates/6590. Accessed January 22 2019.

22. **Calisher CH, Childs JE, Field HE, Holmes KV, Schountz T.** 2006. Bats: important reservoir hosts of emerging viruses. Clin Microbiol Rev **19:**531-545.
23. **Wang LF, Crameri G.** 2014. Emerging zoonotic viral diseases. Rev Sci Tech **33:**569-581.
24. **Young CC, Olival KJ.** 2016. Optimizing Viral Discovery in Bats. PLoS One **11:**e0149237.
25. **Li W, Shi Z, Yu M, Ren W, Smith C, Epstein JH, Wang H, Crameri G, Hu Z, Zhang H, Zhang J, McEachern J, Field H, Daszak P, Eaton BT, Zhang S, Wang LF.** 2005. Bats are natural reservoirs of SARS-like coronaviruses. Science **310:**676-679.
26. **Li Y, Ge X, Zhang H, Zhou P, Zhu Y, Zhang Y, Yuan J, Wang LF, Shi Z.** 2010. Host range, prevalence, and genetic diversity of adenoviruses in bats. J Virol **84:**3889-3897.
27. **Towner JS, Amman BR, Sealy TK, Carroll SA, Comer JA, Kemp A, Swanepoel R, Paddock CD, Balinandi S, Khristova ML, Formenty PB, Albarino CG, Miller DM, Reed ZD, Kayiwa JT, Mills JN, Cannon DL, Greer PW, Byaruhanga E, Farnon EC, Atimnedi P, Okware S, Katongole-Mbidde E, Downing R, Tappero JW, Zaki SR, Ksiazek TG, Nichol ST, Rollin PE.** 2009. Isolation of genetically diverse Marburg viruses from Egyptian fruit bats. PLoS Pathog **5:**e1000536.
28. **Pritchard LI, Chua KB, Cummins D, Hyatt A, Crameri G, Eaton BT, Wang LF.** 2006. Pulau virus; a new member of the Nelson Bay orthoreovirus species isolated from fruit bats in Malaysia. Arch Virol **151:**229-239.
29. **Sasaki M, Setiyono A, Handharyani E, Kobayashi S, Rahmadani I, Taha S, Adiani S, Subangkit M, Nakamura I, Sawa H, Kimura T.** 2014. Isolation and characterization of a novel alphaherpesvirus in fruit bats. J Virol **88:**9819-9829.
30. **Barr J, Smith C, Smith I, de Jong C, Todd S, Melville D, Broos A, Crameri S, Haining J, Marsh G, Crameri G, Field H, Wang LF.** 2015. Isolation of multiple novel paramyxoviruses from pteropid bat urine. J Gen Virol **96:**24-29.
31. **Anthony SJ, Epstein JH, Murray KA, Navarrete-Macias I, Zambrana-Torrelio CM, Solovyov A, Ojeda-Flores R, Arrigo NC, Islam A, Ali Khan S, Hosseini P, Bogich TL, Olival KJ, Sanchez-Leon MD, Karesh WB, Goldstein T, Luby SP, Morse SS, Mazet JA, Daszak P, Lipkin WI.** 2013. A strategy to estimate unknown viral diversity in mammals. MBio **4:**e00598-00513.
32. **Speare R, Skerratt L, Foster R, Berger L, Hooper P, Lunt R, Blair D, Hansman D, Goulet M, Cooper S.** 1997. Australian bat lyssavirus infection in three fruit bats from north Queensland. Commun Dis Intell **21:**117-120.
33. **Haydon DT, Cleaveland S, Taylor LH, Laurenson MK.** 2002. Identifying reservoirs of infection: a conceptual and practical challenge. Emerg Infect Dis **8:**1468-1473.
34. **Wang LF, Walker PJ, Poon LL.** 2011. Mass extinctions, biodiversity and mitochondrial function: are bats 'special' as reservoirs for emerging viruses? Curr Opin Virol **1:**649-657.
35. **Wilkinson GS, South JM.** 2002. Life history, ecology and longevity in bats. Aging Cell **1:**124-131.
36. **Plowright RK, Eby P, Hudson PJ, Smith IL, Westcott D, Bryden WL, Middleton D, Reid PA, McFarlane RA, Martin G, Tabor GM, Skerratt LF, Anderson DL, Crameri G, Quammen D, Jordan D, Freeman P, Wang LF, Epstein JH, Marsh GA, Kung NY, McCallum H.** 2015. Ecological dynamics of emerging bat virus spillover. Proc Biol Sci **282:**20142124.
37. **Teeling EC, Springer MS, Madsen O, Bates P, O'Brien S J, Murphy WJ.** 2005. A molecular phylogeny for bats illuminates biogeography and the fossil record. Science **307:**580-584.
38. **Zhang G, Cowled C, Shi Z, Huang Z, Bishop-Lilly KA, Fang X, Wynne JW, Xiong Z, Baker ML, Zhao W, Tachedjian M, Zhu Y, Zhou P, Jiang X, Ng J, Yang L, Wu L, Xiao J, Feng Y, Chen Y, Sun X, Zhang Y, Marsh GA, Crameri G, Broder CC, Frey KG, Wang LF, Wang J.** 2013. Comparative analysis of bat genomes provides insight into the evolution of flight and immunity. Science **339:**456-460.
39. **Zhou P, Tachedjian M, Wynne JW, Boyd V, Cui J, Smith I, Cowled C, Ng JH, Mok L, Michalski WP, Mendenhall IH, Tachedjian G, Wang LF, Baker ML.** 2016. Contraction of the type I IFN locus and unusual constitutive expression of IFN-alpha in bats. Proc Natl Acad Sci U S A doi:10.1073/pnas.1518240113.

40. **Xie J, Li Y, Shen X, Goh G, Zhu Y, Cui J, Wang LF, Shi ZL, Zhou P.** 2018. Dampened STING-Dependent Interferon Activation in Bats. Cell Host Microbe **23:**297-301 e294.
41. **Tsagkogeorga G, Parker J, Stupka E, Cotton JA, Rossiter SJ.** 2013. Phylogenomic analyses elucidate the evolutionary relationships of bats. Curr Biol **23:**2262-2267.
42. **Lei M, Dong D.** 2016. Phylogenomic analyses of bat subordinal relationships based on transcriptome data. Scientific Reports **6:**27726.
43. **Teeling EC, Madsen O, Van Den Bussche RA, de Jong WW, Stanhope MJ, Springer MS.** 2002. Microbat paraphyly and the convergent evolution of a key innovation in Old World rhinolophoid microbats. Proceedings of the National Academy of Sciences **99:**1431.
44. **Churchill S.** 1998. Australian Bats. Reed New Holland, Sydney, Australia.
45. **Tait J, Perotto-Baldivieso HL, McKeown A, Westcott DA.** 2014. Are flying-foxes coming to town? Urbanisation of the spectacled flying-fox (Pteropus conspicillatus) in Australia. PLoS One **9:**e109810.
46. **Goldspink LK, Edson DW, Vidgen ME, Bingham J, Field HE, Smith CS.** 2015. Natural Hendra Virus Infection in Flying-Foxes - Tissue Tropism and Risk Factors. PLoS One **10:**e0128835.
47. **Edson D, Field H, McMichael L, Vidgen M, Goldspink L, Broos A, Melville D, Kristoffersen J, de Jong C, McLaughlin A, Davis R, Kung N, Jordan D, Kirkland P, Smith C.** 2015. Routes of Hendra Virus Excretion in Naturally-Infected Flying-Foxes: Implications for Viral Transmission and Spillover Risk. PLoS One **10:**e0140670.
48. **Helgen K, Salas L, Bonaccorso F.** 2008. *Pteropus conspicillatus*. http://dx.doi.org/10.2305/IUCN.UK.2008.RLTS.T18721A8510243.en. Accessed 27 August.
49. **Roberts B, Eby P, Tsang SM, Sheherazade.** 2017. *Pteropus alecto*. http://dx.doi.org/10.2305/IUCN.UK.2017-2.RLTS.T18715A22080057.en. Accessed 27 August 2018.
50. **Field H, de Jong C, Melville D, Smith C, Smith I, Broos A, Kung YH, McLaughlin A, Zeddeman A.** 2011. Hendra virus infection dynamics in Australian fruit bats. PLoS One **6:**e28678.
51. **Halpin K, Hyatt AD, Fogarty R, Middleton D, Bingham J, Epstein JH, Rahman SA, Hughes T, Smith C, Field HE, Daszak P.** 2011. Pteropid bats are confirmed as the reservoir hosts of henipaviruses: a comprehensive experimental study of virus transmission. Am J Trop Med Hyg **85:**946-951.
52. **Plowright RK, Field HE, Smith C, Divljan A, Palmer C, Tabor G, Daszak P, Foley JE.** 2008. Reproduction and nutritional stress are risk factors for Hendra virus infection in little red flying foxes (Pteropus scapulatus). Proc Biol Sci **275:**861-869.
53. **Field H, Crameri G, Kung NY, Wang LF.** 2012. Ecological aspects of hendra virus. Curr Top Microbiol Immunol **359:**11-23.
54. **Drexler JF, Corman VM, Muller MA, Maganga GD, Vallo P, Binger T, Gloza-Rausch F, Cottontail VM, Rasche A, Yordanov S, Seebens A, Knornschild M, Oppong S, Adu Sarkodie Y, Pongombo C, Lukashev AN, Schmidt-Chanasit J, Stocker A, Carneiro AJ, Erbar S, Maisner A, Fronhoffs F, Buettner R, Kalko EK, Kruppa T, Franke CR, Kallies R, Yandoko ER, Herrler G, Reusken C, Hassanin A, Kruger DH, Matthee S, Ulrich RG, Leroy EM, Drosten C.** 2012. Bats host major mammalian paramyxoviruses. Nat Commun **3:**796.
55. **Kurth A, Kohl C, Brinkmann A, Ebinger A, Harper JA, Wang LF, Muhldorfer K, Wibbelt G.** 2012. Novel paramyxoviruses in free-ranging European bats. PLoS One **7:**e38688.
56. **Balkema-Buschmann A, Dundon WG, Duprex WP, Easton AJ, Fouchier RAM, Kurath G, Lamb RA, Lee B, Rima BK, Rota PA, Wáng L.** 2018. Proposal 2018.011M.N.v1.Paramyxoviridae. Re-organization of the Family Paramyxoviridae.
57. **Lamb RA, Parks GD.** 2013. *Paramyxoviridae*, p 957-995. *In* Knipe DM, Howley PM (ed), Fields Virology, 6 ed, vol 1. Lippincott Williams & Wilkins, Philadelphia, USA.
58. **Calain P, Roux L.** 1993. The rule of six, a basic feature for efficient replication of Sendai virus defective interfering RNA. J Virol **67:**4822-4830.

59. **Murphy SK, Parks GD.** 1997. Genome nucleotide lengths that are divisible by six are not essential but enhance replication of defective interfering RNAs of the paramyxovirus simian virus 5. Virology **232:**145-157.
60. **Kolakofsky D, Pelet T, Garcin D, Hausmann S, Curran J, Roux L.** 1998. Paramyxovirus RNA synthesis and the requirement for hexamer genome length: the rule of six revisited. J Virol **72:**891-899.
61. **Bowden TR, Westenberg M, Wang LF, Eaton BT, Boyle DB.** 2001. Molecular characterization of Menangle virus, a novel paramyxovirus which infects pigs, fruit bats, and humans. Virology **283:**358-373.
62. **Chua KB, Wang LF, Lam SK, Eaton BT.** 2002. Full length genome sequence of Tioman virus, a novel paramyxovirus in the genus Rubulavirus isolated from fruit bats in Malaysia. Arch Virol **147:**1323-1348.
63. **Shaw ML, Cardenas WB, Zamarin D, Palese P, Basler CF.** 2005. Nuclear localization of the Nipah virus W protein allows for inhibition of both virus- and toll-like receptor 3-triggered signaling pathways. J Virol **79:**6078-6088.
64. **Yu M, Hansson E, Langedijk JP, Eaton BT, Wang LF.** 1998. The attachment protein of Hendra virus has high structural similarity but limited primary sequence homology compared with viruses in the genus Paramyxovirus. Virology **251:**227-233.
65. **Welch BD, Yuan P, Bose S, Kors CA, Lamb RA, Jardetzky TS.** 2013. Structure of the parainfluenza virus 5 (PIV5) hemagglutinin-neuraminidase (HN) ectodomain. PLoS Pathog **9:**e1003534.
66. **Yin HS, Wen X, Paterson RG, Lamb RA, Jardetzky TS.** 2006. Structure of the parainfluenza virus 5 F protein in its metastable, prefusion conformation. Nature **439:**38-44.
67. **Iorio RM, Melanson VR, Mahon PJ.** 2009. Glycoprotein interactions in paramyxovirus fusion. Future Virol **4:**335-351.
68. **Wright PJ, Crameri G, Eaton BT.** 2005. RNA synthesis during infection by Hendra virus: an examination by quantitative real-time PCR of RNA accumulation, the effect of ribavirin and the attenuation of transcription. Arch Virol **150:**521-532.
69. **Curran J, Marq JB, Kolakofsky D.** 1995. An N-terminal domain of the Sendai paramyxovirus P protein acts as a chaperone for the NP protein during the nascent chain assembly step of genome replication. J Virol **69:**849-855.
70. **Wiegand MA, Bossow S, Schlecht S, Neubert WJ.** 2007. De novo synthesis of N and P proteins as a key step in Sendai virus gene expression. J Virol **81:**13835-13844.
71. **Morrison TG.** 2003. Structure and function of a paramyxovirus fusion protein. Biochim Biophys Acta **1614:**73-84.
72. **Chang A, Dutch RE.** 2012. Paramyxovirus Fusion and Entry: Multiple Paths to a Common End. Viruses **4:**613-636.
73. **Lin Y, Bright AC, Rothermel TA, He B.** 2003. Induction of apoptosis by paramyxovirus simian virus 5 lacking a small hydrophobic gene. J Virol **77:**3371-3383.
74. **Nakatsu Y, Ma X, Seki F, Suzuki T, Iwasaki M, Yanagi Y, Komase K, Takeda M.** 2013. Intracellular transport of the measles virus ribonucleoprotein complex is mediated by Rab11A-positive recycling endosomes and drives virus release from the apical membrane of polarized epithelial cells. Journal of virology **87:**4683-4693.
75. **El Najjar F, Schmitt AP, Dutch RE.** 2014. Paramyxovirus glycoprotein incorporation, assembly and budding: a three way dance for infectious particle production. Viruses **6:**3019-3054.
76. **Liljeroos L, Butcher SJ.** 2013. Matrix proteins as centralized organizers of negative-sense RNA virions. Front Biosci (Landmark Ed) **18:**696-715.
77. **Li M, Schmitt PT, Li Z, McCrory TS, He B, Schmitt AP.** 2009. Mumps virus matrix, fusion, and nucleocapsid proteins cooperate for efficient production of virus-like particles. J Virol **83:**7261-7272.

78. **Precious B, Young DF, Andrejeva L, Goodbourn S, Randall RE.** 2005. In vitro and in vivo specificity of ubiquitination and degradation of STAT1 and STAT2 by the V proteins of the paramyxoviruses simian virus 5 and human parainfluenza virus type 2. J Gen Virol **86:**151-158.
79. **Rodriguez JJ, Parisien JP, Horvath CM.** 2002. Nipah virus V protein evades alpha and gamma interferons by preventing STAT1 and STAT2 activation and nuclear accumulation. J Virol **76:**11476-11483.
80. **Audsley MD, Moseley GW.** 2013. Paramyxovirus evasion of innate immunity: Diverse strategies for common targets. World J Virol **2:**57-70.
81. **Ciancanelli MJ, Volchkova VA, Shaw ML, Volchkov VE, Basler CF.** 2009. Nipah virus sequesters inactive STAT1 in the nucleus via a P gene-encoded mechanism. J Virol **83:**7828-7841.
82. **Lo MK, Sogaard TM, Karlin DG.** 2014. Evolution and structural organization of the C proteins of paramyxovirinae. PLoS One **9:**e90003.
83. **Irie T, Okamoto I, Yoshida A, Nagai Y, Sakaguchi T.** 2014. Sendai virus C proteins regulate viral genome and antigenome synthesis to dictate the negative genome polarity. J Virol **88:**690-698.
84. **Wang LF, Yu M, Hansson E, Pritchard LI, Shiell B, Michalski WP, Eaton BT.** 2000. The exceptionally large genome of Hendra virus: support for creation of a new genus within the family Paramyxoviridae. J Virol **74:**9972-9979.
85. **Marsh GA, de Jong C, Barr JA, Tachedjian M, Smith C, Middleton D, Yu M, Todd S, Foord AJ, Haring V, Payne J, Robinson R, Broz I, Crameri G, Field HE, Wang LF.** 2012. Cedar virus: a novel Henipavirus isolated from Australian bats. PLoS Pathog **8:**e1002836.
86. **Zhiqiang W, Li Y, Fan Y, Xianwen R, Jinyong J, Jie D, Lilian S, Yafang Z, Hongning Z, Qi J.** 2014. Novel Henipa-like Virus, Mojiang Paramyxovirus, in Rats, China, 2012. Emerging Infectious Disease journal **20:**1064.
87. **Chan YP, Chua KB, Koh CL, Lim ME, Lam SK.** 2001. Complete nucleotide sequences of Nipah virus isolates from Malaysia. J Gen Virol **82:**2151-2155.
88. **Wang L-F, Collins, P.L., Fouchier, R.A.M., Kurath, G., Lamb, R.A., Randall, R.E. and Rima, B.K.** 2012. Family *Paramyxoviridae*. *In* King AMQ, Adams MJ, Carstens EB, Lefkowitz EJ (ed), Virus Taxonomy: Classification and Nomenclature of Viruses : Ninth Report of the International Committee on Taxonomy of Viruses. Elsevier.
89. **Bonaparte MI, Dimitrov AS, Bossart KN, Crameri G, Mungall BA, Bishop KA, Choudhry V, Dimitrov DS, Wang LF, Eaton BT, Broder CC.** 2005. Ephrin-B2 ligand is a functional receptor for Hendra virus and Nipah virus. Proc Natl Acad Sci U S A **102:**10652-10657.
90. **Negrete OA, Wolf MC, Aguilar HC, Enterlein S, Wang W, Muhlberger E, Su SV, Bertolotti-Ciarlet A, Flick R, Lee B.** 2006. Two key residues in ephrinB3 are critical for its use as an alternative receptor for Nipah virus. PLoS Pathog **2:**e7.
91. **Murray K, Selleck P, Hooper P, Hyatt A, Gould A, Gleeson L, Westbury H, Hiley L, Selvey L, Rodwell B, et al.** 1995. A morbillivirus that caused fatal disease in horses and humans. Science **268:**94-97.
92. **Department of Agriculture, Fisheries and Forestry.** 2013. Guidelines for veterinarians handling potential Hendra virus infection in horses. Version 5.0. https://www.daf.qld.gov.au/__data/assets/pdf_file/0009/97713/2355-guidelines-for-veterinarians-sept-2013.pdf. Accessed 3 March 2016.
93. **Playford EG, McCall B, Smith G, Slinko V, Allen G, Smith I, Moore F, Taylor C, Kung YH, Field H.** 2010. Human Hendra virus encephalitis associated with equine outbreak, Australia, 2008. Emerg Infect Dis **16:**219-223.
94. **O'Sullivan JD, Allworth AM, Paterson DL, Snow TM, Boots R, Gleeson LJ, Gould AR, Hyatt AD, Bradfield J.** 1997. Fatal encephalitis due to novel paramyxovirus transmitted from horses. Lancet **349:**93-95.

95. **Mahalingam S, Herrero LJ, Playford EG, Spann K, Herring B, Rolph MS, Middleton D, McCall B, Field H, Wang LF.** 2012. Hendra virus: an emerging paramyxovirus in Australia. Lancet Infect Dis **12:**799-807.
96. **Middleton D, Pallister J, Klein R, Feng YR, Haining J, Arkinstall R, Frazer L, Huang JA, Edwards N, Wareing M, Elhay M, Hashmi Z, Bingham J, Yamada M, Johnson D, White J, Foord A, Heine HG, Marsh GA, Broder CC, Wang LF.** 2014. Hendra virus vaccine, a one health approach to protecting horse, human, and environmental health. Emerg Infect Dis **20:**372-379.
97. **Queensland Government.** 2018. Summary of Hendra virus incidents in horses. https://www.business.qld.gov.au/industries/service-industries-professionals/service-industries/veterinary-surgeons/guidelines-hendra/incident-summary. Accessed 27 August 2018.
98. **Lieu KG, Marsh GA, Wang LF, Netter HJ.** 2015. The non-pathogenic Henipavirus Cedar paramyxovirus phosphoprotein has a compromised ability to target STAT1 and STAT2. Antiviral Res **124:**69-76.
99. **Centers for Disease Control and Prevention.** 1999. Update: outbreak of Nipah virus--Malaysia and Singapore, 1999. MMWR Morb Mortal Wkly Rep **48:**335-337.
100. **Chua KB, Koh CL, Hooi PS, Wee KF, Khong JH, Chua BH, Chan YP, Lim ME, Lam SK.** 2002. Isolation of Nipah virus from Malaysian Island flying-foxes. Microbes Infect **4:**145-151.
101. **Chua KB, Bellini WJ, Rota PA, Harcourt BH, Tamin A, Lam SK, Ksiazek TG, Rollin PE, Zaki SR, Shieh W, Goldsmith CS, Gubler DJ, Roehrig JT, Eaton B, Gould AR, Olson J, Field H, Daniels P, Ling AE, Peters CJ, Anderson LJ, Mahy BW.** 2000. Nipah virus: a recently emergent deadly paramyxovirus. Science **288:**1432-1435.
102. **Luby SP, Rahman M, Hossain MJ, Blum LS, Husain MM, Gurley E, Khan R, Ahmed BN, Rahman S, Nahar N, Kenah E, Comer JA, Ksiazek TG.** 2006. Foodborne transmission of Nipah virus, Bangladesh. Emerg Infect Dis **12:**1888-1894.
103. **Luby SP, Hossain MJ, Gurley ES, Ahmed BN, Banu S, Khan SU, Homaira N, Rota PA, Rollin PE, Comer JA, Kenah E, Ksiazek TG, Rahman M.** 2009. Recurrent zoonotic transmission of Nipah virus into humans, Bangladesh, 2001-2007. Emerg Infect Dis **15:**1229-1235.
104. **Marsh GA, Wang LF.** 2012. Hendra and Nipah viruses: why are they so deadly? Curr Opin Virol **2:**242-247.
105. **World Health Organisation.** 2018. Effective containment of the Nipah virus outbreak in India highlights the importance of a strong health system. http://www.who.int/csr/disease/nipah/effective-containment-in-india/en/. Accessed 27 August 2018.
106. **Rissanen I, Ahmed AA, Azarm K, Beaty S, Hong P, Nambulli S, Duprex WP, Lee B, Bowden TA.** 2017. Idiosyncratic Mojiang virus attachment glycoprotein directs a host-cell entry pathway distinct from genetically related henipaviruses. Nat Commun **8:**16060.
107. **Pernet O, Beaty S, Lee B.** 2014. Functional Rectification of the Newly Described African Henipavirus Fusion Glycoprotein (Gh-M74a). Journal of Virology **88:**5171-5176.
108. **Lee B, Pernet O, Ahmed AA, Zeltina A, Beaty SM, Bowden TA.** 2015. Molecular recognition of human ephrinB2 cell surface receptor by an emergent African henipavirus. Proceedings of the National Academy of Sciences of the United States of America **112:**E2156-E2165.
109. **Pavri KM, Singh KR, Hollinger FB.** 1971. Isolation of a new parainfluenza virus from a frugivorous bat, Rousettus leschenaulti, collected at Poona, India. Am J Trop Med Hyg **20:**125-130.
110. **Wang LF, Hansson E, Yu M, Chua KB, Mathe N, Crameri G, Rima BK, Moreno-Lopez J, Eaton BT.** 2007. Full-length genome sequence and genetic relationship of two paramyxoviruses isolated from bat and pigs in the Americas. Arch Virol **152:**1259-1271.
111. **Goswami KK, Cameron KR, Russell WC, Lange LS, Mitchell DN.** 1984. Evidence for the persistence of paramyxoviruses in human bone marrows. J Gen Virol **65 (Pt 11):**1881-1888.

112. **Goswami KK, Randall RE, Lange LS, Russell WC.** 1987. Antibodies against the paramyxovirus SV5 in the cerebrospinal fluids of some multiple sclerosis patients. Nature **327:**244-247.
113. **Goswami KK, Lange LS, Mitchell DN, Cameron KR, Russell WC.** 1984. Does simian virus 5 infect humans? J Gen Virol **65 (Pt 8):**1295-1303.
114. **Ford RB.** 2013. Canine Infectious Respiratory Disease, p 55-65. *In* Greene CE (ed), Infectious Diseases of the Dog and Cat, 4th ed. Elsevier Health Sciences.
115. **Day MJ, C. HM, D. SR, A. SR.** 2016. WSAVA Guidelines for the vaccination of dogs and cats. Journal of Small Animal Practice **57:**E1-E45.
116. **Evermann JF, Krakowka S, McKeirnan AJ, Baumgartner W.** 1981. Properties of an encephalitogenic canine parainfluenza virus. Arch Virol **68:**165-172.
117. **Heinen E, Herbst W, Schmeer N.** 1998. Isolation of a cytopathogenic virus from a case of porcine reproductive and respiratory syndrome (PRRS) and its characterization as parainfluenza virus type 2. Arch Virol **143:**2233-2239.
118. **Liu Y, Li N, Zhang S, Zhang F, Lian H, Hu R.** 2015. Parainfluenza Virus 5 as Possible Cause of Severe Respiratory Disease in Calves, China. Emerg Infect Dis **21:**2242-2244.
119. **Phan SI, Chen Z, Xu P, Li Z, Gao X, Foster SL, Teng MN, Tripp RA, Sakamoto K, He B.** 2014. A respiratory syncytial virus (RSV) vaccine based on parainfluenza virus 5 (PIV5). Vaccine **32:**3050-3057.
120. **Chen Z, Zhou M, Gao X, Zhang G, Ren G, Gnanadurai CW, Fu ZF, He B.** 2013. A novel rabies vaccine based on a recombinant parainfluenza virus 5 expressing rabies virus glycoprotein. J Virol **87:**2986-2993.
121. **Huang Y, Chen Z, Huang J, Fu Z, He B.** 2015. Parainfluenza virus 5 expressing the G protein of rabies virus protects mice after rabies virus infection. J Virol **89:**3427-3429.
122. **Li Z, Mooney AJ, Gabbard JD, Gao X, Xu P, Place RJ, Hogan RJ, Tompkins SM, He B.** 2013. Recombinant parainfluenza virus 5 expressing hemagglutinin of influenza A virus H5N1 protected mice against lethal highly pathogenic avian influenza virus H5N1 challenge. J Virol **87:**354-362.
123. **Chen Z, Xu P, Salyards GW, Harvey SB, Rada B, Fu ZF, He B.** 2012. Evaluating a parainfluenza virus 5-based vaccine in a host with pre-existing immunity against parainfluenza virus 5. PLoS One **7:**e50144.
124. **Barr JA, Smith C, Marsh GA, Field H, Wang LF.** 2012. Evidence of bat origin for Menangle virus, a zoonotic paramyxovirus first isolated from diseased pigs. J Gen Virol **93:**2590-2594.
125. **Baker KS, Todd S, Marsh GA, Crameri G, Barr J, Kamins AO, Peel AJ, Yu M, Hayman DT, Nadjm B, Mtove G, Amos B, Reyburn H, Nyarko E, Suu-Ire R, Murcia PR, Cunningham AA, Wood JL, Wang LF.** 2013. Novel, potentially zoonotic paramyxoviruses from the African straw-colored fruit bat Eidolon helvum. J Virol **87:**1348-1358.
126. **Amman BR, Albarino CG, Bird BH, Nyakarahuka L, Sealy TK, Balinandi S, Schuh AJ, Campbell SM, Stroher U, Jones ME, Vodzack ME, Reeder DM, Kaboyo W, Nichol ST, Towner JS.** 2015. A Recently Discovered Pathogenic Paramyxovirus, Sosuga Virus, is Present in Rousettus aegyptiacus Fruit Bats at Multiple Locations in Uganda. J Wildl Dis **51:**774-779.
127. **Lau SK, Woo PC, Wong BH, Wong AY, Tsoi HW, Wang M, Lee P, Xu H, Poon RW, Guo R, Li KS, Chan KH, Zheng BJ, Yuen KY.** 2010. Identification and complete genome analysis of three novel paramyxoviruses, Tuhoko virus 1, 2 and 3, in fruit bats from China. Virology **404:**106-116.
128. **Chua KB, Wang LF, Lam SK, Crameri G, Yu M, Wise T, Boyle D, Hyatt AD, Eaton BT.** 2001. Tioman virus, a novel paramyxovirus isolated from fruit bats in Malaysia. Virology **283:**215-229.
129. **Yaiw KC, Crameri G, Wang L, Chong HT, Chua KB, Tan CT, Goh KJ, Shamala D, Wong KT.** 2007. Serological evidence of possible human infection with Tioman virus, a newly described paramyxovirus of bat origin. J Infect Dis **196:**884-886.

130. **Burroughs AL, Tachedjian M, Crameri G, Durr PA, Marsh GA, Wang LF.** 2015. Complete genome sequence of teviot paramyxovirus, a novel rubulavirus isolated from fruit bats in australia. Genome Announc **3**.
131. **Philbey AW, Kirkland PD, Ross AD, Davis RJ, Gleeson AB, Love RJ, Daniels PW, Gould AR, Hyatt AD.** 1998. An apparently new virus (family Paramyxoviridae) infectious for pigs, humans, and fruit bats. Emerg Infect Dis **4:**269-271.
132. **Chant K, Chan R, Smith M, Dwyer DE, Kirkland P.** 1998. Probable human infection with a newly described virus in the family Paramyxoviridae. The NSW Expert Group. Emerg Infect Dis **4:**273-275.
133. **Albarino CG, Foltzer M, Towner JS, Rowe LA, Campbell S, Jaramillo CM, Bird BH, Reeder DM, Vodzak ME, Rota P, Metcalfe MG, Spiropoulou CF, Knust B, Vincent JP, Frace MA, Nichol ST, Rollin PE, Stroher U.** 2014. Novel paramyxovirus associated with severe acute febrile disease, South Sudan and Uganda, 2012. Emerg Infect Dis **20:**211-216.
134. **Berk AJ.** 2013. *Adenoviridae*, p 1705-1731. *In* Knipe DM, Howley PM (ed), Fields Virology, 6 ed, vol 2. Lippincott Williams & Wilkins, Philadelphia, USA.
135. **Harrach B, Benkö, M., Both, G.W., Brown, M., Davison, A.J., Echavarría, M., Hess, M., Jones M.S., Kajon, A., Lehmkuhl, H.D., Mautner, V., Mittal, S.K., Wadell, G.** 2012. Family *Adenoviridae*, p 125-141. *In* King AMQ, Adams MJ, Carstens EB, Lefkowitz EJ (ed), Virus Taxonomy: Classification and Nomenclature of Viruses : Ninth Report of the International Committee on Taxonomy of Viruses. Elsevier.
136. **Lai C-Y, Lee C-J, Lu C-Y, Lee P-I, Shao P-L, Wu E-T, Wang C-C, Tan B-F, Chang H-Y, Hsia S-H, Lin J-J, Chang L-Y, Huang Y-C, Huang L-M, on behalf of the Taiwan Pediatric Infectious Disease A.** 2013. Adenovirus Serotype 3 and 7 Infection with Acute Respiratory Failure in Children in Taiwan, 2010–2011. PLoS ONE **8:**e53614.
137. **Cooper RJ, Hallett R, Tullo AB, Klapper PE.** 2000. The epidemiology of adenovirus infections in Greater Manchester, UK 1982-96. Epidemiology and Infection **125:**333-345.
138. **Decaro N, Martella V, Buonavoglia C.** 2008. Canine adenoviruses and herpesvirus. Vet Clin North Am Small Anim Pract **38:**799-814, viii.
139. **Zhao J, Zhong Q, Zhao Y, Hu YX, Zhang GZ.** 2015. Pathogenicity and Complete Genome Characterization of Fowl Adenoviruses Isolated from Chickens Associated with Inclusion Body Hepatitis and Hydropericardium Syndrome in China. PLoS One **10:**e0133073.
140. **Domanska-Blicharz K, Tomczyk G, Smietanka K, Kozaczynski W, Minta Z.** 2011. Molecular characterization of fowl adenoviruses isolated from chickens with gizzard erosions. Poult Sci **90:**983-989.
141. **Liu Y, Wan W, Gao D, Li Y, Yang X, Liu H, Yao H, Chen L, Wang C, Zhao J.** 2016. Genetic characterization of novel fowl aviadenovirus 4 isolates from outbreaks of hepatitis-hydropericardium syndrome in broiler chickens in China. **5:**e117.
142. **Benko M, Harrach B.** 1998. A proposal for a new (third) genus within the family Adenoviridae. Arch Virol **143:**829-837.
143. **Kovacs ER, Benko M.** 2011. Complete sequence of raptor adenovirus 1 confirms the characteristic genome organization of siadenoviruses. Infect Genet Evol **11:**1058-1065.
144. **Kovacs GM, LaPatra SE, D'Halluin JC, Benko M.** 2003. Phylogenetic analysis of the hexon and protease genes of a fish adenovirus isolated from white sturgeon (Acipenser transmontanus) supports the proposal for a new adenovirus genus. Virus Res **98:**27-34.
145. **Keeler AM, ElMallah MK, Flotte TR.** 2017. Gene Therapy 2017: Progress and Future Directions. Clin Transl Sci **10:**242-248.
146. **Patel A, Tikoo S, Kobinger G.** 2010. A porcine adenovirus with low human seroprevalence is a promising alternative vaccine vector to human adenovirus 5 in an H5N1 virus disease model. PLoS One **5:**e15301.
147. **Wold WSM, Ison MG.** 2013. Adenoviruses, p 1733-1767. *In* Knipe DM, Howley PM (ed), Fields Virology, 6 ed, vol 2. Lippincott Williams & Wilkins, Philadelphia, USA.

148. **Tan B, Yang XL, Ge XY, Peng C, Liu HZ, Zhang YZ, Zhang LB, Shi ZL.** 2017. Novel bat adenoviruses with low G+C content shed new light on the evolution of adenoviruses. J Gen Virol **98:**739-748.
149. **Kohl C, Vidovszky MZ, Mühldorfer K, Dabrowski PW, Radonić A, Nitsche A, Wibbelt G, Kurth A, Harrach B.** 2012. Genome Analysis of Bat Adenovirus 2: Indications of Interspecies Transmission. Journal of Virology **86:**1888-1892.
150. **King AMQ, Lefkowitz EJ.** 2018. Changes to taxonomy and the International Code of Virus Classification and Nomenclature ratified by the International Committee on Taxonomy of Viruses (2018). doi:10.1007/s00705-018-3847-1.
151. **Hackenbrack N, Rogers MB, Ashley RE, Keel MK, Kubiski SV, Bryan JA, Ghedin E, Holmes EC, Hafenstein SL, Allison AB.** 2017. Evolution and Cryo-electron Microscopy Capsid Structure of a North American Bat Adenovirus and Its Relationship to Other Mastadenoviruses. **91**.
152. **Moens U, Calvignac-Spencer S, Lauber C, Ramqvist T, Feltkamp MCW, Daugherty MD, Verschoor EJ, Ehlers B, Ictv Report C.** 2017. ICTV Virus Taxonomy Profile: Polyomaviridae. J Gen Virol **98:**1159-1160.
153. **DeCaprio JA, Imperiale MJ, Major EO.** 2013. Polyomaviruses, p 1633-1661. *In* Knipe DM, Howley PM (ed), Fields Virology, 6 ed, vol 2. Lippincott Williams & Wilkins, Philadelphia, USA.
154. **Sawinski D, Goral S.** 2015. BK virus infection: an update on diagnosis and treatment. Nephrol Dial Transplant **30:**209-217.
155. **Kean JM, Rao S, Wang M, Garcea RL.** 2009. Seroepidemiology of human polyomaviruses. PLoS Pathog **5:**e1000363.
156. **Zhong S, Zheng HY, Suzuki M, Chen Q, Ikegaya H, Aoki N, Usuku S, Kobayashi N, Nukuzuma S, Yasuda Y, Kuniyoshi N, Yogo Y, Kitamura T.** 2007. Age-related urinary excretion of BK polyomavirus by nonimmunocompromised individuals. J Clin Microbiol **45:**193-198.
157. **Gerits N, Moens U.** 2012. Agnoprotein of mammalian polyomaviruses. Virology **432:**316-326.
158. **Evans GL, Caller LG, Foster V, Crump CM.** 2015. Anion homeostasis is important for non-lytic release of BK polyomavirus from infected cells. Open Biology **5:**150041.
159. **Daniels R, Sadowicz D, Hebert DN.** 2007. A Very Late Viral Protein Triggers the Lytic Release of SV40. PLoS Pathogens **3:**e98.
160. **Misra V, Dumonceaux T, Dubois J, Willis C, Nadin-Davis S, Severini A, Wandeler A, Lindsay R, Artsob H.** 2009. Detection of polyoma and corona viruses in bats of Canada. J Gen Virol **90:**2015-2022.
161. **Kobayashi S, Sasaki M, Nakao R, Setiyono A, Handharyani E, Orba Y, Rahmadani I, Taha S, Adiani S, Subangkit M, Nakamura I, Kimura T, Sawa H.** 2015. Detection of novel polyomaviruses in fruit bats in Indonesia. Arch Virol **160:**1075-1082.
162. **Tao Y, Shi M, Conrardy C, Kuzmin IV, Recuenco S, Agwanda B, Alvarez DA, Ellison JA, Gilbert AT, Moran D, Niezgoda M, Lindblade KA, Holmes EC, Breiman RF, Rupprecht CE, Tong S.** 2013. Discovery of diverse polyomaviruses in bats and the evolutionary history of the Polyomaviridae. J Gen Virol **94:**738-748.
163. **Carr M, Gonzalez G, Sasaki M, Ito K, Ishii A, Hang'ombe BM, Mweene AS, Orba Y, Sawa H.** 2017. Discovery of African bat polyomaviruses and infrequent recombination in the large T antigen in the Polyomaviridae. J Gen Virol **98:**726-738.
164. **Fagrouch Z, Sarwari R, Lavergne A, Delaval M, de Thoisy B, Lacoste V, Verschoor EJ.** 2012. Novel polyomaviruses in South American bats and their relationship to other members of the family Polyomaviridae. J Gen Virol **93:**2652-2657.
165. **Sasaki M, Setiyono A, Handharyani E, Rahmadani I, Taha S, Adiani S, Subangkit M, Sawa H, Nakamura I, Kimura T.** 2012. Molecular detection of a novel paramyxovirus in fruit bats from Indonesia. Virol J **9:**240.
166. **Tang XC, Zhang JX, Zhang SY, Wang P, Fan XH, Li LF, Li G, Dong BQ, Liu W, Cheung CL, Xu KM, Song WJ, Vijaykrishna D, Poon LL, Peiris JS, Smith GJ, Chen H, Guan Y.** 2006. Prevalence and genetic diversity of coronaviruses in bats from China. J Virol **80:**7481-7490.

167. **Amman BR, Carroll SA, Reed ZD, Sealy TK, Balinandi S, Swanepoel R, Kemp A, Erickson BR, Comer JA, Campbell S, Cannon DL, Khristova ML, Atimnedi P, Paddock CD, Crockett RJ, Flietstra TD, Warfield KL, Unfer R, Katongole-Mbidde E, Downing R, Tappero JW, Zaki SR, Rollin PE, Ksiazek TG, Nichol ST, Towner JS.** 2012. Seasonal pulses of Marburg virus circulation in juvenile Rousettus aegyptiacus bats coincide with periods of increased risk of human infection. PLoS Pathog **8:**e1002877.
168. **Baker KS, Todd S, Marsh G, Fernandez-Loras A, Suu-Ire R, Wood JL, Wang LF, Murcia PR, Cunningham AA.** 2012. Co-circulation of diverse paramyxoviruses in an urban African fruit bat population. J Gen Virol **93:**850-856.
169. **Wu Z, Yang L, Ren X, He G, Zhang J, Yang J, Qian Z, Dong J, Sun L, Zhu Y, Du J, Yang F, Zhang S, Jin Q.** 2016. Deciphering the bat virome catalog to better understand the ecological diversity of bat viruses and the bat origin of emerging infectious diseases. ISME J **10:**609-620.
170. **Queen K, Shi M, Anderson LJ, Tong S.** 2015. Other bat-borne viruses, p 217-248. *In* Wang L, Cowled C (ed), Bats and Viruses: A New Frontier of Emerging Infectious Diseases. John Wiley & Sons, New Jersey, USA.
171. **Crameri G, Todd S, Grimley S, McEachern JA, Marsh GA, Smith C, Tachedjian M, De Jong C, Virtue ER, Yu M, Bulach D, Liu JP, Michalski WP, Middleton D, Field HE, Wang LF.** 2009. Establishment, immortalisation and characterisation of pteropid bat cell lines. PLoS One **4:**e8266.
172. **Tong S, Chern SW, Li Y, Pallansch MA, Anderson LJ.** 2008. Sensitive and broadly reactive reverse transcription-PCR assays to detect novel paramyxoviruses. J Clin Microbiol **46:**2652-2658.
173. **Ehlers B, Borchers K, Grund C, Frölich K, Ludwig H, Buhk H-J.** 1999. Detection of New DNA Polymerase Genes of Known and Potentially Novel Herpesviruses by PCR with Degenerate and Deoxyinosine-Substituted Primers. Virus Genes **18:**211-220.
174. **Wellehan JF, Jr., Childress AL, Marschang RE, Johnson AJ, Lamirande EW, Roberts JF, Vickers ML, Gaskin JM, Jacobson ER.** 2009. Consensus nested PCR amplification and sequencing of diverse reptilian, avian, and mammalian orthoreoviruses. Vet Microbiol **133:**34-42.
175. **Vijgen L, Moes E, Keyaerts E, Li S, Van Ranst M.** 2008. A pancoronavirus RT-PCR assay for detection of all known coronaviruses. Methods Mol Biol **454:**3-12.
176. **Messing J.** 1983. New M13 vectors for cloning. Methods Enzymol **101:**20-78.
177. **Li Z, Yu M, Zhang H, Wang HY, Wang LF.** 2005. Improved rapid amplification of cDNA ends (RACE) for mapping both the 5' and 3' terminal sequences of paramyxovirus genomes. J Virol Methods **130:**154-156.
178. **Mungall BA, Middleton D, Crameri G, Bingham J, Halpin K, Russell G, Green D, McEachern J, Pritchard LI, Eaton BT, Wang LF, Bossart KN, Broder CC.** 2006. Feline model of acute nipah virus infection and protection with a soluble glycoprotein-based subunit vaccine. J Virol **80:**12293-12302.
179. **Clayton BA, Middleton D, Bergfeld J, Haining J, Arkinstall R, Wang L, Marsh GA.** 2012. Transmission Routes for Nipah Virus from Malaysia and Bangladesh. Emerging Infectious Diseases **18:**1983-1993.
180. **Bankevich A, Nurk S, Antipov D, Gurevich AA, Dvorkin M, Kulikov AS, Lesin VM, Nikolenko SI, Pham S, Prjibelski AD, Pyshkin AV, Sirotkin AV, Vyahhi N, Tesler G, Alekseyev MA, Pevzner PA.** 2012. SPAdes: a new genome assembly algorithm and its applications to single-cell sequencing. J Comput Biol **19:**455-477.
181. **Wan Y, Renner DW, Albert I, Szpara ML.** 2015. VirAmp: a galaxy-based viral genome assembly pipeline. Gigascience **4:**19.
182. **Biomatters Ltd.** 2018. Assembly and Mapping. *In* (ed), Geneious. https://assets.geneious.com/documentation/geneious/GeneiousManual.pdf.

183. **de Wit E, Bestebroer TM, Spronken MI, Rimmelzwaan GF, Osterhaus AD, Fouchier RA.** 2007. Rapid sequencing of the non-coding regions of influenza A virus. J Virol Methods **139:**85-89.
184. **Audsley MD, Marsh GA, Lieu KG, Tachedjian M, Joubert DA, Wang LF, Jans DA, Moseley GW.** 2015. The immune evasion function of J and Beilong virus V proteins is distinct from that of other paramyxoviruses, consistent with a separate "Jeilongvirus" genus. J Gen Virol doi:10.1099/jgv.0.000388.
185. **Illumina.** 2013. 16S metagenomic sequencing library preparation protocol: preparing 16S ribosomal RNA gene amplicons for the Illumina MiSeq system. Part no. 15044223 Rev B, *on* Illumina. https://www.illumina.com/content/dam/illumina-support/documents/documentation/chemistry_documentation/16s/16s-metagenomic-library-prep-guide-15044223-b.pdf. Accessed 31 October 2017.
186. **Sievers F, Wilm A, Dineen D, Gibson TJ, Karplus K, Li W, Lopez R, McWilliam H, Remmert M, Söding J, Thompson JD, Higgins DG.** 2011. Fast, scalable generation of high‐quality protein multiple sequence alignments using Clustal Omega. Molecular Systems Biology **7**.
187. **Waterhouse AM, Procter JB, Martin DMA, Clamp M, Barton GJ.** 2009. Jalview Version 2—a multiple sequence alignment editor and analysis workbench. Bioinformatics **25:**1189-1191.
188. **Krogh A, Larsson B, von Heijne G, Sonnhammer EL.** 2001. Predicting transmembrane protein topology with a hidden Markov model: application to complete genomes. J Mol Biol **305:**567-580.
189. **Kall L, Krogh A, Sonnhammer EL.** 2004. A combined transmembrane topology and signal peptide prediction method. J Mol Biol **338:**1027-1036.
190. **Petersen TN, Brunak S, von Heijne G, Nielsen H.** 2011. SignalP 4.0: discriminating signal peptides from transmembrane regions. Nat Methods **8:**785-786.
191. **Reed LJ, Muench H.** 1938. A simple method of estimating fifty percent endpoints. American Journal of Epidemiology **27:**493-497.
192. **Simmons CP, Bernasconi NL, Suguitan AL, Mills K, Ward JM, Chau NV, Hien TT, Sallusto F, Ha do Q, Farrar J, de Jong MD, Lanzavecchia A, Subbarao K.** 2007. Prophylactic and therapeutic efficacy of human monoclonal antibodies against H5N1 influenza. PLoS Med **4:**e178.
193. **Pallister J, Middleton D, Wang LF, Klein R, Haining J, Robinson R, Yamada M, White J, Payne J, Feng YR, Chan YP, Broder CC.** 2011. A recombinant Hendra virus G glycoprotein-based subunit vaccine protects ferrets from lethal Hendra virus challenge. Vaccine **29:**5623-5630.
194. **Dups J, Middleton D, Yamada M, Monaghan P, Long F, Robinson R, Marsh GA, Wang LF.** 2012. A new model for Hendra virus encephalitis in the mouse. PLoS One **7:**e40308.
195. **Langford DJ, Bailey AL, Chanda ML, Clarke SE, Drummond TE, Echols S, Glick S, Ingrao J, Klassen-Ross T, Lacroix-Fralish ML, Matsumiya L, Sorge RE, Sotocinal SG, Tabaka JM, Wong D, van den Maagdenberg AM, Ferrari MD, Craig KD, Mogil JS.** 2010. Coding of facial expressions of pain in the laboratory mouse. Nat Methods **7:**447-449.
196. **Staroscik A.** 2015. Copy number calculator for realtime PCR. http://scienceprimer.com/copy-number-calculator-for-realtime-pcr. Accessed 21 January 2017.
197. **Zheng XY, Qiu M, Chen SW, Xiao JP, Ma LZ, Liu S, Zhou JH, Zhang QH, Li X, Chen Z, Wu Y, Chen HF, Jiang LN, Xiong YQ, Ma SJ, Zhong XS, Huo ST, Ge J, Cen SW, Chen Q.** 2016. High prevalence and diversity of viruses of the subfamily Gammaherpesvirinae, family Herpesviridae, in fecal specimens from bats of different species in southern China. Arch Virol **161:**135-140.
198. **Vidgen ME, de Jong C, Rose K, Hall J, Field HE, Smith CS.** 2015. Novel paramyxoviruses in Australian flying-fox populations support host-virus coevolution. J Gen Virol **96:**1619-1625.

199. **Baker KS, Leggett RM, Bexfield NH, Alston M, Daly G, Todd S, Tachedjian M, Holmes CE, Crameri S, Wang LF, Heeney JL, Suu-Ire R, Kellam P, Cunningham AA, Wood JL, Caccamo M, Murcia PR.** 2013. Metagenomic study of the viruses of African straw-coloured fruit bats: detection of a chiropteran poxvirus and isolation of a novel adenovirus. Virology **441:**95-106.
200. **Burroughs AL, Tachedjian M, Crameri G, Durr PA, Marsh GA, Wang LF.** 2015. Complete genome sequence of teviot paramyxovirus, a novel rubulavirus isolated from fruit bats in australia. Genome Announc **3:**e00177–00115.
201. **Patch JR, Han Z, McCarthy SE, Yan L, Wang L-F, Harty RN, Broder CC.** 2008. The YPLGVG sequence of the Nipah virus matrix protein is required for budding. Virology Journal **5:**137.
202. **Ciancanelli MJ, Basler CF.** 2006. Mutation of YMYL in the Nipah virus matrix protein abrogates budding and alters subcellular localization. J Virol **80:**12070-12078.
203. **Gardner AE, Martin KL, Dutch RE.** 2007. A conserved region between the heptad repeats of paramyxovirus fusion proteins is critical for proper F protein folding. Biochemistry **46:**5094-5105.
204. **Vogt C, Eickmann M, Diederich S, Moll M, Maisner A.** 2005. Endocytosis of the Nipah Virus Glycoproteins. Journal of Virology **79:**3865-3872.
205. **Meulendyke KA, Wurth MA, McCann RO, Dutch RE.** 2005. Endocytosis Plays a Critical Role in Proteolytic Processing of the Hendra Virus Fusion Protein. Journal of Virology **79:**12643-12649.
206. **Guillaume V, Aslan H, Ainouze M, Guerbois M, Fabian Wild T, Buckland R, Langedijk JPM.** 2006. Evidence of a Potential Receptor-Binding Site on the Nipah Virus G Protein (NiV-G): Identification of Globular Head Residues with a Role in Fusion Promotion and Their Localization on an NiV-G Structural Model. Journal of Virology **80:**7546-7554.
207. **Bishop KA, Stantchev TS, Hickey AC, Khetawat D, Bossart KN, Krasnoperov V, Gill P, Feng YR, Wang L, Eaton BT, Wang LF, Broder CC.** 2007. Identification of Hendra virus G glycoprotein residues that are critical for receptor binding. J Virol **81:**5893-5901.
208. **Poch O, Blumberg BM, Bougueleret L, Tordo N.** 1990. Sequence comparison of five polymerases (L proteins) of unsegmented negative-strand RNA viruses: theoretical assignment of functional domains. J Gen Virol **71 (Pt 5):**1153-1162.
209. **Jansen van Vuren P, Allam M.** 2018. A novel adenovirus isolated from the Egyptian fruit bat in South Africa is closely related to recent isolates from China. **8:**9584.
210. **McMichael L, Edson D, Smith C, Mayer D, Smith I, Kopp S, Meers J, Field H.** 2017. Physiological stress and Hendra virus in flying-foxes (Pteropus spp.), Australia. PLoS One **12:**e0182171.
211. **Pomeroy LW, Bjørnstad ON, Holmes EC.** 2008. The Evolutionary and Epidemiological Dynamics of the Paramyxoviridae. Journal of Molecular Evolution **66:**98-106.
212. **Beaty SM, Lee B.** 2016. Constraints on the Genetic and Antigenic Variability of Measles Virus. Viruses **8:**109.
213. **Rima BK.** 2015. Nucleotide sequence conservation in paramyxoviruses; the concept of codon constellation. J Gen Virol **96:**939-955.
214. **Sonntag M, Mühldorfer K, Speck S, Wibbelt G, Kurth A.** 2009. New Adenovirus in Bats, Germany. Emerging Infectious Diseases **15:**2052-2055.
215. **Davison AJ, Benko M, Harrach B.** 2003. Genetic content and evolution of adenoviruses. J Gen Virol **84:**2895-2908.
216. **Hassanin A, Nesi N, Marin J, Kadjo B, Pourrut X, Leroy E, Gembu GC, Musaba Akawa P, Ngoagouni C, Nakoune E, Ruedi M, Tshikung D, Pongombo Shongo C, Bonillo C.** 2016. Comparative phylogeography of African fruit bats (Chiroptera, Pteropodidae) provide new insights into the outbreak of Ebola virus disease in West Africa, 2014-2016. C R Biol **339:**517-528.
217. **Buck CB, Van Doorslaer K, Peretti A, Geoghegan EM, Tisza MJ, An P, Katz JP, Pipas JM, McBride AA, Camus AC, McDermott AJ, Dill JA, Delwart E, Ng TF, Farkas K, Austin C,**

Kraberger S, Davison W, Pastrana DV, Varsani A. 2016. The Ancient Evolutionary History of Polyomaviruses. PLoS Pathog **12:**e1005574.
218. **Breed AC, Meers J, Sendow I, Bossart KN, Barr JA, Smith I, Wacharapluesadee S, Wang L, Field HE.** 2013. The distribution of henipaviruses in Southeast Asia and Australasia: is Wallace's line a barrier to Nipah virus? PLoS One **8:**e61316.
219. **Roche SE, Costard S, Meers J, Field HE, Breed AC.** 2015. Assessing the risk of Nipah virus establishment in Australian flying-foxes. Epidemiol Infect **143:**2213-2226.
220. **Breed AC, Field HE, Smith CS, Edmonston J, Meers J.** 2010. Bats without borders: long-distance movements and implications for disease risk management. Ecohealth **7:**204-212.
221. **Tidemann CR, Nelson JE.** 2004. Long-distance movements of the grey-headed flying fox (Pteropus poliocephalus). Journal of Zoology **263:**141-146.
222. **Adams MJ, Lefkowitz EJ.** 2017. Changes to taxonomy and the International Code of Virus Classification and Nomenclature ratified by the International Committee on Taxonomy of Viruses (2017). **162:**2505-2538.
223. **Miller PJ, Boyle DB, Eaton BT, Wang LF.** 2003. Full-length genome sequence of Mossman virus, a novel paramyxovirus isolated from rodents in Australia. Virology **317:**330-344.
224. **Jorgensen ED, Collins PL, Lomedico PT.** 1987. Cloning and nucleotide sequence of Newcastle disease virus hemagglutinin-neuraminidase mRNA: identification of a putative sialic acid binding site. Virology **156:**12-24.
225. **Mirza AM, Deng R, Iorio RM.** 1994. Site-directed mutagenesis of a conserved hexapeptide in the paramyxovirus hemagglutinin-neuraminidase glycoprotein: effects on antigenic structure and function. J Virol **68:**5093-5099.
226. **Langedijk JP, Daus FJ, van Oirschot JT.** 1997. Sequence and structure alignment of Paramyxoviridae attachment proteins and discovery of enzymatic activity for a morbillivirus hemagglutinin. J Virol **71:**6155-6167.
227. **Geoghegan JL, Senior AM, Di Giallonardo F, Holmes EC.** 2016. Virological factors that increase the transmissibility of emerging human viruses. Proc Natl Acad Sci U S A **113:**4170-4175.
228. **Yaiw KC, Bingham J, Crameri G, Mungall B, Hyatt A, Yu M, Eaton B, Shamala D, Wang LF, Thong Wong K.** 2008. Tioman virus, a paramyxovirus of bat origin, causes mild disease in pigs and has a predilection for lymphoid tissues. J Virol **82:**565-568.
229. **Bossart KN, Zhu Z, Middleton D, Klippel J, Crameri G, Bingham J, McEachern JA, Green D, Hancock TJ, Chan YP, Hickey AC, Dimitrov DS, Wang LF, Broder CC.** 2009. A neutralizing human monoclonal antibody protects against lethal disease in a new ferret model of acute Nipah virus infection. PLoS Pathog **5:**e1000642.
230. **Barr J, Todd S, Crameri G, Foord A, Marsh G.** 2018. Animal infection studies of two recently discovered African bat paramyxoviruses, Achimota 1 and Achimota 2. **8:**12744.
231. **Stray SJ, Cummings RD, Air GM.** 2000. Influenza virus infection of desialylated cells. Glycobiology **10:**649-658.
232. **Lunney D, Richards G, Dickman C.** 2008. Pteropus poliocephalus. http://dx.doi.org/10.2305/IUCN.UK.2008.RLTS.T18751A8554062.en. Accessed 5 August 2018.
233. **Carroll D, Daszak P, Wolfe ND, Gao GF, Morel CM, Morzaria S, Pablos-Mendez A, Tomori O, Mazet JAK.** 2018. The Global Virome Project. Science **359:**872-874.
234. **Hull RN, Minner JR, Smith JW.** 1956. New viral agents recovered from tissue cultures of monkey kidney cells. I. Origin and properties of cytopathogenic agents S.V.1, S.V.2, S.V.4, S.V.5, S.V.6, S.V.11, S.V.12 and S.V.15. Am J Hyg **63:**204-215.
235. **Chatziandreou N, Stock N, Young D, Andrejeva J, Hagmaier K, McGeoch DJ, Randall RE.** 2004. Relationships and host range of human, canine, simian and porcine isolates of simian virus 5 (parainfluenza virus 5). J Gen Virol **85:**3007-3016.

236. **Boyd V, Smith I, Crameri G, Burroughs AL, Durr PA, White J, Cowled C, Marsh GA, Wang LF.** 2015. Development of multiplexed bead arrays for the simultaneous detection of nucleic acid from multiple viruses in bat samples. J Virol Methods **223:**5-12.
237. **Bowden TR, Bingham J, Harper JA, Boyle DB.** 2012. Menangle virus, a pteropid bat paramyxovirus infectious for pigs and humans, exhibits tropism for secondary lymphoid organs and intestinal epithelium in weaned pigs. J Gen Virol **93:**1007-1016.
238. **Hiebert SW, Richardson CD, Lamb RA.** 1988. Cell surface expression and orientation in membranes of the 44-amino-acid SH protein of simian virus 5. J Virol **62:**2347-2357.
239. **Rima BK, Gatherer D, Young DF, Norsted H, Randall RE, Davison AJ.** 2014. Stability of the parainfluenza virus 5 genome revealed by deep sequencing of strains isolated from different hosts and following passage in cell culture. J Virol **88:**3826-3836.
240. **Capraro GA, Johnson JB, Kock ND, Parks GD.** 2008. Virus growth and antibody responses following respiratory tract infection of ferrets and mice with WT and P/V mutants of the paramyxovirus Simian Virus 5. Virology **376:**416-428.
241. **Durchfeld B, Baumgartner W, Krakowka S.** 1991. Intranasal infection of ferrets (Mustela putorius furo) with canine parainfluenza virus. Zentralbl Veterinarmed B **38:**505-512.
242. **He B, Lin GY, Durbin JE, Durbin RK, Lamb RA.** 2001. The SH integral membrane protein of the paramyxovirus simian virus 5 is required to block apoptosis in MDBK cells. J Virol **75:**4068-4079.
243. **Choppin PW.** 1964. Multiplication of a myxovirus (SV5) with minimal cytopathic effects and without interference. Virology **23:**224-233.
244. **Durrant DM, Ghosh S, Klein RS.** 2016. The Olfactory Bulb: An Immunosensory Effector Organ during Neurotropic Viral Infections. ACS Chem Neurosci **7:**464-469.
245. **Detje CN, Meyer T, Schmidt H, Kreuz D, Rose JK, Bechmann I, Prinz M, Kalinke U.** 2009. Local type I IFN receptor signaling protects against virus spread within the central nervous system. J Immunol **182:**2297-2304.
246. **Satterfield BA, Dawes BE, Milligan GN.** 2016. Status of vaccine research and development of vaccines for Nipah virus. Vaccine **34:**2971-2975.
247. **World Health Organisation.** 2018. Nipah virus infection. http://www.who.int/csr/disease/nipah/en/. Accessed 29 September 2018.
248. **Reardon T.** 2010. Survey guidelines for Australia's threatened bats. Department of the Environment, Water, Heritage & the Arts, http://www.environment.gov.au/system/files/resources/2f420bf1-d9e4-44ec-a69c-07316cb81086/files/survey-guidelines-bats.pdf.
249. **National Research Council (US) Committee on Animal Models for Testing Interventions Against Aerosolized Bioterrorism Agents.** 2006. Overcoming Challenges to Develop Countermeasures Against Aerosolized Bioterrorism Agents: Appropriate Use of Animal Models doi:10.17226/11640. National Academy of Sciences., Washington DC.
250. **Belser JA, Eckert AM, Tumpey TM, Maines TR.** 2016. Complexities in Ferret Influenza Virus Pathogenesis and Transmission Models. Microbiology and Molecular Biology Reviews **80:**733.
251. **Cuevas-Romero S, Hernandez-Baumgarten E, Kennedy S, Hernandez-Jauregui P, Berg M, Moreno-Lopez J.** 2014. Long-term RNA persistence of porcine rubulavirus (PorPV-LPMV) after an outbreak of a natural infection: the detection of viral mRNA in sentinel pigs suggests viral transmission. Virus Res **188:**155-161.
252. **Zhang L, Collins PL, Lamb RA, Pickles RJ.** 2011. Comparison of differing cytopathic effects in human airway epithelium of parainfluenza virus 5 (W3A), parainfluenza virus type 3, and respiratory syncytial virus. Virology **421:**67-77.
253. **Cohn ML, Robinson ED, Thomas D, Faerber M, Carey S, Sawyer R, Goswami KK, Johnson AH, Richert JR.** 1996. T cell responses to the paramyxovirus simian virus 5: studies in multiple sclerosis and normal populations. Pathobiology **64:**131-135.

254. **Jones BA, Grace D, Kock R, Alonso S, Rushton J, Said MY, McKeever D, Mutua F, Young J, McDermott J, Pfeiffer DU.** 2013. Zoonosis emergence linked to agricultural intensification and environmental change. Proceedings of the National Academy of Sciences **110:**8399.
255. **Queensland Government.** 2018. Reducing the risk of Hendra virus infection. https://www.business.qld.gov.au/industries/farms-fishing-forestry/agriculture/livestock/horses/hendra-virus/reducing-risk. Accessed 3 October 2018.
256. **Calisher CH, Tesh RB.** 2014. Two misleading words in reports of virus discovery: little things mean a lot. Arch Virol **159:**2189-2191.